



# UNIVERSITÀ DEGLI STUDI DI PALERMO

Dottorato Industriale in “Tecnologie e Scienze per la Salute dell’Uomo”  
Dipartimento Biomedico di Medicina Interna e Specialistica DIBIMIS  
Settore Scientifico Disciplinare FIS/07

## DEVELOPMENT & QUALIFICATION OF BIOASSAYS FOR THE DETERMINATION OF THE BIOACTIVITY, PREDICTIVE PHARMACOKINETICS AND POTENTIAL IMMUNOGENICITY OF THERAPEUTIC ANTIBODIES

IL DOTTORE  
**Giulia Anderloni**

IL COORDINATORE  
**Prof. Maurizio Leone**

IL TUTOR  
**Prof.ssa Valeria Vetri**

TUTOR AZIENDALE  
**Dott. Cosimo-Walter D’Acunto**  
**Merck Serono Spa**

CICLO XXXIII  
ANNO CONSEGUIMENTO TITOLO 2020/21

This research was financially supported by Merck Serono S.p.A., Rome, Italy, an affiliate of Merck KGaA, Darmstadt, Germany.

Merck KGaA, Darmstadt, Germany reviewed the manuscript for medical accuracy only before submission. The authors are fully responsible for the content of this manuscript, and the views and opinions described in the publication reflect solely those of the authors.

## Abstract

The critical quality attributes of a given biotherapeutic monoclonal antibody (mAb), its molecular characterization, functional assessment and effector function analysis should be defined and profiled in detail during the life cycle of a biotherapeutic drug. In the past, this product characterization was simple and standardized. In today's complex world of biologics, success demands a more thoughtful approach and drug developers are investing in advanced analytics much earlier in the development process. Indeed, investing in selected sophisticated and state of the art analytics in early developmental phases of a therapeutic monoclonal antibody may mitigate risks by confirming that the drug candidate has the required basic characteristics and functionality. Therefore, recognizing the added value of an early functional characterization of new biological entities (NBE) in the pharmaceutical industry, this work was focused on the development and qualification of novel methodologies defining the proper analytical characterization panel for a new therapeutic monoclonal antibody. In details, this PhD project was specifically designed to identify, develop and qualify with a stepwise approach *in silico* tools and *in vitro* assays aimed at studying the biological activity, predictive pharmacokinetics (PK) and potential immunogenicity of therapeutic drugs in early phase. To this aim Anti-TIGIT mAb was selected as proof of concept molecule. First, an investigation on the mechanism of action of Anti-TIGIT has been carried out and then different approaches were applied to identify the best *in vitro* assay reflecting the mechanism underlying Anti-TIGIT biological effect. Once selected as the best method a cell-based Anti-TIGIT ligand binding bioassay, it was checked for linearity, precision, accuracy and specificity demonstrating its fitting for the purpose. Different alternative assays for the assessment of the mAb's effector functions were also presented and qualified showing the ability of Anti-TIGIT to induce antibody-dependent cell-mediated cytotoxicity (ADCC). Then, the attention was focused on the predictive pharmacokinetics of Anti-TIGIT and specifically on *in vitro* techniques to assess affinity and kinetic of the interaction with neonatal Fc receptor (FcRn) demonstrating that the developed and qualified methods were reliable, precise and accurate. Moreover, forced degradation studies, where the mAb underwent different stresses, were performed demonstrating the assays' suitability for the purpose highlighting the impact of the applied stresses on both Anti-TIGIT biological activity and PK. In addition, to ensure a good comparison and integration of all the findings, several orthogonal assays were also developed, and the results compared demonstrating the equivalence of the methods. In the end, also an *in silico* tool was used to predict the potential immunogenicity of the drug. Altogether the findings of this work elucidate and integrate the strategies applied in different pharmaceutical companies for method development and validation and extend the knowledge on the methodologies used for therapeutic

monoclonal antibodies characterization and stability studies opening new perspectives for the industrial setting.

## Structure of the thesis

The thesis has been structured in seven chapters:

**Chapter 1** briefly introduces the framework of the thesis. Then the general motivations and objectives are described and justified and the description of the development of the present work is outlined.

**Chapter 2** gives an introduction on the thesis topics. Therapeutic monoclonal antibodies, their structure and applications in therapeutic field and their critical quality attributes (CQAs) are presented. The chapter continues elucidating the importance of an early evaluation of CQAs and their impacts on drugs' bioactivity, predictive pharmacokinetics and potential immunogenicity. Then the concept of therapeutic antibodies' biological activity, predictive pharmacokinetics and potential immunogenicity is explored. State of the art methods to evaluate such antibody's properties are presented together with the approaches for assays development and validation. The aim is to present not only the state of the art but also future trends in the field of method development and validation. Finally, Anti-TIGIT monoclonal antibody, used as a proof of concept molecule, is presented to show the proper approaches to be applied to develop and eventually validate analytical methods to assess drug's biological activity, predictive pharmacokinetics (PK) and potential immunogenicity.

**Chapter 3** describes the methods used in this work and it includes the description of a range of techniques such as cell-based assays, ELISA assays, surface plasmon resonance (SPR)-based techniques and AlphaScreen assays.

Following there are three results chapters. All together these chapters showed the strategy applied for the development of a proper analytical strategy for early characterization of therapeutic monoclonal antibodies. **Chapter 4** investigates Anti-TIGIT biological activity, both binding to its main target and its effector functions were explored. The possible assays to be developed for the determination of the bioactivity of therapeutic monoclonal antibodies based on their mechanism of action are shown. Pros and cons of such assays depending on the drug clinical phase are also elucidated. **Chapter 5** investigates the strategies that could be applied for the assessment of monoclonal antibody predictive pharmacokinetics and how they have been optimized to include them in the antibody characterization panel. **Chapter 6** focuses on monoclonal antibody potential immunogenicity assessment using an *in silico* approach.

**Chapter 7** is dedicated to a summary and to comments on the overall obtained results. In **chapter 8** the conclusions of this thesis are reported. Furthermore, the prospects of the work are discussed, particularly the potential use and the advantages of the developed assays for therapeutic mAbs early characterization.

## **Abbreviations**

Ab = Antibody

ADC = Antibody Drug Conjugate

ADCC = Antibody-Dependent Cell Cytotoxicity

ADCP = Antibody-Dependent Cell Phagocytosis

Alpha = Amplified Luminescent Proximity Homogeneous Assay

AM = Assay Medium

CDC = Complement-Dependent Cytotoxicity

CM = Culture Medium

CQA = Critical Quality Attribute

ELISA = Enzyme Linked Immunosorbent Assay

EMA = European Medicines Agency

E-T ratio = Effector cells - Target cells ratio

FDA = Food and Drug Administration

GMP = Good Manufacturing Practices

GOF = Goodness of Fitting

ICH = International Council for Harmonisation of Technical Requirements for Pharmaceuticals for Human Use

Ig = Immunoglobulin

mAb = monoclonal antibody

MOA = Mechanism of action

NBE = New Biological Entity

ORL = Overall Risk Level

PK = Pharmacokinetics

PTM = Post Translational Modification

SPR = Surface Plasmon Resonance

TIGIT = T-cell immunoreceptor with Ig and ITIM domains

WCB = Working Cell Bank

## Contents

1	PROJECT OVERVIEW .....	9
2	GENERAL INTRODUCTION .....	10
2.1	MONOCLONAL ANTIBODIES and THERAPEUTIC FIELD .....	10
2.2	ANTIBODY GENERAL STRUCTURE .....	13
2.3	ANTIBODY CRITICAL QUALITY ATTRIBUTED and THEIR EVALUATION .....	15
2.4	BIOLOGICAL ACTIVITY and MECHANISMS of ACTION of THERAPEUTIC ANTIBODIES .....	20
2.5	BIOASSAY GENERAL OVERVIEW .....	23
2.6	BIOASSAY DEVELOPMENT and VALIDATION .....	27
2.7	PHARMACOKINETICS of THERAPEUTIC MONOCLONAL ANTIBODIES .....	38
2.8	PREDICTIVE PK METHOD QUALIFICATION .....	43
2.9	POTENTIAL IMMUNOGENICITY of BIOTHERAPEUTIC MONOCLONAL ANTIBODIES .....	43
2.10	CASE STUDY: ANTI-TIGIT THERAPEUTIC MONOCLONAL ANTIBODY .....	50
3	MATERIALS and METHODS .....	58
3.1	Anti-TIGIT antibody .....	58
3.2	Cell cultures .....	58
3.3	Bioassays for biological activity determination .....	60
3.5	Assays for predictive pharmacokinetic analysis .....	77
3.6	Software for potential immunogenicity prediction .....	89
4	DEVELOPMENT OF BIOASSAYS TO STUDY ANTI-TIGIT BIOLOGICAL ACTIVITY .....	90
4.1	Introduction and rationale .....	90
4.2	Anti-TIGIT Ligand Binding Assay .....	93
4.3	Anti-TIGIT Competitive ELISA Assay .....	121
4.4	TIGIT-CD155 Blockade Bioassay .....	128
4.5	Anti-TIGIT ADCC activity .....	133
4.6	Forced Degradation Study and Stability-indicating Bioassays .....	152
5	DEVELOPMENT OF BIOASSAYS TO STUDY ANTI-TIGIT PREDICTIVE PHARMACOKINETICS .....	165
5.1	Introduction and rationale .....	165
5.2	SPR PLATFORM .....	166
5.3	ALPHA TECHNOLOGY .....	183
6	POTENTIAL IMMUNOGENICITY <i>IN SILICO</i> ASSESSMENT .....	193
6.1	Introduction and rationale .....	193

6.2	<i>In silico</i> assessment .....	194
7	GENERAL DISCUSSION .....	197
8	CONCLUSIONS .....	205
9	REFERENCES .....	207



## 1 PROJECT OVERVIEW

The critical quality attributes of a given mAb, its molecular characterization, functional assessment and effector function analysis should be defined and profiled in detail during the life cycle of a biotherapeutic drug. Investing in selected sophisticated analytics in early developmental phases of a therapeutic monoclonal antibody may mitigate risks by confirming that the drug candidate has the required basic characteristics and functionality. Therefore, recognizing the added value of an early functional characterization of new biological entities (NBE) in the pharmaceutical industry, this work was focused on the development and qualification of *in silico* and *in vitro* methodologies defining the proper analytical characterization panel for a new therapeutic monoclonal antibody. The main goal of this work was to highlight and integrate the strategies applied in different pharmaceutical companies and extend the knowledge on the methodologies used for therapeutic monoclonal antibodies characterization and stability studies. In details, this PhD project was specifically designed to identify, develop and qualify with a stepwise approach *in silico* tools and *in vitro* assays aimed at studying the biological activity, predictive pharmacokinetics and potential immunogenicity of therapeutic drugs in early phase.

Moreover, since the structure of mAbs are extremely complicated and dynamic, a secondary goal of this work was to identify *in vitro* assays able to detect any chemical or physical degradation pathways that could impact drugs' bioactivity and PK. To this aim forced degradation studies, where the mAb underwent different stresses, were performed demonstrating the assays' suitability for the purpose. In addition, to ensure a good comparison and integration of the findings, several orthogonal assays were also developed, and the results compared demonstrating the equivalence of the methods. Some of the developed procedures were found in the literature but had to be modified and optimized to suit the various characteristics of the monoclonal antibody chosen as proof of concept molecule. Thus, overall, this project required a long time for assays optimization and to understand the complex nature of the selected monoclonal antibody.

## 2

## GENERAL INTRODUCTION

### 2.1

### MONOCLONAL ANTIBODIES and THERAPEUTIC FIELD

It has been more than three decades since the first monoclonal antibody was approved by the United States Food and Drug Administration (US FDA) in 1986, and during this time, the field of therapeutic monoclonal antibodies (mAbs) has dramatically evolved (Lu et al., 2020). Over the past five years, antibodies have become the best-selling drugs in the pharmaceutical market, and in 2018, eight of the top ten bestselling drugs worldwide were biologics. Therapeutic antibodies, including conventional mAbs, antibody-drug conjugate (ADC) and bispecific antibodies (bAbs), have become first line choice to treat diseases such as cancer, metabolic and inflammatory diseases. As a result, an increasing number of mAbs have obtained approval and entered clinical trials (Ecker et al., 2015, Wu et al., 2017). Compared to small molecule drugs, the advantages of these biotherapeutic drugs are mainly manifested through their prolonged half-life, low intrinsic toxicity and high target specificity and affinity to target molecule achieving high level of efficacy. Moreover, as stated in the work of Suzuki et al., modification and refinement by genetic engineering technology and the establishment of recombinant manufacturing technology has made therapeutic mAbs industrial manufacturing possible (Suzuki et al., 2015). As a consequence, mAbs have become a substantial part of many pharmaceutical company portfolios. The development process of mAbs for clinical use is complex, lasts years and requires careful interdisciplinary evaluations to ensure the pharmacology of both the mAb and the target antigen are well-understood. Because of the complex nature of these biotherapeutic drugs and their inherent heterogeneity, a mechanistic understanding of the mode of action along with careful attention to product design and manufacture are critical to assure an effective, consistent and safe product (Chirino A. and Mire-Sluis A., 2004; Weinberg et al., 2005). Indeed, patients receiving mAb-based therapy could fail to respond to the treatment, could develop drug resistance or an unwanted immune response against the drug itself, with the potential development of anti-drug antibodies (ADA). Protein products immunogenicity can impact its safety profile, dose exposure and efficacy. Mechanistic insight should form the basis of biological assays to be applied for monitoring efficacy, safety, lot to lot consistency and manufacturing changes starting from early development phase (Weinberg et al., 2005).

The majority of mAbs-based drugs have been established as one of the most successful therapeutic strategy for cancer.

Tumor-associated antigens recognized by therapeutic mAbs comprehends cluster of differentiation (CD) antigens such as CD20 (which is the target of Rituximab and Obinutuzumab) , glycoproteins

(e.g. EpCAM and Mucin), vascular targets (like VEGF targeted by Bevacizumab), growth factors (HER2 targeted by Trastuzumab, c-MET, ErbB1) and stromal and extracellular matrix antigens.

In addition to targeting antigens involved in cancer cell physiology, antibodies can also function to modulate immunological pathways that are critical to immune surveillance. Antigen-specific immune responses result from a complex dynamic interplay between antigen presenting cells, T lymphocytes, and target cells (Scott et al., 2012).

Indeed, cancer is multifactorial in nature and involve redundant or synergistic action of disease mediators, upregulation of different receptors and crosstalk between their signaling networks. Consequently, blockade of multiple, different pathological factors and pathways may result in improved therapeutic efficacy. This is the case of ipilimumab, an anti-CTLA4 mAb approved for the treatment of metastatic melanoma. The success of this mAb has recently drawn considerable interest in cancer immunotherapy opening the door to other immune-modulating antibodies.

The next most advanced products target PD-1, a marker of activated or exhausted T cells that can trigger apoptosis when bound by its ligand, PD-L1. Of note is that this ligand is found not only on antigen presenting cells, but also on many cancer cells. Both anti-PD-1 and anti-PDL1 therapeutic mAbs have been shown in early clinical trials to result in durable responses in patients with melanoma, renal cell carcinoma, non-small cell lung cancer, and colorectal cancer (Scott et al., 2012). Although immunotherapeutics targeting the inhibitory receptors (IR) CTLA-4, PD-1 or PD-L1 have made substantial clinical progress in cancer, a considerable proportion of patients remains unresponsive to treatment (Andrews et al., 2019) and this is why new mAbs targeting other IRs such as LAG-3, TIM-3 and TIGIT have arisen (Turnis et al., 2015).

Any drug development process must proceed through several stages in order to produce a product that is safe, efficacious, and has passed all regulatory requirements.

The selection of a target antigen is the first step of mAb development. The selection of this target requires extensive knowledge of biological processes involved in the specific disease pathology (Mould and Meibohm, 2016; Mohammed et al., 2019). Then, an appropriate development strategy needs to be designed in order to ascertain the mechanism of action, binding specificity, affinity, kinetics, and potency of the target antigen as well as potential isoforms of the antigen. At this stage, it is also important to see if the target antigen has functional redundancy in other systems to determine the drug effects of a mAb in clinical use. In addition, once a target is identified, appropriate engineering of the mAb can markedly improve its pharmacologic effect (Mould and Meibohm, 2016). After this step, drug candidates are finally tested for their interaction with the drug target. After careful review, one or more lead compounds are chosen. When the candidate molecule shows promise

as a therapeutic, it must undergo to critical quality attributes assessment and should be deeply characterized—the molecule’s size, structure, strengths and weaknesses, optimal conditions for maintaining function, toxicity, bioactivity, and bioavailability must be studied. Characterization studies will therefore undergo analytical method development and validation. These studies are crucial for the fate of the drug candidate and this is why pharmaceutical companies are now investing economical and operative efforts in this phase. Subsequent preclinical testing analyzes the bioactivity, safety, and efficacy of the formulated drug product. This testing is also critical for drug success and, as such, is scrutinized by many regulatory entities. Moreover, studies taking place during the preclinical stage are specifically designed to support the clinical studies that will follow. Indeed, the panel of assays that have been used for characterization purposes are also then used as monitoring strategy to ensure robust process performance over product’s life cycle. Considering the duration of the overall process, it is worthwhile and necessary for pharmaceutical companies to start early with mAb critical quality attributes assessment in order to be able to design the proper analytical panel of in vitro assays to speed up the drug development early phases and increase success rate.

## 2.2

## ANTIBODY GENERAL STRUCTURE

All approved therapeutic mAbs are of the immunoglobulin G class (Tabrizi et al., 2006; Lu et al., 2020). The basic structure of these class of antibody consists of four polypeptide chains, two identical light chains and two identical heavy chains. A cartoon representation is reported in Figure 1. As can be seen, each heavy chain is connected to the light chain through one disulfide bridge forming a heterodimer (H+L). The two heterodimers are joined by similar disulfide bridges to form the basic four chain (H+L)<sub>2</sub> antibody structure with an approximate molecular weight of 150kDa.

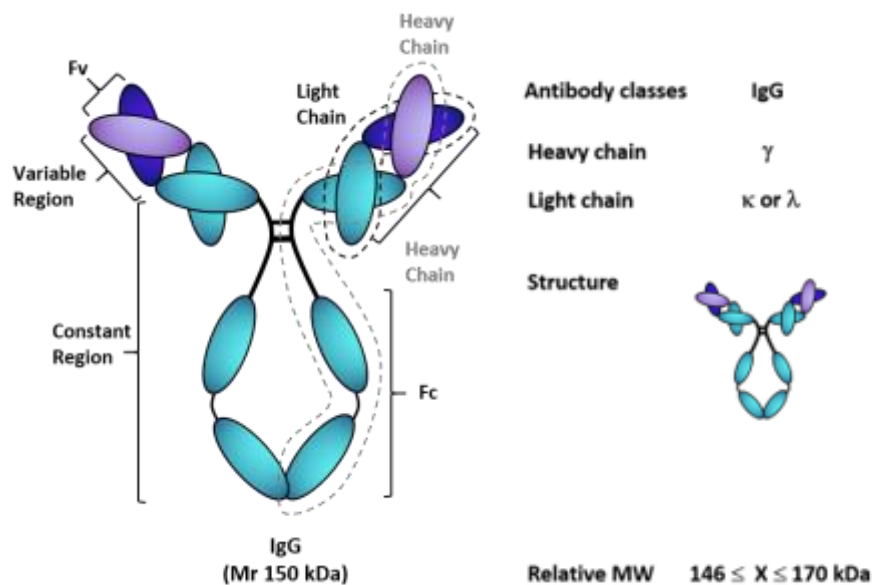


**Figure 1: Schematic representation of Antibody structure.** The constant region of the antibody is depicted in light blue. The variable regions (V regions) are colored in dark blue (VH, variable region of the heavy chain) and in purple (VL, variable region of the light chain). The region of the antibody corresponding to the heavy chain is surrounded by a grey dashed line while the region of the light chain is highlighted by a black dashed line. Modified from *Isabelle Topin – tebu-bio*.

The molecular weight of a light chain (L) is approximately 22 kDa while (H) molecular weight of a heavy chain is 55 kDa. The terminal regions of the two arms of the Y-molecule are called variable regions (V regions: VL for light chain and VH for heavy) and are responsible for the variety between different antibodies. Interestingly, most of the variety within the V regions is concentrated in distinct loop regions called complementary determining regions (CDRs). The three CDRs in each VL and VH constitute the antigen binding site of the antibody molecule, whereas the segments between the CDR regions within VL and VH show much less variation and are thus called framework (FR) regions for their role in maintaining the structure of the antibody molecule. The regions of rather conserved sequences beyond the variable regions are called constant regions: CL in light chain and CH in heavy

chain. The VL, VH, CL and CH1 domains together constitute the Fab (Fragment, antigen binding) portion of IgGs whereas CH2 and CH3 domains constitute the Fc portion (Fragment, crystallizable). While the Fab is responsible for antibody antigen specificity and affinity, the Fc portion contains oligosaccharides that can interact with other components of the immune system to activate effector functions and is responsible for the mAbs extended half-life and placental transport. The Fab and Fc portions of IgGs are linked through a highly flexible hinge region, which in turn covalently connects the two heavy chains through inter-chain disulfide bonds (Vidarsson et al., 2014). It is the hinge structure that confers many of the unique properties to each IgG subclass such as stability, flexibility and distances spanned by the two Fabs and the attendant Fc (Janeway et al., 2001).

These regions (hinge + upper CH2) are involved in binding to both IgG-Fc receptors (FcγR) and C1q. Therefore, as highlighted by Vidarsson et al., the four different IgG subclasses, IgG1, IgG2, IgG3, and IgG4, which are highly conserved, have different effector functions, both in terms of triggering FcγR-expressing cells, resulting in phagocytosis or antibody-dependent cell-mediated cytotoxicity, and activating complement. Typically, IgG1 and IgG3 are potent triggers of effector mechanisms, whereas IgG2 and IgG4 will induce more subtle responses, and only in certain cases (Vidarsson et al., 2014).

The major structural differences among IgG subclasses are shown in the figure below from Vidarsson et al.

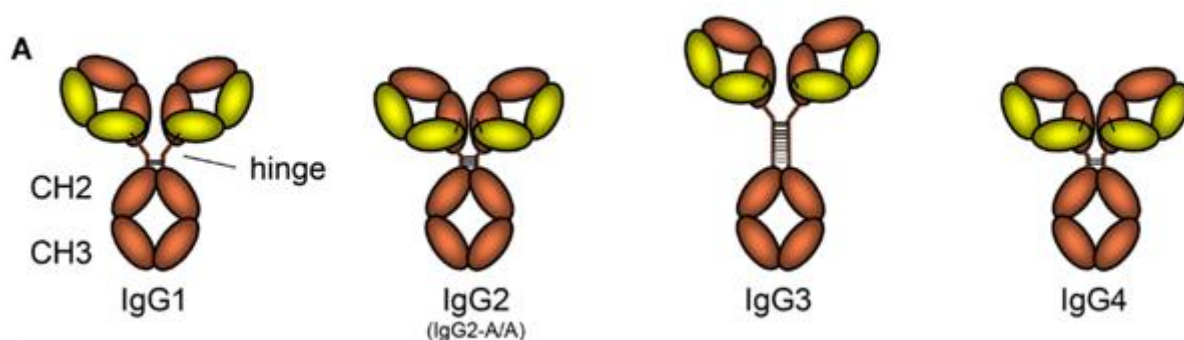


**Figure 2: The schematic layout of the IgG subclasses.** (A) The IgG subclasses, indicating how the different heavy and light chains are linked, the length of the hinge, and the number of disulfide bridges connecting the two heavy chains. The relative flexibility of the Fab arms with respect to the Fc differs between subclasses as follows: IgG3 > IgG1 > IgG4 > IgG2. For orientation, and comparison, the location of the hinge, CH2, and CH3 domains are shown.

Modified from Vidarsson et al., 2014.

In the current range of licensed antibodies, the majority are IgG1. This is likely due to IgG1 displaying potent effector functions, being the most predominant serum subclass, and was the backbone used in early approved Therapeutic Abs. IgG2 or IgG4 has been used when a lack of specific cellular activity is desirable. Interestingly, there are no approved IgG3 Ab, with suggestions that this may be because of (1) an increased likelihood for proteolysis due to an extensive hinge region (Carter, 2006), (2) the many IgG3 allotypes across populations, (3) IgG3 cannot be purified with protein A, or (4) the reduced serum half-life of IgG3 compared to other subclasses (Irani et al., 2015).

## **2.3 ANTIBODY CRITICAL QUALITY ATTRIBUTED and THEIR EVALUATION**

Biotech therapeutics, particularly complex products such as monoclonal antibodies (mAbs), can have numerous quality attributes that can potentially have an impact on bioactivity, pharmacokinetics (PK), safety and/or efficacy of the product. Critical quality attribute (CQA) has been defined as “a physical, chemical, biological, or microbiological property or characteristic that should be within an appropriate limit, range, or distribution to ensure the desired product quality” (ICH guideline Q8 (R2) on pharmaceutical development).

Identifying CQAs for a biotech therapeutic is the first and arguably the most difficult step in implementation of quality by design (QbD) for development and production of biopharmaceuticals. The ultimate objective is to establish linkages between specific product attributes of the biotherapeutic to the expected clinical performance (Reason et al., 2014).

Critical Quality attributes may well be product related, process related or composition/strength/stability CQAs also called obligatory CQA since they are typically specified by Health Authorities (Alt et al., 2016). In this work only product specific CQAs are taken into consideration.

Structural characterization is used to assess the characteristics of biopharmaceutical products. Moreover, the structural data must be supported by functional data to establish a structure-function relationship. In turn, these data can then be used to define the structural components' impact on the activity of the product. Furthermore, the characterization data obtained are essential for product development and regulatory acceptance.

Recombinant therapeutic proteins, including antibodies, contain several chemical and physical modifications. Great effort is expended during process and formulation development in controlling and minimizing this heterogeneity, which may not affect safety or efficacy and, therefore, may not have to be controlled (Goetze et al., 2010). Many of the chemical conversions also occur in vivo and

knowledge about the alterations can be applied to assessment of the potential impact on characteristics and the biological activity of therapeutic proteins.

Identification of CQAs is often performed through a series of product risk assessments conducted over the program lifecycle, the first of which should be performed early in development to bring clarity to the goals of the production process (Reason et al., 2014). Although the criticality of some attributes at this stage is still hypothetical, these “potential CQAs” (pCQAs) serve as both a baseline for development to proceed and a gap analysis to identify which attributes would benefit from further *in-vitro* or *in-vivo* studies to ascertain their true impact on efficacy and safety (Yingda et al., 2019; Rathore, 2009). In the table below a list of the CQA that are highly relevant to mAb developability assessment is reported (Table 1).

**Table 1: mAb quality attributes evaluated during developability assessment.** From Yinda Xu et al., 2019.

Attributes	Objectives and objectives
Primary structure and PTMs	Determine the primary structure and PTMs. The intended primary structure needs to be confirmed. PTMs may impact efficacy and safety
FcRn	Rank ordering mAb candidates based on their binding affinities. Higher binding affinity correlates with longer in vivo half-life
Thermal stability	Rank ordering mAb candidates based on their thermal stability. Higher thermal stability correlates with lower tendency of unfolding and aggregation
Solubility	Rank ordering mAb candidates based on their solubility. MABs with lower solubility pose challenges for process development, especially for high concentration formulation
Viscosity	Rank ordering mAb candidates based on their solubility. MABs with higher viscosity pose challenges for process development, especially for high concentration formulation
Hydrophobicity	Rank ordering mAb candidates based on their hydrophobicity. MABs with lower hydrophobicity correlate with lower tendency to aggregation, lower viscosity and higher solubility
Aggregation propensity	Rank ordering mAb candidates based on their aggregation propensity. Aggregates are the common product-related impurity potentially causing immunogenicity
Charge variants	Compare the charge profiles of mAb candidates. If no difference in safety and efficacy, it is desirable to select mAb with lower level of heterogeneity
Free thiols	Avoid mABs with abnormally high level of free thiols. A high level of free thiols correlates with lower thermal stability, increased tendency to form aggregates and potentially lower antigen binding affinity.
Protein-protein interactions	Rank ordering mAb candidates based on self- or unspecific interactions. Strong self-interaction correlates with higher aggregation propensity, lower solubility and higher viscosity. Strong non-specific interactions may cause shorter half-life.

As the molecule progresses through development and more is learned about the relationship between product attributes and their impact (or non-impact) on potency, pharmacokinetics (PK), safety and immunogenicity, these pCQAs can be further refined and accordingly designated as CQAs as the product approaches the licensure application (Reason et al., 2014). In accordance with the guideline ICH Q9, the identification of the CQAs is accomplished by using a risk-based analysis aimed at assessing the criticality of each quality attribute and consists in three consecutive steps: Severity assessment, Occurrence assessment and Detectability assessment. This approach considers the overall risk level (ORL), by combining the criticality of the quality attributes (severity), the capability of the process to keep a quality attribute under control (occurrence), and the capability of the in-process and final controls in detecting a deviation of a quality attribute (detectability).



$$\text{Overall risk} = f \left( \text{Severity}, \text{Occurrence}, \text{Detectability} \right)$$

The assessment of the ORL is iterative, is evolving during development, and should be revisited when new information becomes available such as the molecular design and known attributes of the molecule, based on prior and accumulated knowledge, published literature, and pharmacopeial requirements or after a comprehensive understanding of the molecular structure, including structure-function relationship studies and pharmacokinetics (PK) and pharmacodynamics (PD) studies in relevant models. A new assessment could be performed also after an analytical data collection (e.g., from characterization studies), a data collection from clinical and non-clinical studies that have been performed with the molecule or molecule variants, and with other relevant molecules and/or from other applicable published information and/or after comparability studies consecutive for example to a process change.

The output of the assessment of criticality of quality attributes is used during the development of the product for driving the development of the manufacturing process, building process knowledge and understanding, characterizing and validating the process, defining the Control Strategy, and finally demonstrating the comparability of pre- and post-change products. More in detail, the first step represents the evaluation of potential CQAs (pCQA) which links the expected quality profile to attributes potentially impacting biological activity, pharmacokinetics (PK), immunogenicity and safety. As defined in ICH guideline Q8 (R2), the quality target product profile (QTPP) forms the basis of design for the development of the product. It defines the intended use in clinical setting, the route of administration, the dosage form, the delivery systems, the dosage strength(s), the container closure system, the therapeutic moiety release or delivery and attributes affecting pharmacokinetic characteristics appropriate to the drug product dosage form being developed, as well as the drug product quality criteria (i.e., sterility, purity, stability and drug release) appropriate for the intended marketed product. In accordance with the guideline ICH Q9, the identification of the pCQAs is accomplished by using a systematic scientific- and risk-based analysis aimed at assessing the criticality of each quality attribute which may potentially be relevant for the new biological entities (NBEs) under development.

Attributes which, according to the QTPP, are not relevant for the mechanism of action, are excluded from the pCQA list and justified. All other attributes theoretically possible for the molecule and product under study, based on literature for products belonging to the same class (e.g., antibodies

produced in CHO cells) are listed and described, independent of their actual presence or absence in the molecule under study, thus providing an exhaustive list. Attributes are grouped whenever scientifically justified, considering the following different categories:

1. **Sequence variants:** The confirmation of the intended amino acid sequence is a prerequisite for further analysis and development of a mAb lead candidate (Yingda et al., 2019). These comprehend, for example, misincorporation (primary sequence variants), N-terminal heterogeneity and C-terminal heterogeneity. Several studies have shown the presence of low abundance sequence variants in bio therapeutic products that are likely caused by the naturally occurring low frequency errors during transcription and translation. Nevertheless, selection of mAb candidates and clones with minimal sequence variants is possible by extensive characterization through for example mass spectrometry (MS) (Yingda et al., 2019).
2. **Glycosylation-related variants:** This group of modifications are known to be involved with safety and efficacy issues. For example, as reported in literature, galactose- $\alpha$ 1,3-galactose ( $\alpha$ -gal) and N-glycolylneuraminic acid (NGNA) are immunogenic. These glycan structures could be produced by non-human mammalian cell lines like Chinese Hamster Ovary (CHO) cells that are usually the preferred expression system when structural complexity, mammalian-type glycosylation, and other post-translational modifications are considered critical for the recombinant protein's activity or stability. Even neither  $\alpha$ -gal neither NGNA have effect on the therapeutic protein's activity, pre-existing antibodies that are cross-reactive with these non-human glycans have been detected in humans increasing the risk of allergenicity (Chamberlain P. and Rup B., 2020). Moreover, high mannose has been shown to cause shorter in vivo half-life and enhanced antibody-dependent cell-mediated cytotoxicity (ADCC) due to the lack of core-fucose (Yu et al., 2012). Additionally, the afucosylation level must be monitored because of its correlation with enhanced ADCC which could be either beneficial or harmful depending on the mAb's mechanism of action (MOA) (Shields et al., 2002; Jiang et al., 2011; Yingda et al., 2019).
3. **Other variants and post-translational modifications (PTMs):** including, for instance, oxidation, deamidation, glycation. This group of modifications are also known to be linked with safety and efficacy issues.
4. **Aggregates that could lead to the formation of high molecular weights:** Aggregates are the most commonly observed product-related impurities, requiring close monitoring due to immunogenicity concerns (Rosenberg, 2006; Singh et al., 2010). Therefore, it is a critical component of developability assessment. In addition to utilizing predictive tools, aggregation

propensity should be directly measured during extended characterization and forced degradation studies (Yingda et al., 2019).

5. **Fragments or low molecular weights:** This group of modifications could be generated in relations to the cell lines and cell culture parameters such as temperature, pH, media composition and formulation. In literature it is not reported an effect on products activity, but they could be potentially involved in immunogenicity because these modifications are not present in either human endogenous IgG or degradation products.
6. **CQAs expressing biological function:** including, but not limited to, potency and binding affinities. These attributes represent a measure of biological functions, which in turn will depend on the impact of other CQAs. Therefore, they could be seen as biological properties describing the cumulative effect of physico-chemical variants, thus considered as CQA for elaboration of an appropriate analytical testing strategy (characterization or control).
7. **Formulation-related attributes:** in relation to formulation components.
8. **Obligatory CQAs** (in relation to compendial requirement or Regulatory expectations, recognized as necessary to ensure patient safety or product identification): including, for instance, pH, osmolality, identity, strength, extractable volume, degree of coloration, appearance, visible and subvisible particles, sterility and adventitious agents.
9. **Process related impurities:** they are considered in a separate category despite being also mandatory, since these need to be evaluated through different types of studies (i.e., clearance studies); they can be subdivided into two categories, such as:
  - a. a first category including host cell-derived and bioactive substances (for instance, host cell DNA, host cell protein, or residual Protein A from chromatography resins used in the purification process);
  - b. a second category including non-bioactive components which may pose a potential safety risk.

Accumulated knowledge on the mAb, studies with related molecules, general (platform) antibody understanding, published literature, in silico evaluation, and pharmacopeial requirements should be used to complete the assessment and build related justifications. The pCQAs needs to be then subjected to the subsequent steps (step 2, occurrence; step 3, detectability) of the CQA risk assessment exercise, to identify final CQAs and to support definition of an appropriate analytical panel for the preliminary Control Strategy.

The second step (step 2) analyses the actual presence of the attribute, to assess relevance for the molecule under study, and the capability of the process to keep a quality attribute under control which, although not used to establish criticality, provides indications for the Preliminary Hazard Risk Level (PHRL) useful for the definition of the testing strategy.

These steps are then followed by a third step (step 3), which evaluates the capability of the analytical panel to capture a significant variation of CQAs, thus defining the overall risk level (ORL).

Finally, the capability of the analytical methods implemented at the time of the risk assessment to detect a deviation of a CQA is assessed. The Overall Risk Level (ORL) is calculated by multiplying the preliminary hazard risk level (PHRL) by the Detection (D) score:

$$\text{ORL} = \text{PHRL} \times \text{D}$$

The ORL provides the level of risk that a CQA deviates because of a lack of process capability, combined with the capability of the analytical panel to detect it. The ORL is also helpful for identifying the need for developing / implementing additional or improved analytical method to be included in the CS.

The overall result of the risk assessment for the therapeutic mAb will reflect the current knowledge and will be subjected to subsequent iterative revision and re-evaluation as process and product knowledge evolves or increases through additional manufacturing experience.

## **2.4 BIOLOGICAL ACTIVITY and MECHANISMS of ACTION of THERAPEUTIC ANTIBODIES**

Biological activity is an important quality attribute for mAb-based biologics and should be appropriately assessed. As shown before, the antibody molecule has two distinct tasks. The Fab portion of mAbs is important for antibody-antigen interactions while the Fc portion is crucial for defining the antibody effector functions and pharmacokinetic properties of IgG molecules (Jefferis, 2007). The Fc region of the antibody is involved in modulating immune response through the binding of specific proteins, such as Fc receptors (FcγRIIIa) as well as complement proteins like C1q, the first component of the complement cascade. Thus, the Fc region of mAbs is the most important region for ADCC, complement-dependent cytotoxicity (CDC), and antibody-dependent cellular phagocytosis (ADCP). In contrast, the antigen-binding region binds to a wide array of antigens defining mAbs

specificity. Biotherapeutic antibodies can have multiple and complex MOA, in the figure 3 the most common ones are summarized (Suzuki et al., 2015).

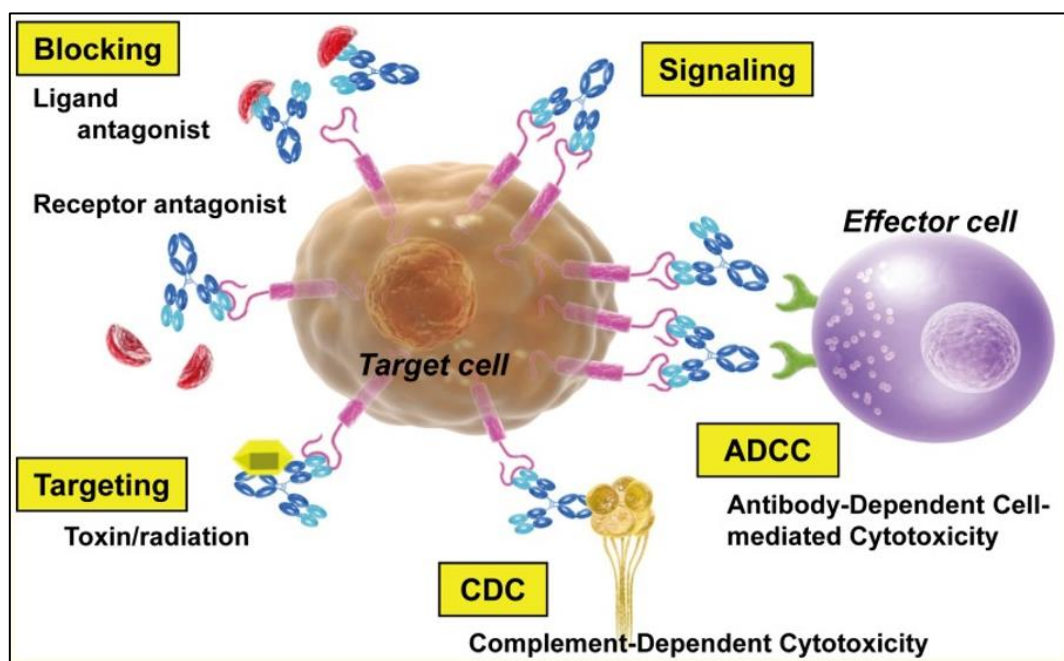


**Figure 3: Mechanisms of action of therapeutic antibodies.** The efficacy of therapeutic antibodies comes from various natural direct functions of antibodies such as neutralization, ADCC or CDC activity or indirect functions when the mAb is used as a drug delivery carrier. Adapted from Suzuki et al. (2015).

The biological activity of antibodies and their derivatives is achieved by various means. They can have direct effects by binding for example with cell surface receptors or they can have indirect effects through the conjugation to drugs, toxins, radioisotopes, or cytokines permitting the specialized delivery of therapeutic or diagnostic agents (Redman et al., 2015; Borghaei et al., 2006).

The most obvious mode of action is the binding of the antibody to its antigen, thereby interfering with its activity and interaction with binding partners (also called “neutralization”) (Chames et al., 2009). When the signaling in the tumor through these ligands or receptors is reduced, it can result in cellular activity being lost, proliferation being inhibited, pro-apoptotic programs being activated, or cells being re-sensitized to cytotoxic agents (Cavallo et al., 2007). The antigen could be a soluble ligand, or a receptor displayed at the cell surface. Infliximab, adalimumab and certolizumab (all anti-  $\text{TNF}\alpha$ ), bevacizumab (anti-vascular endothelial growth factor) and avelumab (anti PD-L1) are classical examples of antigens belonging to the first category while trastuzumab (anti-HER2) and abrituzumab (anti integrin alpha-V (ITGAV) ) are directed against membrane receptors.

Direct effects of antibodies on cell proliferation and apoptosis are generally tested in vitro using cell lines exposed to the antibody for 24–96 hours. Proliferation could be measured by standard techniques including absolute live cell count (in Bürker chambers or by flow cytometry using calibration beads), <sup>3</sup>H-thymidine or BUdR uptake, in some cases clonogenic assays, or CFSE staining and flow cytometry analysis at different times. Cell death can be assayed by a variety of techniques such as MTT, WSP1, alamar blue, or similar intracellular enzyme-based assays, which basically measure the number of live cells in a treated sample compared to control. Interestingly, in the last twenty years, several methods have been developed for the generation of bispecific antibodies that have the ability to bind two distinct antigens. These products are interesting candidates for cancer therapy because of their unique biological properties including increased specificity, high target selectivity and prolonged half-life. The main antigens that have been used as targets for bispecific antibodies are overexpressed by tumor cells, such as EGFR (Epidermal growth factor receptor), HER2 (Human epidermal growth factor receptor 2), CD19, CD20, EpCAM (epithelial cell adhesion molecule), MUC-1 (mucin 1, cell surface associated) and CEA (Carcino-Embryonic Antigen) (Zafir-Lavie et al., 2007).

As mentioned before, antibodies can be also applied as drug delivery carriers when conjugated to radioisotopes, toxins, drugs or cytokines (Zafir-Lavie et al., 2007). The advantage of these conjugates over conventional drugs is that cytotoxic agents can be delivered directly and at higher local concentrations to tumor tissues, without damaging healthy cells. Antibodies conjugated to drugs (ADCs) or toxins are specifically designed to induce either a block in proliferation or direct cell death (usually through apoptosis). Examples of drugs that have been successfully linked to antibodies include: (1) calicheamicin and duocarmycins which bind to the DNA minor groove, induce double strand breaks and induce apoptosis at low doses (e.g. gentuzumab ozogamicin, CD22-calicheamicin); (2) monomethyl auristatin E (MMAE) and maytansine derivatives such as emtansine (DM1) and DM4, all of which are anti-tubulin agents (e.g. brentuximab vedotin, trastuzumab-DM1), and (3) toxin fragments such as pseudomonas exotoxin fragments PE38 (e.g. monetumomab pasutodox, a CD22-PE38) (Golay and Introna, 2012).

Moreover, antibodies could bind and/or cross-link to target molecules and thus stimulate several signal pathways are also under research. However, these agonistic antibodies have not been placed on the market at this point (Suzuki et al., 2016).

In addition to the biological activity provided through the variable region by directly binding to the specific antigen, some antibodies have a mechanism of action that is indirectly mediated through the Fc region of the antibody (the so-called antibody “effector functions”).

ADCC is the antibody induced lysis of a target cell by an activated effector cell. To trigger ADCC, the antibody binds to a specific antigen expressed on the surface of a target cell. Immune-effector cells (such as macrophages and NK cells) that express receptors able to bind to the Fc, are then recruited activating the immune-effector cells to lyse the target cell (Zafir-Lavie et al., 2007). ADCC induction can be analyzed by employing effector cells from different sources, such as peripheral blood mononuclear cells (PBMC) and genetically modified cell lines (e.g., transfected NKs or Jurkat cells), and different approaches can be used for detection and results interpretation depending on the type of effector cells used. A deeper discussion on ADCC mechanism and in vitro assays to assess this mAbs’ activity are reported in the results section of this work.

CDC instead is triggered when the C1 complex, which is comprised of three different proteins, binds the antibody–antigen complex, activates a cascade of complement proteins, and causes a complex to form that attacks the membrane. This results in lysis of the target cell (Suzuki M., Kato C., Kato A., 2016). CDC has been proposed to be an important mechanism of action of several unconjugated therapeutic antibodies, such as rituximab (an anti-CD20) and alemtuzumab (anti-CD52).

Both ADCC and CDC are interactions that involve components of the host immune system and, among the therapeutic antibodies being developed for cancer, there are presumably products that utilize more than one mechanism (ADCC, CDC, and neutralizing functions) in their pharmacological actions.

## **2.5 BIOASSAY GENERAL OVERVIEW**

In pharmaceutical and biotech companies, to measure and monitor product attributes and ensure their identity, purity, strength (potency) and stability, biological and physical-chemical analytical tests are routinely used (from Food and Drug Administration guidance).

The critical quality attributes of mAbs, such as its structure, post-translational modifications, and its functions at biomolecular and cellular levels, need to be defined and profiled in details starting from the developmental phases of a biological drug. Particularly, as Wang stated in his work, structural characterization, functional assessment, and effector functions analysis of mAbs, are reviewed with respect to the critical parameters and the methods used for obtaining them (Wang et al., 2018).

Indeed, success in the clinic begins with the identification, characterization and validation of a comprehensive panel of in vitro assays. The proper combination of in vitro assays can deliver critical information from different perspectives that serves as better predictors for the transition to in vivo studies, the market and the post-licensure life cycle management.

In the end, the establishment of an efficient platform for products 'analysis is critical to guarantee quality and consistency of mAbs production.

Here, the attention is focused on two essential aspects of the analytical package for mAb-based drugs highlighted in the figure 4: functional analysis that includes mAbs potency (equilibrium dissociation constants, binding activity, and biological potency) and effector functions.

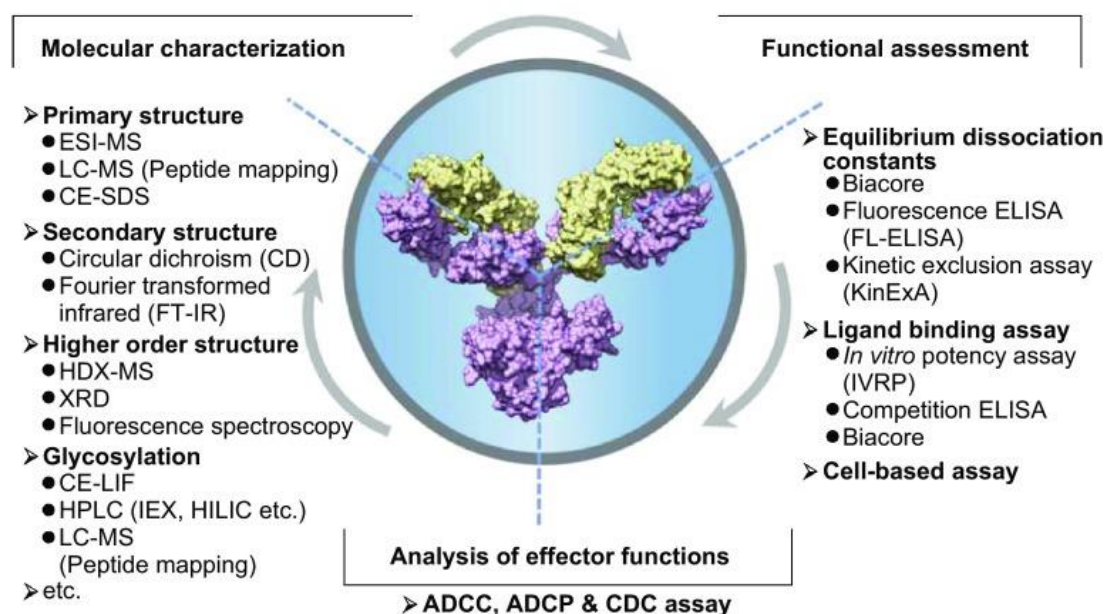


**Figure 4: Overview of the methods of molecular structural analysis and functional assessment.** As a complex macro-molecule protein, the molecular characteristics and functions are critical quality attributes for monoclonal antibodies. A series of physicochemical and biological methods should be developed to evaluate these critical quality attributes carefully. In addition to the general molecular characterization (on the left panel), particular attention should be given to the biological function-associated analyses that are listed in the right panel and bottom panel. In the figure as an example of a monoclonal antibody an IgG1 is represented (PDB: 1IGY). From Wang et al. (2018).

Function is a critical attribute for mAb-based biologics. The methods applied for functional studies could be cell-based and/or non-cell-based or can involve in vivo animal studies or any combination of these (from Food and Drug Administration guidance). However, in vitro assays are usually preferred to the in vivo ones for early phase drugs, since they are easier to implement, show higher



reproducibility and applicability, they have minor ethical impacts and are of course less expensive. Function of mAbs could be assessed through different tools analyzing biotherapeutic drug's ligand binding ability, its cells-based functions and affinity constant.

Antibody-antigen (Ab-Ag) interaction is critical for the function of mAbs. As a key parameter of Ab-Ag interaction, the equilibrium dissociation constant ( $K_D$ ) can be used to predict the interaction status under certain conditions (Wang et al., 2018). SPR-based technology, AlpaScreen technology, fluorescence ELISA (FL-ELISA), and kinetic exclusion assays (KinExA) are commonly used to determine the  $K_D$  value even if based on different mechanisms. A detailed description of these technologies is reported in the following chapters.

The *in vitro* binding activity is used as a surrogate method to analyze mAb candidates, so ligand-binding assay (*in vitro* potency assay) are particularly useful during early development phase. ELISA and surface plasmon resonance (SPR)-based technology are two most popular methods for ligand-binding analysis. Different forms of ELISA and SPR-based assays can be used to evaluate the binding ability of mAbs. Here, a stable and soluble antigen is needed to represent the *in vivo* target of mAbs. With regards to ELISA, the final result is  $EC_{50}$  value that is the effective concentration needed for 50% of maximal binding. With the use of a reference standard, the ratio of  $EC_{50}$  values can be obtained by dividing the  $EC_{50}$  value of the standard and the  $EC_{50}$  value of test mAb. This value indicates the binding activity of the test mAb compared to that of the standard (Wang et al., 2018). In summary, if the mechanism of action of therapeutic mAbs is expected to be binding activity to a specific ligand, the binding assay can be used as lot release assay along with the cell-based assay during clinical development phases. Upon the product licensure, these ligand binding assays could be substituted with assays more representative of the mode of action (MOA) of the drug such as cell-based assays. Indeed, even though the ligand-binding assay can be performed readily with desirable precision and accuracy, the mechanism of action could involve downstream events post ligand-binding. Thus, the sole measure of the binding activity may not reflect the mAb potency in a faithful manner having implications also from a regulatory perspective (Wang et al., 2018).

Biological assays can also measure potency of bio therapeutic mAbs by evaluating the activity of a product's active ingredient(s) within a living biological system (Cell-based assays). Potency tests are performed as part of product conformance testing, comparability studies and stability testing. Similarly, potency measurements are used to demonstrate that only product lots that meet defined specifications or acceptance criteria are administered during all phases of clinical investigation and

following market approval (from Food and Drug Administration guidance). Companies are continuously challenged with developing assays that are functionally relevant while reflecting the complex MOA of drugs. Functional cell-based assay could better reflect the mechanism of action of a therapeutic mAb than a ligand binding assay. Moreover, compared to binding assay, cell-based bioassay could better detect the impact of chemical modifications, such as deamidation, oxidation and other stresses on both drugs' structure and activity. Therefore, during clinical development of mAb-based drugs and post licensure life-cycle management, cell-based assays represent the best choice for both product characterization and stability studies. Indeed, potency determination, is necessary for regulatory submission and lot release of all biopharmaceutical products and this is why bioassays are central and critical for product development and manufacturing. An understanding of the MOA and receptor interactions of a mAb is important for considering the strategy for biological activity assessment in both the characterization study and the stability study. For example, as reported by Wang et al., mAbs with different targets generally induce an early response (signaling pathway) or a late response (proliferation, cytokines) and so the "simple" evaluation of the binding to a target would not be completely representative of the *in vivo* situation. A downstream marker (early response, late response or cell adhesion, etc.) that is normally inhibited with the use of the mAb should be defined. For example, to evaluate the potency of a vascular endothelial growth factor (VEGF)-specific antibody (such as bevacizumab), knowing that VEGF targets VEGF receptor-2 (VEGFR-2) and subsequently activates calcineurin-nuclear factor of activated T cell (NFAT) signaling, a reporter gene assay (using engineered NFAT-RE-luc2P/KDR HEK293 cell line) was developed. Moreover, many therapeutic antibodies recognize cell surface receptors or transmembrane ligands, such as rituximab which targets CD20 or avelumab that target PD-L1. Therefore, based on the different MOA, several types of cell-based assays for potency determination are presented in the literature: cell proliferation/cell death assays where cell proliferation or cell death induced by the biopharmaceutical product can be quantitatively measured; reporter gene assays, where the tested molecule could trigger a series of events leading to the expression of a detectable reporter gene (Debnath et al., 2010); cell-signaling assays, where the drug activates or inhibit a signaling cascade that results in a specific therapeutic effect (e.g. an increase or a decrease in certain signaling molecules); cell-based ligand binding assay where the specific binding of the mAb to its target is measured (Hunter and Cochran, 2016). As highlighted in this chapter section 2.2, while the Fab fragment is mainly associated with binding specificity, the Fc portion is critical for the function of IgG at the cell level and for its metabolic fate. For candidate molecules, complement activation and other effector functions are important, and should be well-evaluated during development. These effector functions include

ADCC, CDC, and ADCP. Assays for measuring Fc functions can be technically demanding. Both the difference of assay formats and of cell combinations have significant impact on the sensitivities of this type of assays. New and old antibodies are most commonly assessed in vitro using standard ADCC assays, that is by loading target cells with  $^{51}\text{Chromium}$  ( $^{51}\text{Cr}$ ) or membrane permeable acetoxymethyl ester fluorescence dyes, such as calcein-AM or DELFIA-BATDA. Labelled targets are then incubated with antibody and purified NK cells or peripheral blood mononuclear cells as effector cells, at various effector to target (E:T) ratios, usually for 4 hours. At the end of the incubation, the released radioisotope or fluorescent dye is then measured in a suitable instrument, with or without enhancing solutions. Although the use of primary cells may provide a more physiologically relevant model, the criteria of low assay variability and robustness may not be satisfied (Parekh et al., 2012). Continuous cell lines may overcome these limitations. However, identifying or producing a suitable cell line can be difficult and arduous. Furthermore, the clinical relevance of data generated by engineered/artificial cell lines may also be challenged because of the use of a homogenous cell population over-expressing the targets/receptors. A solution could be the use of different assay formats and cell combinations in order to obtain results that are more relevant to the physiological/pathophysiological conditions in patients (Parekh et al., 2012). In the CDC assay instead, baby rabbit complement is used in replacement of NK cells (Duensing and Watson, 2018). For the ADCP assay, macrophage and target cells are labeled with different dyes, and when the test antibody is added, the ADCP is detected with the use of flow cytometry-based techniques (Wang et al., 2018). Although these biological assays are mainly used in house for characterization or for demonstrating similarity and are not as robust as release assays, they should anyhow be qualified for the intended use and should be sufficiently sensitive.

In the end it is evident that a detailed analysis of the biological activity of the mAb, demonstrating the MOA (including Fab-and/or Fc-mediated functions), ability to bind to Fc gamma and neonatal Fc receptors, as well as to complement C1q should be provided starting from the early phase of product development.

## **2.6 BIOASSAY DEVELOPMENT and VALIDATION**

In the pharmaceutical community, risks associated to safety of human and animal health care products are addressed by guidelines and regulations covering not only the development, production and testing of these products, but including also procedures related to the use of analytical methods. Assay development and validation are indeed an integral part of the underlying quality system (Ederveen,

2010). The importance assigned to them, especially to the validation study, is reinforced by the presence of several regulatory and guidance documents covering this subject describing the fundamental principles, boundaries and specifications that are important in producing accurate and reproducible results during the manufacturing and testing of medicines (Ederveen, 2010).

Validation is a fundamental feature in any analytical method to be applied for GMP purposes since it is closely related to the quality and reliability of the produced results. A method of analysis is characterized by its performance parameters that must be in accordance with previously defined requirements that the method of analysis should satisfy. Above all, the performance parameters depend on the type of method and its intrinsic characteristics (Songara and Prakashkumar, 2010).

Moreover, good manufacturing practice (GMP) requires that test methods used for assessing compliance of pharmaceutical products with quality requirements should meet appropriate standards for accuracy and reliability as stated by official agencies and professional bodies like the Food and Drug Administration (FDA), the European Medicines Agency (EMA), and the International Committee on Harmonisation (ICH).

Assay validation could therefore be defined as “the process of demonstrating and documenting that the performance characteristics of the procedure and its underlying method meet the requirements for the intended application and that the assay is thereby suitable for its intended use” (USP 1033).

According to international guidelines, the validation of bioanalytical methods can be performed following a clinical phase-specific approach. However, validation parameters should always include relative accuracy, specificity, intermediate precision and linearity and range while the robustness study could be performed during development phase or in a later phase. Independently from the clinical phase, assessment of bioassay performance should be a continuous process and should be guided by a validation protocol describing the goals and design of the validation study.

Critical steps in the overall life cycle of a “fit-for-purpose assay” comprehend method selection, feasibility, development, suitability testing, performance characterization, performance verification, documentation, maintenance and improvement (Songara and Prakashkumar, 2010).

A schematic representation of these steps is graphed in the following figure (Figure 5).

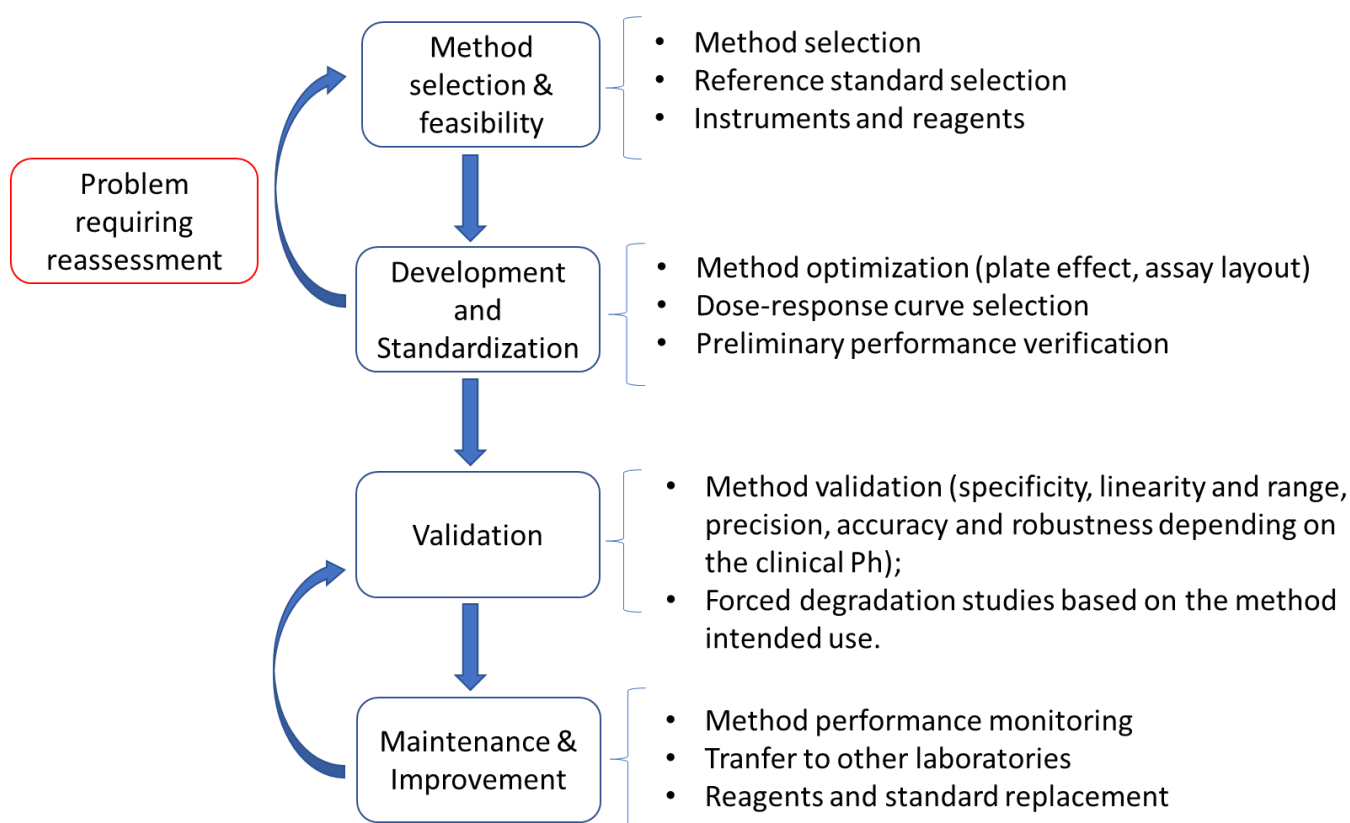


**Figure 5: Bioassay life cycle management.** The main stages of method validation are summarized in a flow chart: method selection and feasibility assessment are followed by assay development and standardization. If something during this stage needs to be reoptimized or did not met the requirements, the method feasibility should be reassessed. After method standardization, the validation study begins. During its routine usage the performance of the procedure are continuously monitored and if necessary improved. If a critical reagent or a reference standard need to be replaced (i.e. for a reagent stock-out) then the method should be revalidated. Modified from Ederveen (2010).

During method selection and feasibility, the gathering of the drug's background information is the first step. All the information of literature connected with the drug is reviewed for biological and structural properties and appropriate analytical methods with reference to relevant books, journals, health authorities' guidelines and other publications. As previously discussed, cell-based bioassays are inherently complex and variable. To control for this variability, a methodical, stepwise approach is used to design and select the assay type that best reflects the MOA(s) of the therapeutic (White et al., 2019).

Indeed, the choice of the method is related to the purpose and the required output of the experiment and the MOA of the drug candidate and is therefore an important aspect of the overall validation

process. Other factors can influence the suitability of a method as well. Clear examples of such factors are logistical and operational limitations like running costs, equipment availability, reagent availability, and biosecurity (Ederveen, 2010).

In the feasibility phase the required resources and the assay format are investigated and selected. The fitting for the purpose of the assay is also evaluated. Materials like antibodies, primers, cell banks and reagents are selected. Reference materials are obtained, aliquoted and certified.

At this stage for cell-based assays it is fundamental the selection of the cell line to be used since the choice of cell type, cell handling and bioassay design could influence bioassay performance (White et al., 2019). Primary cells typically isolated from human blood or tissue, immortalized cell lines of human or nonhuman origin or ready to use cells modified to overexpress the receptor or ligand that is targeted by the therapeutic, could be used.

Whenever is possible, the use of primary cells should be avoided due to donor-to-donor variability and costs. However, primary cells may be required when the MOA of the therapeutic agent is complex or multiple receptors are involved and a transfected cell line cannot fully represent all interactions (White et al., 2019).

When cells are cultured, it is important to monitor morphology, magnitude of response, doubling time and cell viability, among other parameters. Cell culture and assay performance should be controlled over time and a limit established for the allowable number of cell passages (working window), before routinely starting a new culture (White et al., 2019). For this reason, at industry level when an immortal cell line is selected and its feasibility is evaluated for a particular bioassay, a working cell bank (WCB) is prepared and used to ensure the reproducibility of the assay response over time. Once the working cell bank is going to stock out a new WCB will be prepared and qualified for that specific assay.

Method feasibility assessment is followed by assay development and standardization.

A method should be developed with the goal to rapidly test preclinical samples, formulation prototypes, and commercial samples (Sharma et al., 2018). An operator should always keep in mind that a well-developed assay is easy to validate.

Experiments are conducted to find the optimal conditions for parameters like bioassay incubation time and temperature, equipment settings, reagents, etc. While performing optimization, one parameter is changed at a time and a set of conditions are isolated, before utilizing trial and error approach (Sabir et al., 2015). The method robustness will be then further checked in the forthcoming validation study. In this stage, the proper dose-response curve of the mAb reference material is identified. Bioassays usually present a nonlinear relationship between the response and the analyte

such as log-concentration with a sigmoidal shape (White et al., 2019). The model commonly used for curve-fitting analysis of symmetric sigmoidal curves is the 4-Parameter Logistic (4-PL) regression model described by the following equation:

$$Y = \frac{(A-D)}{\left(1+\left(\frac{x}{C}\right)^B\right)} + D$$

Where Y is the response, A is the minimum value that can be obtained (response at zero analyte concentration or bottom/lower asymptote of the reference material dose-response curve), D is the maximum value that can be obtained (response at infinite analyte concentration or top/upper asymptote of the reference material dose-response curve), C is the inflection point (also known as EC50 that corresponds to the point where “Y = (A + D)/2”), B is the Hill slope that defines the steepness of the curve at point C and x is the analyte concentration (White et al., 2019). A 4-PL function requires a sufficient number of concentrations or dilutions to fit the model and several guidelines recommend a minimum of eight concentration points to define a 4-PL curve. At least two concentration points are commonly used to define each asymptote (parameters A and D) and at least three concentration points in the linear part of the curve as shown in the representative dose-response curve below (Figure 6).

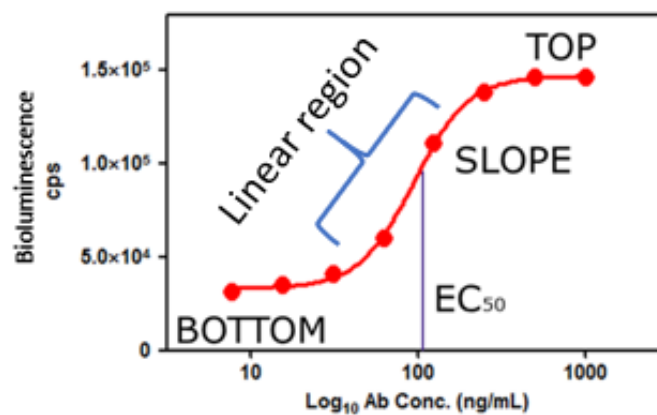


**Figure 6:** A representative example of a bioassay dose-response curve. On the Y axis is reported the observable response (bioluminescence measured in count per second (cps)) while in the X axis is reported the Log<sub>10</sub> of the antibody concentration. When the relation between drug dose (X-axis) and drug response (Y-axis) is plotted

on a linear scale, the resulting curve is usually hyperbolic. If the drug dose is plotted on a base 10 logarithmic scale, this produces a sigmoidal dose-response curve. This representation is more useful because it expands the dose scale in the region where drug response is changing rapidly and compresses the scale at higher doses where large changes have little effect on response.

The ‘linear’ region of a 4-PL function, highlighted with the blue parenthesis in the figure 6, is often defined as the range of concentrations where assay’s output is directly proportional to the concentration of the test sample (White et al., 2019). The validity of a given mathematical model as a descriptor of the concentration–response relationship should be firstly assessed during the development phase as suggested in the work of John R White and colleagues. To achieve this, analysis of the residuals (meaning the differences between the observed response and the response predicted by the fitted model at a given concentration) is recommended. If the model is appropriate, residuals would be randomly and independently distributed around zero. For a further description on residuals ‘analysis the reader should refers to the section on the validation parameters evaluation. When a curve is not symmetric around its inflection point instead, evaluation of an alternative model may be necessary, and typically a 5-PL model will produce a better fit for asymmetric curves. Once the proper mAb dose response curve is designed, the plate layout and plate effect should be evaluated. 96-well plates format is usually used for the set-up of both binding assays and cell-based bioassays. This format helps to facilitate and speed up bioassay’s execution allowing the possibility for the operator to use multichannel pipettes to prepare or add dilutions and reagents and to use plate washers and plate readers. Microtiter plate assays have multiple potential sources of variability that can affect bioassay performance and thus impact the accuracy of results. The most common comprehend variations in cell plating and cell growth rate, inconsistent cell response, biased results due to the location of the sample in assay plates, order of addition of standard, control sample(s), test samples and critical reagents, analyst-to-analyst, plate-to-plate and run-to-run variability (White et al., 2019). Among these variables, the microtiter plate is for sure a dominant contributing source of location-based error and thus should be assessed early in method development phase. Indeed, standard 96-well microplate assays are prone to edge and bowl effects and such plate location effects can badly bias potency estimates. One of the most common plate-related bias is for example the so-called ‘edge effect’, where the response from peripheral wells differs from the response observed in the inner wells of a microtiter plate.

To minimize location effects, several approaches have been applied and reported in the literature. The most common practices include: 1) the use of techniques that help minimize the edge effect such as



the use of plate hotels; 2) the inclusion of replicates (wells or plates); 3) careful consideration on the placement of standard, control, and test samples in the plate (plate layout); 4) the use of randomization or pseudo-randomization (row or column); 5) exclusion of outer rows and/or columns; 6) use of automation (White et al., 2019). An integral part of bioassay development is the assessment of plate layout to identify possible positional issues. Experimentally it can be evaluated by testing throughout the plate the reference material full dose–response curve loaded into columns 1–12 or rows A–H of multiple plates, depending on the bioassay design. Then all full-dose response curves are compared in terms of EC50, R2, Top, Bottom and Hill Slope values. If no ‘edge effect’ is observed, all wells of the microtiter plate may be used. If an edge effect is highlighted, this bias may be addressed by utilizing only the inner-80 or inner-60 wells of the plate. In this case, it is important to note that the use of only a portion of the assay plate significantly decreases sample throughput. An alternative or complementary approach is represented by randomization, pseudo-randomization, replication and plate design that can be used to minimize plate location and plate-to-plate bias.

Within the plate, plate effects could be also mitigated by ensuring that test and reference samples have equal exposure to the edges. The choice of the number of replicates may vary based on the application and variability of the bioassay (release, stability, comparability or characterization), and the expected throughput and precision needed (White et al., 2019). Usually, within a plate, at least two replicates per dose level are employed.

Preliminary performance verification, including linearity and range, detection limits and accuracy and precision of the assay, is finally checked. Moreover, at this stage, it is also possible to start testing stressed samples in order to verify the ability of the system to detect changes in the biological activity of the drug demonstrating its stability indicating properties. Once the method has been developed the following step is assay validation.

Method validation is the process used to confirm that the analytical procedure employed for a specific test is suitable for its intended use. Results from method validation can be used to judge the quality, reliability and consistency of analytical results; it is an integral part of any good analytical practice (Sharma et al., 2018). Indeed, as an example, if a bioassay in this phase is demonstrated to be too variable or not amenable for a quality control environment, it may be advisable to move that bioassay to the characterization panel.

Therefore, all measurements susceptible to variations in analytical conditions should be suitably controlled. An assay is considered valid and may only be used to generate data of an unknown sample if the criteria for the specific assay run are met (the so-called System suitability criteria). The verification process, whereby it is established that the conditions are suitable for a specific type of

sample and that this sample is “similar” to the reference material, is called sample suitability. Whereas in the system suitability process the functionality of the method is evaluated by means of assay controls (‘does the test/equipment itself properly work?’), in the sample suitability process the functionality of the method is evaluated in relation to the product or sample to be tested (‘is the test suitable for this particular type of sample?’).

Once the method is standardized, the assay is ready for the first qualification experiments, in which validation parameters are established.

If the results comply with the requirements, the assay is ready to be used for its final purpose, otherwise, the assay goes back to the previous stage for additional optimization and standardization (Ederveen, 2010).

During method’s performance validation, the performance of the assay is demonstrated, showing that the assay is reproducible when it is performed e.g. on different days, by different technicians, with the range of samples for which the assay is intended, etc. Also, small fluctuations in assay conditions, that could occur under normal situations, are mimicked and the results should demonstrate that the assay is robust.

Typical parameters recommended by FDA, USP, and ICH to be evaluated during a validation exercise of a cell-based assay are as follow 1. Specificity 2. Linearity & Range 3. Precision (Repeatability, Inter-session variability and Intermediate precision) 4. Accuracy (Recovery) 5. Robustness. In addition, also proper system suitability criteria should also be determined to ensure the goodness of the assay’s results. Moreover, if a non-cell-based assay, such as ELISA, is used for sample stability testing or characterization purpose also the limit of detection (LOD) and limit of quantification (LOQ) should be assessed. If a procedure is a validated quantitative analytical procedure that can detect changes in a quality attribute(s) of the drug substance and drug product during storage, it is considered a stability indicating test. In order to demonstrate this assay’s feature a proper forced degradation stress study should be also performed.

In the following part of this paragraph a deep discussion on each validation parameter is provided.

#### Specificity:

An ICH guideline defines specificity as the “ability to assess unequivocally the analyte in the presence of other compounds that may be likely to be present” (ICH Q2 (R1), 2005). Typically, these might be impurities, degradants, matrix, etc. In the case of cell-based assays specificity analysis consists mainly in the evaluation of the possible effects of the matrix components on both the assay and the active drug. To determine whether the product formulation has an impact on the bioassay method (e.g. by inducing cell’s proliferation/death), the matrix is diluted with the same dilution scheme as

the reference material and tested on the same plate as the standard. The dose-response curve of the standard is interpolated in the fitting algorithm defined during the development study (e.g. 4-parameter logistic 4PL algorithm), whereas the curve of the matrix is analyzed by linear regression. If the p-value of the linear regression is greater than 0.05, an impact of the product formulation on the method can be excluded. To determine whether the product formulation has an impact on the biological activity of the active principle, different matrix dilutions have to be tested in the bioassay. In order to test a wider range of matrix dilutions, a sample with the highest concentration available is used in the specificity experiments. The sample is diluted to the target concentration according to the developed procedure. Each dilution step is performed in matrix sequentially, in order to mimic the matrix dilution performed when samples at different concentrations are tested. If the linear regression of potencies obtained when the sample is diluted in the tested buffer at different concentrations results in a line with a slope that is not significantly different from zero (p-value greater than 0.05), the matrix does not affect the bioactivity of samples under the tested conditions.

In addition to these experiments, to prove that the method is specific for the developed product, a different molecule can be tested, and no biological response should be detected.

#### Dilutional linearity

The dilutional linearity study is the core of a method validation and it consists of a series of runs that are required to establish the Linearity, Accuracy, Precision and Range of a bioassay method. As a result, the design of the dilutional linearity study is of crucial importance for proving that the developed assay meets Phase I/II or Phase III/Market requirements. The approach here described is widely based on USP <1033>. As these experiments are going to be used to calculate the precision of the method, it is crucial that the experimental design includes all the sources of variability that could occur in routine testing. In bioassays, the most prominent sources of variability are 1) different operators, 2) different lots/supplier of a critical reagent or 3) different cell passages (for cell-based assays performed with continuous cell cultures).

The linearity of an analytical method is defined as its ability (within a given range) to obtain test results that are directly proportional to the concentration (amounts) of analyte in the sample.

The linearity of a method is a measure of how well a calibration plot of response vs. concentration approximates a straight line. Linearity can be assessed by performing single measurements at several analyte nominal concentrations (e.g. 50%, 71%, 100%, 141% and 200% of its potency or 60%, 77%, 100%, 120% and 144% depending on the assay range evaluated during development).

A log-log linear regression analysis of all measured potency values versus the target potency levels is then performed. The resulting plot slope, intercept and correlation coefficient ( $R^2$ ) of the linear regression curve provide the desired information on linearity as stated in ICH Q2(R1).

If all acceptance criteria are fulfilled at all levels, all potency levels should be included in the linear range. Also, checking the residuals of the regression curve should be a good practice as mentioned before.

Precision of a method expresses the closeness between a series of measurements performed on multiple sampling of the same homogeneous sample under similar analytical conditions. In the validation of cell-based assays, the variability of the method is studied with the variance component analysis, where three precision levels are analyzed: 1) Repeatability (or intra-assay precision), which is a measure of the variability among the runs (or replicates) of an analytical session. Here the measurements are taken under same operating conditions, same analyst over a short period of time. 2) Between-assay (or inter-assay precision), which measures the variability between different analytical sessions 3) Intermediate precision (IP), which measures the total variability of the method by taking into account both the repeatability and between-assay component (e.g. the method is tested on multiple days, instruments, analysts etc.).

The ICH guidelines suggest that repeatability should be conformed duly utilizing at least 9 determinations with specified range for the procedure or a minimum of 6 determinations at 100 % of the test concentration and this is why the linearity experiments' results are commonly used to determine bioassay's precision.

The accuracy of a measurement is defined as the closeness of agreement between an accepted reference value and the measured value. In a method with high accuracy, a sample (whose "true value" is known) is analyzed and the measured value is identical to the true value (Ravisankar P. and Sankar R., 2015). Typically, the accuracy of a method is expressed as relative bias (RB) and is calculated with the following formula on each run of the dilutional linearity study:

$$Relative\ Bias = 100 * \left( \frac{Measured\ Potency}{Target\ Potency} - 1 \right) \%$$

Once the relative bias has been calculated for each run at each level, it is important to check the conformance to the acceptance criteria set at the beginning of the validation study. Furthermore, it is important to investigate the presence of a bias across levels as this would not allow the comparison of samples with different measured potencies. To do so, data should be fitted in a linear regression

curve. A significant p-value ( $p < 0.05$ ) is an indication of a bias across the levels and if so, an evaluation of the impact of the extreme potency levels (e.g. 50% and 200%) on the bias should be performed. If the bias is caused by the potencies obtained at one or both extreme levels, these should not be considered when determining the linear range of the method.

In addition, the limit of detection (LOD) and the limit of quantitation should be also considered if the method to be validated is an ELISA assay.

LOD is determined by the analysis of samples with known concentration of analyte and by establishing that minimum level at which the analyte can reliably detected, but not necessarily quantitated as precise value, under the stated experimental conditions (Ravisankar and Sankar, 2015). The detection limit is generally expressed in the concentration of analyte (ppm) in the sample. Several approaches like visual evaluation, signal-to-noise ratio, standard deviation of the response and standard deviation of the slope of the linearity plot, are recommended by the ICH for determining the detection limit of sample, depending on instrument used for analysis, nature of analyte and suitability of the method. The formula for calculating LOD is:

$$\text{LOD} = 3.3 * \delta / S$$

Where  $\delta$  = standard deviation of intercepts of calibration curves. S = the slope of linearity plot.

The limit of quantitation instead is the least concentration of drug in a sample which is estimated with appropriate precision and accuracy under the affirmed experimental conditions. ICH recommends the same methods used to estimate the LOD. The formula for calculating LOQ is:

$$\text{LOQ} = 10 * \delta / S$$

Where  $\delta$  = standard deviation of response. S = Mean of slopes of the calibration curves.

Both LOD and LOQ are not evaluated for cell-based assay and for this reason the methods applied for their determination and the statistical evaluation are not here reported in detail.

Finally, also bioassay robustness should be carefully evaluated considering that, as reported in the ICH Q2(R1) guideline, it is defined as the measure of the capability of an analytical method to remain unaffected by small deliberate changes in method parameters, providing an indication of its reliability in routine analyses.

Although the evaluation of the method robustness is performed during the development phase, analysis of critical parameters during the validation study is also recommended, especially for Ph III products. Method parameters that need to be studied are defined through a risk assessment, which determines their criticality.

The variable method parameters in cell-based assays may involve cell number/well; incubation of pre-plated cells, incubation of critical reagents, bioassay incubation time and incubation of bioassay read-out.

The study of the robustness starts from a DoE (Design of Experiment), in which, based on the experience and the knowledge of the method, key factors are identified and tested in a defined range. The goal of this kind of approach is to find out which variables have the biggest impact on the method performance by performing the minimum number of experiments.

Once the method is validated/qualified, depending on its intrinsic characteristics, it could be routinely applied for characterization studies and/or release and stability testing to ensure the quality of the tested product over time. If one or more critical parameters impacting on the tested drug and/or the method change, a risk assessment should be performed to decide if a revalidation study is needed. Clear examples of this situation are a change in the drug's formulation buffer, a change in production process that can significantly affect product's CQAs or a method change after troubleshooting or an optimization.

## **2.7 PHARMACOKINETICS of THERAPEUTIC MONOCLONAL ANTIBODIES**

Early screening and optimization of mAbs is mainly focused on properties such as affinity, potency and stability for selection of lead constructs, while pharmacokinetic (PK) properties, that can influence both efficacy and safety of a drug, are usually characterized later in development and on a small number of lead mAb candidates (Avery et al., 2018). Compared to the well-defined field of small molecule therapeutics, in vitro assays used as preclinical tools to predict human PK for mAbs have yet to be established for large molecule therapeutics.

Implementing such tools for identifying mAbs at risk for inadequate PK during drug development will ultimately reduce the time and the investments needed for drug discovery and development by improving the lead mAb selection process.

The inclusion of PK developability criteria together with the implementation of pharmacokinetic modelling and simulation in drug product development will indeed provide a rational, scientifically based framework for efficient decision making regarding the selection of potential drug candidates; for maximum information gain from the performed experiments; and for conduct of fewer, more focused clinical trials with improved efficiency and cost effectiveness (Rodgers and Chou, 2016; Elloumi et al., 2012; Reichert et al., 2005; Beck et al., 2019).

As a confirmation, during the last 5 years, a decision-making go/no-go strategy has been introduced into the drug discovery process, using pharmacokinetic principles to reduce the risks and maximize the benefits of selecting superior drug candidates (Caldwell et al., 2003).

Indeed, a previously published survey on the causes of failure in drug development indicated that inappropriate pharmacokinetics were a major cause and some reports have suggested »15% of Phase 1 clinical studies fail due to inadequate PK or pharmacodynamics properties (Cook et al., 2014; Walker, 2004, Mahmood and Green, 2005; Jones et al., 2019). Moreover, from another survey on 18 development projects, there is evidence that a PK/PD guided approach contributes to streamline the drug development process.

Since PK is defined as “the study of the effects of a living organism on an administered drug”, inappropriate pharmacokinetic behavior includes factors such as low bioavailability due to high extraction or poor absorption characteristics, low target tissue distribution, short elimination half-life leading to short duration of action and excessive variability due to genetic or environmental factors. For example, Dobson et al. showed a short half-life and a fast rate of clearance for MEDI1912, an anti-nerve growth factor (NGF) antibody for the potential treatment of chronic pain, due to an aberrant self-association and non-specific tissue binding (Dobson et al., 2016).

Moreover, Dostalek et al. reported unexpectedly fast non-specific clearance, poor target tissue distribution and limited efficacy for a humanized monoclonal antibody against fibroblast growth factor receptor 4 in athymic NCr nude mice (Dostalek et al., 2017).

These kinds of observations have led to an increased emphasis on pharmacokinetic input to the drug discovery process throughout the pharmaceutical industry. Much progress has been made in developing tools for the prediction of drug absorption, drug clearance and drug–drug interactions, in addition to the scaling of pharmacokinetic parameters from animals to man (Walker, 2004).

While there are readily available papers and other online material on pharmacokinetic topics such as its technical terms, model definitions and calculation methods (Dunnington et al., 2018); there are some gaps when it comes to how the science of pharmacokinetics is used in drug development.

Pharmacokinetic (PK) modeling and simulation is indeed one such innovative tool intended to help in early go or no-go decisions and significantly improve development efficiency. Indeed, due to time constraints and the availability of only small quantities of each candidate at the drug discovery stage, evaluations through *in silico*, *in vitro* and small animal studies have become fundamental.

*In vitro* PK models cannot incorporate all variables observed *in vivo* but they do provide valuable information for the drug-development process since they have many favorable characteristics, such as flexibility, adaptability, relatively low cost, good correlation with human and animal data and no

ethical concerns as compared with animal experiments, which make them excellent experimental platforms. Several authors have touched on various aspects (Dunnington et al., 2018).

The PK of mAbs is generally characterized by a slow systemic clearance (CL) and low volume of distribution, resulting in a long terminal elimination half-life (11-30 days in humans). Multiple biophysical, biochemical, and biological characteristics of a mAb have been linked to CL. These properties comprehend isoelectric point (pI), charge, size, hydrophobicity, nonspecific binding, off-target binding, degree and type of glycosylation (including mannose, sialic acids, galactose, and fucose), binding affinity toward Fc $\gamma$  receptors and the target, immunogenicity, injection route and interactions with neonatal Fc receptor (FcRn) which in turn could have ramifications on mAb's efficacy and safety (Igawa et al., 2011).

For example, therapeutic mAbs with high terminal mannose glycans exhibit fast elimination from systemic circulation and lower efficacy (Goetze et al., 2011; Kanda et al., 2007), while Igawa et al. showed that lowering the total pI by 1–2 units resulted in longer half-lives and slower elimination rates (Igawa et al., 2011).

Among the above-mentioned properties, protection and recycling of mAbs mediated by the neonatal Fc receptor (FcRn) is well documented as one of the most important factors for the evaluation of predictive PK (Jones et al., 2019; Avery et al., 2018; Chung et al., 2019).

FcRn binding constitutes a major consideration for *in vivo* pharmacokinetic analysis of antibody drugs, hence, comprehensive profiling of FcRn binding is commonly required by regulatory agencies as an integral part of Fc assessment.

FcRn consists of two polypeptides, a 48–52 kDa class I major histocompatibility complex-like protein ( $\alpha$ -FcRn) and a 14 kDa  $\beta$ 2-microglobulin ( $\beta$ 2 m) and it is widely expressed on the surface of endothelial cells, macrophages, monocyte-derived dendritic cells. The FcRn/IgG interaction occurs with high affinity at acidic pH in the endosomes of vascular endothelial cells and bone marrow-derived cells and increase *in vivo* mAb stability and efficacy by circumventing lysosomal IgG degradation.

Specifically, FcRn binds to the CH2-CH3 portion of the Fc domain of IgG in the slightly acid environment of endosomes (pH = 6). Then, the receptor facilitates the recycling of IgGs to the cell surface and the subsequent release in circulation upon exposure of the FcRn/IgG complex to the physiological extracellular pH environment as shown in the figure below (Figure 7).



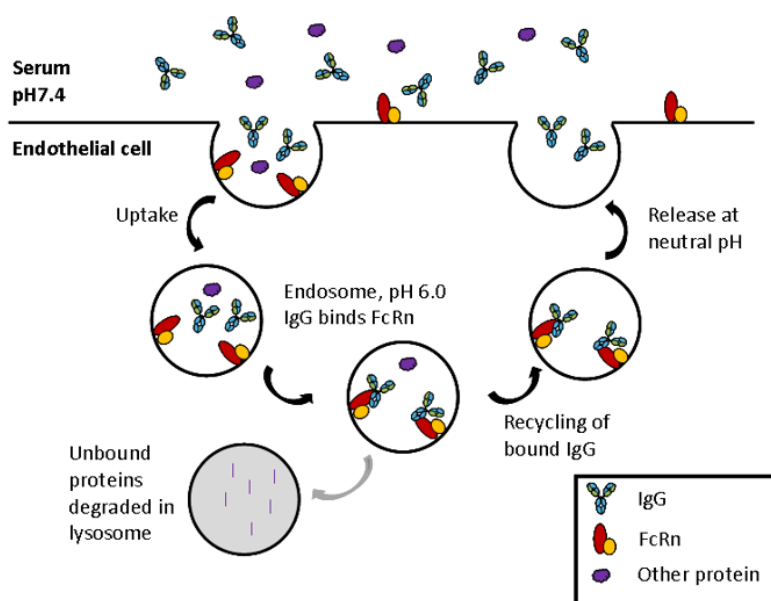


**Figure 7: FcRn mediated recycling of IgGs.** In the early endosome IgG interacts with FcRn at pH 6.0. The FcRn-IgG complex is then recycled back to the cell surface and IgG released at neutral pH thus rescuing IgG from lysosomal degradation.

From <https://absoluteantibody.com/antibody-resources/antibody-overview/other-antibody-interactions/>

Therefore, having a robust, accurate, precise and qualified FcRn binding assay that can ensure that the Fc domain of an IgG-based therapeutic is intact, functional, and can bind to FcRn, is advisable prior to the start of pre-clinical and clinical studies. Such an assay could also potentially be useful to allow for the detection of any subtle structural changes that may occur in the Fc domain of an IgG-based therapeutic during manufacturing process (Mathur et al., 2013).

Having the changes and possible impacts on FcRn binding and PK under control, is an advantage offered by analytical biochemistry to the control strategy of products and processes.

Manufacturing process changes are often necessary during drug development and after approval in order to improve product quality, increase production capacity, enhance product stability, or increase convenience for the administration of the product to patients. According to the ICH Q5E guideline, the demonstration of comparability for biological products means that the pre- and post-change products are highly similar and any difference in quality attributes have no adverse impact on the safety or efficacy of the product. In principle, if pre- and post-change products exhibit similar pharmacokinetic (PK) properties, it is reasonable to assume that such changes would result in comparable efficacy and safety (Zhuang et al., 2018). The comparability exercises are required by the guidelines and the predictive PK is one of the comparability attributes that most needs to be monitored due to its criticality as also highlighted before (ICH Q5E).

One of the challenges for the establishment of a relationship of FcRn binding and PK are the different methodologies, tools and assay designs used to verify and measure the interaction between IgG and FcRn. Employment of diverse technologies with their specific limitations and advantages further contributes to variability in the *in vitro* measurements. Regardless of the method used for measuring FcRn–IgG interactions it is important to design assay format which minimize assay artifacts and produces consistent results (Bajardi-Taccioli et al., 2015).

A comprehensive review by Dostalek et al. summarized the various *in silico*, *in vitro*, and *in vivo* tools in predicting PK liability of lead candidates (Dostalek et al., 2017).

Here we will describe FcRn assays that should be considered during drug discovery and discuss approaches that could be included in the pharmacokinetic screening part of the lead candidate generation process to de-risk unexpected pharmacokinetic behaviors of Fc-based therapeutic mAbs. Most of these tools can be formatted in a high throughput fashion to screen large numbers of candidates and use very small amounts of materials available during early discovery stage (Dostalek et al., 2017).

FcRn binding to Fc domain of an immunoglobulin can be analyzed with cell-based assays, arguably more physiologically relevant and with cell-free assays using a wide variety of techniques (Schlothauer et al., 2013).

The latter include surface plasmon resonance (SPR) (Biacore, ProteOn), biolayer interferometry (BLI, Octet), isothermal titration calorimetry (ITC), enzyme-linked immunosorbent assays (ELISA), AlphaScreen proximity assays, affinity chromatography and asymmetrical flow field flow fractionation.

The cell-based FACS assay uses cells expressing FcRn on the surface and labeled IgG to measure the affinity while ELISA immobilizes the target (FcRn or IgG) on a plate and detects the bound target (IgG or FcRn) captured with secondary antibody conjugated with horseradish peroxidase or other enzymes as reported by Qiang Wu in his work.

However, among the cell-free technologies, SPR-based biosensor assays represent the gold standard, likely due to the fact that they can provide real-time quality data on binding specificity and kinetics over a wide range of binding affinities allowing high flexibility.

While there are several assay formats and tools available, there is still room for improvements for sensitivity, reproducibility/consistency, as well as time requirements and costs (Wu et al., 2015).

## **2.8 PREDICTIVE PK METHOD QUALIFICATION**

Analytical data are fundamental for product licensure and are indeed used through all the bio therapeutic product development lifecycle to ensure the right strategy for the evaluation of product quality, attribute criticality and process control.

As highlighted before, analytical procedures must be appropriately validated before their implementation for routine use for product release and stability studies as per ICH Q2(R1)5 procedure validation guideline. For non-routine analytical characterization methods, rigid adherence to procedure validation guidance it is not mandatory. Based on the intended use of the test method, the level of confidence required could be different. At least the assay must be scientifically sound and generally suitable for the intended use and operationally robust (Saxena, 2010). Indeed, it is important to underline that they are not intended for QC applications.

As stated in the research article of Gabrielson et al., “scientific judgment should be used to tailor the demonstration of fitness-for-purpose to suit the specific procedure, based on the type of measurement being made, the attribute being measured, and the purpose of the test”. This exercise is referred to as “procedure qualification” through which the operator should be able to demonstrate that the procedure exhibits the performance necessary to satisfy its requirements and achieve it (Gabrielson et al., 2020). Methods applied only for Characterization or Comparability studies does not necessarily need be fully validated. However, even if there are no predetermined method performance specifications as for validation studies, there may be minimal method performance capability requirements based on an intended purpose (Ritter et al., 2013).

Indeed, the key criteria for evaluation of an analytical method should include method specificity, preliminary accuracy and precision, linearity and range and system suitability. A method cannot fail qualification; it should be reoptimized until it achieves an acceptable performance.

## **2.9 POTENTIAL IMMUNOGENICITY of BIOTHERAPEUTIC MONOCLONAL ANTIBODIES**

The field of biotherapeutics is in fast development however, despite their clinical and commercial successes, the use of therapeutic mAbs has also some drawbacks associated to their potential immunogenicity (Jiskoot et al., 2016). Immunogenicity occurs when the patient’s immune system perceives as non-self or danger the biological product and launches specific immune responses against it.

Even though the similarities with endogenous proteins for which patients are immune tolerant, some patients develop antibodies against these therapeutic proteins. This class of antibodies are called anti-drug antibodies (ADA) and represent a major limitation to the use of biotherapeutic proteins (BP). The clinical consequences of ADA can range from clinically asymptomatic to severe life-threatening conditions such as hypersensitivity reactions (e.g. anaphylaxis); moreover, they may decrease the efficacy of BPs by neutralizing them or modifying their clearance. ADA may also cross-react with closely related endogenous counterparts of BPs, thereby compromising physiological functions (Schellekens, 2002). ADA that develop in patients treated with a mAb can be divided in two main categories: neutralizing ADA (ntADA) that directly block or interfere with the drug's target binding, and non-neutralizing ADA (i.e., binding ADA, bADA) that recognize other epitopes on the drug (Bendtzen, 2015) and thereby do not straightly impact the drug's pharmacodynamic activity. NtADA are generally considered to be more critical in the clinical setting than bADA because they directly reduce a drug's efficacy resulting in the loss of clinical response. However, bADA could result in a clinically similar outcome to the one of ntADAs (e.g., reduced therapeutic efficacy) by compromising bioavailability or accelerating drug clearance from the circulation (Vaisman-Mentesh et al., 2019). In addition, they can also be precursor or triggers for the generation of ntADAs through the phenomenon of epitope spreading.

In both cases, as stated in the paper of Putnam et al., ntADA and bADA substantially alter the PK and pharmacodynamics of the mAb being administered (Putnam et al., 2010).

Different types of biopharmaceutical products produce two markedly different unwanted immune reactions, identified as classical immune reactions to neo-antigens and breakdown of immune tolerance (Schellekens, 2002).

Reaction to neo antigens usually occurs after a single administration and tends to be a fast reaction. In this case antibodies are induced by a classical immune response stimulated by T-cells.

Antigen presenting cells (APCs) uptake the mAb, then digest it and finally present the peptides (T-cell epitopes) via appropriate major histocompatibility complex (MHC) Class II molecules on their surface as shown in the figure below (figure 8).

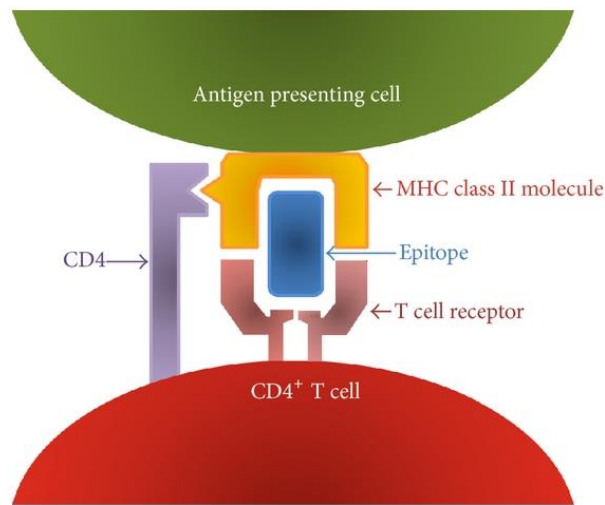


**Figure 8: Antigen peptide presentation to MHC class II molecule.** T cells recognize a complex of a peptide fragment and MHC (Human Leucocyte Antigen (HLA) in humans).

From Paul et al., 2013.

These peptides are recognized by T cells that induce B cells differentiation in antibody-secreting (short- and long-lived) plasma B cells. Some of the activated B cells also become memory cells, which maintain the pool of long-lived plasma cells and react rapidly to rechallenge by producing short-lived plasma cells (Singh, 2011).

This type of immune response has a high incidence, while the antibodies are generally neutralizing and persist for a long time. The clinical consequence, most of the time, is a loss of product efficacy. B cells can also be activated without cognate T-cell help through the so-called T-cell-independent pathway.

This pathway is typically induced by antigens of bacterial or viral origin displaying repetitive epitopes termed pathogen-associated molecular patterns, but it could also be stimulated by aggregates in biotherapeutics. Due to lack of affinity maturation, this pathway usually results in a response of the IgM type, which is transient, of low titer, and poor specificity (Singh, 2011).

Breakdown in immune tolerance against self-antigens instead is a slow process that can take years to become clinically evident (Porter, 2001). The likelihood of breakage of tolerance to proteins of human origin or recombinant autologous proteins is strongly related to the abundance of the endogenous protein. Indeed, for low abundance proteins, the immunologic tolerance is not complete. T and B cells specific for low-abundance proteins (autoantigens) are not always completely eliminated during early development and, under particular conditions (e.g., presence of molecules with adjuvant-like characteristics), these might generate an immune response (Singh, 2011).

Immunogenicity of mAbs and the generation of ADA has been suggested to be dependent on the interplay between factors related to the intrinsic complexity of the drug itself and to the patient, or to the drug's route and frequency of administration (the so-called extrinsic factors) (Bloem et al., 2017; Krishna and Nadler, 2016).

Protein related factors comprehend protein sequence and structure, homology with respect to human amino acid sequences, post translational modifications, presence of T and B cell epitopes and proteins' source. Also, the nature of the biotherapeutic mAb (e.g., immunostimulatory vs. immunosuppressive; agonist vs. antagonist) concurs to the observed effect. Moreover, cell-surface binding therapeutic antibodies generally will have more potential to be immunogenic than those that interact with soluble targets (Singh, 2011).

It is crucial to keep in mind all these drug's intrinsic factors since during drug design, on the basis of previous knowledge and experience, it is possible to mutate mAb's sequences to avoid fragmentation and aggregation hotspots, as well as antigenic epitopes, while maintaining its biological activity (Singh, 2011).

The extrinsic factors can be product-, treatment- and patient-related factors.

Product-related factors comprehend proteins' expression system, complexities of the manufacturing process, production contaminants (i.e. aggregates and impurities) and formulation excipients. Appropriate formulation of a protein product is highly important, particularly with respect to stabilization, because if this is inadequate the protein may aggregate or denature increasing its immunogenic potential (Delves and Roitt, 2000). Aggregation and adduct formation of proteins may indeed reveal new epitopes or lead to the formation of multivalent epitopes, which may stimulate the immune system (Guideline for Immunogenicity Assessment, EMEA, 2017). This is supported by the fact that removal of aggregates (present as visible or sub-visible particles) has been associated with reduced immunogenicity in preclinical in vivo studies. Formulation becomes even more crucial for products that may not be optimally stored or handled.

Treatment-related factors include dose, route and frequency of administration and treatment duration. The route of administration can influence the immunogenicity of the protein but, as underlined in the work of Schellekens, does not confer immunogenicity per se. Evidence suggests that the subcutaneous (s.c.) environment is relatively hostile to an already immunogenic protein (Schellekens, 2005). Subcutaneous administration indeed localizes and prolongs the exposure of the biotherapeutic to a small area within close proximity of the lymph nodes where B and T cells are present. Intravenous (i.v.) administration is also likely to elicit an immune response, but to a lesser degree than

intramuscular (i.m.) administration, which in turn is more immunogenic than intranasal administration.

Finally, patient-related factors comprise patient's immune status, genetic factors such as HLA allotype, medical history, presence of pre-existing antibodies et al. The type of disease has a role in the generation of treatment-related immune response, likely due to the immune status of the patient. Indeed, patients with weak or compromised immune system or those on immunosuppression therapy are less likely to develop ADAs than those with a healthy immune system (Singh, 2011). As reported by Kosmas et al., Rituximab, a human mouse chimeric antibody anti CD20 surface antigen, interestingly did not cause a human anti-chimeric antibody (HACA) response in patients with B-cell lymphocytic leukemia. This was possibly due because of a B-cell depletion elicited by the antibody that prevents the formation of HACA response (Kosmas, 2002). Furthermore, the patients were also treated with immunosuppressive drugs. In contrast, when Rituximab is administered to patients with autoimmune disease such as systemic lupus erythematosus and primary Sjögren's syndrome, 65% and 27% of patients developed HACA, respectively, despite immunosuppressive therapy (Van Walle et al., 2007; Singh, 2011). Moreover, short-term therapy is less likely to be immunogenic than long-term therapy, although intermittent treatment is more likely to elicit a response than continuous therapy as Schneider suggested (Jahn and Schneider, 2009). Also, lower doses are generally more immunogenic than higher doses, a behavior that is probably ascribable to the fact that the immune system is generally less tolerant of low-abundance proteins as shown in a primate study with adalimumab (anti-TNF alpha) (Singh, 2011). High-dose regimens are therefore sometimes used as a mode of therapy to induce tolerance (e.g., for Factor VIII) (Singh, 2011).

In addition, variations at any of the steps of the process can lead to clinically relevant changes in efficacy and/or safety of the final product at any of the following stages:

- Molecule design and cell-line selection
- Upstream processing (from thawing working cell bank to harvest)
- Downstream processing (post-harvest to bulk formulation)
- Drug product (fill finish to clinic/pharmacy)

The upstream (bioreactor/fermentation, harvest) process for example determines the type of host cell impurities that may ultimately remain in the final product. The current state of purification processes however is such that impurities are routinely reduced to levels well below what is considered a safety risk. Product variants instead are not as easily eliminated, and a certain minor fraction of some or all of these variants makes its way into the final bulk solution, generally in the low percentage levels.

The biotherapeutic mAb is also subjected to different stresses during manufacturing process (see, e.g., Cromwell et al., 2006) including high-concentration and high-temperature steps, different ranges of pH, ionic strengths, shear stresses, extractable and leachable materials and light stress.

Different temperatures could be encountered by the drug when in the bioreactor or in the fermenter or during storage while filtration and filling equipment could lead to shear stresses and risk of shedding metal particles (Singh, 2011). Indeed, tungsten metal embedded in the neck of syringe barrels (during forming) has been shown to cause oxidation and aggregation.

Exposure to light could occur during all the above-mentioned operations, especially bright light during inspection, even if brief, as well as light exposure during use.

These structural changes could be present in only a small fraction of the molecules, making them difficult to detect analytically, but still sufficient to raise an unwanted immune response.

In the end, as Porter also concludes in his work, no particular property of the mAb can be identified as an obvious predictor of immunogenicity in humans (Porter, 2001). This lack of correlation is indeed a manifestation of the complexity of this subject.

Therefore, immunogenicity risk management of biotherapeutics is important for successful drug development (Wadhwa et al., 2015). On the other hand, due to the enormous investments and costs in the whole process of developing a biotherapeutic drug candidate, it is worthwhile and necessary to assess the immunogenicity starting from the early stage of the drug discovery process.

#### 2.9.1 Current methods used for immunogenicity evaluation

Here we review the literature on the models used to study immunogenicity during the early development phase of a drug candidate before clinical evaluation.

Non-clinical in vitro or in vivo studies aiming at predicting immunogenicity in humans are normally not required. However, head-to-head comparative immunogenicity studies after changes are made to the manufacturing process of a given biologic (e.g. mAbs to compare the pre- and post-change versions of the product) are sometimes requested by regulatory agencies (Guideline on Immunogenicity Assessment, EMEA, 2017). When changes to the manufacturing process of an individual product are made, the comparability exercise is a stepwise process (ICH Q5E). If the initial physicochemical and biological testing indicates a difference between the pre- and post-change versions of the product, the potential consequences to safety and efficacy need to be considered, including immunogenicity. Ongoing consideration has been given to the use of emerging technologies (novel in silico, in vitro and in vivo models), which might add value to inform on the



potential risk for immunogenicity. None of these tools, however, is considered clinically validated by Health agencies and this is why they are not yet officially required in guidance documents. A limitation in prediction of the relative immunogenicity of BPs is the variance in the immunogenicity potential determined by *in silico* and *in vitro* techniques (Brinks et al., 2011). No single assay can provide all the necessary information on the immunogenicity profile of a biotherapeutic, therefore, bioanalytical strategies using a panel of assay is commonly used.

The current approached used by many companies foresee the *in silico* analysis of the protein of interest through different software, *in vitro* tests using mainly classic 2D assays with PBMC-derived cells or immune cell lines to follow protein uptake, immune cell maturation and pro-inflammatory cytokines released and *in vivo* tests using different animal models (Groell et al., 2018).

Apart from improvements in product quality, an important aspect of the design of the molecule that is becoming computationally tractable is the removal of epitopes that lead to recognition by T cells. *In silico* prediction tools have been developed to identify the potential T-cell epitope content of a protein. Because the T-cell epitopes presented by MHC Class II molecules are linear, sequence-based screening to evaluate the binding potential of overlapping peptides to the binding pockets of common HLA Class II alleles is performed. Immunogenicity potential of the whole sequence can be scored, allowing the possibility to identify, modify, or completely remove epitopes to prevent their display by MHC (Baker and Jones, 2007; Rosenberg and Worobec, 2004). Such guidance can be useful in early development of new biologics, although the models currently lack adequate validation (Koren et al., 2007) and do not capture the complex interplay between in tolerance and immunogenicity that determines clinical outcomes (Barbosa and Celis, 2007).

The *in vitro* assays used to assess the potential immunogenicity of an NBE should be selected based on the mode of action of the mAb candidate and the characteristics of the final product. The type of immunogenicity studies, should be justified on the basis of the observed difference(s), the potential impact, and knowledge gained with the product and product class before (ICH Q5E).

These *in vitro* assays are characterized by high intrinsic variability and poor standardization considering the difficulties encountered in manipulating PBMCs. Moreover such *in vitro* tools are expensive, and this is why an immunogenicity risk preassessment should be performed with *in silico* software.

Indeed, *in silico* assessment can be applied to reduce the amount and complexity of the *in vitro* screening by identifying linear T cell epitopes that are present throughout the protein sequence (neo or modified T cell epitopes). Among the different tools that could be used, to cite a few, there are IEDB, CHOPPI and Tepitope.

## **2.10 CASE STUDY: ANTI-TIGIT THERAPEUTIC MONOCLONAL ANTIBODY**

In this work all the experiments and the developed methodologies refer to a specific case study. Indeed, Anti-TIGIT antibody was selected.

Anti-TIGIT was chosen as proof of concept molecule since it is a classical IgG1 monoclonal antibody like the majority of antibody-based biotherapeutics and therefore the findings and the issues faced during this work could be also translated to other IgG1. The specific objective of this case study was to illustrate the approaches to be applied for the development and qualification of assays for the assessment of mAb's biological activity, predictive PK and potential immunogenicity together with the important factors that need to be considered in this context providing valuable inputs.

Anti-TIGIT antibody has been developed with immunomodulatory purposes.

Immunotherapy has been recognized as a key strategy to control tumor progression. Among these immunotherapies, the use of immune checkpoint inhibitors is one of the most promising and Anti-TIGIT belongs to this class of molecules.

Inhibitory immune checkpoint receptors have been shown to perform critical roles in the maintenance of immune homeostasis but also have a significant role in cancer progression and autoimmune disease (Qin et al., 2019; Akinleye and Rasool, 2019). Immune checkpoints are a normal part of the immune system, they are engaged when proteins on the surface of immune cells called T cells recognize and bind to partner proteins on other cells, such as some tumor cells. These proteins are called immune checkpoint proteins. When the checkpoint and partner proteins bind together, they send an “off” signal to the T cells blocking the immune system from destroying the cancer.

Indeed, immunotherapy drugs called immune checkpoint inhibitors work by blocking checkpoint proteins from binding with their partner proteins. This prevents the “off” signal from being sent, allowing the T cells to kill cancer cells.

Several immune checkpoint receptors such as Cytotoxic T-Lymphocyte Associated protein 4 (CTLA-4), T Cell immunoreceptor with immunoglobulin and Immunoreceptor Tyrosine-based Inhibitory Motif (TIGIT), T cell immunoglobulin and mucin domain-containing protein 3 (Tim3), Programmed Cell Death protein 1 (PD-1) and Lymphocyte Activation Gene-3 (LAG-3) have been discovered and are shown in the figure below (Figure 9). Blocking these receptors with monoclonal antibodies has proven to be an effective strategy to enhance anti-tumor immune responses and promote immune-mediated tumor rejection (Mahoney et al., 2015; Melero et al., 2015; Johnston et al., 2014).

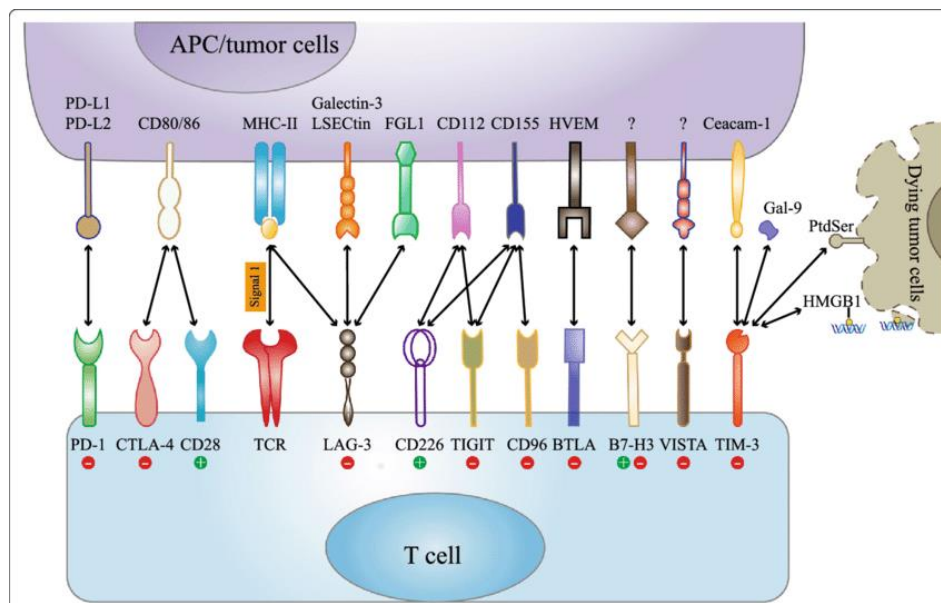


**Figure 9: Graphical representation of major immune checkpoint inhibitors and their respective ligands.**

Various immune checkpoint molecules expressed on T cells were shown with their ligands. Immune checkpoints such as PD-1, CTLA-4, LAG-3, TIM-3, TIGIT bound with their respective ligands on APCs and/or tumor cells, triggering a negative or positive signal to T cells response

From Qin et al., 2019.

TIGIT is an immune inhibitory receptor expressed on subsets of activated T cells and natural killer (NK) cells. TIGIT has an extracellular Ig variable domain, a type 1 transmembrane domain and a cytoplasmic tail that contains an immunoreceptor tyrosine-based inhibitory motif (ITIM) and an Ig tail-tyrosine (ITT)-like motif. TIGIT has different binding partners belonging to the family of Poliovirus receptor-like proteins: CD155, CD113 and CD112. This family mainly includes cell surface molecules that mediate cell adhesion, cell polarization and tissue organization, but several members also function as receptors for herpes and poliovirus.

CD155, also called NCL5 or poliovirus receptor (PVR) is a cognate receptor binding TIGIT with a high affinity (1-3 nM). CD155 is expressed on antigen-presenting cells (APCs), T cells and various non-hematopoietic cell types including tumor cells (Anderson et al., 2016). It also contains an immunoreceptor tyrosine-based inhibitory motif (ITIM) in its cytoplasmic tail (Yu et al., 2009).

CD113 or Nectin-3 instead binds with lower affinity (~40 nM) to TIGIT and its expression is limited to non-hematopoietic tissues like placenta, testis, kidney, liver and lung (Harjunpää and Guillerey, 2019).

CD112 has a weaker binding affinity than CD155 (Zhu et al., 2016; Deuss et al., 2017; Yu et al., 2009). CD112 is expressed by endothelial cells, hematopoietic cells and immune cells including

activated T cells and B cells, CD14<sup>+</sup> cells, dendritic cells (DCs) as well as by various tumors (Chauvin et al., 2015). TIGIT binds CD112 relatively tightly at its ectodomain as a heterotetrametric assembly where two central TIGIT molecules were flanked by two CD112 protomers. CD112 is implicated in the formation of cell junction and it is closely related to tumorigenesis, since it is overexpressed in several types of cancer (myeloid leukemia, multiple myeloma and epithelial cancers) (Sanchez-Correa et al., 2019).

Poliovirus receptor (PVR)–like proteins are an emerging group of Immunoglobulin superfamily with T cell co-signaling functions (Yu et al., 2009, Chan et al., 2012; Pauken and Wherry, 2014). This group of molecules share PVR signature motifs in the first Ig variable–like (IgV) domain and are originally known to mediate epithelial cell–cell contacts (Takai et al., 2008; Yu et al., 2009).

Three receptors compete with TIGIT for its binding partners. CD226 (DNAM) is a co-stimulatory receptor that is also binding to CD155 but with a lower binding affinity of 115 nM and to CD112 with an even lower affinity (Yu et al., 2009). CD226 is expressed on NK cells, naïve and activated T cells and monocytes, potentiating NK and T cell cytotoxicity and thereby immunosurveillance (Yeh et al., 2018). CD96 is a co-inhibitory receptor like TIGIT and binds to CD155 with an affinity of 38 nM. CD96 is expressed by both T and NK cells (Eriksson et al., 2012). CD112R is a newly identified co-inhibitory receptor binding to CD112 with a high affinity of 8.8 nM that is mainly expressed on T cells and inhibits T cell receptor mediated signals.

TIGIT has at least three strategies to inhibit lymphocytes and these are explained in the following figure (Figure 10): it mediates TIGIT signaling, antigen presenting cells (APC) modulation and CD226 interference.

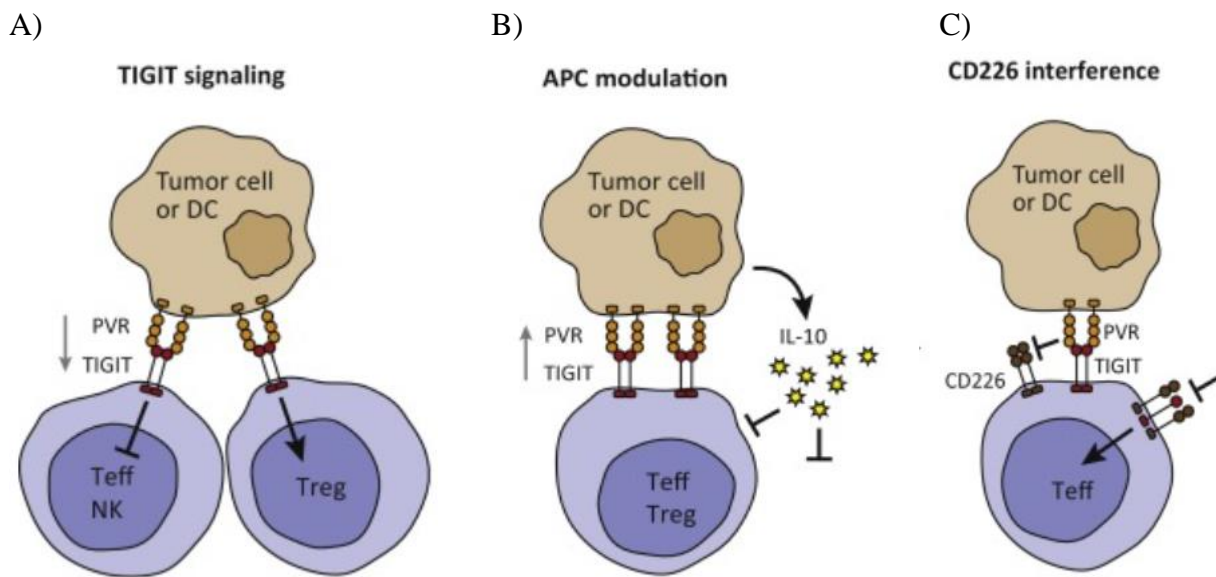


**Figure 10: TIGIT different modes of action.** TIGIT can inhibit lymphocytes through three distinct mechanisms of action. A) TIGIT can bind to PVR and then signal through the UTIM and/or ITT motifs on its intracellular tail. B) TIGIT can bind to PVR inducing PVR signaling in the near dendritic cells or tumor cells. C) TIGIT can bind with high affinity to PVR thus inhibiting CD226 signaling or disrupting CD226 homodimerization.

Adapted from Manieri et al., 2016.

TIGIT can act as a receptor binding to CD155 on dendritic cells (DC) or tumor cells. The ligation of CD155 with TIGIT results in TIGIT phosphorylation at Tyr225 at its ITT-like motif, recruiting SHIP1 (SH2-containing inositol phosphatase 1) via adaptor molecule Grb2. Recruitment of SHIP1 to the TIGIT tail blocks signal transduction through the PI3K (phosphoinositide 3-kinase) and MAPK (mitogen-activated protein kinase) pathways and results in NK cell inhibition (Li et al., 2014; Liu et al., 2013). Phosphorylated TIGIT can also recruit SHIP1 via adaptor molecule  $\beta$ -arrestin 2, suppressing NF- $\kappa$ B activity and IFN- $\gamma$  production in NK cells. TIGIT has been shown to inhibit T cell activation and effector function in a cell-intrinsic manner. TIGIT engagement downregulates components of the TCR complex itself (e.g. TCR $\alpha$ , CD3 $\epsilon$ ) as well as central regulators of the TCR signaling cascade such as PLC $\gamma$  (Joller et al., 2011). At the same time, however, TIGIT engagement induces anti-apoptotic molecules such as Bcl-xL as well as upregulation of the receptors for IL-2, IL-7, and IL-15, which promote T cell survival<sup>14</sup>.

TIGIT expressed on T cells can also act as a ligand for CD155 on DCs. In this case, the ligation results in phosphorylation of CD155 itself and of the mitogen-activated protein kinases (MAPKs) Erk

and p38 in the DCs. The result is an immunosuppressive effect on the T cells via enhanced production of interleukin 10 and diminished production of proinflammatory interleukin (Xu et al., 2009).

The third inhibitory biological activity of TIGIT is its capacity to compete and interfere with the engagement and costimulatory signaling of co-stimulatory receptor CD226. Due to its much higher binding affinity TIGIT expressed on T cells outcompetes CD226 in the competition for their shared ligand CD155, 3. TIGIT has higher affinity for CD155 than CD226 (PVR-TIGIT interaction is between 1–3 nM while the PVR-CD226 interaction is 119 nM). In addition, TIGIT can directly block homodimerization of CD226 and thereby impairs its co-stimulatory function (Johnston et al., 2014) as graphed in the figure below (Figure 11).

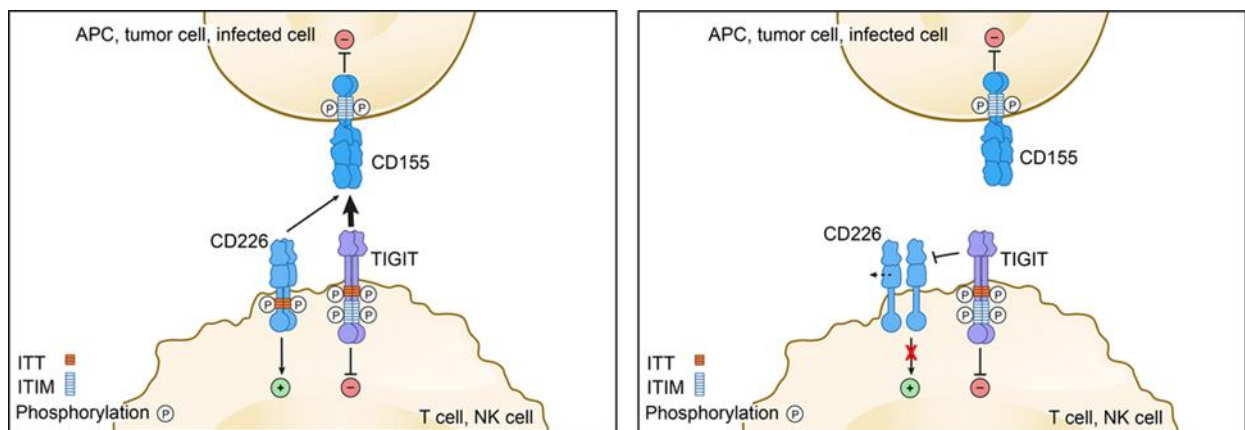


**Figure 11: *In vivo* MOA of TIGIT/CD155.** Figure showing the competition between Anti-TIGIT and CD226 for the binding to CD155.

Consistent with TIGIT mechanism of action, Anti-TIGIT treatment promoted upregulation of immune genes associated with activation of T and NK cells, Th1 response and cytotoxic activity as depicted below in figure 12. More specifically, Anti-TIGIT promoted dose-dependent increases in T and NK cell activation in tumors, as well as increased infiltration of T cells into the tumor.

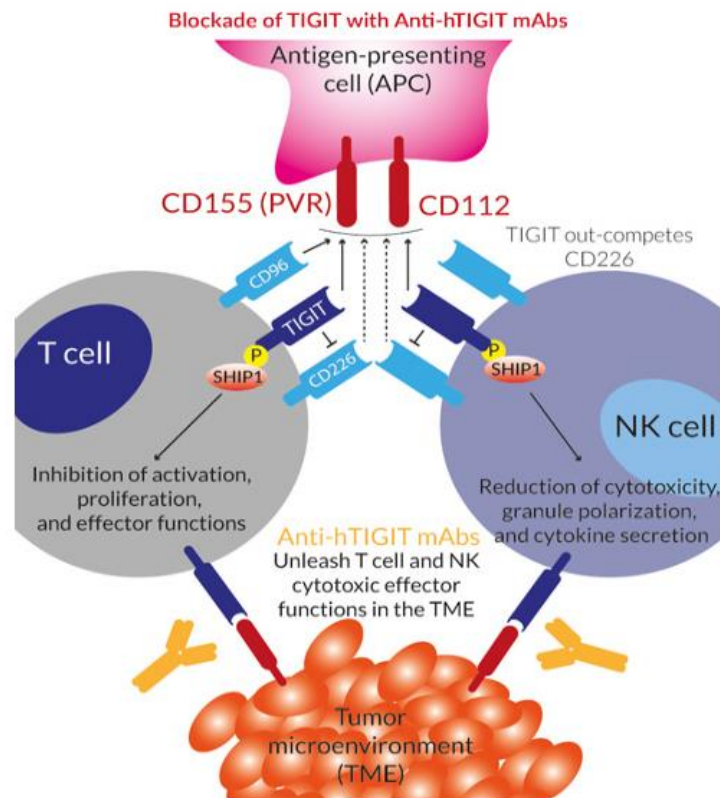


**Figure 12: Blocking of TIGIT with Anti-TIGIT mAbs.**

From <https://www.invivogen.com/anti-htigit>

TIGIT targeting antibodies have shown enhanced antitumor functions in several studies especially against solid tumors in combination with immunotherapeutic agents like anti PDL1. Indeed, TIGIT and PD-1 are often co-expressed in tumor-infiltrating T cells in preclinical murine models and human patients (Johnston et al., 2014; Wang et al., 2018). Combined blockade of TIGIT and PD-L1 in a mouse model resulted in complete tumor rejection and induced tumor antigen-specific protective memory responses. Accordingly, co-blockade of TIGIT with PD-1 additively improved proliferation, cytokine production, and degranulation in CD8<sup>+</sup> tumor-infiltrating lymphocytes from melanoma patients. TIGIT not only synergizes with PD-1 but also with Tim-3 in impairing protective anti-tumor responses (Kurtulus et al., 2015). These data indicate that TIGIT synergizes with other co-inhibitory molecules to dampen effector T cell responses and promote T cell dysfunction, thus representing promising target for cancer immunotherapy (Anderson A.C. et al., 2016).

The Anti-TIGIT antibody used in this work is a fully human monoclonal antibody (IgG1) designed to bind to TIGIT (T cell immunoglobulin and ITIM domain) and prevent its interaction with poliovirus receptor (PVR) also called NECL5 or CD155. Anti-TIGIT is a fully human IgG1 antibody and it comprised of two heavy chains (HC) and two kappa light chains (LC) as shown in figure 13.

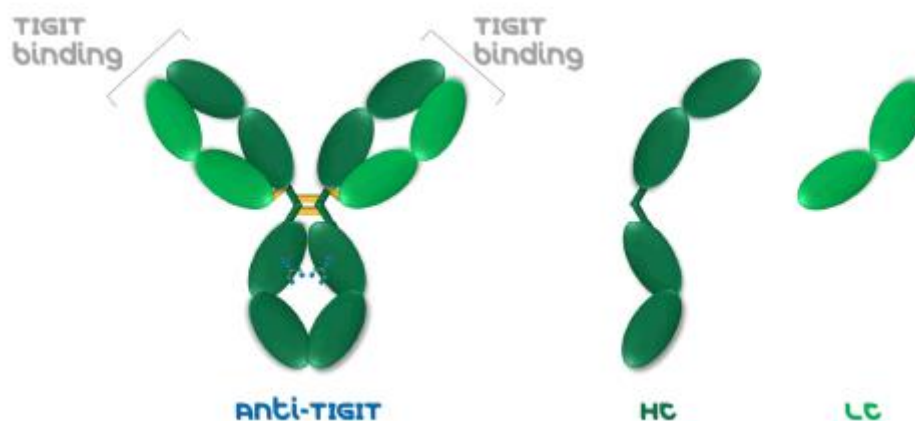


**Figure 13: Anti-TIGIT mAb's structure**

Considering Anti-TIGIT complex structure and relevant biological functions, the main challenges that will be faced during this work will be the development and qualification of dedicated methods with higher precision and accuracy allowing to ensure reliable results meeting the requirements of health authorities. Indeed, cell-based potency and bioassays are considered among the most challenging methods required during the drug development process considering both the variability associated with the use of the cells and the difficulties in establishing methods as relevant as possible to the real *in vivo* situation.

Both *in silico* and *in vitro* methods to measure recruitment of effector functions, induction or inhibition of a variety of secondary and tertiary activities, and antibody potential immunogenicity will be explored helping the definition of a specific analytical panel to foster product knowledge and that could serve during all the phases of biotherapeutic antibodies production.

Moreover, another challenge will be to develop assays that are fully customizable methods and to produce applying them data packages ready to be used for monoclonal antibody characterization and stability studies.



## Aim

This project aims to provide a unique insight into the bioanalytical tools tailored to support biotherapeutic antibodies production process throughout the product lifecycle. Indeed, early stage adoption of methods to characterize monoclonal antibody-based products can be beneficial at all stages, from clone selection to optimization of a manufacturing process to reduce risk in biologics development, to help in decisions making during a product lifecycle and to fulfill regulatory requirements. For maximum risk mitigation, key binding and functional activities should be assessed as early as possible in development. To achieve a level of product understanding that helps ensure the quality of the final product, sensitive and robust assays are essential. Therefore, the main aim of this PhD project was the elaboration of an analytical panel including reliable methods required for compliance with national and international regulations. All together these *in silico* tools and *in vitro* assays will serve to assess therapeutic monoclonal antibodies' biological activity, predictive pharmacokinetics and potential immunogenicity. For such purpose, the specific case study of Anti-TIGIT monoclonal antibody is presented.

### **3 MATERIALS and METHODS**

All the experimental methods applied in this work including samples preparation are here detailed. Moreover, a short overview of the theoretical basis of the techniques used is given.

#### **3.1 Anti-TIGIT antibody**

Anti-TIGIT antibody is the proof-of-concept molecule of this work.

This monoclonal antibody is expressed in CHO (Chinese Hamster Ovary) cell line using a fed-batch cell culture process.

A vial from the CHO cell bank is thawed and expanded in wave bags and, finally, inoculated in a 2000 L bioreactor. The crude harvest is clarified and purified by three chromatographic steps (affinity chromatography, AEX, CEX) and a nano-filtration step for viral clearance. A concentration/diafiltration step is needed to obtain a pre-formulated drug substance.

Drug Product (DP) process instead consists in the thawing and pooling of the DS, a mixing to homogenize the solution and a double sterile filtration before the filling in vial, stoppering and capping. Final Anti-TIGIT is designed as a parenteral drug product at 20 mg/mL as concentrated Infusion for intravenous (IV) route of administration.

#### **3.2 Cell cultures**

##### 3.2.1 Cellular viability assessment

To measure cellular viability of all the cell lines the Vi-Cell XR Cell Viability Analyzer from Beckman Coulter was used. The Vi-Cell automated cell counter that is based on a trypan blue cell viability assay can determine cell vitality (absolute, % and cells/mL), cell concentration, and cell growth rates and doubling time.

##### 3.2.2 CHO-s-myc huTIGIT ECD cell line

###### Basic maintenance

The cells have been used for both cell-based ligand binding bioassay (chapter 3, section 2) and as target cells in ADCC bioassay (chapter 3, section 5).

These cells are engineered CHO cells that constitutively express on their surface the extracellular portion of human TIGIT. CHO-S-myc-huTIGIT ECD cell line has been produced in EMD Serono Research and Development Institute (Billerica) by transfection and selection for surface expression of human TIGIT extracellular domain. The wild type cells are adherent cell line while these cells can

be cultured both in suspension and in adhesion by adding fetal bovine serum (FBS) to the culture medium.

All cultured cells were kept in a humidified incubator at 37 °C, 100 % relative humidity and 5 % CO<sub>2</sub>. For routine maintenance, T75 cm<sup>2</sup> tissue culture flasks (Nunc or equivalent) were utilized for culturing the cells. The culture medium used was the ProCHO5™ (Lonza) that has been developed to facilitate the production of recombinant proteins in CHO cells under suspension. It is made up of 0.1% Pluronic® F-68. It does not contain L-glutamine, phenol red, hypoxanthine, or thymidine. To the complete medium 400 µg/mL of Hygromycin B (Gibco) and 4 mM of L-Glutamine (Euroclone) are added. The CHO-S-myc-huTIGIT cells have a cellular duplication time of approximately 24 hours. For their maintenance, they are passed every 3-4 days as described below.

Upon detachment via scraper, transfer the cells in a 50mL Falcon test tube and centrifuge the cells at 300×g for 7 minutes. Withdraw the medium and resuspend the cells in 10mL of CM and then count the cells with an automatic cell counter (Beckman Coulter) by setting the instrument reading window from 7 to 20 µm. Dispense 1–2 ×10<sup>6</sup> cells in a 75cm<sup>2</sup> flask in final 20 mL of CM in order to obtain a confluent plate for the next passage. Confluent flasks were either used for initiating experiments or passaged further.

#### Master and Working Cell Bank Preparation

As reported in the United States Pharmacopeia (USP) <1032>, extensive characterization is necessary to ensure the quality and longevity of cell banks for use in the QC environment. Indeed, the general health and metabolic state of the cells at the time of bioassay can greatly influence the test results. After a cell line has been characterized in terms of thawing and culturing conditions, growth rate, morphology and functionality, is ready for banking. Analysts typically prepare a two-tiered bank (Master and Working). A Master Cell Bank is created as the source layer for the next Working Cell Bank. The Working Cell Bank is derived by expansion of one or more vials of the Master Cell Bank. During bioassay development, a working cell bank (WCB) was generated starting from a vial of MCB and stored in liquid nitrogen. After method validation the working cell bank was qualified to be used in routine tests both in terms of performance and for sterility and mycoplasma. The sterility analysis was done by the Microbiological & Biological QC laboratory while the mycoplasma test was performed in house using the MycoAlert™ Mycoplasma Detection Kit by Lonza (LT07-118) following manufacturer instructions. During the qualification study of the WCB, it is important to monitor for changes in morphology, magnitude of response, half maximal effective concentration (EC<sub>50</sub>), doubling time and cell viability, among other parameters. Cell culture and assay performance should be monitored during all the analytical working window to establish a limit for the allowable

number of cell passages that guarantee the same bioassay performance, before routinely starting a new culture. All manipulations of the cells were performed in a biological safety cabinet and all the equipment used were previously sterilized.

### 3.2.3 TIGIT Effector Cells (Jurkat T cells) and CD155 aAPC/CHO-K1 Cells

These are engineered cell lines provided by Promega (Cat n°J2092) and were used for the TIGIT/CD155 Blockade bioassay development (chapter 3, section 4).

Jurkat cells are an immortalized human leukemic T-cell line expressing human TIGIT with a luciferase reporter driven by a native promoter that can respond to both TCR activation and CD226 co-stimulation. CD155 aAPC/CHO-K1 cells are engineered to express human CD155 with an engineered cell-surface protein designed to activate the TCR complex in an antigen-independent manner.

For cell freezing and thawing and cell maintenance and banking the protocols supplied by the manufacturer were followed.

### 3.2.4 Effector Cells (Jurkat T cells expressing FcγRIIIa receptor, V158 high affinity variant)

These ADCC Bioassay Effector Cells are Jurkat T cells engineered to express FcγRIIIa receptor, V158 (high affinity) variant, and an NFAT response element driving expression of firefly luciferase (NFAT-RE). The cells were provided by Promega (ADCC Bioassay Effector Cells, Propagation Model(a–c) (Cat. # G7102).

For cell freezing and thawing and cell maintenance and banking the protocols supplied by the manufacturer were followed.

## **3.3 Bioassays for biological activity determination**

A number of assays to study the biological activity of biotherapeutic drugs were developed in the frame of this PhD study. The essentials of these (after the validation or qualification step) and the appropriate calibrations are described in this section.

Before entering in detail in each bioassay, a description on how the main bioassay's parameters (linearity and range, precision, accuracy and specificity) were evaluated is reported.

### **3.3.1 Bioassay performance verification approaches**

The bioassay's parameters that have been studied in this work and that are also recommended by FDA, USP, and ICH to be evaluated for a cell-based assay are as follow 1. Specificity 2. Linearity &

Range 3. Accuracy (Recovery) 4. Precision (Repeatability, Inter-session variability and Intermediate precision). In addition, also proper system suitability criteria should be determined to ensure the goodness of the assay's results.

### 3.3.1.1 Specificity

Two different approaches were used to evaluate the specificity of a cell-based assay: the first approach assess the effects of the Anti-TIGIT matrix on the bioassay while the second strategy verify if the matrix could have an impact on the bioactivity of active drug interfering. The two complementary approaches are summarized in the table below:

**Table 2: Summary of the approach and the acceptance criteria of the specificity study.**

<b>Approach</b>	<ol style="list-style-type: none"> <li>1. <u>Matrix effect on the assay</u>: Anti-TIGIT matrix is diluted as the relevant samples.</li> <li>2. <u>Matrix effect on the active drug</u>: BKAA1801 sample is diluted into Anti-TIGIT matrix up to different concentration levels so as to determine the effect of different matrix dilutions.</li> </ol>
<b>Data analysis</b>	<ol style="list-style-type: none"> <li>1. Linear regression of the response plotted versus each relevant sample concentration.</li> <li>2. Linear regression of the response plotted versus each relevant dilution applied.</li> </ol>
<b>Acceptance criteria</b>	<ol style="list-style-type: none"> <li>1. No matrix interference in Potency calculation: The slope of the regression line is not statistical different from zero (<math>P\text{-value} \leq 0.05</math>)</li> <li>2. No impact on the Potency results: The slope of the regression line is not statistical different from zero (<math>P\text{-value} \leq 0.05</math>).</li> </ol>
<b>No. of runs/Approach</b>	<u>Approach 1</u> : 1 run <u>Approach 2</u> : 2 runs
<b>No. of total runs</b>	3

A detailed explanation on how to verify bioassay's specificity is also given in Chapter 2, section 6.

### 3.3.1.2 Dilutional Linearity

The dilutional linearity study is the core of a method validation and it consists of a series of runs that are required to establish the Linearity, Accuracy, Precision and Range of a bioassay method.

In the table below experimental set up of the experiments is reported. This approach is the same applied during the development of a bioassay with the exception that only one operator is involved so a total of three runs are performed.

**Table 3: Experimental design for the evaluation of the Performance Verification of the Bioassay.** The relevant sample is tested at 50%, 71%, 100%, 141% and 200% of its nominal concentration as suggested by USP<1033> for bioassay linearity evaluation. Three different operators are involved in the study and each of them performs 3 independent runs (total runs = 9) at each concentration level.

<b>Experimental design</b>	A representative sample is tested at 50%, 71%, 100%, 141%, and 200% of its concentration.
<b>No. of Analysts</b>	3
<b>No. of runs/Analyst</b>	3
<b>No. of total runs</b>	9

#### Linearity and Range

From the runs above the linearity and range of the bioassay are determined by following the approach shown in the table 4.

**Table 4: Summary of the approach, data analysis and acceptance criteria of the linearity study.** The linear regression of the potency values (response) obtained for each Anti-TIGIT nominal concentration tested should be analyzed to evaluate bioassay's linearity.

<b>Approach</b>	Linear response among the Potencies at the different levels
<b>Data analysis</b>	Linear regression of the response plotted versus each tested concentration.
<b>Acceptance criteria</b>	$R^2 \geq 0.95$ Variability of each point $CV \leq 25\%$ Relative Bias (%) $\leq 25\%$

In order to demonstrate that the bioassay is linear among the nominal tested concentrations (50%-200%) the  $R^2$  of the linear regression needs to be  $\geq 0.95$  while the variability of each point and the relative bias should be  $\leq 25\%$ . The relative bias is the difference between the observed response and

the response predicted by the fitted model at a given concentration (also defined as analysis of residuals).

### Accuracy

Bioassay's accuracy is evaluated following the approach summarized in the table 5:

**Table 5: Summary of the approach, data analysis and acceptance criteria of the accuracy study.**

<b>Approach</b>	Bias obtained between the measured Potency and the target value for each concentration level.
<b>Data analysis</b>	$\text{Relative bias (\%)} = \left( \frac{\text{Measured Potency}}{\text{Target Potency}} - 1 \right) \times 100$
<b>Acceptance criteria</b>	<p>Relative Bias at the target (100%) <math>\leq 15\%</math></p> $\text{Upper Acceptance Limit (UAL)} = \left( \frac{115}{100} - 1 \right) \times 100 = 15\%$ $\text{Lower Acceptance Limit (LAL)} = \left( \frac{100}{115} - 1 \right) \times 100 = -13\%$ <p>-13% (LAL) <math>\leq</math> 90% confidence intervals for relative bias at each level <math>\leq</math> +15% (UAL)</p>

### Precision

In the table below (table 6) the strategy applied for bioassay's precision evaluation is shown.

**Table 6: Summary of the approach, data analysis and acceptance criteria of the precision study.**

<b>Approach</b>	<p>According to the assay format, the Potency is released as average of three independent runs. These three runs compose the analytical session usually performed by the same operator. Precision is measured as:</p> <ul style="list-style-type: none"> <li>– <u>Repeatability</u>: Intra-session variability</li> <li>– <u>Between analytical session variability</u>: Inter-session variability</li> <li>– <u>Intermediate precision</u>: Total assay variability</li> </ul>
<b>Data analysis</b>	<p>The ANOVA of variance components will be applied to estimate the contribution of multiple factors to the variability of the response when the data are completely nested or hierarchical.</p> <ul style="list-style-type: none"> <li>– <u>Intra-session variability</u>: this value reflects the variability of the method within the analytical session performed for release. The analytical session performed at the QC lab will also be included in this evaluation. It will be calculated as follows:  <math display="block">\%CV \text{ Repeatability} = \frac{\sqrt{\text{Variance of Replicate component}}}{\text{Overall mean}} \times 100</math></li> <li>– <u>Inter-session variability</u>: this value reflects the variability of the method when different results are compared, such as different time points in Stability studies or different samples in Comparability and Biosimilarity exercises. The analytical session performed at the QC lab is also included in this evaluation; consequently, this variability also reflects the Reproducibility. It will be calculated as follows:  <math display="block">\%CV \text{ Between session e Reproducibility} = \frac{\sqrt{\text{Variance of Session component}}}{\text{Overall mean}} \times 100</math></li> <li>– <u>Intermediate precision (IP; Total assay variability)</u>: this value expresses the overall variability from measurements taken under a variety of normal test conditions. It includes different days, different analysts, different equipment, etc. It will be calculated as follows:  <math display="block">\%CV \text{ IP} = \frac{\sqrt{\text{Variance of Replicate component} + \text{Variance of Session component}}}{\text{Overall mean}} \times 100</math></li> <li>– <u>Reproducibility</u>: A complete analytical session (three runs) is performed at QC laboratory and compared with the average of the analytical sessions performed at the source lab. The maximum value obtained is considered for the Reproducibility. This value reflects the variability of the method between laboratories.</li> </ul>
<b>Acceptance Criteria</b>	<p>Repeatability (Intra-session): <math>CV\% \leq 15\%</math> at each level  Between (Inter-sessions) variability: <math>CV\% \leq 15\%</math> at each level  Intermediate Precision: <math>CV\% \leq 15\%</math> at each level  Reproducibility <math>\leq 20\%</math></p> <p>Also, the following criteria has to be met at each level:</p> $\frac{SS - RS}{SS} \times 100 \pm \text{Intermediate precision}$ <p><i>SS = Potency obtained at Source Site; RS = Potency obtained at Receiving Site</i></p>



	Cases in which these criteria are not met should be discussed with the Receiving Lab to evaluate their impact on the outcome of the Reproducibility study.
--	--

### 3.3.1.3 System suitability

In the table below (table 7) the approach for system suitability criteria evaluation is summarized. As per the other validation parameters a deeper explanation can be found in material and methods session.

**Table 7: Summary of the approach, data analysis and acceptance criteria for the evaluation of the System suitability criteria (Goodness of fitting, EC50, Fold increase and similarity parameters).**

<b>Approach</b>	<p>Defining specific ranges of suitable parameters in order to verify that the system is working within the conditions tested during the validation in a way to make the acceptance criteria applicable for each single test.</p> <p>The following parameters are defined as System Suitability criteria:</p> <ul style="list-style-type: none"> <li>– Goodness of fit (<math>R^2</math>) of the dose-response curve of both reference and samples</li> <li>– EC<sub>50</sub> of the reference material</li> <li>– Fold increase of the response (Top/Bottom ratio) of the reference material</li> <li>– Similarity of the dose-response curves</li> </ul>
<b>Data analysis</b>	Ranges are evaluated considering each reference curve generated during the validation study.
<b>Acceptance criteria</b>	<p>To be defined as follows:</p> <ul style="list-style-type: none"> <li>– Goodness of fit (<math>R^2</math>): average <math>-nxSD^*</math> (not less than 0.95), depending on the values distribution</li> <li>– EC<sub>50</sub>: average <math>\pm nxSD^*</math>, depending on the values distribution</li> <li>– Fold increase (Top - Bottom difference): average <math>-nxSD^*</math>, depending on the values distribution (<i>the difference between Top and Bottom will be applied</i>)</li> <li>– Similarity (Top and Slope ratio): average <math>\pm nxSD^*</math>, depending on the values distribution</li> </ul> <p>Should the variability be so high not to allow the SD* approach (negative values or too wide range), the Min and Max values obtained will be considered.</p> <p>*SD= standard deviation</p>

### 3.3.2 Cell Based Ligand Binding Bioassay

The following procedure describes the in-vitro method used for the determination of the biological activity of the Anti-TIGIT samples that has been developed and validated in the frame of this work. The method is based on the ability of Anti-TIGIT antibody to bind in a dose-dependent manner to the TIGIT expressed by the CHO-S-myc-huTIGIT ECD cells.

Below the main solutions and reagents used in this assay are listed:

- Protein A coating solution: Protein A stock solution is diluted in D-PBS 1X without  $\text{Ca}^{2+}$  and  $\text{Mg}^{2+}$  until reaching a final working concentration of 5  $\mu\text{g/mL}$ .
- Blocking Buffer/Assay buffer (AB): 1.5% BSA in D-PBS 1X without  $\text{Ca}^{2+}$  and  $\text{Mg}^{2+}$ .
- Washing Buffer (WB): 1X D-PBS without  $\text{Ca}^{2+}$  and  $\text{Mg}^{2+}$  and 0.05% Tween 20.
- ATPLite solution: 50% Cell Titer Glo and 50% D-PBS 1X without  $\text{Ca}^{2+}$  and  $\text{Mg}^{2+}$ .

The analytical procedure is schematized in the figure 14:

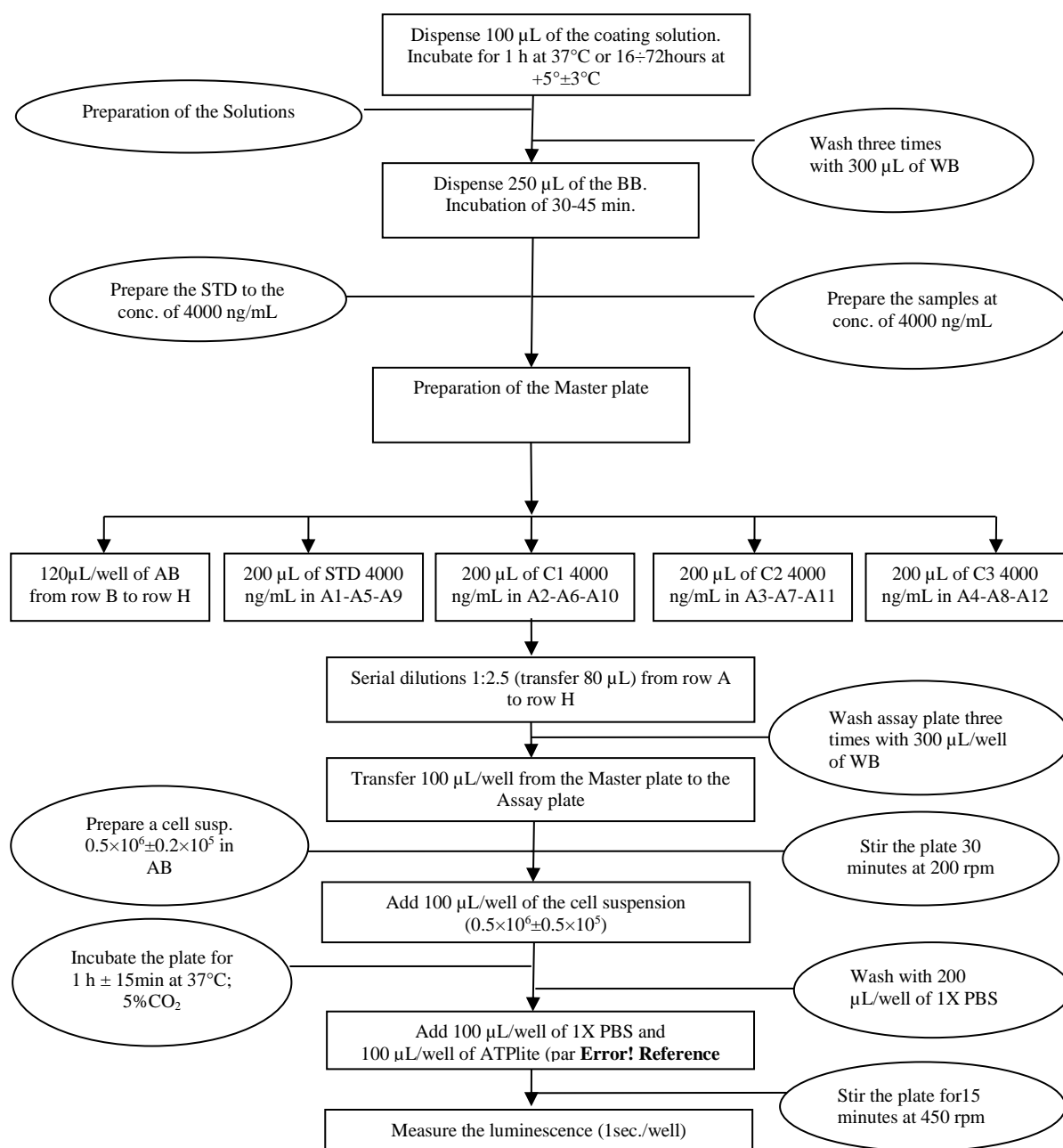


**Figure 14: Schematic representation of the bioassay workflow.** The step-by-step protocol for Anti-TIGIT ligand binding bioassay, established after method validation, is shown. The bioassay plate layout foresees that samples are allocated to columns and dose levels are assigned to rows.

Abbreviations: BB= blocking buffer; AB = assay buffer; WB = washing buffer; cell susp. = cell suspension; STD = assay standard

For data analysis the signal (expressed as count per second, cps) is plotted against the Log of Anti-TIGIT concentrations and fitted by 4 Parameter Logistic Marquadt algorithm (4PL) on transformed concentrations in Log10. Data processing and graphing have been performed by using the GraphPad

Prism software. In the electronic spreadsheet of the GraphPad Prism software were inserted the concentration values of Anti-TIGIT in ng/mL in the abscissa column (x) and the CPS values obtained for the Standard and the samples under testing in the ordinate column (y). The relative values of the EC<sub>50</sub> for the Standard and the samples under analysis are directly derived from the “Table of Results” that appears at the end of the described operations. The values of Top, Bottom and Slope are calculated by dividing the values obtained from the standard curve by the values obtained from the samples under analysis. The concentration of Anti-TIGIT that is able to induce 50% of the maximum effect (EC<sub>50</sub>) is calculated. The biological activity of a sample (potency) is expressed as % of activity with respect to a reference material as per the following equation:

$\text{Potency}_{\text{campione}} = \frac{\text{EC}_{50\text{standard}}}{\text{EC}_{50\text{campione}}} \times 100$	EC <sub>50</sub> standard	EC <sub>50</sub> obtained by the Standard
	EC <sub>50</sub> sample	EC <sub>50</sub> obtained by the sample

The sample potency is released as the average of results obtained in three independent experiments.

### 3.3.3 Anti-TIGIT competitive ELISA assay

The following procedure describes the ELISA method developed for the determination of the biological activity of the Anti-TIGIT samples as an alternative assay to the CBA assay.

The enzyme-linked immunosorbent assay (ELISA) is a commonly used analytical biochemistry assay for detecting and quantifying a specific protein in a complex mixture originally described by Engvall and Perlmann (1971). ELISAs are typically performed in 96-well or 384-well polystyrene plates, which passively bind antibodies and proteins. It is this binding and immobilization of reagents that makes ELISAs easy to design and perform. Having the reactants of the ELISA immobilized to the microplate surface makes it easy to separate bound from non-bound material through several washing steps during the assay. There are several formats used for ELISAs, for our assay we selected the competitive ELISA format. The method consists in a competition between a labeled molecule (biotinylated CD155) and Anti-TIGIT mAb for the binding to the antigen (TIGIT) captured on the plate. A decrease in signal will indicate the binding of Anti-TIGIT mAb to the antigen molecules when compared to assay wells with labeled molecule alone.

Below the main reagents and solutions used in this assay are listed:

- Recombinant Human CD155/PVR Fc Chimera Biotin Protein, CF (BIO-TECHNE)
- Human TIGIT/VSTM3 Protein His-Tag (Sino Biological)

- Coating buffer: Human TIGIT/VSTM3 Protein His-Tag stock solution is diluted in D-PBS 1X without  $\text{Ca}^{2+}$  and  $\text{Mg}^{2+}$  until reaching a final working concentration of 1  $\mu\text{g/mL}$ .
- Washing buffer: 1X D-PBS without  $\text{Ca}^{2+}$  and  $\text{Mg}^{2+}$  and 0.05% Tween 20.
- Blocking buffer: 1X D-PBS without  $\text{Ca}^{2+}$  and  $\text{Mg}^{2+}$ , 1% of 7.5% BSA.
- Assay buffer: 1X D-PBS without  $\text{Ca}^{2+}$  and  $\text{Mg}^{2+}$  and 1% of 7.5% BSA.

The analytical procedure after the optimization stage is schematized in the workflow in figure 15:

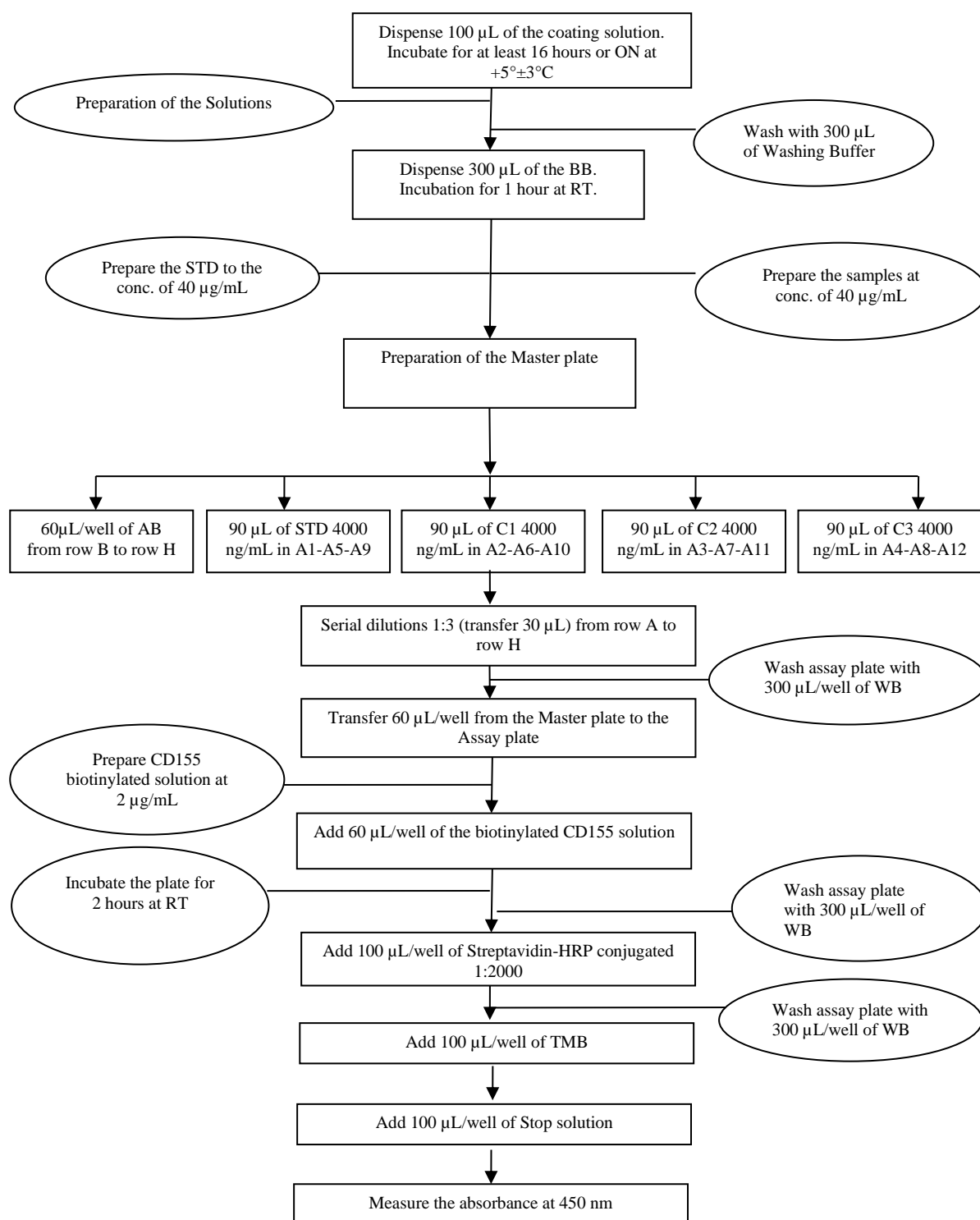


**Figure 15: Schematic representation of the Anti-TIGIT Sandwich ELISA assay.** In the picture the main steps of the bioassay are depicted. The first passage is the 96-well plate coating with TIGIT followed by the addition of Anti-TIGIT dose response curve and a fixed concentration of biotinylated CD155 that competes with the mAb for the binding to TIGIT. After 2 hours of incubation at room temperature, the assay plate is washed three times before the incubation with TMB solution. After 5 minutes the chemiluminescence is

detected. The signal will be inversely proportional to the quantity of Anti-TIGIT bound to TIGIT on the plate wells since the Streptavidin HRP will detect only the biotinylated CD155 bound to the antigen. After each step washing steps are foreseen to ensure that only specific (high affinity) binding events are maintained to cause signal at the final step.

The data are elaborated using a graphing software such as GraphPad PRISM. The data is fitted to the function 'log(inhibitor) vs. response -- Variable slope' with the goal to determine the IC<sub>50</sub> of the inhibitor meaning the concentration that provokes a response half way between the maximal (Top) response and the maximally inhibited (Bottom) response as shown in the representative figure below (figure 16).

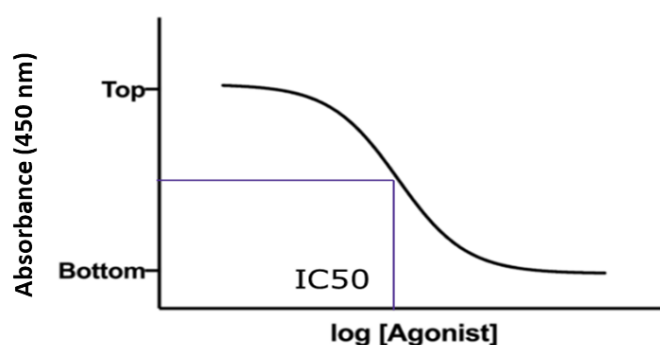


**Figure 16: A typical dose response curve of the competitive ELISA assay.** The curve is obtained by measuring the optical densities (OD) at 450 nm and plotting them against the logarithm of the agonist concentration. The IC<sub>50</sub> is the concentration of agonist that gives a response halfway between Bottom and Top.

This model does not assume a standard slope but rather fits the Hill Slope from the data, and therefore is called a variable slope model. It is also called a four-parameter logistic curve (4PL) and is described by the following equation:

$$Y = \frac{(A-D)}{\left(1 + \left(\frac{x}{C}\right)^B\right)} + D$$

Where Y is the response, A is the minimum value that can be obtained (Bottom of the dose response curve), D is the maximum value that can be obtained (Top of the dose response curve), C is the inflection point (or IC<sub>50</sub>), B is the Hill slope and x is the analyte concentration (White et al., 2019). For a detailed explanation of the 4PL model see paragraph 1.7 “Bioassay Development and Validation” of this work.

The potency of the tested sample is determined by dividing the IC<sub>50</sub> of the Standard dose response curve with the IC<sub>50</sub> of the sample as follows:

$\text{Potency}_{\text{campione}} = \frac{\text{IC}_{50\text{standard}}}{\text{IC}_{50\text{campione}}} \times 100$	<b>IC<sub>50</sub>standard</b>	IC <sub>50</sub> obtained by the Standard
	<b>IC<sub>50</sub>sample</b>	IC <sub>50</sub> obtained by the sample

The sample final potency is released as the average of results obtained in three independent experiments.

### 3.3.4 TIGIT/CD155 Blockade Bioassay

The following procedure describes the TIGIT/CD155 Blockade Bioassay that has been used as a starting point for the development of a cell-based assay for the determination of the biological activity of the Anti-TIGIT samples that is more reflecting the MOA of the drug. To this aim, the TIGIT/CD155 Blockade Bioassay, Propagation Model (cat n° J2092) from Promega was used.

The reagents used and protocols that were followed for this assay were the one supplied by the manufacturer. As it is shown in chapter 3, section 4 the optimization of this assay for the establishment of a new cell-based assay for Anti-TIGIT was stopped for the difficulties encountered during the experiments.

### 3.3.5 Antibody-dependent cellular cytotoxicity assay

The Antibody-dependent cellular cytotoxicity (ADCC) Reporter Gene Assay measures reporter gene signal generated by ADCC pathway activation in engineered Jurkat T effector cells. The effector cells were provided by Promega (cat # G7102) as previously discussed in this chapter (2.2.4) of this chapter. As target cells the CHO-S-myc-huTIGIT ECD (paragraph 2.2.1 of this chapter) were used from #15 to #29. All the reagents used are the ones recommended by supplier's protocols.

The Promega bioassay has been optimized and qualified in the frame of this work as follow.

First CHO-S-myc-huTIGIT ECD are centrifuged and resuspended at  $0.3 \times 10^6$  cells/mL. Then 12000 cells/well of this suspension are added in a 96 well white plate. Anti-TIGIT standard and samples are diluted in polypropylene tubes to a final concentration of 20000 ng/mL. Then Anti-TIGIT reference and samples dose response curves ranging from 30000 ng/mL to 0.096 ng/mL are prepared in the master plate before to transfer them to the assay plate with CHO cells. Jurkat effector cells are then centrifuged at 190 g x 10 minutes and resuspended at  $3.75 \times 10^6$  cells/mL. Then, 150,000 cells/well



of this suspension are added in the plate obtaining a target/effector cells (T/E) ratio of 1:12.5. The plate is incubated for 24 hours in incubator at +37°C with 5% CO<sub>2</sub>.

The final Anti-TIGIT dose response curves range from 10000 ng/mL to 0.032 ng/mL.

The next day, 120 µL/well of the BioGlo Reagent are added to the plate and the emitted luminescence is measured (1 second/well) with a Luminescence counter (Tecan Infinite F200).

For data analysis Anti-TIGIT concentrations (X values) are Log10 transformed and the analytical response (Y value) expressed as cps. The dose response curve of Reference Standard and samples are fitted by 4PL and the Anti TIGIT concentration able to induce an ADCC Activity on the CHO-S-myc-huTIGIT ECD cells at 50% of the maximum possible (EC50) is automatically calculated using the Graphpad Prism software.

The ADCC activity of a sample is expressed as % of activity with respect to a reference material as per the following equation:

$\text{Potency}_{\text{campione}} = \frac{\text{EC}_{50\text{standard}}}{\text{EC}_{50\text{campione}}} \times 100$	EC <sub>50</sub> standard	EC <sub>50</sub> obtained by the Standard
	EC <sub>50</sub> sample	EC <sub>50</sub> obtained by the sample

The sample potency is released as the average of results obtained in three independent experiments.

### 3.4 Stressed samples preparation

To confirm the stability indicating properties of the qualified cell-based assays the following stressed samples were prepared starting from Anti-TIGIT drug substance (DS) batch BKAA1801-BDS.

**Table 8: List of the stressed samples tested in this study together with their measured protein content.**

Sample	Concentration mg/mL
Anti-TIGIT Reference material IRS 2018/01	19.42
Thermal stress +50 °C for 8 Weeks	19.66
Thermal stress +40 °C for 8 Weeks	19.08
Deglycosylated	15.51
Oxidized	17.81

Below the stressing protocol are summarized:

**Oxidation:** In a certain volume of DS 2 volumes of 1% hydrogen peroxide were added to yield a solution 0.33% in hydrogen peroxide. The sample was incubated 60 minutes at room temperature. At the end of incubation time, the reaction was quenched with a 0.3 M Methionine solution in a way to obtain a 40 mM final concentration of Methionine within the sample. Then the sample was buffer exchanged 5 times in a ratio 1:5 with buffer and finally concentrated to the starting volume. In order to purify the sample, the proper dimensions and cut-off Amicon Ultra characteristics fit for the experimental purposes must be chosen.

In order to choose the Amicon membrane with the fit cut-off it is necessary to consider the molecular weight (MW) of the molecule ( $MW \gg$  Amicon cut-off) and the attitude of the molecule to generate fragments and the dimensions of the fragments that can originate and that could be lost in case the membrane filter has a too high porosity.

Moreover, the aim of the study and thus the impact that the possible removal of fragments through the purification procedure might have on the study conclusions need to be taken in to account.

The most employed cut-off available have a membrane with a porosity for 3, 10, 30, 50, 100 kDa.

In addition, dependently on the sample volume that needs to be treated, the Amicon with the dimensions fit for the purpose according to the following Table (table 9) should be chosen.

**Table 9: Different Amicon formats.** Depending on the sample to be buffer exchanged, its MW and the purpose of the experiment a specific Amicon should be selected.

Amicon	Format	Minimum Volume Capacity	Maximum Volume Capacity	Volume Range of the Sample under Treatment
Amicon Ultra-2	2 mL Eppendorf	70 $\mu$ L	500 $\mu$ L	100-125 $\mu$ L
Amicon Ultra-4	15 mL Falcon	100 $\mu$ L	4 mL	125-1000 $\mu$ L
Amicon Ultra-15	50 mL Falcon	300 $\mu$ L	15 mL	1-3.75 mL

For the procedure on how to use Amicon Ultra Centrifugal filters see supplier's protocol.

**Deglycosylation:** Deglycosylation is commonly performed via an enzymatic reaction with N-Glycosidase F (PNGase-F), an enzyme able to hydrolyze the N-glycosidic bond between Asparagine residues and GlcNAc residues. In of 700 µg DS sample was added an equal volume of 0.2M Tris buffer pH 8.5 and 0.25 U (100 µL) of PNGase-F enzyme, where PNGase-F is added in excess considering that 1 U (400 µL) is able to deglycosylate 18 g of mAb with 2 N-Glycosylation sites in 4 hours. As the PNGase-F enzyme has a molecular weight of 35 kDa, the enzyme can only be removed with an Amicon with a cutoff of 50 kDa or larger, as long as the protein of interest has a molecular weight above 50 kDa like Anti-TIGIT. In case the protein has a molecular weight below 50 kDa or if the generation of low molecular weight species is expected and it is relevant to the study, a purification approach (described below) by protein A cartridge, able to bind proteins with a Fc portion, should be employed. In a third event where the protein of interest has a molecular weight below 50 kDa and does not have a Fc portion, it is necessary to employ other purification approaches such as a semi-prep ion exchange or a purification by SEC. The above-mentioned cases are summarized in the following Table (table 10).

**Table 10: Purification procedures summary.** Based on the molecular weight of the sample, the three main modes on how to purify deglycosylated samples are shown.

MW of the Molecule under study	Purification Procedure	Usage note
> 50 kDa	Amicon with 50 kDa cut-off	In the case where the formation of fragments during the stress procedure <b>is not</b> relevant to the study aim
	Protein A Cartridge	In the case where the formation of fragments during the stress procedure <b>is</b> relevant to the study aim
< 50 kDa	Protein A Cartridge	Molecule <b>with</b> an Fc portion
	Semi-prep IE or SEC	Molecule <b>without</b> an Fc portion

Purification procedure with Protein A cartridge: dependently on the sample volume to purify, cartridge with different size can be employed (1 mL or 5 mL). For additional details on the purification procedure and on the cartridge characteristics, dependently on the volume of the sample to be purified, refer to the cartridge User Manual.

The sample fractions are then screened by Nanodrop for the sample concentration and the aliquots containing protein are joined together and are then buffer exchanged with the respective placebo as described before and concentrated to the starting volume.

Thermal stressing: The sample was kept at +40°C ±3°C and +50°C±3°C for 8 weeks.

#### Concentration determination by NanoDrop

After all degradation procedures the protein concentration of the stressed samples was verified by measuring the absorbance at 280 nm (A<sub>280</sub>) with NanoDrop Spectrophotometer.

Three different lectures of each sample should be performed and then the final concentration is calculated using the following formula:

$$\text{Sample Concentration} \left( \frac{\text{mg}}{\text{mL}} \right) = \frac{\frac{[A_{280}(1) + A_{280}(2) + A_{280}(3)]}{3}}{\epsilon \left( \frac{\text{mL}}{\text{mg} * \text{cm}} \right) * l (\text{cm})}$$

Where A<sub>280</sub> is the absorbance of the sample at 280 nm,  $\epsilon_{280}$  is the molecule extinction coefficient and I is the pathlength.

### **3.5 Assays for predictive pharmacokinetic analysis**

Two different assays to study the predictive pharmacokinetic (PK) of biotherapeutic drugs were developed in the frame of this PhD study. The essentials of these (after the validation or qualification step) and the appropriate calibrations are described in this section.

#### **3.5.1 SPR based methods**

In the following paragraph the in-vitro method used to analyze the interaction and binding affinity (expressed as equilibrium dissociation constant,  $K_D$ ) between Anti-TIGIT samples and Neonatal Fc receptor (FcRn) is described. This is not a mere standard procedure, but it has been optimized in the frame of this work. Binding kinetics of Anti-TIGIT reference material against human FcRn was measured at pH 6.0 at +25°C using a Biacore T200 from GE Healthcare. The method is based on surface plasmon resonance principles, an optical technique that measures changes in refractive index near a metal surface over time as shown in figure 17 A. In a typical SPR experiment, one molecule (the Ligand) is immobilized to a sensor chip and binding to a second molecule (the Analyte) is measured under flow. Response is measured in resonance units (RU) and is proportional to the mass and refractive index on the surface of the biosensor. For any given interactant, the response is proportional to the number of molecules bound to the surface. Response is recorded and displayed on a sensorgram in real time as seen in figure 17 C.

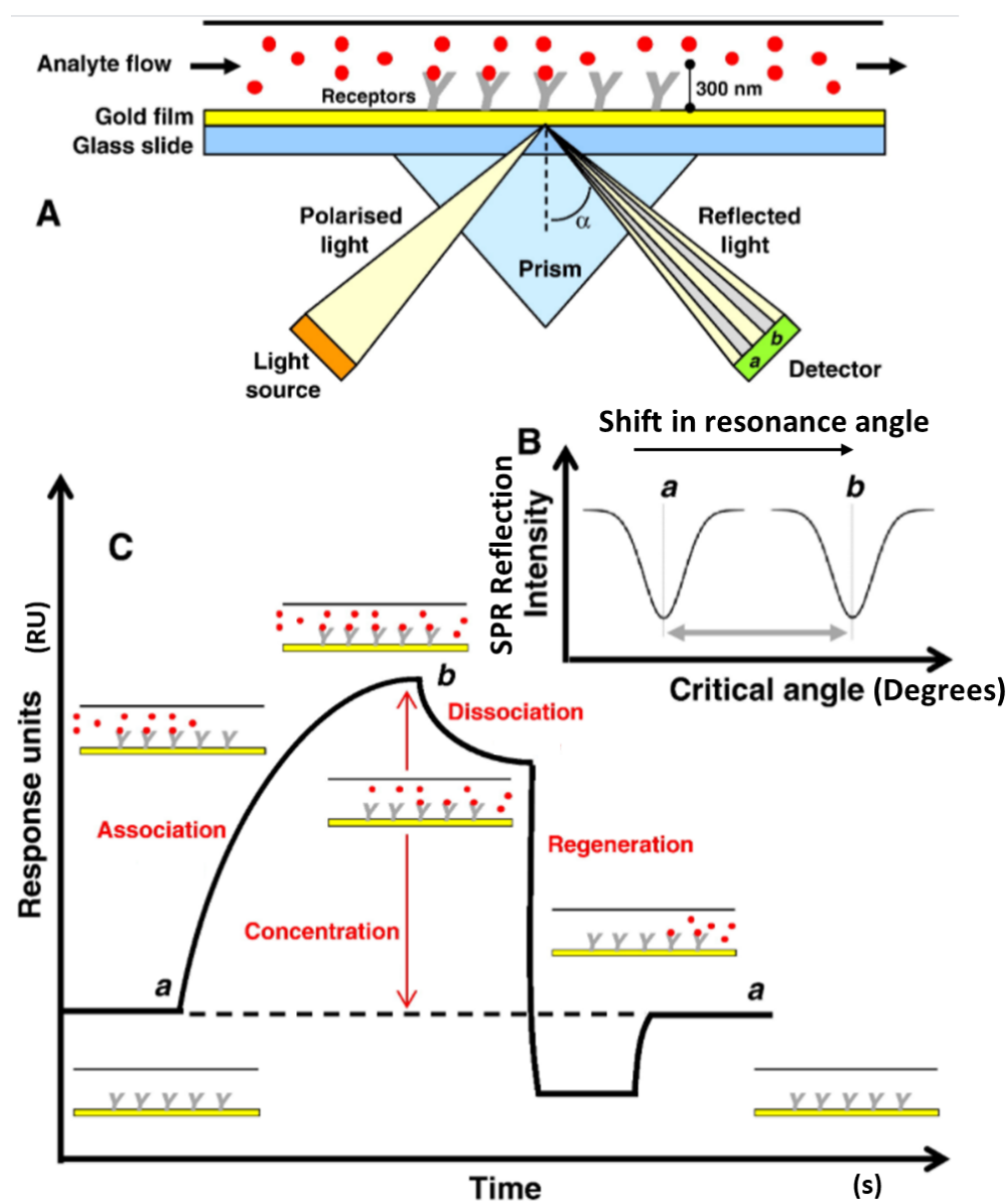


**Figure 17: Illustration of the Basic Principle of an SPR measurement of the binding of an analyte molecule to a receptor molecule.** A) A standard Biacore instrument set up for an SPR experiment is shown. The underlying principle of an SPR measurement is to attach (immobilize) a molecule termed ligand onto a sensor chip surface and measure the change in refractive index of the surface when another molecule (interaction partner called analyte), injected through an aqueous solution, binds to it. The SPR phenomenon occurs on the surface of a conducting material (such as gold or other metals) at the interface of two media (usually glass and liquid) when it is illuminated by a polarized light at a specific angle. As shown above, when a beam of incident polarized monochromatic light is shone through a prism at a thin-layer of gold coating one surface of a glass sensor chip, the prism causes the light to be reflected at the gold-coated surface. At a particular angle of incidence, absorption of some of the light by the electrons in the gold excites charged density waves, called "surface plasmons", which propagate along the metal surface. Plasmon

resonance leads to a reduction in the intensity of the reflected light at that specific angle known as resonance angle. B) Change in the critical angle of incident light from angle  $a$  to angle  $b$  on binding of an analyte molecule to a receptor molecule. The angle at which the intensity of refracted light is most significantly reduced (resonance angle) depends not only on the gold layer but also occurs as a function of the refractive index of the medium just above the gold surface i.e. the running buffer. SPR is thus highly sensitive to changes in the environment close to the gold-aqueous solution interface. A change in the refraction index at the surface of the sensor (due to for example analyte binding or dissociation occurring near the surface) may hence be monitored as a shift in the resonance angle and is recorded as a sensorgram (C). If interaction between the immobilized receptor molecule and the analyte molecule occurs, the refractive index at the surface of the gold film changes and this is seen as an increase in signal intensity. Resonance or response units (RU) are used to describe the increase in the signal, where 1 RU is equal to a critical angle shift of  $10^{-4}$  deg. At the start of the experiment all immobilized receptor molecules have not been exposed to analyte molecules and the RU correspond to the starting critical angle  $a$  (baseline in the sensorgram). Analyte molecules are injected into the flow cell; if they bind to the immobilized ligand molecules, there is an association phase during which binding sites become occupied and the shape of this curve can be used to measure the rate of association. When a steady state is achieved (all binding sites occupied) the RU correspond to the changed final critical angle  $b$  (maximum of response). This maximum RU relates to the concentrations of immobilized receptor and analyte molecules and so can be used to measure the binding affinity (KD). When analyte molecules are removed from the continuous flow there is the dissociation phase during which binding sites become free and the shape of this curve can be used to measure the rate of dissociation. The surface can then be regenerated and returned to the critical angle  $a$  to start the experiment again.

Modified from Patching 2014.

### Old SPR-based method

Before entering in detail in the novel SPR-based technique developed and qualified during this PhD project, the main features of the old reference SPR method are highlighted in the figure below (figure 18).

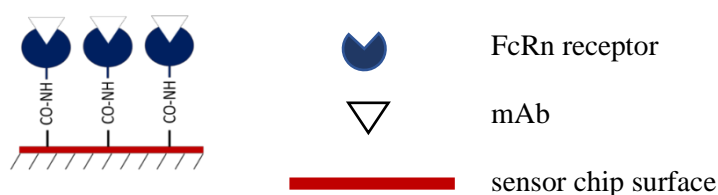


**Figure 18: Representative layout of SPR method.** FcRn is bound to the sensor chip and the mAb is flowed on the receptor.

Briefly, the SPR-method layout foresees the direct immobilization of FcRn (ligand) on a sensor chip surface and the IgG (analyte) injection over the immobilized ligand at different concentrations through a multi-cycle analysis. Each injection of analyte concentration is done in a separate cycle. This means that the surface is regenerated at each cycle by reverting the binding between FcRn and IgG, as shown in Figure 19. At the end of the analysis, all the curves are put together in one sensorgram as displayed in figure 20.

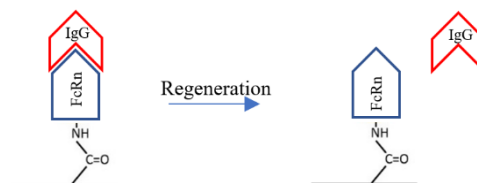


**Figure 19: Representation of regeneration step.** The regeneration procedure foresees the removal of the analyte from the ligand bound on the sensor chip. It is important to choose the mildest regeneration conditions that completely dissociate the complex. Moreover, the selected regeneration conditions must not cause damage to the ligand. The most frequent method used is to inject a low pH-buffer such as 10 mM Glycine pH 1.5-2.5. This works probably because most proteins become partly unfolded and positively charged at low pH. Protein binding sites will repel each other, and the unfolding will bring the molecules further apart.



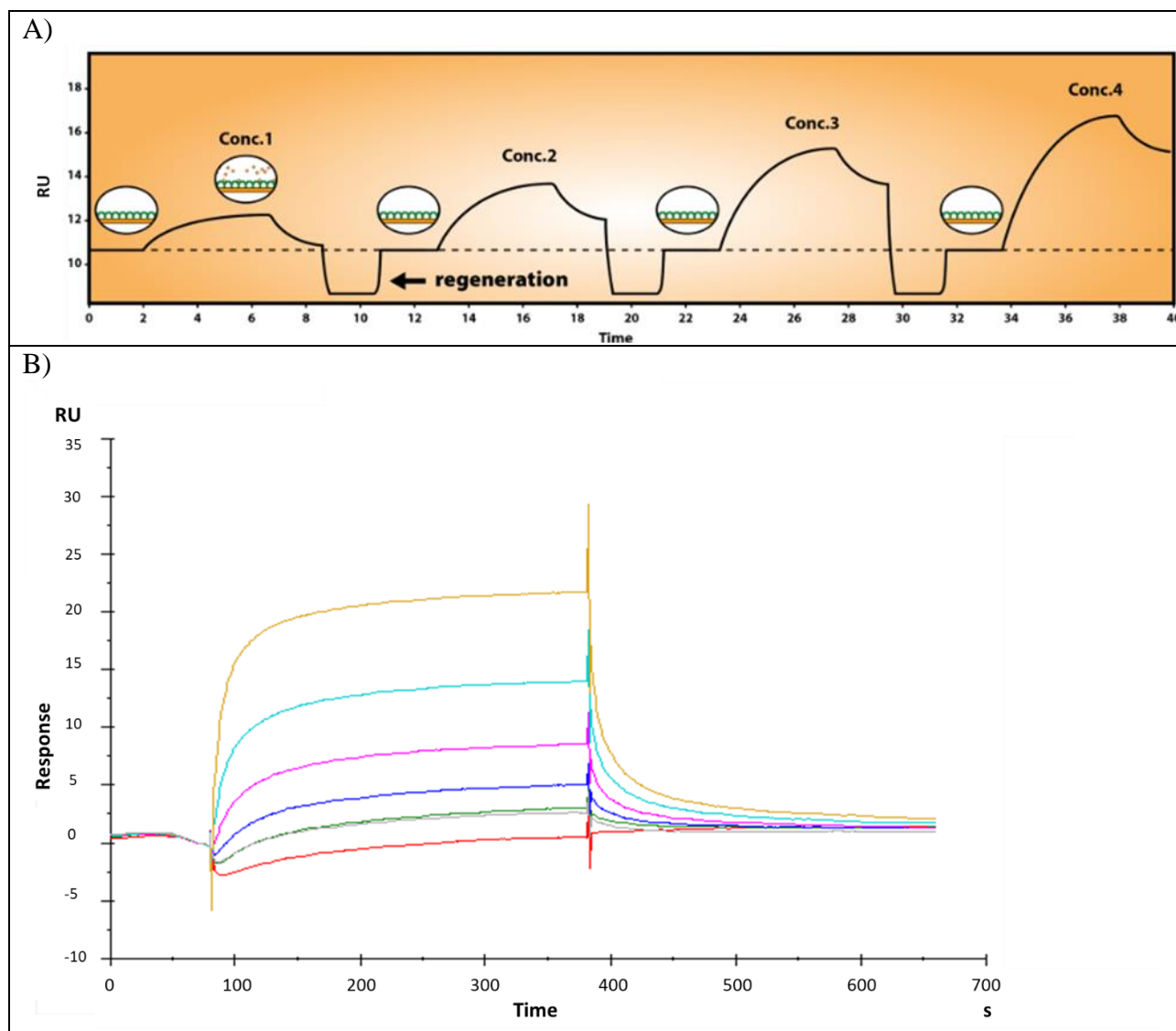


**Figure 20: Example of a multi cycle kinetics analysis.** A) In a multi cycle kinetic experiment, the analyte sample is injected over the surface with immobilized ligand. After sample injection (Conc. 1), the analyte is let to dissociate. Rest of the bound analyte is removed by injecting a suitable regeneration solution. After that, next sample concentration (indicated as Conc. 2) is injected in a similar manner as the first sample. Abbreviations: Conc. = concentration

From <https://www.bionavis.com/en/life-science/technology/kinetictitration/>

B) Representative sensorgram of multi-cycle analysis generated with current SPR method performed in the company. The different concentrations of the analyte injected over the ligand are represented with different colors. Each sensorgram is obtained through separated analysis by injecting each analyte concentration over the immobilized FcRn. All mAb responses at different concentrations are expressed as relative unit (RU) monitored over time (s).

Considering that during the different analytical cycles the immobilized ligand loses activity,  $R_{max}$  local is used as fitting parameter in order to mitigate the decreasing trend of the signal in KD evaluation. The obtained sensorgram is elaborated using the “two state reaction” fitting model in order to determine the KD value for the FcRn/IgG complex. A detailed explanation of this fitting model will be given later in this work in the section 5.1.2.

#### New SPR-based method

The development of this new SPR-based method is one goal of the present research project. The details of the procedures and the list of the main reagents and solutions are provided below:

- HBS-EP + buffer 10X (GE Healthcare)
- Series S Sensor Chip CM5 (GE Healthcare)
- Amine coupling kit (GE Healthcare)
- Tetra His Antibody, BSA-free (Quiagen)
- Human FcRn/FCGRT/B2M, His-Tag, Biotin-labeled (BPS Bioscience)
- Streptavidin Recombinant Protein, His-Tag (Abnova)
- Running and sample dilution buffer: it is a solution of 50mM NaPO<sub>4</sub>, 150 mM NaCl and 0.05% Tween20 pH 6.0. Once prepared, filter the solution with a 0.22 µm membrane before use.

To determine Anti-TIGIT/FcRn binding affinity, a double capturing approach is used. In particular, biotinylated FcRn is used as ligand; its biotin tag portion is captured by His Tagged Streptavidin that is captured by the Tetra His Antibody immobilized through amine coupling on to the sensor surface. Below the main parameters of the optimized SPR method are summarized (table 11).

**Table 11: Main parameters of the optimized method**

<b>Biacore instrument</b>	Biacore T200
<b>Sensor Chip</b>	Series S Sensor Chip CM5
<b>Flow cell 1</b>	It is used as reference flow cell (with no immobilized ligand)
<b>Flow cell 2</b>	It is the measurement flow cell (functionalized flow cell)
<b>Flow rate</b>	10 $\mu$ L/min
<b>Approach</b>	Single kinetic approach
<b>Startup</b>	10 cycles
<b>Capturing molecules</b>	Tetra His Antibody 20 $\mu$ g/mL + His tagged Streptavidin 8 $\mu$ g/mL
<b>Ligand</b>	Biotinylated FcRn 3 $\mu$ g/mL
<b>Analyte</b>	Anti-TIGIT mAb
<b>Analyte concentrations</b>	From 400mM to 25 mM (step dil 1:2)
<b>Running buffer</b>	50 mM NaPO <sub>4</sub> , 150 mM NaCl and 0.05% P20 pH 6.0
<b>Regeneration buffer 1</b>	10 mM pH 2.0 Glycine-HCl
<b>Regeneration buffer 2</b>	3 M Guanidine Hydrochloride

In details, the Tetra His Antibody was immobilized by amine coupling onto Biacore CM5 sensor chip. The running buffer for the immobilization procedure was HBS-EP+ pH 7.4. For each flow cell (measurement and reference flow cells) the surface is activated using the manufacturer's instructions. After the immobilization step and before the analysis, the buffer must be switched from the immobilization buffer to the running buffer. The following step is the chip conditioning with capturing solutions. This step is aimed at identifying the working concentrations of the two capturing solutions, FcRn and Streptavidin, in order to have a FcRn capture level in the range of 200-400 RU (relative units). Starting using FcRn 3  $\mu$ g/mL and Streptavidin 8  $\mu$ g/mL. Depending on the reagent lots used these conditions may need to be adjusted. For both FcRn and Streptavidin the contact time is 60 seconds and the flow rate selected is 5  $\mu$ L/min.

Flow cell 1 is prepared as a blank surface (reference flow cell) and therefore is prepared by omitting the FcRn capturing step (no ligand injection). Flow cell 2 (measurement flow cell) instead contained also the captured FcRn. Before adding the analyte, it is necessary to perform 10 start-up cycles for system equilibration. Start-up cycles are identical to analysis cycles except that the sample is replaced by running buffer. This because the response from a newly prepared sensor chip often could show some instability during the first few cycles, and start-up cycles allow the response to stabilize to a baseline before the first analysis cycle is performed.

Then Anti-TIGIT reference material and samples (analytes) are diluted into running buffer and a serial dilution was created with a 2-fold dilution factor to give five concentrations of 25, 50, 100, 200 and 400 nM. Anti-TIGIT or buffer was injected for 3-minutes at 30  $\mu$ L/min and dissociation time is set at 2 minutes. The buffer blanks were used to double-reference the analyte binding data before

fitting. At the end of each cycle two regeneration steps are performed: Glycine pH 2.0 is flowed for 30 seconds at 30  $\mu\text{L}/\text{min}$  while 3M Guanidine for 15 seconds at the same flow rate to remove ligand together with the bound molecules. This way the capturing molecule is ready to bind fresh ligand in the next cycle.

Data evaluation is performed with Biacore T200 evaluation software by using as evaluation algorithm the “Two state reaction”. An example of the result obtained is shown in the figure below (figure 21).

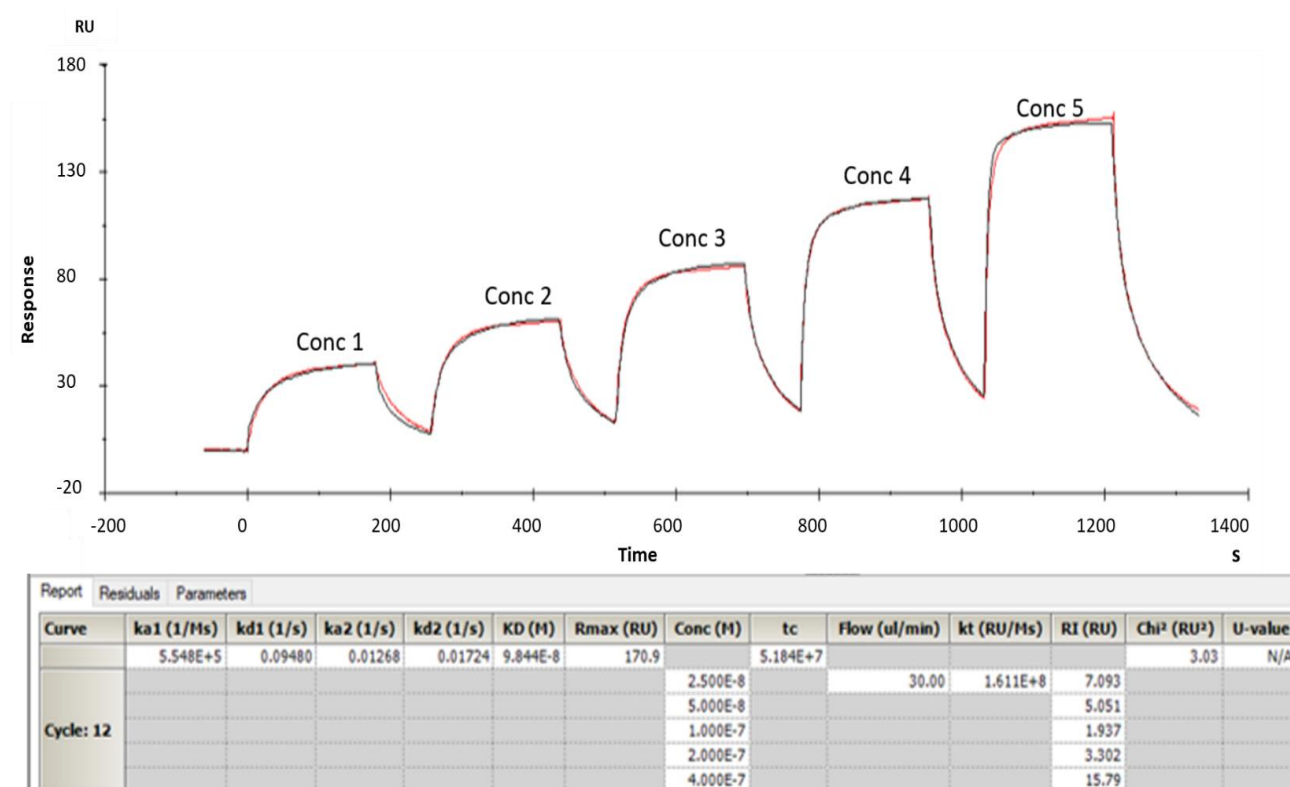


**Figure 21: A representative example of the results obtained at the end of SPR analysis.** In the figure the Anti-TIGIT reference material sensorgram run at the beginning of the analysis is shown. In red is graphed the experimental sensorgram while in black the sensorgram fitted by the software. As expected, when the concentration of the Anti-TIGIT injected increased (from conc 1 to conc 5), the generated signal increased accordingly sine there is more Anti-TIGIT bound to FcRn. In the table on the bottom all the main data retrieved from the analysis after the elaboration with Biacore software are highlighted. Abbreviations: ka= association rate constant, kd= dissociation rate constant, KD= equilibrium dissociation constant, Rmax= maximum response, Conc = concentration expressed in M, tc= flow rate-independent component of the mass transfer constant, kt= transfer constant, RI= refractive index.

Samples results are generated as Relative Binding (KD%) versus the reference material, according to the following formula:

$$\text{KD (\%)} = (\text{KD Reference material} / \text{KD sample}) * 100$$

The final sample KD% is released as the average of results obtained in two independent analytical runs.

### 3.5.2 AlphaScreen technology

AlphaScreen is a bead-based, non-radioactive Amplified Luminescent Proximity Homogeneous Assay. Alpha technology is based on mode of energy transfer prevailing between Donor and Acceptor beads based on singlet oxygen. Singlet oxygen lifetime allows this molecule to travel up to 200 nm in solution before decaying to its ground state, hence offering an unsurpassed equivalent distance for proximity. The assay format comprises two discrete ligand - or receptor - coated polystyrene beads, designated as “Donor” and “Acceptor” beads, which form pairs in the presence of analyte. The pairs must be within about 200 nm for a chemiluminescent signal to be generated. Donor beads contain a photosensitizing agent (phthalocyanine) that excites ambient oxygen to a singlet state when irradiated at 680 nm (Eglen et al., 2008). Excitation of each Donor bead generates approximately 60,000 oxygen singlets per second, resulting in a highly amplified response upon interaction with Acceptor beads. A schematic representation of the assay principle is graphed below (Figure 22):

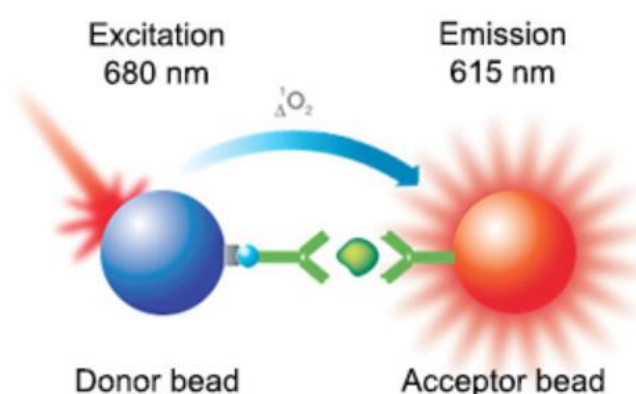


**Figure 22: Schematic representation of Alpha technology.** The Alpha bead-based technology relies on PerkinElmer's exclusive amplified luminescent proximity homogeneous assay (AlphaScreen®) and uses a luminescent oxygen-channeling chemistry. An antibody to the analyte or a generic conjugated or tagged protein binds to the donor beads and a second antibody to the analyte is directly conjugated to Alpha acceptor beads. In the presence of the analyte, the two beads come into close proximity. The excitation of the donor beads at 680 nm generates singlet oxygen molecules that trigger a series of chemical reactions in the acceptor beads resulting in a sharp peak of light emission at 615 nm.

From: <https://beantownbiotech.com/home/assays/alphascreen-and-alphalisa/>

In all AlphaScreen assays, the Acceptor beads comprehend three chemical dyes: thioxene, anthracene and rubrene. Thioxene reacts with singlet oxygen to produce light energy at a wavelength of 370 nm, which is then transferred to anthracene and subsequently to rubrene that emits light at wavelengths of 520-620 nm.

An AlphaScreen method has been qualified in this work as an orthogonal method to SPR to analyze the interaction between an IgG1 and Fc neonatal receptor (FcRn). To this aim, FcRn is used as ligand, captured by Nickel Chelate Donor beads by its His-tagged tail. Anti-TIGIT is used as analyte, diluted in a range from 15nM to 0.0375nM and captured by Acceptor beads coated with anti-whole IgG Fab fragment.

Below the main reagents and solutions used in this assay are listed:

- AffiniPure F(ab')<sub>2</sub> Fragment Rabbit Anti-Human IgG (H+L) (Jackson ImmunoResearch)
- AlphaScreen Unconjugated Acceptor Beads, 5 mg (Perkin Elmer)
- Nickel Chelate Alpha Donor beads, 1 mg (Perkin Elmer)
- Human FCGRT & B2M Heterodimer Protein, His tag (Sino Biological)
- Assay buffer: It is a solution of 50 mM NaPO<sub>4</sub>, 75 mM NaCl and 0.05% P20 pH 5.8. Once prepared, the solution should be filtered with a 0.22 µm membrane. Prior to use add casein to a final concentration of 0.1%.

All the measurements were performed by using the EnVision plate reader from Perkin Elmer.

Before the binding affinity assay, the conjugation of the F(ab')<sub>2</sub> Fragment Anti-Human IgG to the Acceptor beads is performed accordingly to manufacturer's instruction. Beads suspensions are handled and loaded under dim light and kept protected from light using aluminum foil during incubation steps. All assay reagents need to be pre-equilibrated, and all steps should be performed at room temperature. (Variation in temperature can have a significant effect on the signal amplitude). As first step Anti-TIGIT reference and sample dose response curves are prepared. Standard and samples are diluted in Assay buffer to a final concentration of 60 nM. For the preparation of the Master Plate, 96-well transparent plates with a flat bottom are used. 60 nM reference material and samples are loaded in duplicates in row A accordingly to a 2-7 layout as shown in figure 23. Then the reference and the samples are diluted in master plate with a step dilution 1:3 in assay buffer.

	1	2	3	4	5	6	7	8	9	10	11	12
A		STD	UNK1	UNK2	UNK3	UNK4	STD	UNK1	UNK2	UNK3	UNK4	
B												
C												
D												
E												
F												
G												
H		Blank	Blank	Blank	Blank	Blank	Blank	Blank	Blank	Blank	Blank	

**Figure 23. Master plate layout.** In the picture an example of the layout is depicted. The reference material (STD= standard) is loaded in column 2 and 7 while the unknown samples (UNK1, UNK2 and UNK3) are loaded in position 3-8, 4-9, 5-10 and 6-11 respectively. In row H the blank sample is loaded. Column 1 and 12 are empty.

The solution of FcRn is prepared obtaining a final concentration of 80 nM. Anti-TIGIT dilutions are transferred from each well of the master plate to the respective well of the assay plate (1/2 AreaPlate-96, White Perkin Elmer). Master plate and assay plate has the same layout. Then FcRn solution is added to the assay plate. The assay plate is incubated for 1 hour at room temperature before the addition of the 1:1 mixture of conjugated Acceptor and Donor beads. The final Anti-TIGIT dose response curve ranges from 15 nM to 0.0206 nM, FcRn concentration in assay plate is 20 µg/mL and the concentration of the beads' mixture is 10 µg/mL. After one hour incubation at +23°C, the plate is read through EnVision reader with excitation wavelength of 680 nm and emission filter for 570 nm with 100 nm bandwidth. Excitation time is set to 180 ms and the total measurement time is 550 ms. Considering that the presence of Anti-TIGIT will bring the Acceptor and Donor beads in close proximity, the higher is Anti-TIGIT concentration, the higher will be the detected signal. Data are analyzed with GraphPad Prism software. Concentrations of Anti-TIGIT (X values) are transformed using  $X = \text{Log}(X)$ , then the data are plotted using 4-parameter nonlinear regression. The relative values of the EC<sub>50</sub> for the Standard and the samples under analysis are directly derived from the "Table of Results" that appears. The biological activity (Potency) of the samples is expressed as percentage of the bioactivity of the sample compared to the standard and calculated as follows:

$\text{Potency}_{\text{campione}} = \frac{\text{EC}_{50\text{standard}}}{\text{EC}_{50\text{campione}}} \times 100$	EC <sub>50standard</sub>	EC <sub>50</sub> obtained by the Standard
	EC <sub>50sample</sub>	EC <sub>50</sub> obtained by the sample

The final potency value of the sample is calculated from the average among potency values measured in two independent analytical runs.

### 3.5.3 Artificially degraded samples preparation

To confirm the stability indicating properties of the qualified assays for the binding to FcRn the following stressed samples were prepared starting from Anti-TIGIT reference material IRS Anti-TIGIT 2018/01.

**Table 12: List of the stressed samples tested in this study together with their measured protein content.**

Sample	Concentration mg/mL
<b>Anti TIGIT Reference material IRS 2018/01</b>	19.42
<b>Deamidated</b>	8.5
<b>Oxidized 0.01%</b>	16
<b>Oxidized 0.1%</b>	14.6

The reagents that were used for samples' preparation are listed in paragraph 3.4 of this chapter.

For the generation of the two samples with different oxidation percentage the same approach reported in paragraph 2.4 was used except for changing the concentration of H<sub>2</sub>O<sub>2</sub> from 0.33% to 0.01% and 0.1% respectively. This because it was verified that an oxidation with 0.33% H<sub>2</sub>O<sub>2</sub> was too aggressive for Anti-TIGIT.

Deamidation: A volume of DS was diluted with an equal volume of ammonium bicarbonate pH 9.2 1 M and incubated at +37°C for 3 days. At the end of incubation, the sample was buffer exchanged to the formulation buffer until pH was the same as the formulation buffer and then concentrated to the starting DS volume.

Samples' concentrations were measured by NanoDrop Spectrophotometer as reported in paragraph 2.4 of this chapter.



### **3.6 Software for potential immunogenicity prediction**

For the potential immunogenicity assessment, a Merck internal software based on the Immune Epitope Database (IEDB) was used.

IEDB is a freely available resource funded by the National Institute of Allergy and Infectious Diseases. It catalogs experimental data on antibody and T cell epitopes studied in humans, non-human primates, and other animal species in the context of infectious disease, allergy, autoimmunity and transplantation. The IEDB also hosts tools to assist in the prediction and analysis of epitopes.

Computational prediction of T cell epitope candidates is currently being used in several applications including vaccine discovery studies, development of diagnostics, and removal of unwanted immune responses against protein therapeutics (Paul et al., 2016).

Specifically, the tool was used for T Cell Epitopes prediction based on MHC (Major Histocompatibility Complex) class II binding. This tool employs different methods to predict MHC Class II epitopes, including a consensus approach which combines NN-align, SMM-align and Combinatorial library methods (Fleri et al., 2017).

The instructions for the use of the software can be found on IEDB site (<http://tools.iedb.org/tepitool/>).

## **4 DEVELOPMENT OF BIOASSAYS TO STUDY ANTI-TIGIT BIOLOGICAL ACTIVITY**

### **4.1 Introduction and rationale**

Biologics testing is a critical process during development and production as these large molecules are sensitive to and altered by changes in their manufacturing process and therefore quality, safety, and efficacy must be continually monitored and in order to meet strict regulatory requirements.

Therefore, analytical method development and validation of fit-for-purpose bioassays is critical to the successful development and quality assessment of new pharmaceuticals. However, the development, standardization and implementation of bioassays is a challenging task because of the intrinsic variability of the response of living organisms (i.e. cultured cells), the use of critical reagents, and other uncontrollable sources of variability that affect the system's performance (Camacho-Sandoval et al., 2018).

The development of bioassays requires a deep understanding of the mechanisms of action of the therapeutic mAb under study; this is fundamental during the design of the assay, because allows defining the critical characteristics to be evaluated and helps the selection of the most appropriate analytical approaches for their assessment (Camacho-Sandoval et al., 2018).

In general, in order to identify the best options for the bioassays to be developed, all the available information on Anti-TIGIT in literature (as it relates to the molecule of interest) have been searched, focusing on:

- Mechanism(s) of Action (Known, Likely and Plausible)
- Binding to Cell-Surface Ligands or Receptors
- Potential Off-Target Effects Not Related to Primary MOAs
- Effector Functions
- Clearance Mechanisms
- Amino Acid Sequence, Post-Translational Modifications and their relevance (e.g., Glycosylation Profile)
- Degradation Hot Spots

- Sequence Regions Important for Ligand or Receptor Binding (e.g., mAb's complementary determining regions, CDRs)
- Structural Motifs Important for Binding (e.g., helices)

An IgG molecule can perform two main functions through different regions of its structure. While one part of the antibody, the antigen binding fragment (Fab), recognizes the antigen, the other part of the antibody, known as the crystallizable fragment (Fc), is responsible for the so-called antibody effector functions, such as binding to the complement, and binding to cell receptors on macrophages and monocytes.

As reviewed in the General Introduction (Section 2.10), the first mechanism of action of Anti-TIGIT is based on the inhibition of the interaction between TIGIT and its binding partner CD155 (PVR). This inhibition results in different effects depending on the way of signaling and the cell types involved. Blockade of TIGIT signaling using CD155 as ligand should result in activation of NK and T effector cell function and inhibition of Treg cell inhibitory function. Blockade of CD155 signaling using TIGIT as ligand should induce the production of immunostimulatory cytokines like IL-12 by dendritic cells (DCs). In addition, blockade of TIGIT/CD155 binding leaves CD155 free for binding to the co-stimulatory receptor CD226, resulting in T cell activation.

Anti-TIGIT also blocks the interaction between TIGIT and its binding partner CD112. However, the expected effect is not clear as it has to be still addressed if the TIGIT:CD112 interaction has functional relevance in mediating inhibitory functions.

The second known mechanism of action of Anti-TIGIT is based on its effector-function competent Fc region. Binding to this region by NK cells or macrophages can result in depletion of TIGIT-(over-)expressing cells like regulatory T cells.

In the following figures the Anti-TIGIT regions which are critical for mAb biological activity are presented in relation to:

- CDRs and target interaction (CDRs are reported according to Martin) (Martin, 2010);
- FcRn binding (Dall'Acqua et al., 2002), which represents a major regulator of antibody PK;
- FcγR binding region functional for ADCC activity (Siberil et al., 2012);
- C1q binding region functional for CDC activity.

During this PhD study all the functions related to these mAb's region have been explored. Accordingly, bioassays that could be used or for QC testing and release or for characterization purposes have been developed following a stepwise approach to define a proper analytical panel for Anti-TIGIT bioactivity assessment.

The first part of this study regards the development and validation of a bioassay to quantify the biological activity of Anti-TIGIT related to its main mechanism of action while the second part is focused on Anti-TIGIT effector functions. In the end, the evaluation of the stability indicating properties of the qualified assays is performed.

## 4.2 Anti-TIGIT Ligand Binding Assay

### 4.2.1 Development study

Design strategies for bioassays are driven by the drug's intended physiological MOA. Unlike other analytical techniques, bioassays are almost always unique for each therapeutic. A well-designed bioassay will accurately capture the biological activity of a drug candidate.

Current published methods used to measure the activity of biologic drugs targeting TIGIT rely on primary human T cells and measurement of functional endpoints such as cell proliferation, cell surface marker expression, and interferon gamma (IFN $\gamma$ ) and interleukin-2 (IL-2) production. These assays are laborious and highly variable due to their reliance on donor primary cells, complex assay protocols and unqualified assay reagents. As a result, these assays are limited in their ability to provide a mechanism of action-based quantitative measure of drug-induced cellular response with the assay precision and accuracy required for use in a quality control environment.

It is generally agreed by regulatory agencies that a phased approach to the development of bioassays should be implemented and it is often advantageous to start with a ligand binding method for the early phase of product development.

Based on this assumption, on the collected information on Anti-TIGIT and on regulatory requirements for bioassay for the bioactivity determination of a drug candidate, we identified these possible options:

1. A classical direct ELISA assay (ligand-binding assay, LBA);
2. A cell-based ligand binding bioassay (CBA).

Ligand-binding assay (LBA) has been widely utilized as an easy and robust method for starting an antibody developing campaign. However, LBA still has some significant drawbacks, such as difficulties in obtaining high-quality and reproducible recombinant ligands, lack of native conformations, and assay matrix disturbance. These restrictions of LBA may cause inevitable result bias and less representativeness of *in vivo* condition. Cell-based binding assay (CBA) thereby is required by most regulatory guidelines as a further complement of LBA for determining the mechanism of action and bioactivity of therapeutic antibodies. In contrast to LBA, CBA employs native cellular antigens, no need for synthesizing and purifying recombinant ligands. Moreover, the cell-based system offers a more physiologically relevant environment, and it exerts higher sensitivity

to small changes, such as glycosylation patterns and conformational alterations, thus providing valuable insight upon functional mechanism and potency. Based on this assumption the second format has been selected for Anti-TIGIT biological activity determination.

The development study was performed according to the internal guideline of Merck Serono and according to USP <1032> with the final goal of developing a cell-based assay exhibiting specificity, simplicity, and robustness with the appropriate assay precision, accuracy, and linearity required for antibody potency and stability testing.

The assay format was developed considering the target of Anti-TIGIT and the known affinity of the Fc portion of antibodies to bind protein A (Boyle and Reis, 1987).

Indeed, immobilized Protein A adsorbents have been extensively used for purification of IgGs (Boyle et al., 1993; Hou et al., 1991; Klein et al., 1994) and in solid-phase immunoassays for the coating.

Protein A is a highly stable surface receptor produced by *Staphylococcus aureus* with a molecular weight of 42 kDa in its native form which is capable of binding up to 5 molecules of IgG (Yang et al., 2003). Optimal binding occurs at pH 8.2, with high affinity ( $K_a = 10^8/\text{mole}$ ).

The second step was the cell type selection that should ideally be relevant to the MOAs of the therapeutic. The choice of cell type is usually between a primary cell typically isolated from human blood or tissue, and an immortalized established cell line derived from human or nonhuman origin (White et al., 2019). Primary cells may be required when the MOA of the therapeutic agent is complex or multiple receptors are involved in the MOA and a transfected cell line cannot fully represent all interactions. Unless primary cells are absolutely required, they should be avoided due to considerable donor-to-donor variability. Cell lines can also be modified to overexpress the receptor or ligand that is targeted by the therapeutic and this was the case of Anti-TIGIT.

The selected target cells for the Anti-TIGIT Ligand Binding Bioassay are the CHO-S-myc huTIGIT ECD cells which are engineered CHO cells that constitutively express on their surface the extracellular portion of human TIGIT. CHO-S-myc-huTIGIT ECD cell line has been produced in EMD Serono Research and Development Institute (Billerica) by transfection and selection for surface expression of human TIGIT extracellular domain. The wild type cells CHO-K1 is an adherent cell line while these cells can be cultured both in suspension and in adhesion by adding FBS to the culture medium. This alternative is given by the c-Myc over-expression, that not only enhances growth rate but also adds further transforming characteristics altering the attachment and detachment rates and

serum dependency as reported in the work of Ifandi and Al-Rubeai (Ifandi and Al-Rubeai, 2003). To let the cells acquiring the adherent morphology, the amount of FBS required in culture media is 10%.

To determine the best condition for the cells' growth and for the bioassay, in the first experiment of the development phase both cell culturing conditions were tested in Anti-TIGIT ligand binding assay (see Chapter 3, "Materials and Methods" for the bioassay's detailed protocol).

The preliminary experiment shows Anti-TIGIT dose-response curves with comparable EC<sub>50</sub> (82.06 ng/mL for adhesion cells vs 92.35 ng/mL for suspension cells) and comparable slopes for both cells morphologies as reported in figure 24. Both curves showed the typical sigmoidal shape where the signal intensity (bioluminescence) increases with Anti-TIGIT concentration. When the two curves are compared a 3-fold higher signal is obtained when using suspension cells with respect to adherent cells. This different behavior could be due to the increased number of exposed TIGIT molecules on the surface of suspension cells. Moreover, these cells, showed an increased viable cell density when kept in culture and being already free-floating, do not require trypsinization, hence are easier to split and to keep in culture for operators.

Based on these considerations, the suspension cells as target cells to develop the Anti-TIGIT potency assay were selected.

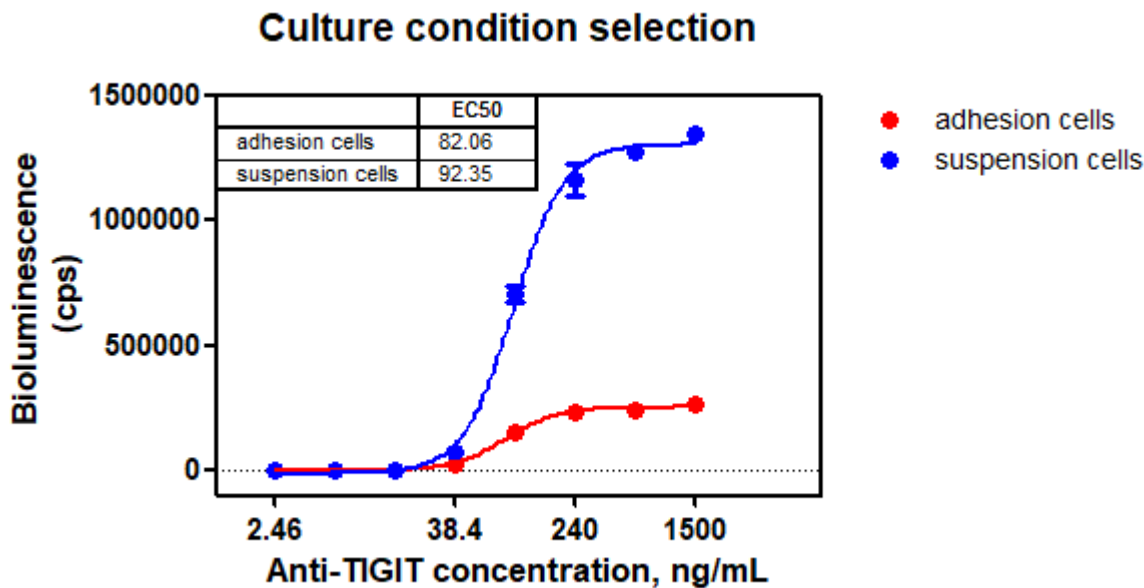


**Figure 24: Preliminary Anti-TIGIT dose-response curve.** Two Anti-TIGIT dose response curves obtained using two different cell culturing conditions are shown. For both dose response curves when the Anti-TIGIT concentration increased the signal expressed in count per seconds (cps) given by the CHO cells increased. The

red dose response curve was obtained using adhesion CHO cells and the blue one was obtained with cells grown in suspension. Considering the difference in terms of maximum signal obtained, the suspension cells as target cells to develop the Anti-TIGIT potency assay were chosen.

Moreover, since cells and cell-derived reagents in general require distinct characterization and control measures to ensure operational consistency over time in the bioassay, a homogeneous, stable analytical CHO-S-myc-huTIGIT ECD cell bank was prepared and frozen as reported in Materials and Methods chapter (Gazzano-Santoro et al., 2014).

The cell-seeding density and the incubation time for bioassay execution have been selected based on in-house experience from another ligand binding bioassay:

- Cell density:  $0.5 \times 10^6 \pm 0.2 \times 10^6$  cells/mL;
- Incubation Time: 1 hour  $\pm$  15 minutes.

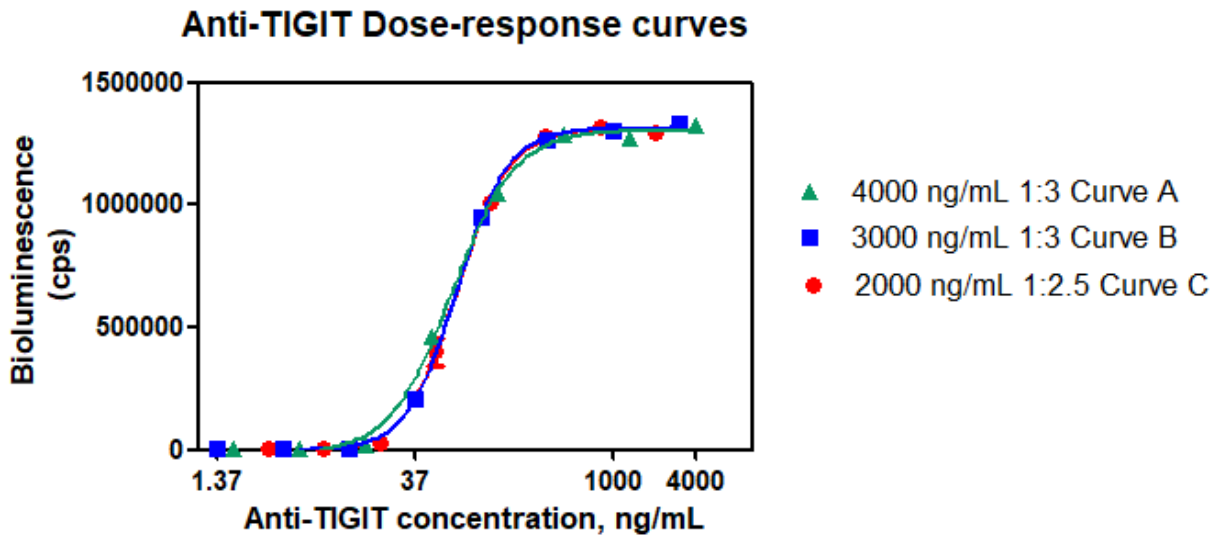
To develop an appropriate Anti-TIGIT full dose-response curve with a sigmoidal shape and well-defined bottom and top plateau to describe the bioactivity of the mAb, different curves with eight concentration points have been tested with CHO-s-myc-huTIGIT ECD cells.

To achieve this, different assay conditions were analyzed with a trial-and-error method. Different Anti-TIGIT dose-response curve concentration ranges starting from 4000, 3000 and 2000 ng/mL were tested. These concentrations were selected based on the previous knowledge we had on both developing CBA and on Anti-TIGIT affinity to TIGIT. Moreover, two different Anti-TIGIT step dilutions (1:2.5 and 1:3) were used.

Results are shown in the figure below (Figure 25).



A)



B)

Anti-TIGIT (ng/mL)		
Curve A (1:3)	Curve B (1:3)	Curve C (1:2.5)
4000	3000	2000
1333	1000	800
444.44	333.33	320
148.15	111.11	128
49.38	37.04	51.20
16.46	12.35	20.48
5.49	4.12	8.19
1.83	1.37	3.28

**Figure 25: Anti-TIGIT dose-response curves.** A) Anti-TIGIT dose-response curves obtained with different Anti-TIGIT starting concentrations and step dilutions. Curve A is colored in green and represent the dose-response curve obtained when starting from 4000 ng/mL of Anti-TIGIT with a step dilution 1:3. Curve

B is graphed in blue and starts from an Anti-TIGIT concentration of 3000 ng/mL with a step dilution 1:3. Curve C represented in red starts from 2000 ng/mL with a step dilution 1:2.5. All the curves are comparable in terms of Top, Bottom, Hillslope and EC50 values. For this reason, curve C starting from a lower Anti-TIGIT concentration was chosen. B) In the table, Anti-TIGIT concentration points of the different dose-response curves (ng/mL) are shown.

All the tested dose-response curves, with two different step-dilution (Curve A and B 1:3 and Curve C 1:2.5) were found to be symmetrical around their inflection point and to fit the 4PL algorithm with a  $R^2 = 0.998$  (Curve A),  $R^2 = 0.9998$  (Curve B) and  $R^2 = 0.9997$  (Curve C) respectively. As such, Curve C, using less amount of Anti-TIGIT, was the selected for bioassay development.

After selecting the proper Anti-TIGIT dose-response curve, the target cells and the bioassay incubation time, the plate effect was established. The setup of cell-based bioassays is typically amenable to a 96-well plate format. This format allows analysts to set up assays using multichannel pipettes or, alternatively, automated liquid handling systems to prepare or add dilutions, add reagents, and so on. It also allows for the use of plate washers and plate readers that facilitate the performance of the assays as highlighted by White et al (White et al., 2019). Microtiter plate assays have multiple potential sources of variability that can affect bioassay performance and thus impact the accuracy of results. These include variations in cell plating and cell growth rate, inconsistent cell response, biased results due to the location of the sample in assay plates, order of addition of standard, test samples and critical reagents, analyst-to-analyst, plate-to-plate and run-to-run variability. Among these variables, the microtiter plate is a dominant contributing source of location-based error and for this reason it should be evaluated early in bioassay development. To minimize or protect against potential plate location effects, different approaches have been reported in the literature (Lundholt et al., 2003; Robinson et al., 2014; Roselle et al., 2016). The most common practices include: 1) the use of techniques that help minimize the edge effect (e.g., plate hotels, heat-transfer plate and others); 2) the inclusion of replicates; 3) careful consideration on the placement of standard and test samples in the plate (plate layout); 4) the use of randomization or pseudo-randomization (row or column); 5) exclusion of outer rows and/or columns; 6) use of automation.

In the case of CBA such as the one of Anti-TIGIT, triplicates are usually required to allow for accurate measurement in a 96-well plate format. Moreover, based on in-house experience, the loading mode 1-5-9 has been selected for this bioassay to minimize the plate effect.

Once the cell line, cells culture and seeding conditions, plate layout and incubation time have been defined, the overall bioassay workflow was designed as shown below in figure 26.

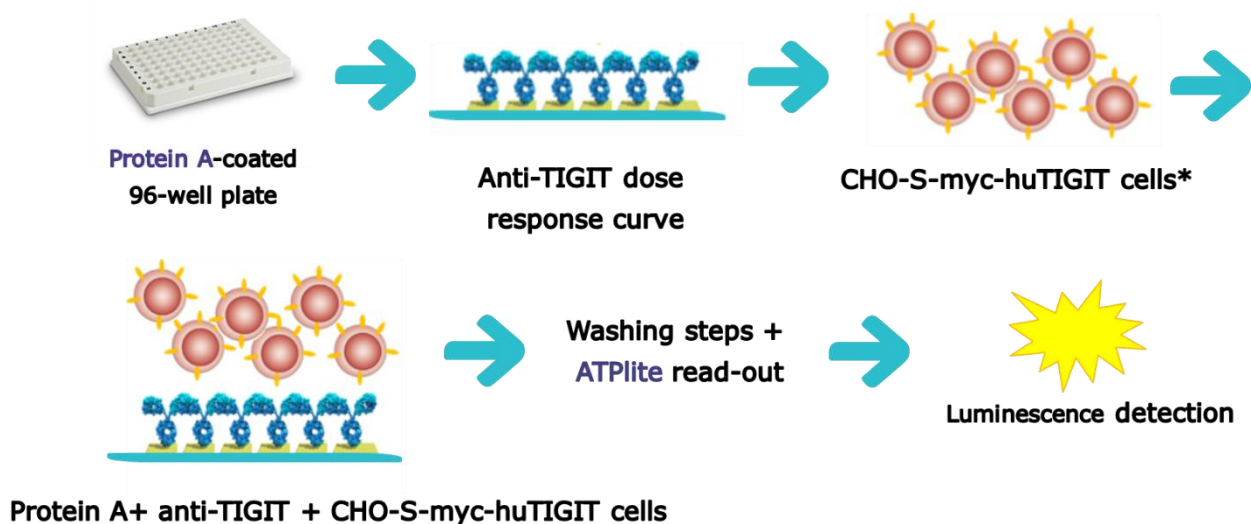


**Figure 26: Schematic representation of the new cell-based ligand binding bioassay.** In the picture the main steps of the bioassay are depicted. The first passage is the 96-well plate coating with protein A followed by the loading of Anti-TIGIT reference and samples full dose response curves. After 30 minutes of incubation, the properly diluted cell suspension is added to the assay plate. All the reagents are let incubating for 1 hour at +37°C. Then, after three washing steps the ATPlite solution is added to each well and the luminescence is detected for 1 second/well on a luminometer.

The final developed bioassay presents several advantages including high throughput (3 different samples per plate can be analyzed), short assay time (hours vs days of other cell-based assays), easiness of execution for the operators and low costs. Considering all the aforementioned points, it was then decided to go on with the preliminary performance verification to verify the performance of the optimized assay.

#### 4.2.1.1 Preliminary Performance Verification

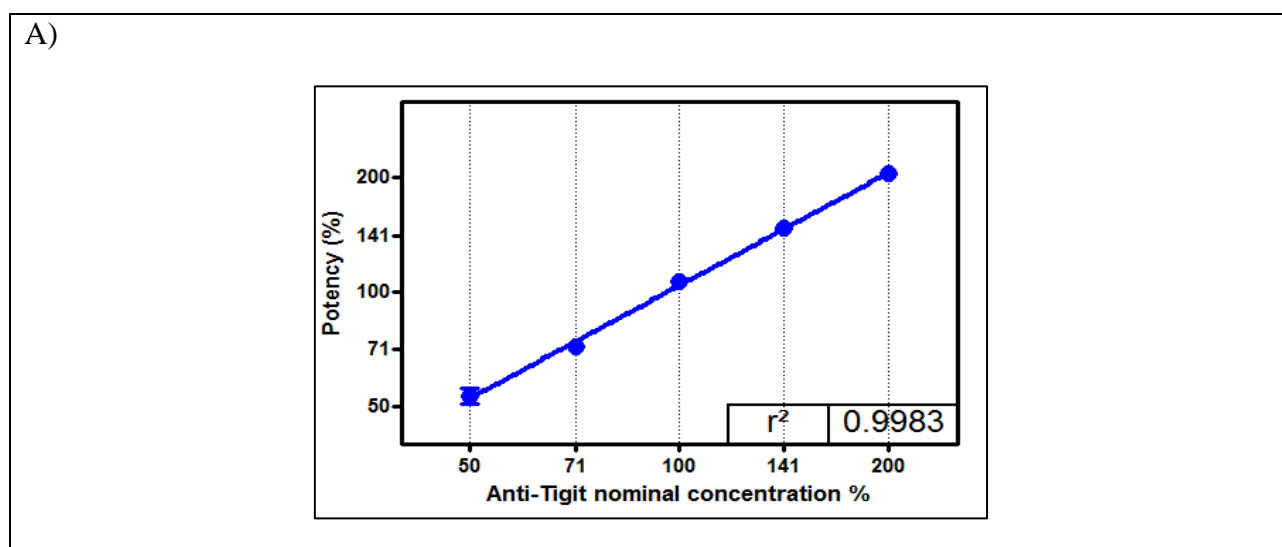
As a general approach for bioassay development, as seen in Chapter 2, the preliminary performance verification needs to be checked to confirm the feasibility of the assay for the intended purpose. To evaluate the performance of the Anti-TIGIT Ligand Binding bioassay, preliminary 1) goodness of fitting (GOF) of the reference dose-response curve, 2) bioassay linearity and range and 3) precision

and accuracy were estimated on the basis of the experiments performed during this development study.

Evaluating model GOF is a key piece of early assay development. Different approaches to evaluate the GOF are proposed in the literature (Robinson et al., 2014); here we used the  $R^2$  evaluation which is based on the ratio between sum of squares regression and total sum of squares. The coefficient of determination (or  $R^2$ ) determines how well the Anti-TIGIT curve fits the 4PL algorithm. The  $R^2$  ranges from 0.0 to 1.0: the closer the  $R^2$  to 1.0, the better the curve fits the model. The  $R^2$  values calculated in all the bioassays performed during this development study were collected and used to estimate a preliminary goodness of fitting. The average  $R^2$  was found to be = 0.99, thus confirming that the developed Anti-TIGIT dose-response curve properly fits the 4PL algorithm. A more extensive GOF analysis was performed in the following validation study.

The linearity of an analytical method is its ability to obtain test results that, within a given range, are directly proportional to the concentration of the analyte in the samples while the range is the interval between the upper and lower concentrations of analyte for which it has been demonstrated that the analytical procedure has a suitable level of precision, accuracy and linearity.

For the approach and analysis applied for the preliminary linearity evaluation refer to Chapter 3. Anti-TIGIT potency values at each concentration level and the linear regression obtained by plotting each Potency value against each Anti-TIGIT nominal concentration level are shown in the figure below (Figure 27):



B)					
Exp	Potency Ratio				
	50%	71%	100%	141%	200%
<b>1</b>	53	71	109	156	213
<b>2</b>	49	71	110	143	189
<b>3</b>	58	73	100	145	213
<b>Average</b>	<b>53</b>	<b>72</b>	<b>106</b>	<b>148</b>	<b>205</b>
<b>Recovery</b>	<b>100</b>	<b>95</b>	<b>100</b>	<b>99</b>	<b>96</b>
<b>%CV</b>	<b>8</b>	<b>2</b>	<b>5</b>	<b>5</b>	<b>7</b>

**Figure 27: Anti-TIGIT bioassay preliminary linearity verification.** A) Linear regression of the response obtained by plotting the calculated Potencies of Anti-TIGIT versus each nominal concentration (50%, 71%, 100%, 141% and 200%). B) In the table are shown the calculated Potencies values, the percentage of recovery and the coefficient of variation (CV) at each Potency level. Abbreviations: Exp = experiment; %CV= coefficient of variation (%).

The linear behavior of the data showed in figure 28 is evident and the  $R^2$  of the linear regression curve confirms it. The analytical range (50% - 200% of bioactivity) has also been confirmed based on the precision and accuracy results at each concentration point. Indeed, from the experiment run in the linearity study, also preliminary precision and accuracy were estimated. Both were found within the acceptance criteria stated at the beginning of the study (see chapter 3) thereby demonstrating the method suitability for its application in a GMP environment. These preliminary values were just an indication of the method suitability and they could not be considered as acceptance criteria in routine analysis. Indeed, system suitability parameters and acceptance criteria of the final bioassay procedure have been set based on results from the forthcoming validation study.

#### 4.2.2 Validation study

In this section the validation of Anti-TIGIT ligand binding bioassay is presented. This study was aimed at establishing the performances of the bioassay in order to confirm the GMP requirements. Indeed, the validation of the methodologies used for the assessment of critical quality attributes of biopharmaceuticals is a key requirement for manufacturing under GMP environment. The validation

exercise must be focused on the evaluation of characteristics that warranty the robustness of the assay under the experimental conditions in which it will be performed. However, the validation exercise of bioassays and the stringency to evaluate each characteristic will depend on the nature of each assay, the knowledge gained during its development, as well as its intended purpose (e.g., R&D, Manufacturing, Quality Control, Batch Release, or Biosimilarity exercise).

The Anti-TIGIT ligand binding assay was validated in terms of Linearity, Accuracy, Precision and Specificity according to ICH Q2(R1) and USP <1033>. System suitability and similarity criteria were also established in order to ensure the performance of the method in routine analyses and keep all the possible sources of variability under control.

Considering that bioassay validation should include samples that are representative of materials that will be tested in the bioassay and should effectively establish the performance characteristics of the procedure, the samples used for this study were Anti-TIGIT reference material (also referred as IRS Anti-TIGIT 2018/01) and a DP representative of the manufacturing process called BKAA1801 (table 13).

**Table 13: List of samples used in the validation study together with their code and concentration.**

Sample	Code	Concentration
<b>Anti-TIGIT Reference Material</b>	IRS Anti-TIGIT 2018/01	19.42 mg/ml
<b>Test sample</b>	BKAA1801	20.72 mg/ml

The first parameters that have been evaluated were the linearity, accuracy, and precision of the method. The same experimental design applied during the preliminary verification study was used except that here three different operators were involved as per International guidelines request (Bioassay Validation Design of the USP <1033>). Therefore, a total of nine independent runs for each Anti-TIGIT concentration level were performed instead of only three increasing the possible sources of variability and the statistical power. For a detailed explanation on the applied approach and analysis refer to Materials and Methods, chapter 3.

Representative Anti-TIGIT dose-response curves at each level are shown in figure 28. As expected, the lower is the concentration of the sample tested, the higher is the EC<sub>50</sub> of the dose-response curve

and the lower its biological activity is. All the curves are well described in the range of potency from 50% to 200%. Moreover, all the analyses have been accepted upon evaluating the F-Test for the similarity of the three parameters of the curve (Top, Bottom and Slope).

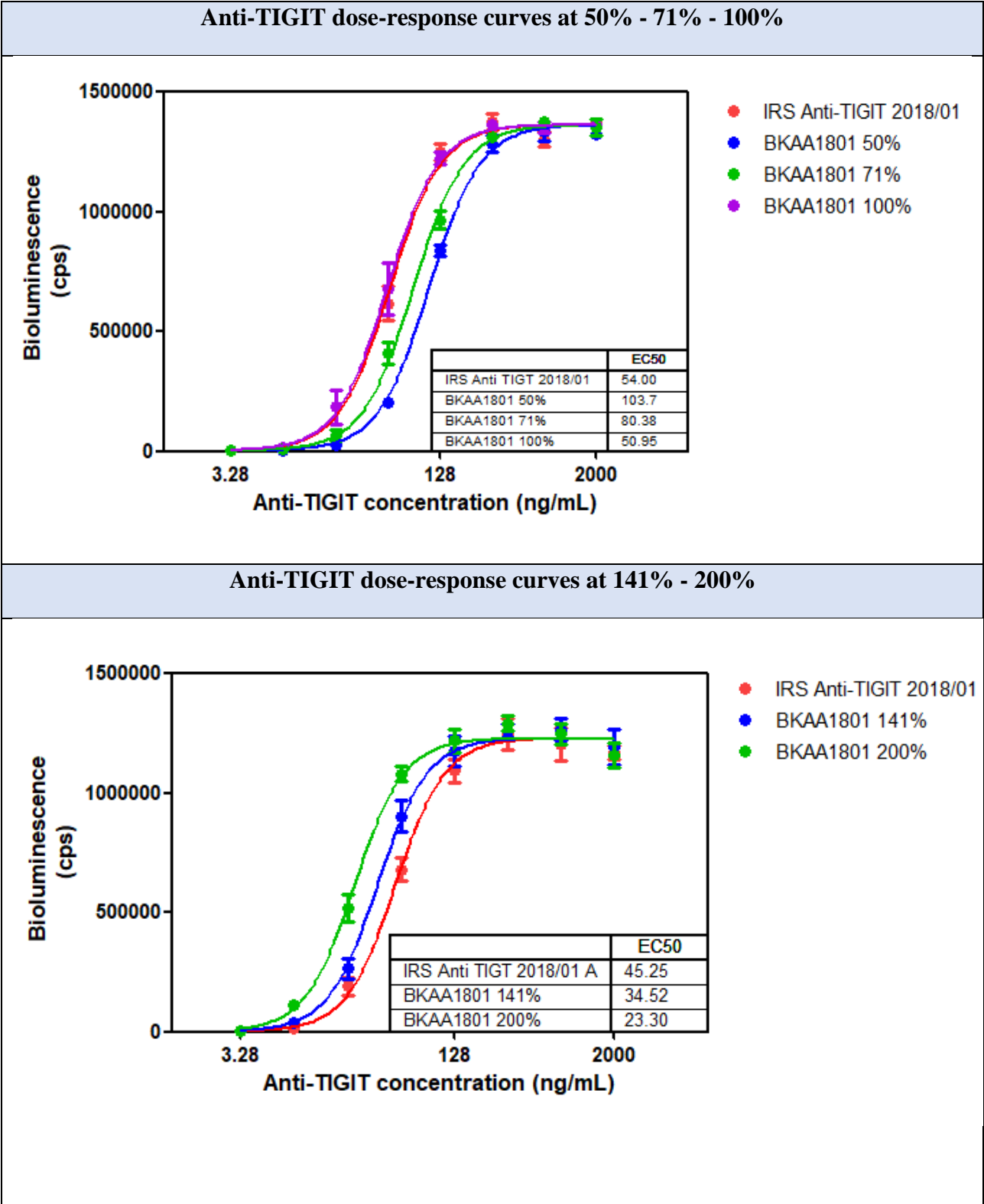
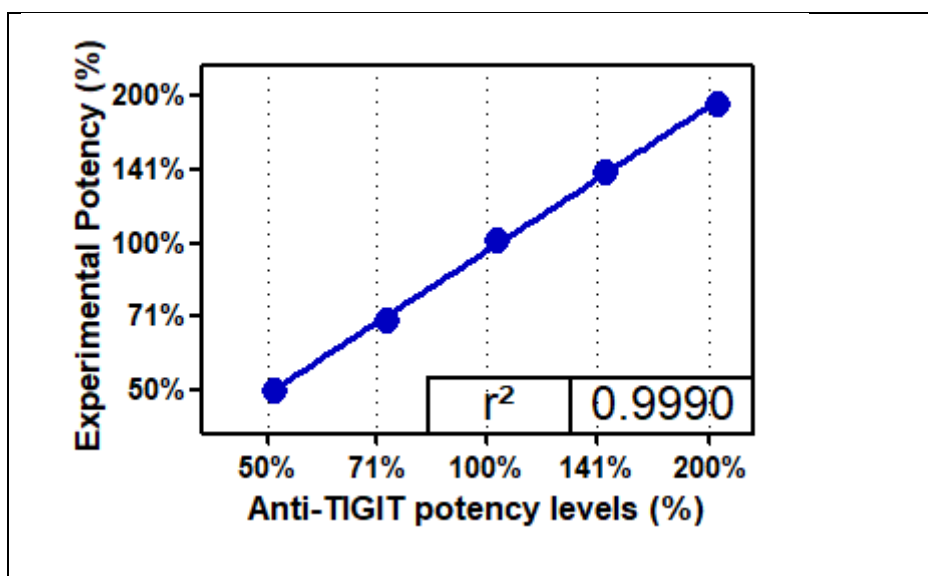


**Figure 28: Anti-TIGIT reference material dose response curve and DP dose-response curves at 50%, 71%, 100%, 141% and 200% potency levels.** All the dose response curves are well defined within the potency range 50%-200%. The reference material dose response curve is graphed in red. In the graph on the top the dose response curve of the sample at 50% is in blue, the one of the sample at 71% is graphed in green while the dose-response curve of the sample at 100% is graphed in violet. In the graph on the bottom in blue is represented the sample at 141% while in green the dose response curve of the sample at 200%. In both graphs also the EC50 values of each curve are reported.

#### 4.2.2.1 Linearity and Range

From the runs above the linearity of the bioassay has been determined following the approach reported in Chapter 3.

Results are shown in figure 29.





Analytical session	Run	Experimental Potency				
		50%	71%	100%	141%	200%
1	1	50	65	106	141	205
	2	51	70	99	154	209
	3	51	70	113	144	200
2	1	52	67	106	131	194
	2	51	77	101	142	198
	3	50	75	111	141	192
3	1	44	61	83	122	162
	2	45	65	85	128	170
	3	46	63	91	124	160
Average		49	68	99	136	188

**Figure 29: Anti-TIGIT bioassay linearity.** On top is shown the linear regression of the response obtained by plotting the calculated Potencies of Anti-TIGIT versus each nominal concentration (50%, 71%, 100%, 141% and 200%). In the table below the calculated Potency values (Experimental Potency) at all the concentration levels coming from each run are reported. The final Potency at every level is obtained as average of all the Potency measured. The values are shown without decimal numbers, but the calculations were performed considering seven significant digits that are the maximum that can be entered in GraphPad Prism software.

As the  $R^2$  of the linear regression curve is 0.9990, the method was assessed to be able to give a linear response between 50% and 200% of Potency, as such the preliminary results obtained during the development study were confirmed. Moreover, the values for Slope and Y-intercept when  $X=0.0$  are from 0.9189 to 1.035 and from -0.0871 to 0.1468 respectively, at 95% of confidence intervals confirming the linearity.

#### 4.2.2.2 Accuracy

Bioassay's accuracy has been evaluated following the approach summarized in chapter 3. The experimental design to evaluate the linearity, accuracy, precision and range involves the use of a real sample (i.e., BKAA1801). Hence, the Expected potency for the calculation of the relative bias was calculated taking into consideration the real Potency of the sample at the 100% level.

The Potency of the sample BKAA1801 at the 100% level was calculated as average of the results generated from the nine runs performed and was found to be 99%. Therefore, the Expected potency at each level was recalculated considering the real potency value at 100% level. In order to assess the

conformance of the obtained relative bias values to the acceptance criteria, an equivalence test was applied. Therefore, 90% confidence intervals of relative bias values obtained at each level were calculated using a statistical software according to the following formula:

$$90\% C.I. = x \pm t * \frac{s}{\sqrt{n}}$$

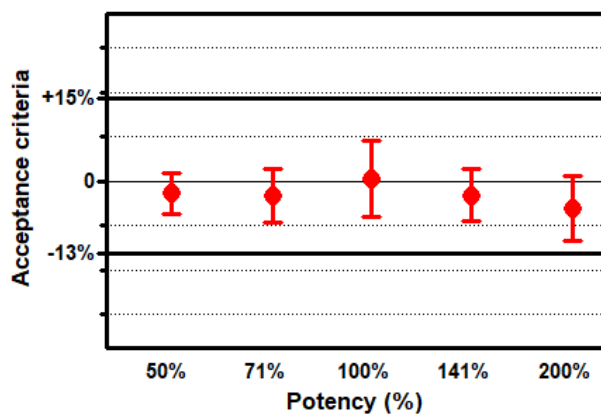
Where x is the mean, t is a statistical constant from the t-table, with degrees of freedom (df) equal to the number of measurements minus one (df= 9-1=8), s is the standard deviation and n is the number of runs performed.

Results of this calculation are shown in figure 30.

### A. Relative bias results and 90% Confidence Intervals

Analytical session	Run	Relative Bias				
		50%	71%	100%	141%	200%
1	1	0	-7	7	1	4
	2	2	0	0	10	6
	3	2	0	14	3	1
2	1	4	-4	7	-6	-2
	2	2	10	2	1	0
	3	0	7	12	1	-3
3	1	-12	-13	-16	-13	-18
	2	-10	-7	-14	-9	-14
	3	-8	-10	-8	-11	-19
Average		-2	-3	0	-3	-5
Lower 90% CI		-6	-7	-6	-7	-11
Upper 90% CI		2	2	7	2	1

### B. Plot of 90% CI for Relative Bias vs acceptance criterion



### C. Trend analysis of Relative Bias across defined Potency range

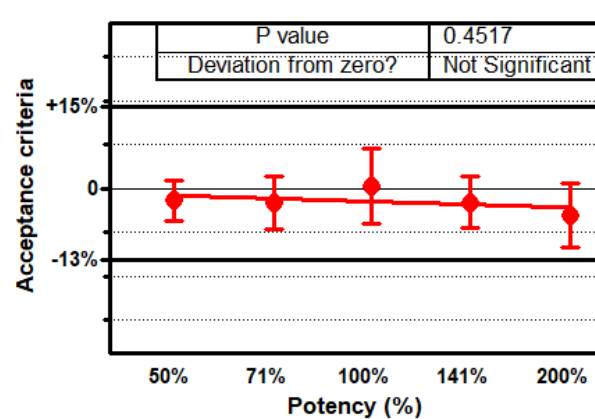


**Figure 30: Anti-TIGIT bioassay Accuracy.** A) Calculation of Relative bias and 90% Confidence Intervals (CI). Considering that residuals are randomly and independently distributed around zero, the fitted model is appropriate. B) Plot of 90% CI for Relative Bias at each level versus the acceptance criterion (i.e. -13%; +15%). All 90% CIs are within the acceptance region, thus indicating that the Anti-TIGIT bioassay is accurate between 50% and 200% of Potency. C) Trend analysis performed on the accurate range of the method. As the p-value of the linear regression is greater than 0.05 (i.e., 0.4517), the same bias is ensured between 50% and 200% Potency levels.

The average of the Relative Bias falls within the acceptance range (i.e., -13%; +15%), thus indicating that the method is accurate at each level. As the p-value of the linear regression is greater than 0.05 (i.e. 0.4517), there is an acceptable bias between 50% and 200%. Moreover, residuals are randomly and independently distributed around zero. Plotting residuals against dose from the model indicated that there is a random deviation suggesting that the model is appropriate. In conclusion, the bioassay should be considerate accurate between 50% and 200% of Potency giving reliable results also when testing samples with unusual potencies (e.g., stressed samples).

#### 4.2.2.3 Precision

Bioassay's precision was evaluated following the approach reported in Chapter 3. As shown in the table below (table 14), the contribution to the variability of the method comes predominantly from between-session (inter-session) variability rather than from the repeatability (intra-session variability). The intra- and inter-session variability percentage (CV%) was found within the acceptance criteria set for these parameters at the beginning of this validation study, i.e., 15%. As for the overall method variability, the highest Intermediate Precision obtained among all levels was found to be 12% at the 100% Potency level.

**Table 14: Precision results (ANOVA of variance components).** All the potency values obtained at each level are shown together with the calculation of the related variability (Between session, Repeatability and Intermediate precision of the method). The final acceptance criteria for the Intermediate Precision was set to  $\leq 12\%$ . All the values in the table are shown without decimal numbers but the calculation was performed considering seven significant digits that are the maximum that can be entered in Graphpad software. The values referred to the variance are reported as obtained from Statgraphics software.

<b>Analytical session</b>	<b>Replicates</b>	<b>50%</b>	<b>71%</b>	<b>100%</b>	<b>141%</b>	<b>200%</b>
<b>1</b>	<b>1</b>	50	65	106	141	205
	<b>2</b>	51	70	99	154	209
	<b>3</b>	51	70	113	144	200
<b>2</b>	<b>1</b>	52	67	106	131	194
	<b>2</b>	51	77	101	142	198
	<b>3</b>	50	75	111	141	192
<b>3</b>	<b>1</b>	44	61	83	122	162
	<b>2</b>	45	65	85	128	170
	<b>3</b>	46	63	91	124	160
<b>4</b>	<b>1</b>	47	68	96	137	195
	<b>2</b>	50	68	102	138	187
	<b>3</b>	52	76	102	137	207
<b>Average</b>		49	69	100	137	190
<b>Analytical session's variance</b>		10,6481	19,8981	120,315	111,694	435,787
<b>Replicates' variance</b>		2,16667	15,4167	25,8333	23,25	39,75
<b>Between session (%)</b>		<b>7</b>	<b>6</b>	<b>11</b>	<b>8</b>	<b>11</b>
<b>Repeatability (%)</b>		<b>3</b>	<b>6</b>	<b>5</b>	<b>4</b>	<b>3</b>
<b>Intermediate precision (%)</b>		<b>7</b>	<b>9</b>	<b>12</b>	<b>9</b>	<b>11</b>

All acceptance criteria set for Linearity, Accuracy and Precision were met. As a result, the Range of the Anti-TIGIT bioassay was established from 50% to 200% of Potency.

All together these results confirmed that the Anti-TIGIT ligand binding bioassay is precise, accurate and given these features it could be applied in a GMP environment for lots testing and stability studies.

#### 4.2.2.4 Specificity

For products or intermediates associated with complex matrices, specificity (sometimes called selectivity) involves demonstrating lack of interference from matrix components or product-related components that can be expected to be present. This can be assessed via parallel dilution of the Standard sample with and without a spike addition of the potentially interfering compound. If the curves are similar and the potency conforms to expectations of a Standard-to-Standard comparison, the bioassay is specific against the compound (USP <1033>).

The potential influence of Anti-TIGIT matrix composition on both the assay's performance and active drug's bioactivity has been evaluated. Anti-TIGIT matrix composition is reported in table 15.

**Table 15: Anti-TIGIT matrix composition.** The components, together with their function and amount are here reported.

Component	Function	Amount
Anti-TIGIT	Active ingredient	20 mg/ml
L-histidine	Buffering agent	20 mM
L-Methionine	Antioxidant agent	10 mM
Trehalose	Stabilizing agent	8%
Tween 20	Surfactant	0.05%
Water for injection	Vehicle	q.s.*

\*q.s.: *quantum satis* (for as much as required).

The composition of the matrix component plays a fundamental role as each matrix component has different functions.

**L-histidine** is a well know buffering agent that is commonly used in the final formulation of many commercialized monoclonal antibodies, with histidine helping to stabilize the antibody during storage in addition to its buffering function. Moreover, Histidine has been shown to stabilize mAb structures at elevated temperatures and during lyophilization, and it can reduce the viscosity of concentrated

mAb solutions (Baek et al., 2019). Cantoni et al. however reported that micromolar concentrations of L-histidine increase the cytotoxicity of hydrogen peroxide in a number of cell lines including CHO cells. For this reason, even if the Anti-TIGIT ligand binding assay foresee only one hour of incubation between CHO cells and Anti-TIGIT and the matrix is really diluted, it is important to assess possible matrix effect on assay performance (Cantoni et al., 1994).

**L-Methionine** instead is a well-known radical scavenger/sacrificial agent. Indeed, when Saha et al. tested the ability of five different excipients (Methionine, Tryptophan, Arginine, Sucrose and Trehalose) to prevent protein oxidation they were able to demonstrate that Methionine was the most effective one (Luo and Levine, 2009). The protection from methionine was evident both in terms of the minimal loss of monomer and minimal generation of aggregates or degradants and in terms of thermodynamic stability (Shah et al., 2018). The disaccharide trehalose has also been known to increase thermodynamic stability of mAbs (Chi et al., 2003). **Tween20** instead is a commonly used surfactant. Surfactants are generally added in mAbs formulations to reduce the exposure of hydrophobic regions and so decreasing protein-protein interactions and interface-induced aggregation, also prevented by competition for adsorption sites. In addition, surfactants have been shown to act as chemical chaperones, increasing rates of protein refolding and thus reducing aggregation. For example, Gerhardt et al. showed that addition of polysorbate 20 to a solution containing various concentrations of a humanized IgG1 antibody reduced particle formation during incubation with siliconized glass syringes possibly because polysorbate 20 binding to the protein interferes with protein-protein interactions required for protein gelation at the silicone oil-water interface (Le Basle et al., 2020).

The two different approaches applied to evaluate the specificity are summarized in section 3.3.1.1.

In order to verify whether the Anti-TIGIT matrix has an effect on the bioassay, the Anti-TIGIT sample buffer was diluted following the same dilution scheme used for the IRS Anti-TIGIT 2018/01. As shown from figure 31 the slope of the regression line of the curve of the matrix was not found statistically different from zero ( $P\text{-value} > 0.05$ ), thus suggesting that its composition does not have a significant effect on the bioassay.

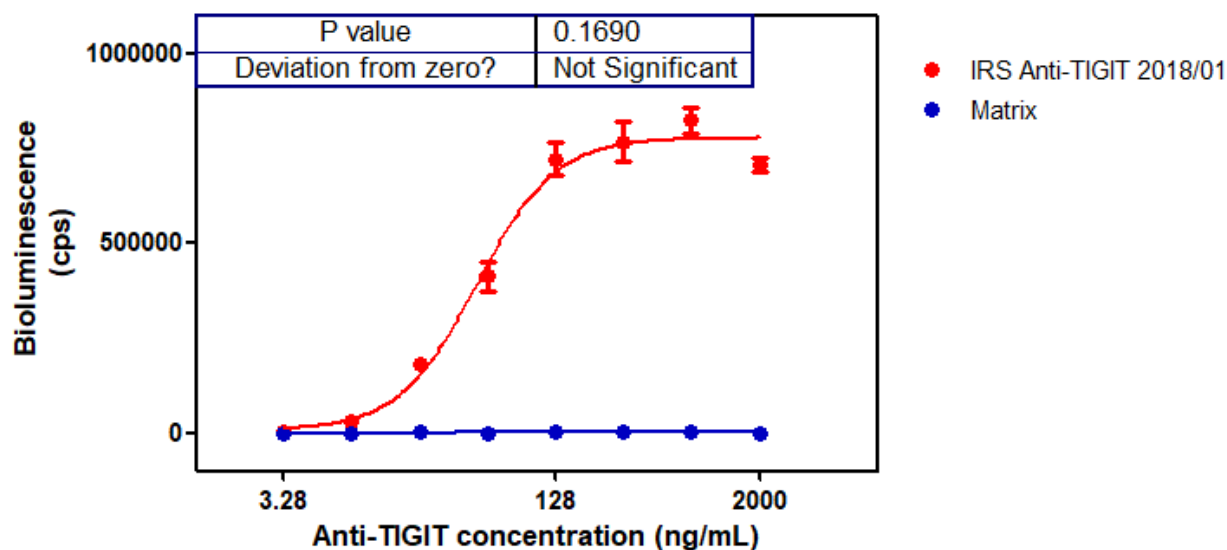


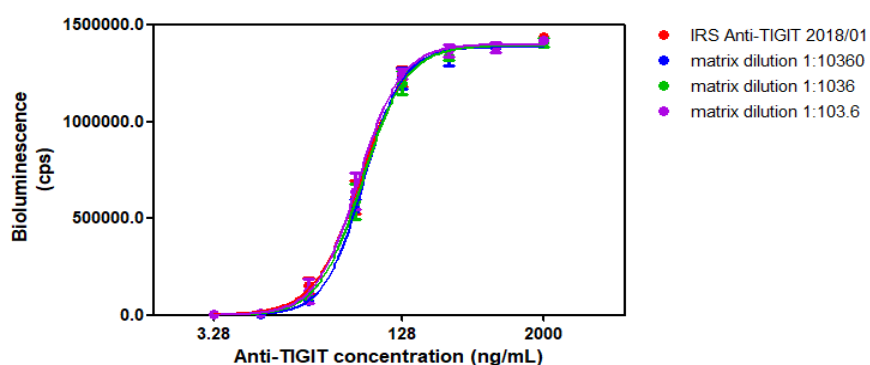
**Figure 31: Specificity: matrix effect on the bioassay.** Anti-TIGIT matrix was tested by diluting it with the same dilution scheme applied for Anti-TIGIT IRS 2018/01. The dose response curve of the standard is graphed in red while the curve of the matrix in blue. As shown by the blue curve, no signal is detected in the bioassay when the matrix is loaded without the active drug. Indeed, the slope of the regression line of the matrix curve was found not statistically different from zero (P-value = 0.1690).

To evaluate the matrix effects on the active compound, the sample BKAA1801 was selected since it is representative of Anti-TIGIT manufacturing process and because it has a higher concentration with respect to the reference material (20.72 mg/mL vs 19.42 mg/mL). Indeed, as suggested in the ICH guideline, to test a wider range of matrix dilutions, the sample with the highest concentration available should be used in the specificity experiments. The sample is diluted to the target concentrations and each dilution step is performed in matrix sequentially, in order to mimic the matrix dilution performed when samples at different concentrations are tested. For this reason, the sample BKAA1801 was tested by diluting it in Anti-TIGIT buffer up to different concentrations: 20.72 mg/mL, 2.72 mg/mL, 0.272 mg/mL and 0.0272 mg/mL mimicking real samples. This way, the matrix in the bioassay was diluted and tested at 1:10360, 1:1036 and 1:103.6 and 1:10.36 respectively. The experiment has been performed twice in order to confirm the first result obtained.

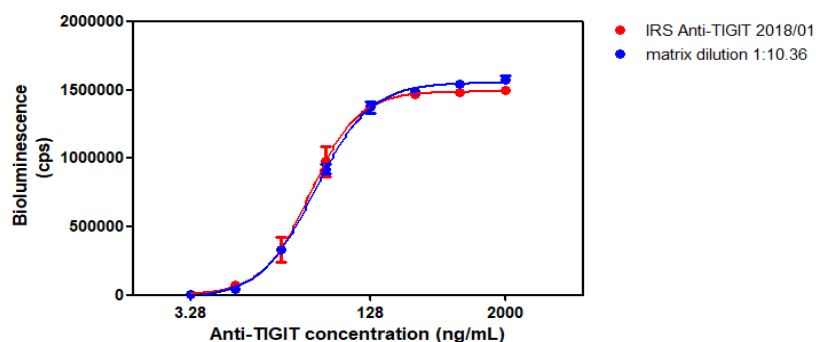
Specificity elaboration is reported in figure 32.



### Anti-TIGIT buffer 1:10360/1:1036/1:103.6



### Anti-TIGIT buffer 1:10.36



#### Matrix dilution

#### Potency (n=2)

1:10360

93%

1:1036

93%

1:103.6

100%

1:10.36

93%

### Matrix effect (1:10.36 – 1:10360)

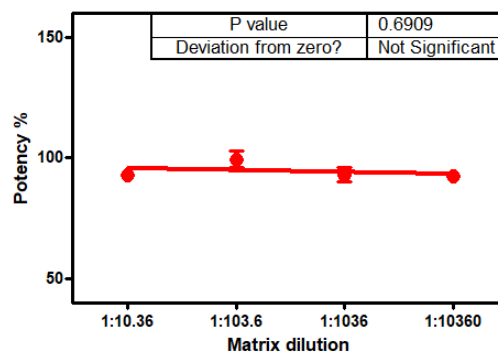


**Figure 32: Specificity: matrix effect on samples.** Anti-TIGIT matrix was tested at different dilutions (1:10360; 1:1036, 1: 103,6; 1:10,36) in order to exclude that it has possible effects on drug's bioactivity evaluations. The linear regression of potencies obtained when the sample is diluted in the tested buffer at different concentrations results in a line with a slope that is not significantly different from zero (p-value greater than 0.05) proving that the matrix does not affect the bioactivity of the samples under the tested conditions. Abbreviation: n= number of tested performed for the analysis.

The linear regression of potencies obtained when the BKAA1801 sample is diluted in Anti-TIGIT buffer at different concentrations results in a line with a slope that is not significantly different from zero (p-value = 0.6909). Therefore, this result suggests that Anti-TIGIT buffer does not have an effect on the bioactivity of samples when its dilution is between 1:10.36 and 1:10360, mimicking the dilution of samples concentrated between 0.0207 mg/ml to 20.7 mg/ml. As a result, only Anti-TIGIT samples concentrated more than 0.0207 mg/ml can be analyzed in the bioassay without any matrix interference.

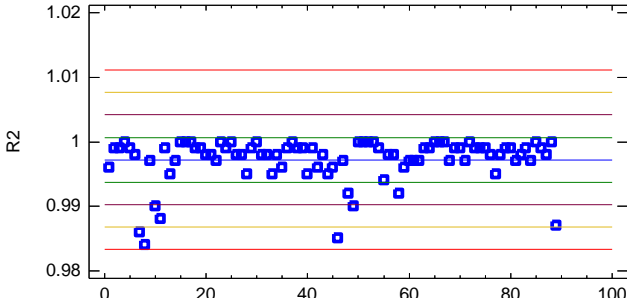
#### 4.2.2.5 System Suitability

Prior to calculating the potency of a test article, an assessment of the assay performance should be conducted. Indeed, once a method is defined linear, accurate and precise within a certain range and specific in order to be applied in routine QC analysis, it is fundamental to define system suitability criteria to guarantee the performances of the bioassay over time. System and sample suitability criteria are a panel of assay performance criteria, established during assay development and confirmed during assay validation, to ensure the assay is in a controlled state during the testing. System and sample suitability are applied individually to each plate, and each test article on the plate. For the approach used and the statistical analysis refer to Chapter 3, section 3.3.1.3.

#### Goodness of fit assessment

$R^2$  values from both the Reference material and sample curves were collected and the values distribution analyzed and used to establish the acceptance criteria. As shown below (table 16) based on the generated data, the  $R^2$  parameter was set to 0.99, at three SD below the calculated average  $R^2$ .

**Table 16: Goodness of fit.** All the  $R^2$  of the reference and tested samples were collected in order to identify the criteria for  $R^2$  parameter. Abbreviations: Exp= experiment, SD= standard deviation.

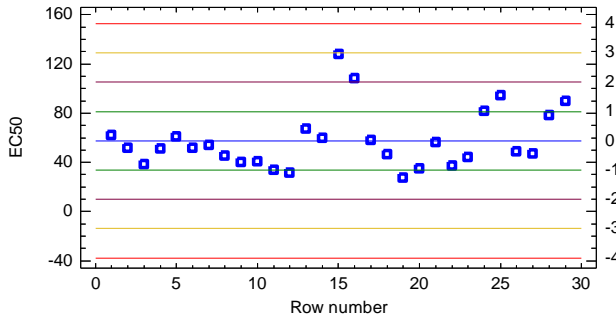
Exp	R <sup>2</sup>	Exp	R <sup>2</sup>	Exp	R <sup>2</sup>	Exp	R <sup>2</sup>	Exp	R <sup>2</sup>	Exp	R <sup>2</sup>
1	0.996	16	1.000	31	0.998	46	0.985	61	0.997	76	0.998
2	0.999	17	1.000	32	0.998	47	0.997	62	0.997	77	0.995
3	0.999	18	0.999	33	0.995	48	0.992	63	0.999	78	0.998
4	1.000	19	0.999	34	0.998	49	0.990	64	0.999	79	0.999
5	0.999	20	0.998	35	0.996	50	1.000	65	1.000	80	0.999
6	0.998	21	0.998	36	0.999	51	1.000	66	1.000	81	0.997
7	0.986	22	0.997	37	1.000	52	1.000	67	1.000	82	0.998
8	0.984	23	1.000	38	0.999	53	1.000	68	0.997	83	0.999
9	0.997	24	0.999	39	0.999	54	0.999	69	0.999	84	0.997
10	0.990	25	1.000	40	0.995	55	0.994	70	0.999	85	1.000
11	0.988	26	0.998	41	0.999	56	0.998	71	0.997	86	0.999
12	0.999	27	0.998	42	0.996	57	0.998	72	1.000	87	0.998
13	0.995	28	0.995	43	0.998	58	0.992	73	0.999	88	1.000
14	0.997	29	0.999	44	0.995	59	0.996	74	0.999	89	0.987
15	1.000	30	1.000	45	0.996	60	0.997	75	0.999		
Average		0.997202		<div>Outlier Plot with Sigma Limits</div> <div>Sample mean = 0.997202, std. deviation = 0.00348757</div> 							
SD		0.00348757									
Average - 3xSD		0.99									

*Yellow line =  $\pm 3xSD$  – Purple line =  $\pm 2xSD$  – Green line =  $\pm 1xSD$*

### EC<sub>50</sub> parameter

The range for this parameter was calculated only based on the EC<sub>50</sub> values of the IRS Anti-TIGIT 2018/01 dose-response curves obtained in the Linearity and Specificity experiments. EC<sub>50</sub> of the samples was not included as it depends on their own biological activity. Variability of all EC<sub>50</sub> values was also calculated. Results are reported in table 17.

**Table 17: EC<sub>50</sub> analysis.** All the EC<sub>50</sub> of the reference IRS Anti-TIGIT 2018/01 were collected to determine the EC<sub>50</sub> acceptance criteria range (27-129 ng/mL). Also, EC<sub>50</sub> variability was calculated (CV  $\leq$  56%).

Exp	EC <sub>50</sub>	Exp	EC <sub>50</sub>	Exp	EC <sub>50</sub>	Exp	EC <sub>50</sub>
1	62.3	9	39.9	17	57.9	25	94.2
2	51.5	10	40.8	18	46.3	26	48.7
3	38.6	11	33.8	19	27.1	27	47.0
4	51.1	12	31.4	20	34.9	28	78.3
5	60.9	13	67.1	21	56.4	29	89.7
6	51.4	14	59.8	22	37.3		
7	54.0	15	127.8	23	44.0		
8	45.3	16	108.1	24	81.8		
Average		57.50		<div>Outlier Plot with Sigma Limits</div> <div>Sample mean = 57.4966, std. deviation = 23.7886</div> 			
SD		23.789					
Min. value		27					
Average +3xSD		129					
95% upper bound CI of SD		32.1729					
CV%		56					

*Yellow line =  $\pm 3xSD$  – Purple line =  $\pm 2xSD$  – Green line =  $\pm 1xSD$*

Abbreviations: SD= standard deviation, CI= confidence interval, CV% = coefficient of variation expressed as a percentage.

Based on the above data, the majority of EC<sub>50</sub> values were distributed in the range of  $\pm 3xSD$ . However, as the calculation of the lower EC<sub>50</sub> limit (i.e., Average – 3xSD) results in a negative number, the minimum EC<sub>50</sub> value obtained in the validation study was set as the lower range limit. Therefore, the EC<sub>50</sub> range was set between 27 and 129 ng/ml.

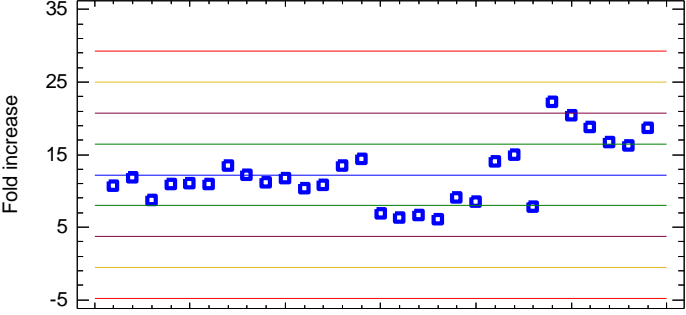
#### Fold increase evaluation

The Fold increase is a measure of the extent of the bioassay response to the tested drug. As this value depends on the nature of the tested sample, Fold increase was only calculated on the IRS Anti-TIGIT 2018/01 dose-response curves. As the interpolation of the IRS dose-response curves to the 4PL algorithm resulted in negative Bottom values, the fold increase of the response could not be derived from the ratio between Top and Bottom values. Therefore, it was calculated as follows:

Fold increase = Top value of the IRS dose-response curve – Bottom value of the IRS dose-response curve

Based on the data distribution shown in table 18, the CPS values deriving from the difference between top and bottom asymptotes ranged between  $\pm 3\text{xSD}$ .

**Table 18: Fold increase analysis.** In the table for each experiment that was considered the values of the Top, of the Bottom and the difference Top- Bottom (Fold increase or FI) are shown. Moreover, the average of the FI, the standard deviation, the minimum value obtained for the FI and the average + 3xSD are shown. The final range for the FI was set considering for the lower value the minimum value since the average – 3xSD was negative while for the upper range the average + 3XSD was selected.

Exp	Top	Bottom	Top-Bottom	Exp	Top	Bottom	Top-Bottom	Exp	Top	Bottom	Top-Bottom
1	1092000	22217	1069783	11	1021000	-11380	1032380	21	1398000	341	1397659
2	1170000	-8963	1178963	12	1098000	14353	1083647	22	1489000	193	1488807
3	868773	674	868099	13	1407000	61266	1345734	23	779071	6927	772144
4	1086000	-6870	1092870	14	1445000	12157	1432843	24	2249000	21544	2227456
5	1102000	-503	1102503	15	711761	23239	688522	25	2049000	12929	2036071
6	1094000	3219	1090781	16	634713	8282	626431	26	1896000	18676	1877324
7	1363000	19058	1343942	17	663997	-1656	665653	27	1723000	49784	1673216
8	1212000	-3580	1215580	18	598825	-10460	609285	28	1643000	23537	1619463
9	1112000	-6185	1118185	19	860536	-43150	903686	29	1888000	20093	1867907
10	1170000	916	1169084	20	833078	-13280	846358	30			
Average			1222220								
SD			426562								
Min. value			609285								
AVG +3xSD			2501906								
<div>Outlier Plot with Sigma Limits</div> <div>Sample mean = 1.22222E6, std. deviation = 426562.</div> <div>(X 100000.)</div> <div></div> <div>Fold increase</div> <div>Row number</div>											

*Yellow line =  $\pm 3\text{xSD}$  – Purple line =  $\pm 2\text{xSD}$  – Green line =  $\pm 1\text{xSD}$*

Abbreviations: SD= standard deviation.

However, as the lower value of the range was found to be negative, the minimum value obtained in the validation study was used to set the range. Therefore, the fold increase for the Anti-TIGIT bioassay has to comply with the following acceptance criteria:

Parameter	Acceptance criteria
<b>Fold increase (Top – Bottom)</b>	$6.09 \times 10^5 - 2.5 \times 10^6$ CPS

#### Similarity assessment

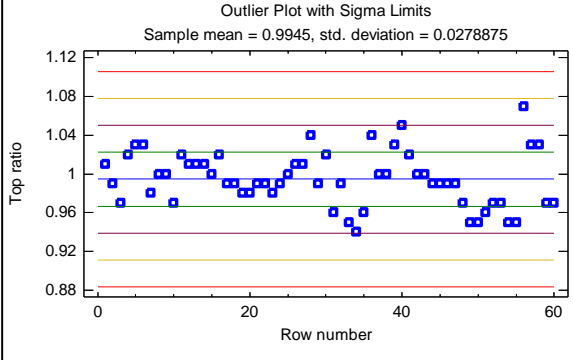
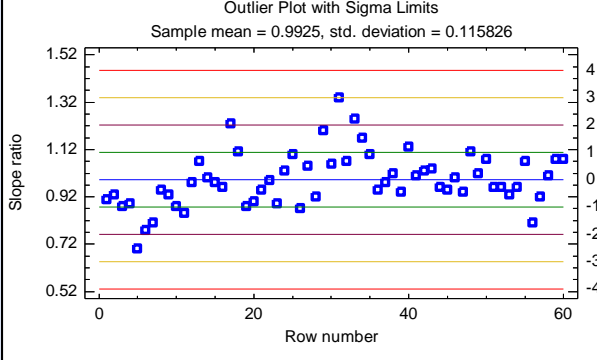
Similarity between Sample and Reference dose-response curves was assessed by calculating Top and Slope ratios as follows:

$$\text{Top/Slope ratio} = \frac{\text{Top/Slope value of IRS dose-response curve}}{\text{Top/Slope value of Sample dose-response curve}}$$

The Bottom ratio was not calculated due to the occurrence of negative values of bottom asymptotes after the interpolation to the 4PL algorithm.

Results are shown in table 19.

**Table 19: Similarity results (Top ratio and Slope ratio).** All the Top and Slope ratio were collected to determine the acceptance criteria ranges. The acceptance criteria for the Top ratio was found to be 0.9-1.1 and the acceptance criteria for the Slope ratio 0.6-1.3. Abbreviations: SD= standard deviation.

Exp	Top ratio	Slope ratio	Exp	Top ratio	Slope ratio	Exp	Top ratio	Slope ratio
1	1.01	0.91	21	0.99	0.95	41	1.02	1.01
2	0.99	0.93	22	0.99	0.99	42	1.00	1.03
3	0.97	0.88	23	0.98	0.89	43	1.00	1.04
4	1.02	0.89	24	0.99	1.03	44	0.99	0.96
5	1.03	0.70	25	1.00	1.10	45	0.99	0.95
6	1.03	0.78	26	1.01	0.87	46	0.99	1.00
7	0.98	0.81	27	1.01	1.05	47	0.99	0.94
8	1.00	0.95	28	1.04	0.92	48	0.97	1.11
9	1.00	0.93	29	0.99	1.20	49	0.95	1.02
10	0.97	0.88	30	1.02	1.06	50	0.95	1.08
11	1.02	0.85	31	0.96	1.34	51	0.96	0.96
12	1.01	0.98	32	0.99	1.07	52	0.97	0.96
13	1.01	1.07	33	0.95	1.25	53	0.97	0.93
14	1.01	1.00	34	0.94	1.17	54	0.95	0.96
15	1.00	0.98	35	0.96	1.10	55	0.95	1.07
16	1.02	0.96	36	1.04	0.95	56	1.07	0.81
17	0.99	1.23	37	1.00	0.98	57	1.03	0.92
18	0.99	1.11	38	1.00	1.02	58	1.03	1.01
19	0.98	0.88	39	1.03	0.94	59	0.97	1.08
20	0.98	0.90	40	1.05	1.13	60	0.97	1.08
<b>Top ratio</b>						<b>Slope ratio</b>		
								
<b>Average</b>		0.995	<b>Average</b>		0.993			
<b>SD</b>		0.0279	<b>SD</b>		0.1158			
<b>Average -3xSD</b>		0.9	<b>Average -3xSD</b>		0.6			
<b>Average +3xSD</b>		1.1	<b>Average +3xSD</b>		1.3			

*Yellow line =  $\pm 3xSD$  – Purple line =  $\pm 2xSD$  – Green line =  $\pm 1xSD$*

Based on the data distribution, the majority of Top and Slope ratios were distributed in the range of  $\pm 3 \times \text{SD}$ . Hence, Top and Slope ratio ranges were set as follows:

Parameter	Acceptance criteria
Top ratio	0.9 – 1.1
Slope ratio	0.6 – 1.3

At the end of this validation all acceptance criteria defined at the beginning of the study were met, thus confirming that the method is suitable for QC release tests and stability studies.

In addition, this methodology could be standardized for the evaluation of other biomolecules exploiting their biological activity through the binding of an extracellular receptor.



### **4.3 Anti-TIGIT Competitive ELISA Assay**

Other alternatives more representative of the MOA of the biotherapeutic drugs than cell-based ligand binding bioassays have also been explored.

Therefore, we tried to develop a new bioassay for Anti-TIGIT that could be also used as an orthogonal method to the cell-based ligand binding. The first choice was a competitive ELISA (Enzyme linked immunosorbent assay). ELISA is a highly sensitive, specific and readily available technique, routinely used in almost every laboratory (Syedbasha et al., 2016). Ligand-binding assay (LBA) is as an analytical method that measures the binding ability of an analyte to its specific target and as such it represents the first step for antibody functional assessment. Indeed, it can provide direct evidence if the antibody candidate can bind to specific antigen properly. Specifically, for therapeutic monoclonal antibodies, which rely on specific binding activities to deliver certain clinical effects, binding affinities and selectivity play a vital role in determining drug efficacy and safety. Therefore, Ligand-binding assays are commonly required by regulatory agencies, such as FDA and EMA, as an essential part of the submission package.

Competitive ELISA is a strategy that is commonly used in most of the laboratories working in an industrial setting. Particularly, the method that has been developed consists in a competition between a labeled molecule (biotinylated CD155) and our antibody (Anti-TIGIT) for the binding to the antigen (TIGIT) captured on the plate. A decrease in signal will indicate the binding of Anti-TIGIT mAb to the antigen molecules when compared to assay wells with labeled molecule alone. Among the different strategies that exist specifically for the detection step, we selected the indirect one that uses a biotin-streptavidin complex for amplification. The competitive ELISA is the most popular ELISA format since it offers several advantages with respect to the cell-based ligand binding assay. It has a rapid set-up and it is fast to develop; it excludes the variability related to the use of the cells and it could be performed every day and would be easily transferred to Quality Control laboratories.

Before starting with the bioassay development, several parameters were evaluated including coating/capture conditions (coating buffer, TIGIT antigen optimal concentration, incubation time); plate blocking achieved with the addition of irrelevant protein or other molecule to cover all unsaturated surface-binding sites of the microplate wells; biotinylated CD155 fixed concentration to be used; Anti-TIGIT dose-response curve and probing/detection with the appropriate read-out (Streptavidin HRP-conjugated dilution).

The first step is immobilization of the antigen of interest (TIGIT) that is accomplished by direct adsorption to the assay plate. The most common method for coating plates involves preparing a 1–10 µg/mL solution of protein in the appropriate coating buffer. In this situation the ELISA coating buffer selection is crucial. Indeed, the coating buffer is used to help immobilizing the selected molecules on microtiter plates. Key factors in immobilization of antibodies on to microtiter plates can be the pH of the coating buffer and the time and the coating conditions (room temperature or +5°C) since the adsorption occurs passively through hydrophobic interactions between non-polar protein residues and the plastic. Selecting a coating buffer between pH 7.4 and pH 9.6 can have an effect on the steric structure of antibody binding and thus affect its immobilization. Testing of coating buffers can help increase mobility and performance of immobilized antibodies.

The two most common coating buffers are 1X PBS at pH 7.5 and Bicarbonate buffer at pH 9.6 that have been both tested here with a TIGIT coating concentration of 0.5 µg/mL and 1 µg/mL. In the same experiment, after the coating of the plates, a biotinylated CD155 dose response curve has been tested in order to identify the CD155 suboptimal concentration for the ELISA ligand binding bioassay. In the figure below a representative result (Figure 33):

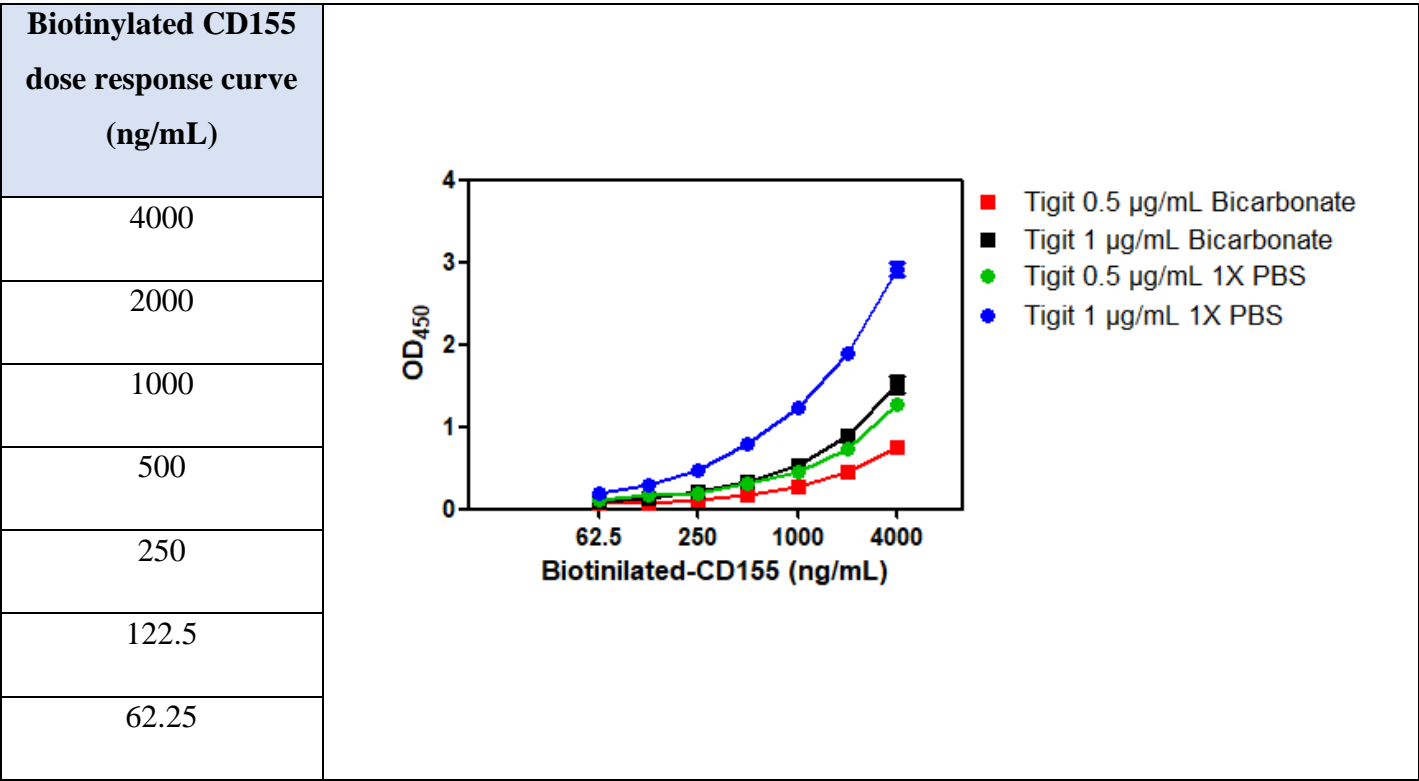


**Figure 33: Coating buffer selection and CD155 suboptimal concentration to be use for ELISA development.** As shown from the curves using 1X PBS as coating buffer (blue and green curves), the obtained OD values are higher than when using Bicarbonate (black and red curves). As expected, signals are higher also when increasing the TIGIT coating concentration (1 µg/mL vs 0.5 µg/mL). Based on the OD values obtained, the CD155 concentrations selected to be further tested in the assay are 500 ng/mL and 1000 ng/mL.

1X PBS as coating buffer, 1 µg/mL of TIGIT as coating concentration and 0.5 µg/mL of Biotinylated CD155 have been initially selected for assay development. An example of the preliminary Anti-TIGIT dose response curve applying the conditions above is reported in figure 34.

As shown below the Anti-TIGIT dose response curve perfectly fits the 4PL algorithm by showing well defined top and bottom plateau and having a R<sup>2</sup> equal to 0.99.

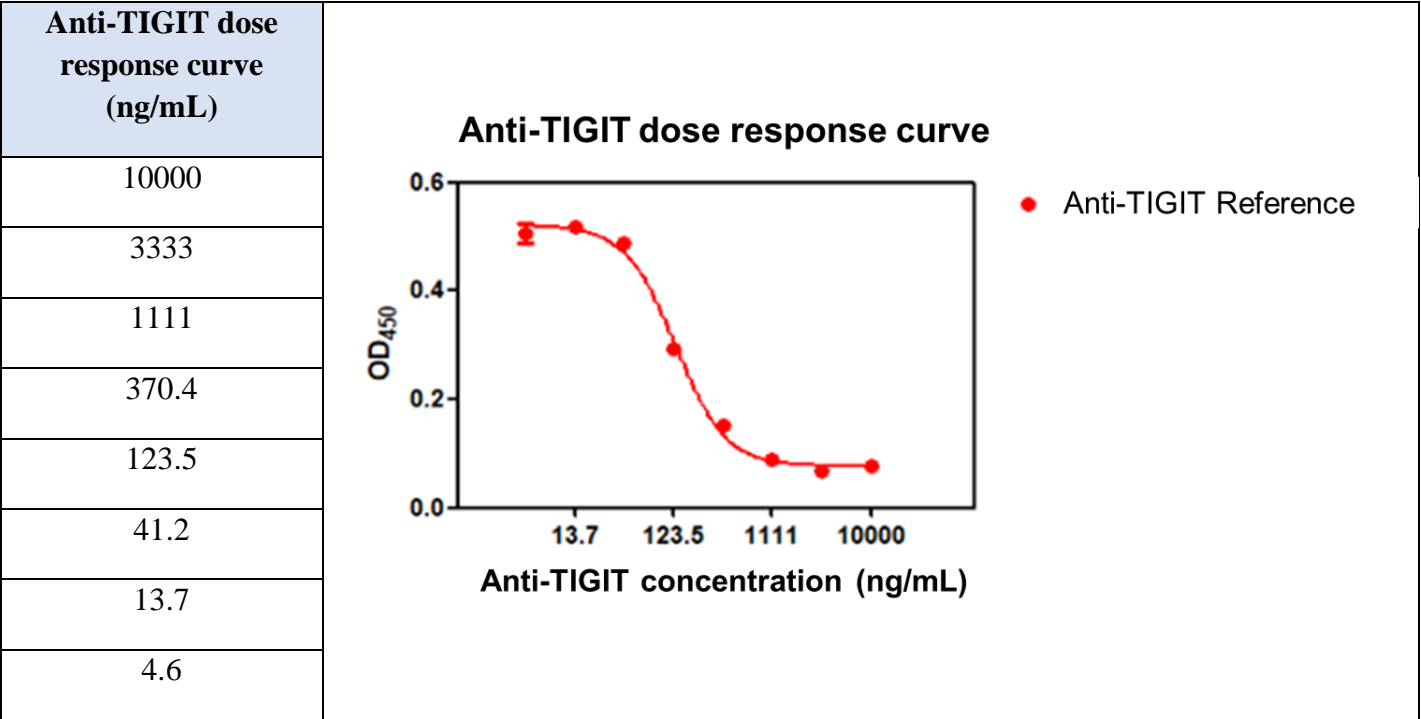


**Figure 34: Anti-TIGIT dose response curve.** On the left it is reported a table with the Anti-TIGIT concentrations of the 8 points dose-response curve. On the right, a representation of the Anti-TIGIT dose-response curve is graphed.

Since the optimal Anti-TIGIT dose response curve was selected, the following step was to optimize the enzymatic detection step by testing two different Streptavidin-HRP dilutions: 1:4000 and 1:2000.

Horseradish peroxidase is one of the two commonly used enzymes for ELISA applications. Its small size (40KDa) allows more molecules to be coupled with such as streptavidin, and this will boost signal generation. Enzymatic signal generation requires the catalysis of a substrate to produce a colored compound. Here we used TMB as colorimetric substrate. When the desired color intensity is reached, a stop solution is added to provide a fixed end point for the assay.

By reducing HRP dilution step the maximum signal obtained could be increased since the detection step could largely determine the sensitivity of an ELISA. The result of this test is shown in the figure below (figure 35):

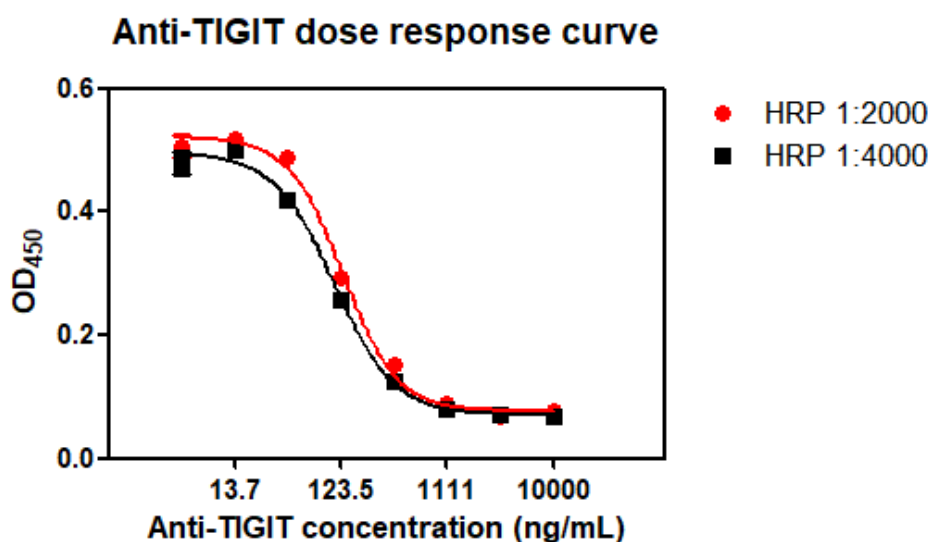


**Figure 35: Streptavidin-HRP dilution selection.** Two different Streptavidin-HRP dilutions have been tested with the same Anti-TIGIT dose response curve. As shown from the figure the red curve (using a dilution of 1:2000) reached higher signals with respect of the black curve (Streptavidin-HRP dilution 1:4000) without impacting the signal background.

Given the obtained signals we decided to use the Streptavidin HRP diluted 1:2000.

Despite of using high concentrated Streptavidin-HRP and high concentration of TIGIT, the final signal intensity is not the one that we expected (OD values around 1.5 at the top of the curve) meaning that the system still requires optimization.

For this reason, other attempts varying different factors were performed in order to increase the overall signal. Among the factors that could affect ELISA signal intensity we considered assay and blocking buffer composition and components concentration, washes (buffer composition, volume, duration and frequency), TIGIT and biotinylated CD155 concentrations and Anti-TIGIT dose-

response curve. Blocking buffers usually consist of formulations of proteins designed to prevent non-specific binding of proteins to the plate. Indeed, the binding capacity of microplate wells is typically higher than the amount of protein coated in each well. The remaining surface area must be blocked to prevent antibodies or other proteins from adsorbing to the plate during subsequent steps.

An optimal blocking buffer maximizes the signal-to-noise ratio and does not react with the antibodies or target protein improving the sensitivity of the assay.

As reported in literature (Steinitz et al., 2000), some systems may benefit from the addition of a surfactant such as Tween-20 (a gentle non-ionic detergent) to the blocking solution. Typically, a final concentration of 0.05% (v/v) Tween-20 is used. Indeed, the blocking buffer that we used is composed by 1X PBS, 1% of 7.5% BSA (serum bovine albumin) and 0.05% Tween-20. Addition of this detergent helps in minimizing hydrophobic interactions between the blocking protein and the antigen.

The same composition, but without BSA, was used for the washing buffer.

Washing steps are necessary to remove non-bound reagents and decrease background, thereby increasing the signal to noise ratio. Non proper washing could cause high background, while excessive washing might induce a decrease in sensitivity caused by elution of the antibody and/or antigen from the well. For this reason, a physiologic buffer was selected.

Given the low signal intensity it was decided to eliminate Tween-20 from the assay buffer since it could interfere with the low affinity binding between TIGIT and Biotinylated CD155. In addition to this modification, both TIGIT and Biotinylated CD155 concentration in the assay have been increased from 0,5 µg/mL to 1 µg/mL while the starting concentration of Anti-TIGIT dose response curve has been set to 20 µg/mL with a step dilution 1:3.

Below an example of the obtained result (Figure 36):

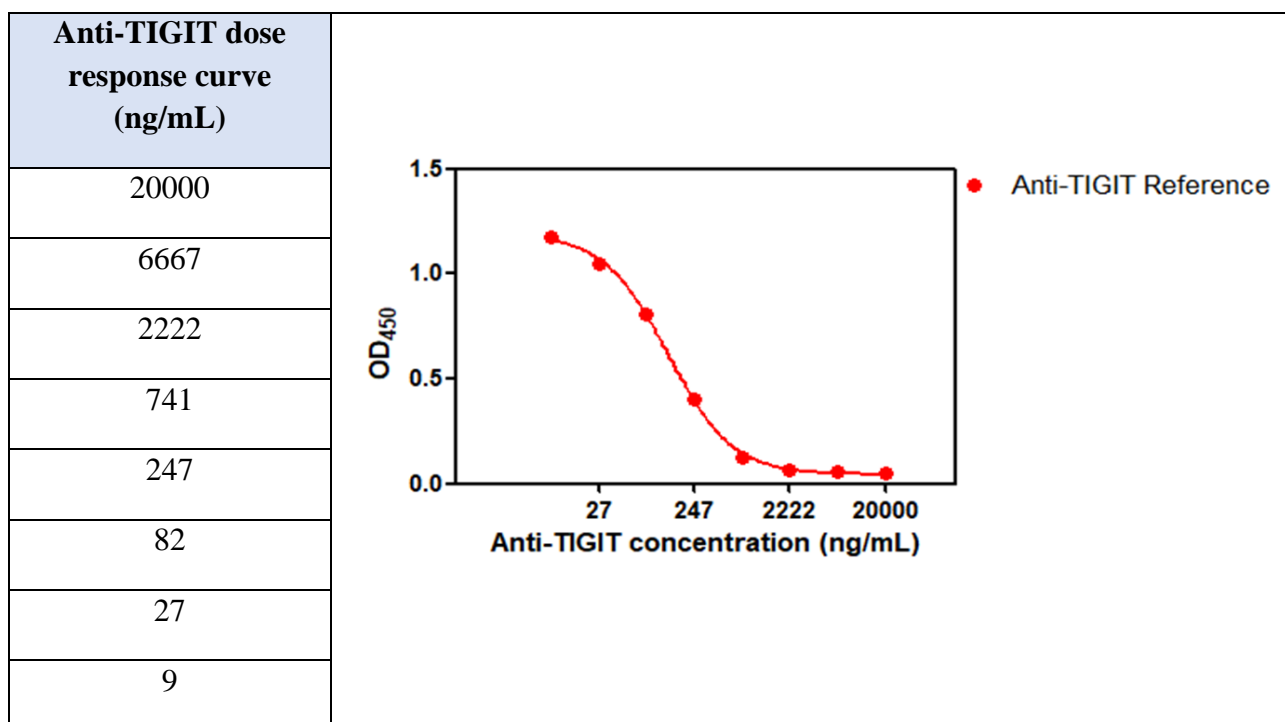


**Figure 36: A representative Anti-TIGIT dose response curve.** On the left the table showed the 8 concentrations point values of the Anti-TIGIT dose response curve while on the right a representative graph of the same dose response curve obtained with the optimized ELISA procedure is shown. After method fine tuning, the reference material dose response curve graphed in red perfectly met our internal requirements. The final signal at the top of the curve is increased with a maximum OD value around 1.5. Moreover, the dose response curve of Anti-TIGIT is symmetrical around its inflection point and well-shaped with properly defined top and bottom plateau. The IC50 value usually obtained is around 200 ng/mL.

After the method adjustments, Anti-TIGIT dose response curve showed a signal with the expected intensity.

The final layout of the assay is graphed in the figure below (figure 37):

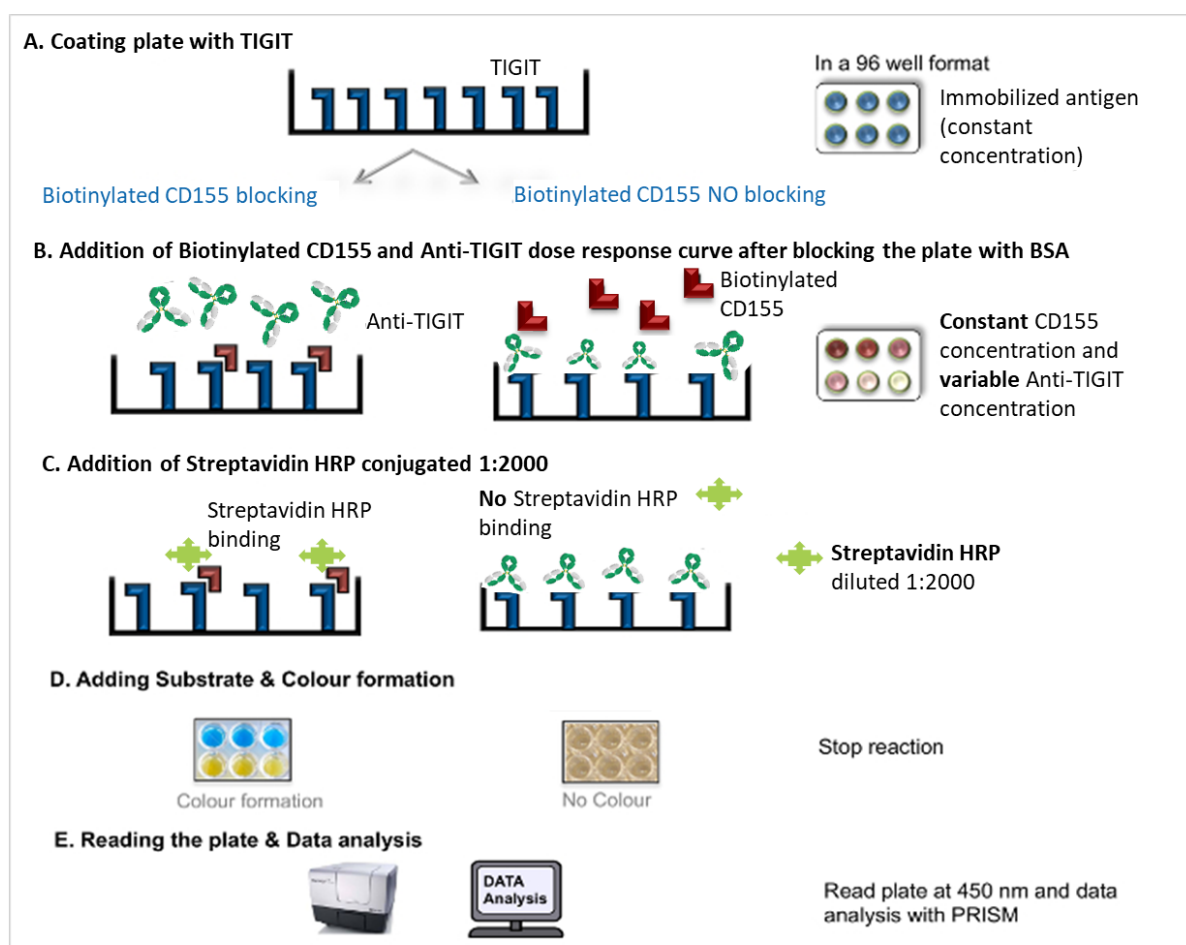


**Figure 37: Competition antibody-antigen-interaction assay.** The step-by-step protocol for competition ELISA is shown. Specifically, the plate is coated at +5°C with TIGIT for at least 16 hours. Then the plate is blocked and Anti-TIGIT 8 points dose-response curve together with a fixed concentration of biotinylated CD155 are added. After 2 hours of incubation time at room temperature to allow antibody-antigen interaction, the Streptavidin HRP (horseradish peroxidase)-conjugated is added to each well and incubated for 30 minutes. This step is followed by the addition of TMB and after 15 minutes of the stop solution. Finally, absorbance at 450 nm is detected. After each step washing steps are foreseen to ensure that only specific (high affinity) binding events are maintained to cause signal at the final step. Modified from Syedbasha et al., 2016.

Experiments to confirm the results and to assess the robustness of the entire system should be performed prior to use this assay as an orthogonal method to the CBA to assess Anti-TIGIT batches biological activity.

#### **4.4 TIGIT-CD155 Blockade Bioassay**

A potential limitation of the competitive ELISA assay is that it reflects an *in vitro* situation. In particular, as highlighted in the work of Syedbasha et al., it is not possible to distinguish if the ligand simply binds to the receptor or if the ligand also activates the receptor by inducing a conformational change or a dimerization, which in turn leads to an intracellular signal (Syedbasha et al., 2016).

For this reason, the main goal of this study was the feasibility assessment of a cell-based method that do not simply measure the binding between Anti-TIGIT and TIGIT but that can also verify the cascade of events leading to the blockade of the TIGIT/CD155 interaction.

This way antibody potency and bioactivity could be better assessed by reflecting the *in vivo* mechanism of action in a more physiologically relevant environment and preserving the native target form. The starting point for this new cell-based assay was the TIGIT/CD155 Blockade Bioassay, a bioluminescent cell-based assay developed by Promega. This Bioassay consists of two genetically engineered cell lines. TIGIT Effector Cells (Jurkat T cells) expressing human TIGIT with a luciferase reporter driven by a native promoter that can respond to both TCR activation and CD226 co-stimulation and CD155 aAPC/CHO-K1 Cells (CHO-K1 cells) engineered to express human CD155 with an engineered cell-surface protein designed to activate the TCR complex in an antigen-independent manner. When the two cell types are co-cultured, TIGIT inhibits CD226 activation and promoter-mediated luminescence. Addition of an Anti-TIGIT antibody blocks the interaction of TIGIT with CD155 or inhibits the ability of TIGIT to prevent CD226 homodimerization, resulting in promoter-mediated luminescence as shown in figure 38.



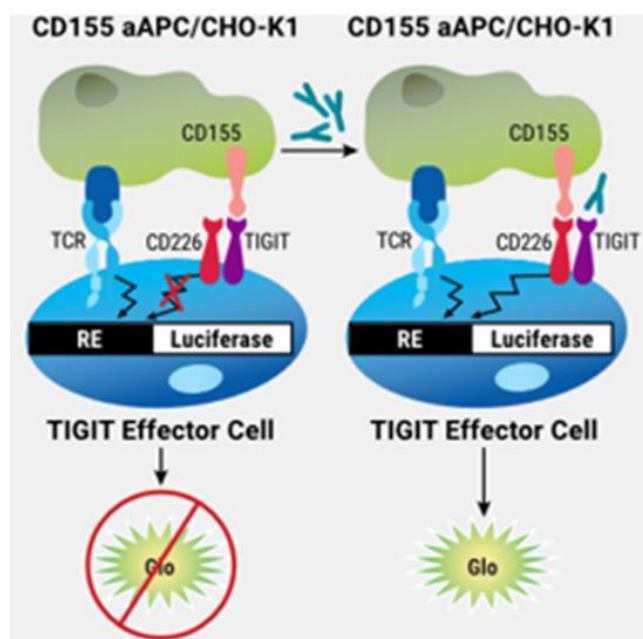


**Figure 38: TIGIT/CD155 Blockade Bioassay Design.** When the two cell lines are co-cultured, TIGIT inhibits CD226 pathway-activated luminescence. The addition of Anti-TIGIT antibody blocks the TIGIT/CD155 interaction, thereby re-establishing CD226 pathway-activated luminescence, which can be detected in a dose-dependent manner by addition of BIo-Glo™ Reagent and quantitation with a luminometer. Figure supplied by Promega, Inc.

The bioassay workflow is simple and can be performed in a two-day time frame. During day 1 the CD155 aAPC/CHO-K1 Cells are pre-plated in 96 wells plates and incubate overnight. The day after the 10 points Anti-TIGIT dose-response curve is added in triplicate to the plate together with the TIGIT Effector Cells. In this way one sample per plate could be tested together with the reference material. The plate is then incubated in incubator. After six hours induction, the assay plate is equilibrated at room temperature for 10-15 min before the addition of the readout reagent and luminescence detection.

The first dose-response curves have been generated applying the standard conditions for this type of assays: for cells number and incubation time we followed what was stated in the supplier's protocol. Anti-TIGIT dose-response curve started from the same Anti-TIGIT concentration (100 µg/mL) with the same step dilution (1:2,5) of the one of Promega but, instead of having 10 points, the one that we tested has 8 points in order to increase the throughput of the assay (in this way up to three samples per plate could be tested instead of only one). Both the signal reached, and the fold increase were low, not comparable with the data provided by the developer (figure 39).

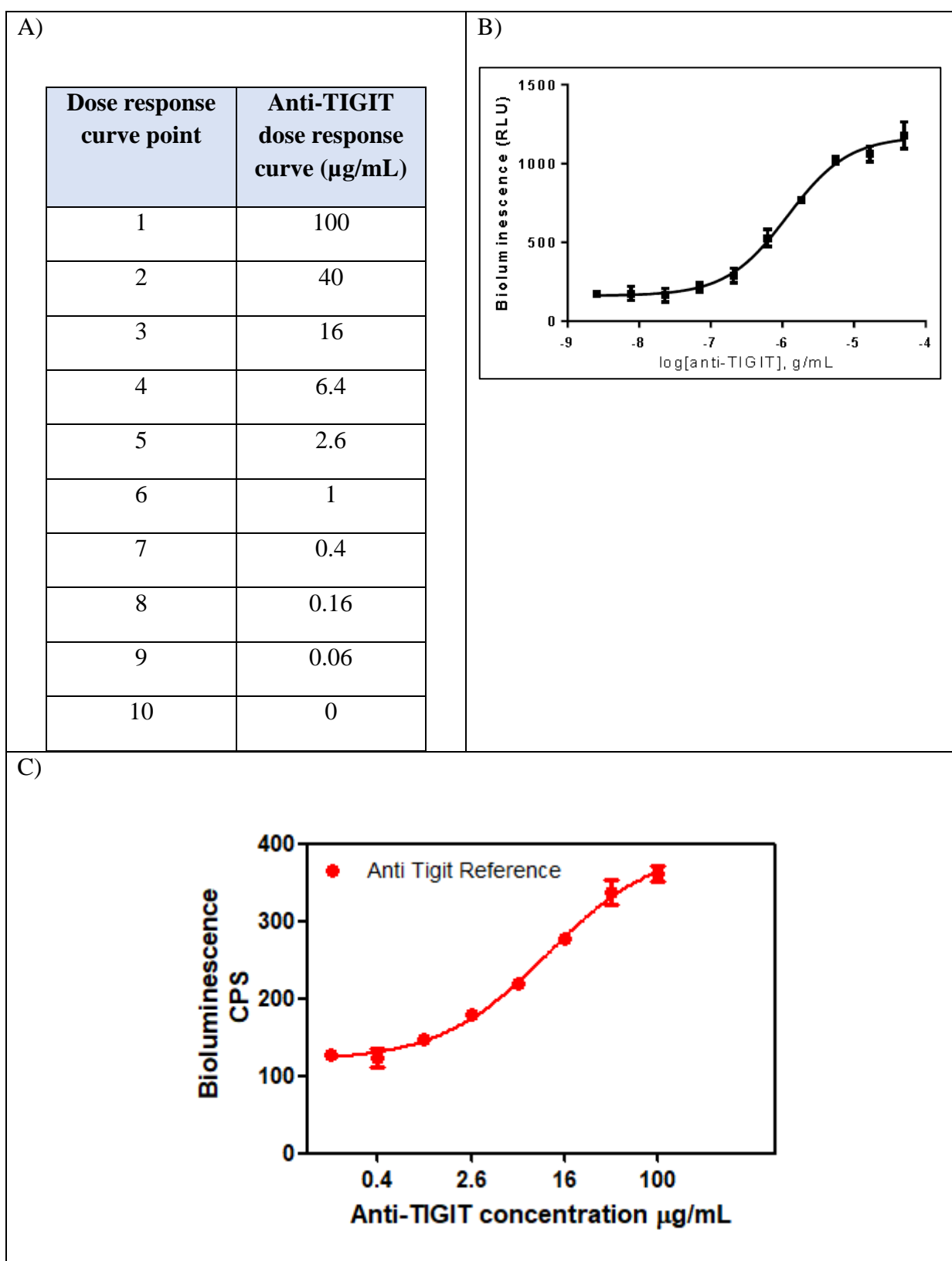


**Figure 39:** Anti-TIGIT dose response curve. A) Anti-TIGIT dose-response curve concentrations. B) Anti-TIGIT dose-response curve obtained from the supplier using an internal Anti-TIGIT positive control (black

curve). The picture was supplied as it is by Promega. C) Anti-TIGIT dose response curve obtained with the proof of concept antibody. As shown from the obtained results the signal reached from the red curve was lower with respect to what is shown for the black curve (350 versus 1300 counts per second, CPS). Moreover, the shape of our Anti-TIGIT dose-response curve was not well defined. Abbreviations: RLU = Luminescence relative units; CPS = Counts per seconds.

After excluding possible problems related to the reagents used for the assay such as 96-well plates, culture and assay media and BioGlo luciferase, different hypothesis for the root causes of the poor signal and not well-defined dose-response curve were formulated.

To track down all the possible reasons of this defect we used a fishbone diagram identifying as concomitant root causes:

- No proper detection. Indeed, it is well-known that assay performance can be greatly affected by instrumental properties and range and sensitivity of the detector;
- Insufficient number of cells per well;
- Not optimized concentration range of Anti-TIGIT to achieve a full dose response with complete upper and lower asymptotes;
- Low functionality of the cells;
- Low affinity of Anti-TIGIT antibody for its target TIGIT.

To overcome the issues highlighted in the previous runs, in the following experiments some of the conditions stated in Promega protocol have been changed including Anti-TIGIT starting concentration (from 100  $\mu\text{g/mL}$  to 400  $\mu\text{g/mL}$ ), the dose-response curve step dilution (from 1:2.5 to 1:3) and the detector used. Indeed, the spectrophotometer Tecan Infinite F200Pro that we used is designed primarily for fluorescence and not luminescence, so its sensitivity was demonstrated to be too low for this type of assay as shown in figure 40. GloMax Discover Multimode Microplate reader was therefore selected as alternative detector since it is designed for plate-reading luminescence detection and present an adjustable gain that could be regulated to obtain the maximal signal. Anti-TIGIT dose response curve obtained after the previously proposed adjustments is shown in the figure 41.

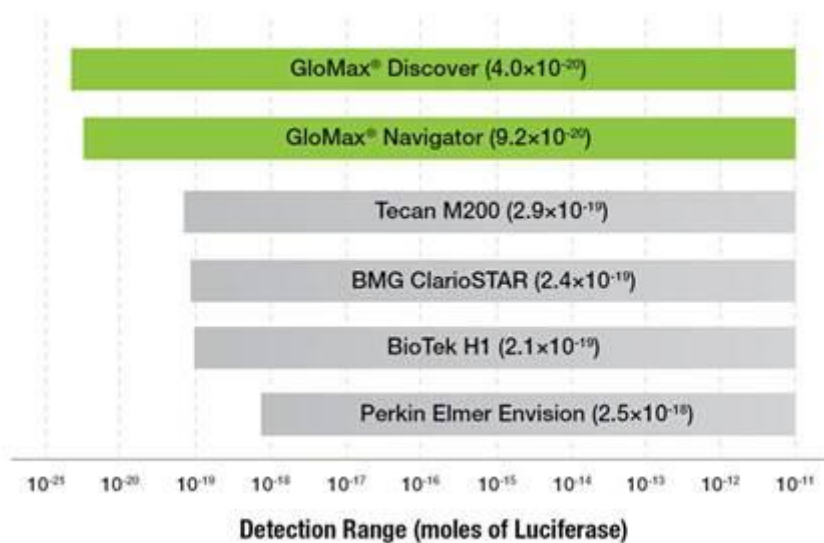


**Figure 40:** Sensitivity of Bio-Glo™ detection on GloMax® Systems and other commercially available plate readers. GloMax Discover System present the highest sensitivity among the tested plate readers.

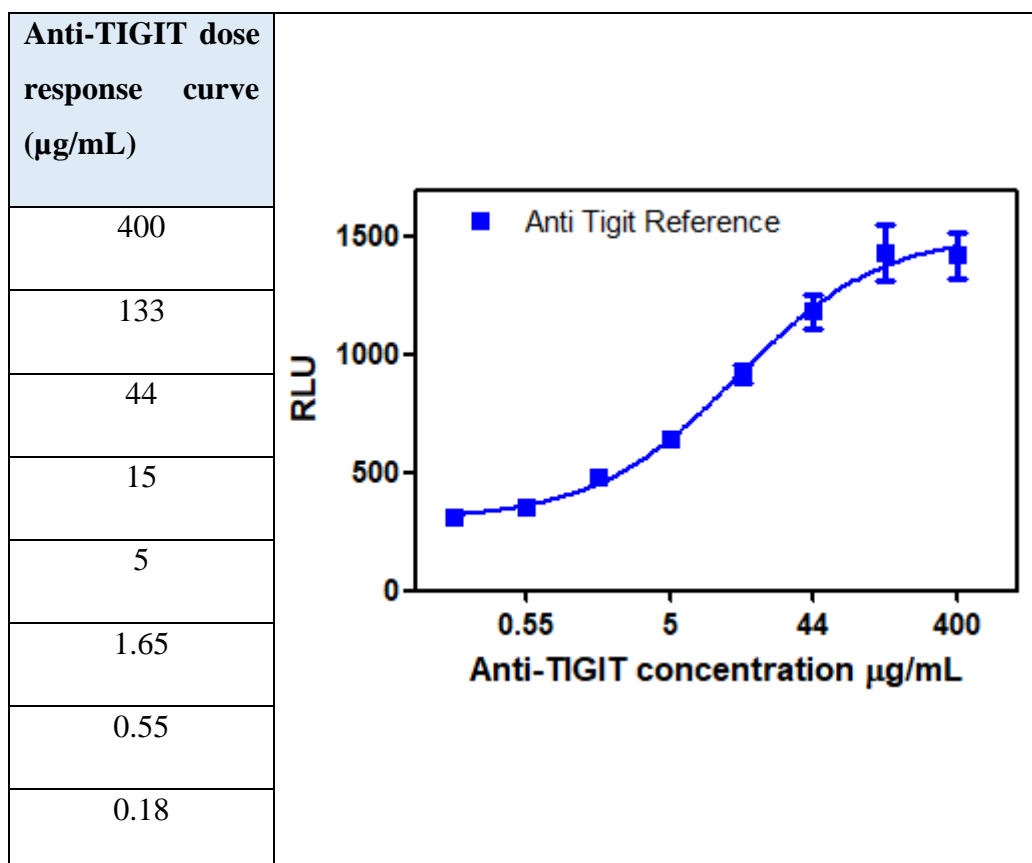


**Figure 41:** Anti-TIGIT dose response curve applying the new conditions. The dose-response curve showed an increased signal in terms of RLU, a well-defined shape and a fold increase comparable with the one of the Promega Anti-TIGIT dose-response curve (figure 40B). Abbreviation: RLU = Luminescence relative units.

By increasing Anti-TIGIT starting concentration and changing the plate reader, the Anti-TIGIT dose response curve become comparable in terms of signal intensity and fold increase to the one of Promega. However, even if the same experimental conditions were repeated, the shape of the curve and its reproducibility do not reflect our performance verification requirements (data not shown). This suggested that not all the parameters were optimized. An increased number of both cell types (CHO and Jurkat) and also a different cell ratio were tested but the results did not change (data not shown). To exclude a problem related to cells' functionality a deeper investigation was conducted by comparing the Promega positive control that is an Anti-TIGIT mouse IgG1 used to validate the TIGIT/CD155 Blockade Bioassay with our Anti-TIGIT antibody in the Blockade Bioassay (data not shown). Based on the obtained results, it was possible to exclude a problem with the cells' responsiveness since the dose-response curve of the Promega positive control was well defined. Anti-TIGIT antibody seems to be less active than Promega mouse positive control explaining the difficulties in developing the blockade bioassay. However, the reduced affinity of Anti-TIGIT antibody for its main target is requested since, as demonstrated in several published works, the overall efficacy of antibody therapies results from the complex interplay between affinity, valence, tumor penetration and retention, and signaling inhibition. Moreover, there are several models demonstrating that there is an inverse relationship between affinity and tumor penetration (termed the binding-site barrier). Successful binding of antigen decreases the concentration of free mAb reducing mAb's diffusion into the tumor. In addition, target antigen is commonly expressed also on normal tissue. This nontarget pool of antigens can reduce treatment effectiveness and increase side-effects especially when considering high affinity mAbs (Rudnick and Adams, 2009).

## **4.5 Anti-TIGIT ADCC activity**

In a case like Anti-TIGIT, the knowledge that multiple immune system-mediated effects are important suggests that early inclusion of effector function capability testing in the characterization package may provide valuable insight. For this reason, to test for these Anti-TIGIT potential effector functions, two cell-based ADCC assays involving different effector cell types were explored. Then

the most promising one has been also qualified to introduce it in the final analytical panel for the characterization of early phase new biological entities.

Effector functions are defined as the abilities of an antibody to mediate activation of components of the immune system. Antibody effector functions are a clinically relevant part of the humoral immune response and form an essential link between innate and adaptive immunity. MAbs' effector functions are induced via the constant (Fc) region of the antibody. The most well-known Fc-mediated effector functions are antibody-dependent cell-mediated cytotoxicity (ADCC), antibody-dependent cellular phagocytosis (ADCP), and complement-dependent cytotoxicity (CDC) (Van Erp et al., 2019). Fc antibody portion can interact with various effector molecules including complement proteins and specialized Fc-receptors (Woof and Burton, 2004). The known classes of FcR include Fc $\gamma$ R, which bind IgG; Fc $\alpha$ R, which bind IgA; and Fc $\epsilon$ R, which bind IgE as shown in the table 20. Among the subclasses of immunoglobulin G (IgG) antibodies (IgG1, IgG2, IgG3 and IgG4), IgG1 and IgG3 antibodies exhibit relatively stronger binding to the major Fc $\gamma$ R required for effector functions (Hansel et al., 2010). Fc $\gamma$ R are the most important for tumor cell clearance by myeloid cells and are comprised of activating Fc $\gamma$ RI (CD64), Fc $\gamma$ RIIA (CD32A), Fc $\gamma$ RIIIA (CD16A), and inhibitory Fc $\gamma$ RIIB (CD32B) receptors (Zahavi et al., 2018).

Fc $\gamma$ RIIIa is the only activating Fc $\gamma$ R expressed on NK cells, and it is thought to play a pivotal role in ADCC induced by IgG1 subclass mAbs. Correlations between Fc $\gamma$ RIIIa polymorphism (F158V) and response to rituximab or other mAbs supported Fc $\gamma$ RIIIa significance in clinical efficacy as highlighted in the paper of Tada et al (Tada et al., 2014).

**Table 20: Human Leucocyte FcγR, FcαR and FcεR.** Relative affinities of various ligands for each receptor are indicated in decreasing order, starting from the isotype with the highest affinity. Abbreviations: DC= dendritic cells, INF-γ= interferon γ; ITAM= immunoreceptor tyrosine-based activation motif; ITIM= immunoreceptor tyrosine-inhibitory motif; HR= high responder; LR= low responder; NA= neutrophil antigen; N.D.= not determined; NK= natural killer; SIgA= secretory IgA.

From Woof and Burton, 2004.

Fc receptor (FcR)	Major isoforms expressed	Allotype	Specificity for human Ig*	Affinity for monomer Ig	Signalling motif	Cellular distribution
FcγRI (CD64)	FcγRIa	–	IgG1=3>4 IgG2 doesn't bind	High	γ-chain ITAM	Monocytes, macrophages, neutrophils (IFN-γ stimulated), eosinophils (IFN-γ stimulated)
FcγRII (CD32)	FcγRIIa	LR	IgG3≥1=2 IgG4 doesn't bind	Low	α-chain ITAM	Monocytes, macrophages, neutrophils, platelets and Langerhans cells
	FcγRIIa	HR	IgG3≥1>>>2 IgG4 doesn't bind	Low	α-chain ITAM	Monocytes, macrophages, neutrophils, platelets and Langerhans cells
	FcγRIIb	–	IgG3≥1>>2>4	Low	α-chain ITIM	Monocytes, macrophages and B cells
	FcγRIIc	–	N.D.	Low	α-chain ITAM	Monocytes, macrophages, neutrophils and B cells
FcγRIII (CD16)	FcγRIIIa	–	N.D.	Medium	γ-chain ITAM	Macrophages, NK cells, γδ T cells and some monocytes
	FcγRIIIb	NA1, NA2	IgG1=3>>>2=4	Low	No signalling motif Anchored in the membrane by GPI linkage	Neutrophils and eosinophils (IFN-γ stimulated)
FcεRI	FcεRI	–	IgE	Very high	γ-chain ITAM β-chain also present, but its role is unclear	Mast cells, basophils, Langerhans cells and activated monocytes
FcεRII (CD23)	FcεRIIa	–	IgE	Low	C-type lectin	B cells
	FcεRIIb	–	IgE	Low	C-type lectin	B cells, T cells, monocytes eosinophils and macrophages
FcαRI (CD89)	FcαRIa	–	Serum IgA1=2, SIgA1=SIgA2	Medium	γ-chain ITAM	Neutrophils, monocytes, some macrophages, eosinophils, Kupffer cells and some DCs

The phenomenon of ADCC is characterized by a cascade of intracellular signalling events started with the interaction between target cell, antigen-bound antibody and Fc receptor on effector cells that results in conformational changes and clustering of activating Fc receptors (Kato et al., 2000; Radaev et al., 2001). Once activated, the effector cells induce target cell death through three key mechanisms: cytotoxic granules release, Fas signaling, and production of reactive oxygen species. The release of perforins and granzymes from effector cell granules is the main and best characterized mechanism utilized in ADCC (Zahavi et al., 2018). The signalling cascade include signalling through the calcineurin and nuclear factor of activated T cells (NFAT) signalling pathway (Nimmerjahn and

Ravetch, 2008). The signalling started with a series of tyrosine phosphorylation events which allow  $\text{Ca}^{2+}$  to enter through  $\text{Ca}^{2+}$  channels, thereby increasing cytoplasmic  $\text{Ca}^{2+}$  concentration. This increase in  $\text{Ca}^{2+}$  induce the dephosphorylation of pNFAT2 by the calcineurin enzyme with subsequent translocation to the nucleus of NFAT. This translocation of NFAT2 up-regulates the synthesis of cytotoxic immune-modulators, including interleukin-2 (IL-2) and granzyme and perforin are released from effector cells and mediate lysis of target cells (Hsieh et al., 2017). Considering the main events characterizing ADCC; relevant cell-based assays required at least an effector cell, an antigen-bearing target cell, mAbs, and a readout to measure cytotoxicity (Lewis et al., 2019). Killing of targets is an endpoint of ADCC pathway activation and is used in classic ADCC bioassays. As effector cells classic methods use primary donor peripheral blood mononuclear cells (PBMCs) or purified natural killer (NK) cells that express Fc Receptors on their surface. These assays generally use freshly isolated PBMCs that are difficult to use in pharmaceutical development settings because fresh blood is required (Parekh et al., 2012). Moreover, these procedures are done often using blood from individuals who are not genotyped, and this could affect assay's outcome. Indeed, there could be major differences in IgG binding among the Fc $\gamma$ RIII allotypes (Koene et al., 1997; Wu et al., 1997) and this correlates with mAb efficacy in vivo. These bioassays are also labor intensive, have high inherent assay variability and can result in high background readings. In addition, the current reference method for measuring cytotoxicity is the  $^{51}\text{Cr}$ -release method. This assay has been considered the gold reference standard as it is the most sensitive and biologically relevant assay for cytotoxicity (Rossignol et al., 2017) and provides a good signal/background ratio. These characteristics result in good performances in terms of accuracy, precision and robustness, at least for a complex bioassay, such as an ADCC assay (Rossignol et al., 2017). However, taking into consideration the advances in environmental protection and operator safety, the use of radionuclides is increasingly constraining and costly and is hard to implement in an industrial context.

Several non-radioactive alternatives to the  $^{51}\text{Cr}$ -release assay have been described and are commercially available. Miller et al. reported that an enzyme-linked immunosorbent assay (ELISA)-based bridging assay using recombinant Fc $\gamma$ RIIIa protein can be used as a surrogate assay for ADCC activity while Parekh et al. (Parekh et al., 2012) developed an ADCC-reporter gene assay measuring the activation of Fc $\gamma$ RIIIa-expressing reporter cells with excellent performance in accuracy, precision and robustness.

Here, two different assay formats involving two different types of effector cells have been explored during the development stage, to obtain the best compromise between assay performance, high



throughput and work time for single assay. The two types of effector cells selected for the evaluation of ADCC activity of Anti-TIGIT are FcγRIIIA engineered NK cells and FcγRIIIA/NFAT-RE/luc2 engineered Jurkat T cells. Both assay formats overcome many of the limitations of traditional methods by eliminating the requirement for primary cell culture and do not use radioactive materials.

The main purpose of the study was to rationalize which of these ADCC effector cells best simulate the expected response in human subjects and to identify which effector cells and assay best fit ADCC bioassay needs during antibody drug development.

CHO-S-myc-hu TIGIT ECD cell line has been used as target cell for both the tested formats. These cells are the same used for the development and validation of the cell-based ligand binding bioassay for the study of Anti-TIGIT biological activity (section 4.2).

#### 3.5.1 ADCC via Immortal NK Effector cells

The clinical efficacy of many targeted mAb therapies has been demonstrated to be at least in part NK cell dependent. Trastuzumab (a humanized anti-HER2 mAb), Cetuximab (a chimeric mAb anti-EGFR) and Rituximab (a chimeric IgG1 mAb targeting CD20), to name a few, are clear examples of NK cell-mediated anti-tumor activity via ADCC (Wang et al., 2015). Considering this, in the first bioassay format engineered NK cells were used as bioassay effector cells in order to try to mimic the in vivo situation.

NK cells are naturally potent cytotoxic effector cells for cancer therapy. However, there are technical challenges to obtain sufficient numbers of functionally active NK cells from patient's blood since they represent only 10% of the lymphocytes (Klingemann et al., 2016).

An immortalized cell line mimicking NK behavior is commercially available. Such cells are an interleukin-2 (IL-2) dependent NK cell line derived from the peripheral blood of a 50-year-old Caucasian man with rapidly progressive non-Hodgkin lymphoma in 1992 and shows strong cytotoxic NK activity. According to the manufacturer information, the cells have the following characteristics: surface marker positive for CD2, CD7, CD11a, CD28, CD45, CD54, CD56bright; surface negative for CD1, CD3, CD4, CD5, CD8, CD10, CD14, CD16, CD19, CD20, CD23, CD34, HLA-DR (Gong et al., 1994). The advantage of applying immortalized cell line mimicking NK cells is that they have an easier cell preparation process, and therefore lower costs and required operator time, versus repeated use of primary NK cells isolated from whole blood.

A CD16 enhanced mutation of such cell line is commercially available as well, derived by retrovirally transduction with the aim to express CD16 receptor (FcγRIII) and have been used as effector cells to mimic the natural ADCC mechanism. There are two different NK CD16 mutant cell lines, each of them expressing one specific isoform of CD16 receptor: low affinity 158-F variant carrying phenylalanine in position 158 and 158-V high affinity variant having a valine at amino acid 158. Even if FcγRIIIA V-158 on NK cells confers a higher binding affinity for a variety of IgG antibodies than does the F-158 variant and contributes to enhanced ADCC activity (Koene et al., 1997; Chung et al., 2014b; Yamane-Ohnuki et al., 2004) both cell lines were tested in this ADCC bioassay format.

This bioassay allows to analyse the end point of the ADCC process by measuring the signal directly from dead target cells giving an accurate *in vitro* representation of the natural mechanism.

Different Anti-TIGIT eight points dose response curves have been tested to identify the best antibody concentration range. Furthermore, the best E:T cells ratio, cell seeding and Target and Effector cells working windows have been assessed. Incubation times of all the experimental stages have been also evaluated. After exploring different types of read out, the Delfia (Dissociation-Enhanced Lanthanide Fluorescent Immunoassay) EuTDA cytotoxicity assay was selected. This assay is considered a valid alternative to <sup>51</sup>Cr release assay since it shows comparable sensitivity for cytotoxicity assays without using radioactive compounds (Blomberg et al., 2011). This assay read out is based on loading target cells with an acetoxymethyl ester of the fluorescence enhancing ligand (BATDA, bis(acetoxymethyl)2,2':6,2''-terpyridine-6,6''-dicarboxylate) (Figure 42). Briefly, target cells are stained with BATDA reagent. The ligand quickly penetrates the cell membrane. Within the cell the ester bonds are hydrolyzed to form a hydrophilic ligand (TDA) which no longer passes the membrane. While the cells are intact, TDA remains in the cell. When mAbs and effector cells are placed in contact with the loaded target cells, upon lysis the TDA is released into the supernatant. After the TDA is mixed with DELFIA Europium solution, the Europium and TDA form a highly fluorescent and stable chelate (EuTDA). Therefore, the measured fluorescence signal correlates directly with the amounts of lysed cells. Europium solution in fact is not fluorescent in its unaltered state.

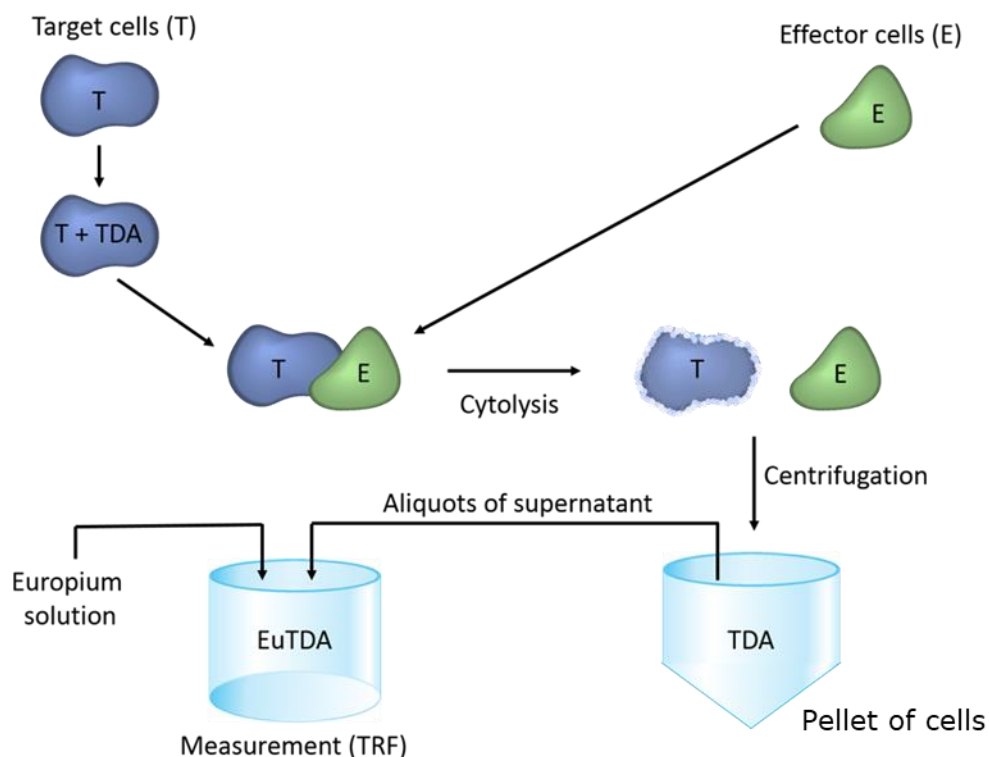


**Figure 42: Workflow of the EuTDA assay.** In the picture the principles of this ADCC bioassay are depicted. Target cells are stained with BATDA. Then target cells are loaded to the plate together with effector cells at a certain E:T ratio and let incubate at 37°C, 5% CO<sub>2</sub>. After a proper incubation, the assay plate is centrifuged, and the supernatant collected and transferred to a new plate. Finally, Europium solution is added, and the time-resolved fluorescence detected. Abbreviations: TFR = Time-Resolved Fluorescence

Modified from Perkin Elmer (<https://www.perkinelmer.com/lab-products-and-services/application-support-knowledgebase/delfia/delfia-cell-cytotoxicity-assays.html>).

Both cell lines were maintained in culture but showed a very low growth rate. Since the high affinity variant NK.CD16V did not reach the minimum number of cells needed for the assay as poorly viable and inefficient in duplication, a feasibility test has been done only with the low affinity variant NK.CD16F.

The following parameters were tested:

- 8 points Anti-TIGIT antibody dose response curve 20000÷0.002 ng/ml with a step dilution 1:10
- Effector/Target ratio 20:1

- Label condition for target cells 2.5 $\mu$ L/mL, 0.45 hour at 37 °C 5% CO<sub>2</sub>

No dose response effect was measured due to a low BATDA reagent incorporation and a very low number of effector cells. Moreover, the low affinity of the receptor expressed on the effector cells is not promoting the interaction, already not favoured by the other conditions.

Several mitigation parameters have been tested such as changing BATDA incubation times and staining protocol. However, no curve was obtained leading to the conclusion that the negative outcome of the assay was mostly due to bad performance of the effector cells. Also, an alternative approach using PBMCs was tested but even in that case no response effect was obtained. In conclusion BATDA approach did not provide satisfactory results.

### 3.5.2 ADCC-RGA via Immortal Jurkat T Effector cells

ADCC Reporter Gene Assay is a bioluminescent cell-based assay using Jurkat T cells that express the Fc $\gamma$ RIIIa receptor and a luciferase reporter driven by an NFAT-response element (NFAT-RE). These engineered effector cells have been implemented to address need for improved precision and accuracy of classic NK cell ADCC bioassays (Hsieh et al., 2017). The ADCC Reporter Gene Assay measures reporter gene signal generated by ADCC pathway activation in engineered Jurkat T effector cells. Jurkat Bioassay Effectors Cells purchased from Promega are engineered Jurkat cells stably expressing the Fc $\gamma$ RIIIa receptor, V158 (high affinity) variant, and a NFAT response element driving expression of firefly luciferase. This format is a surrogate ADCC assay measuring relevant pathway activation in the effector cells as an alternative to measuring target cell death (Cheng et al., 2014). This assay quantifies the signal from the effector cells due to the translocation of NFAT2 protein into the nucleus and the consequent transcription of the luciferase reporter gene, with luminescence signal readout (Cheng et al., 2014). For this reason, ADCC reporter Bioassay provides partial but relevant indication of ADCC MOA process. Its biological relevance with respect to PBMC ADCC assays has been already discussed in the literature. Parekh et al. to demonstrate the comparability among the two ADCC assay formats tested antibodies with different levels of fucosylation (Parekh et al., 2012) since it is well known that fucosylation of the Fc-glycan is inversely linked to Fc $\gamma$ RIIIa binding and ADCC activity (Shields et al., 2002). Their ADCC-reporter gene assay was similarly sensitive to changes in the Fc-glycosylation of mAbs as the PBMC based-ADCC assay. Moreover, researchers were also able to demonstrate that the induction of luciferase activity in the ADCC-reporter assay was comparable to the amount of cell death in the PBMC based assay after incubation with anti-CD20 antibodies of different isotypes having different efficiency in inducing antibodies effector functions

(Parekh et al., 2012). In addition, as underlined by Cheng et al., this ADCC reporter gene assay is widely used in drug development for its high stability and precision and ability to ensure a good throughput of analysis. For the intended aim, the assay would be appropriate, upon development and qualification, to support side by side testing and antibody characterization for industrial purposes.

Briefly, target cells are seeded with Anti-TIGIT antibody and after the incubation Jurkat effector cells are added. The FcγRIIIa/Anti-TIGIT binding results in the activation of NFAT-RE-mediated luciferase activity (Figure 43). The bioluminescent signal is detected and quantified using Bio-Glo™ Luciferase Assay System and a standard luminometer.

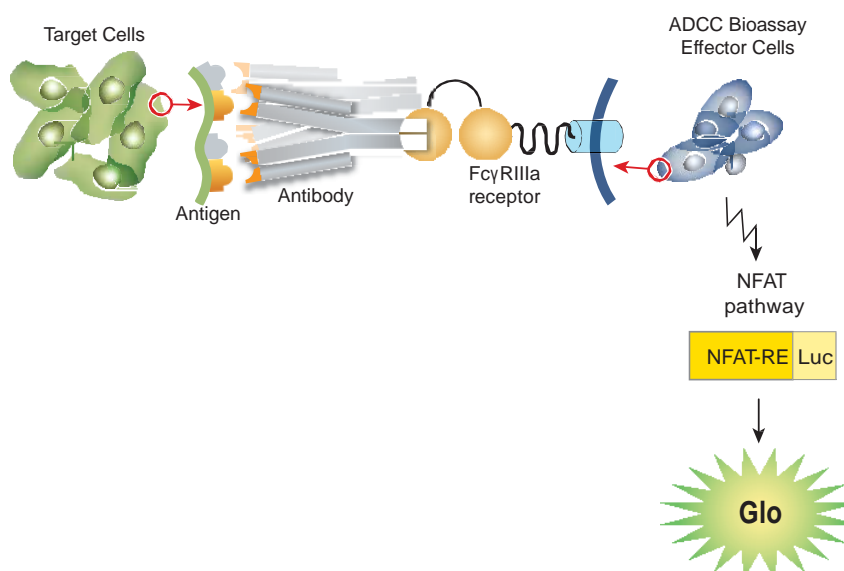


**Figure 43: Representation of the ADCC RGA assay.** The ADCC Reporter Gene Bioassay uses an alternative readout at an earlier point in ADCC MOA pathway activation: the activation of gene transcription through the NFAT (nuclear factor of activated T-cells) pathway in the effector cells. In addition, the ADCC Reporter Bioassay uses engineered Jurkat cells stably expressing the FcγRIIIa receptor, V158 (high affinity) variant, and an NFAT response element driving expression of firefly luciferase as effector cells. Antibody biological activity in ADCC MOA is quantified through the luciferase produced as a result of NFAT pathway activation; luciferase activity in the effector cell is quantified with luminescence readout. Figure supplied by Promega, Inc.

According to the ICH-Q2 analytical method guidelines, the experimental conditions were carefully optimized before starting the development of the assay. The parameters applied in this feasibility step are summarized in the table below.

**Table 21: Main parameters checked for ADCC RGA assay during the feasibility study.**

<b>Parameters</b>	
<b>Target cells</b>	CHO-S-myc-hu TIGIT ECD
<b>Effector cells</b>	Engineered Jurkat cells stably expressing the FcγRIIIa receptor, V158 (high affinity) variant, and a NFAT response element
<b>Ratio Target:Effector</b>	1:12.5
<b>Bioassay incubation time</b>	24 hrs at 37°C, 5%CO <sub>2</sub>

Applying these conditions several dose-response curves, with different step dilutions, were tested. Among all, two curves showed both well described top and bottom and the easiness of run.

For the dose-response curve number 1 the starting concentration of Anti-TIGIT was 10000 ng/mL while dose response curve 2 started from 5000 ng/mL. Moreover, the two curves had different dilution steps has highlighted below (figure 44):

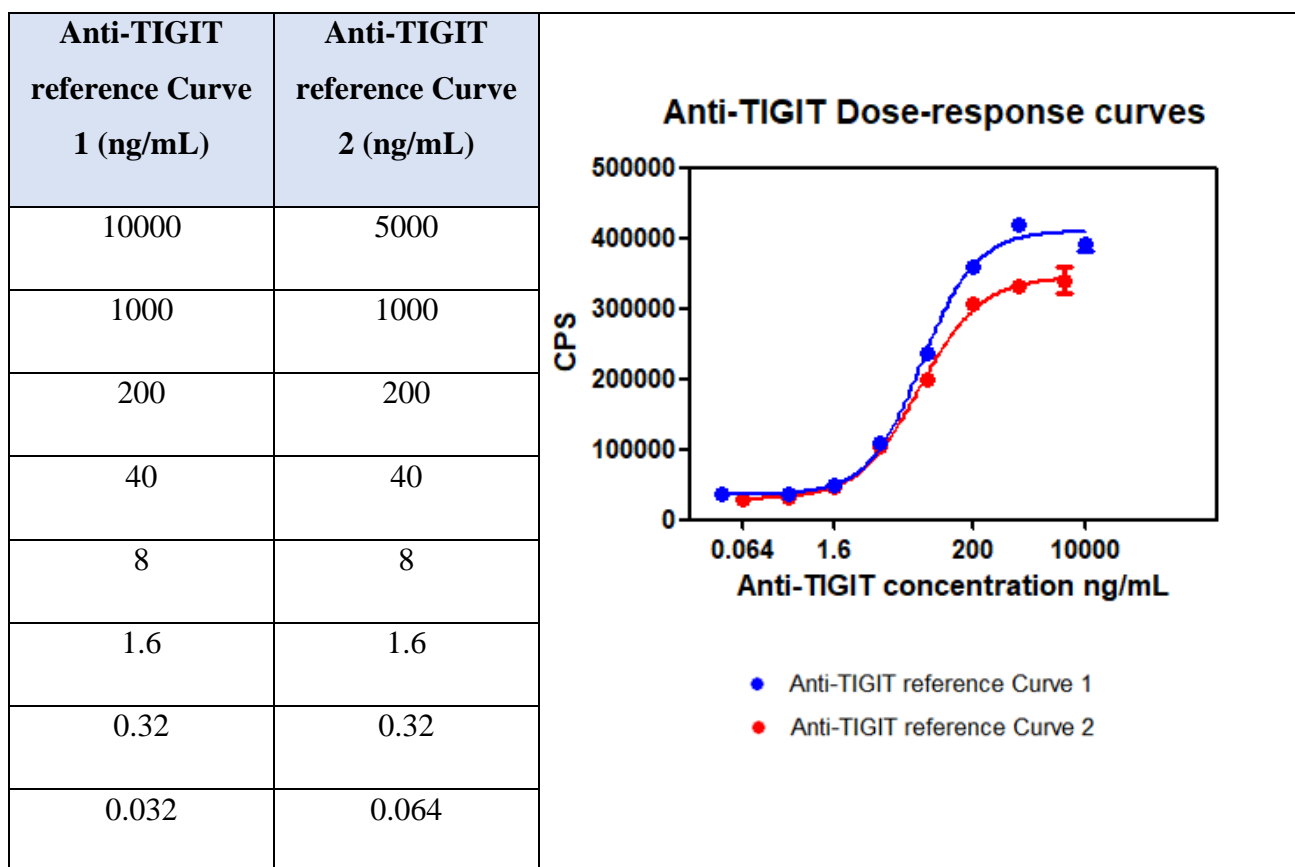


**Figure 44: Representative Anti-TIGIT dose-response curves.** Both curves were obtained by plotting luciferase signal versus Anti-TIGIT concentration. The Anti-TIGIT dose response curve 1 is graphed in blue while the curve 2 in red. The two curves have comparable shapes and EC<sub>50</sub> (33.27 ng/mL for Curve 1 vs 30.53 ng/mL for Curve B).

The experiment has been repeated in order to confirm the results and allow the selection of the best Anti-TIGIT dose-response curve. Results are shown in figure 45.

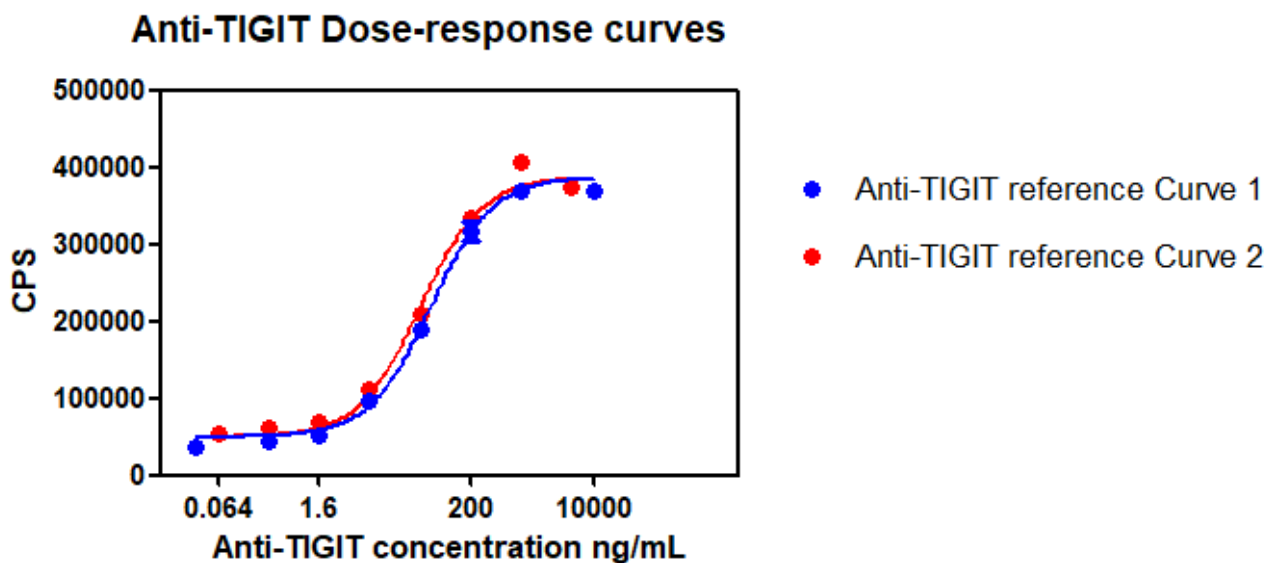


**Figure 45: Anti-TIGIT Dose response curves obtained in the second experiment.** The results shown in the previous experiment (figure 44) were confirmed. Curve 1 shows the same shape of the first experiment reported above while Curve 2 shows a small hook effect in the upper part.

The two dose-response curves showed the same signal intensity in terms of CPS (count per second) but Curve 1 has a better-defined top plateau. Since Curve 1 properly describes Anti-TIGIT reference biological behaviour in both the experiments, it has been selected for the bioassay qualification.

Before starting the qualification also, the specificity of the assay was checked. In this experiment, serial dilutions of Anti-TIGIT were incubated for 6 hours of induction at 37°C with engineered Jurkat effector cells (ADCC Bioassay Effector Cells), with or without ADCC Bioassay Target Cells (CHO-S-myc-huTIGIT).

As shown in figure 46, the ADCC Reporter Bioassay exhibits the clear specificity desired for a bioassay since a good assay response is only obtained when target cells with the correct surface antigen, the correct specific antibody, and effector cells expressing FcγRIIIa are present. If any one of these is missing, no response is detected. In addition, this result attests that the signal is only due to an activation of FcγRIIIa, confirming that Anti-TIGIT antibody is able to mediate ADCC.



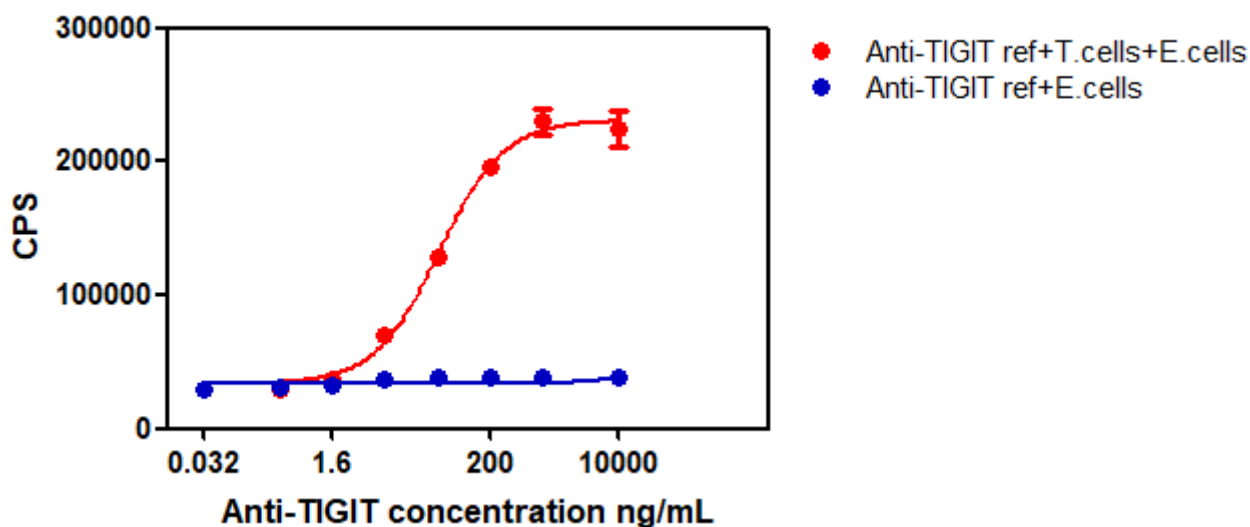


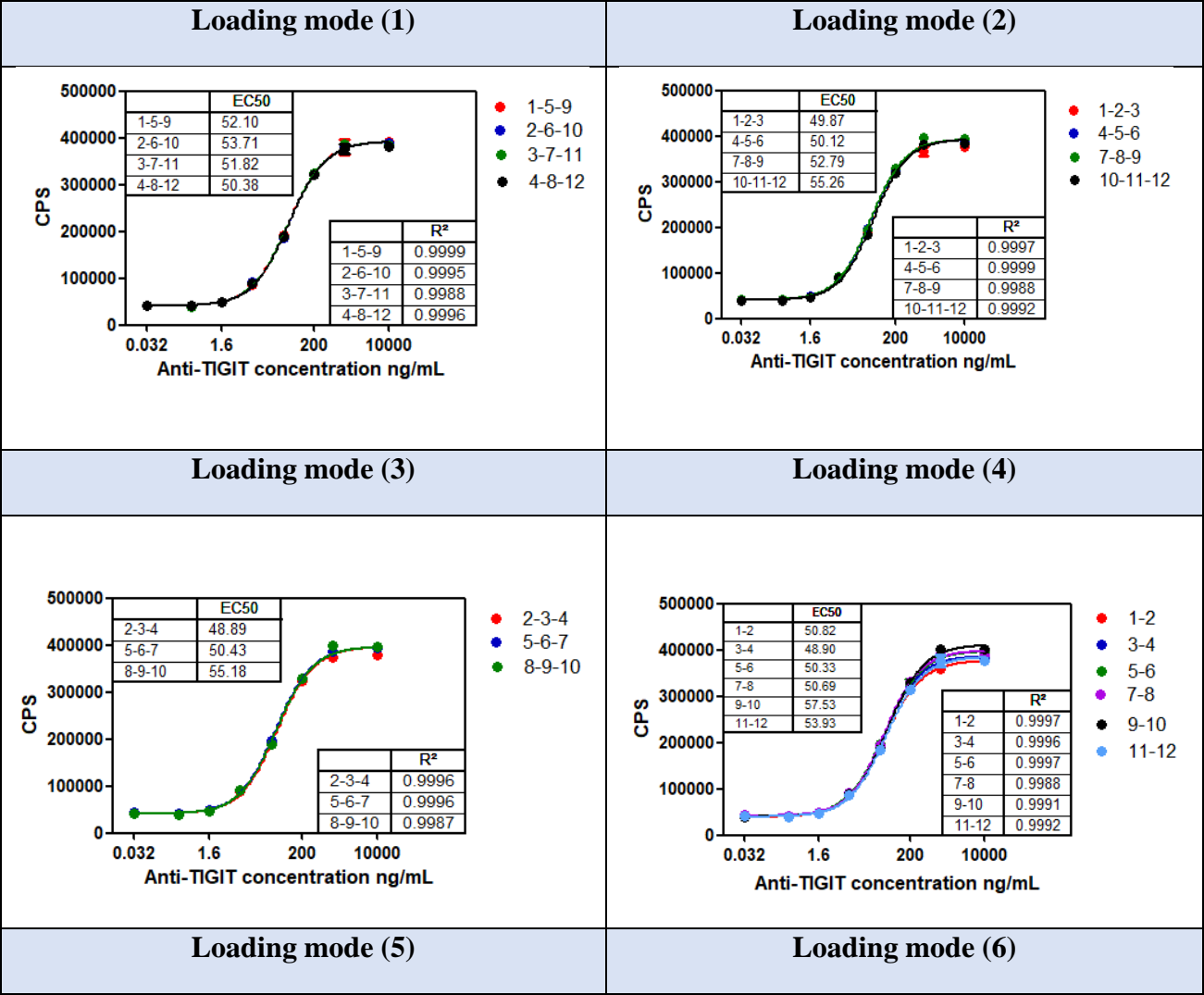
**Figure 46: Specificity of the ADCC Reporter Bioassay.** Anti-TIGIT dose response curve in the complete assay format is depicted in red. When Anti-TIGIT concentration increases also the measured signal is higher. In the same graph Anti-TIGIT dose response curve when target cells are not loaded to assay plate is sketched in blue. As expected, when in the plate target cells are not added as in this case, no response is detected in the assay (flat curve). Abbreviations: T. cells = Target cells; E. cells= Effector cells.

From the analytical method point of view, considering the results obtained with both assay formats, the ADCC RGA's approach that guarantees a higher throughput and reproducibility has been selected to be used for Anti-TIGIT characterization purposes. Moreover, the engineered Jurkat cells rather than NK cells were selected for ADCC assay since Jurkat cells share the same ability to activate the appropriate pathways for cellular activation after the crosslinking of Fc $\gamma$ RIIIa as that of NK cells and in addition, they are much more simple to handle than NK cell line.

For the development of the ADCC RGA assay the same approach used for Anti-TIGIT ligand binding bioassay was applied. Therefore, the plate effect and the preliminary performance verification were assessed as reported in chapter 3 of this work.

As a rule, since uniformity of response throughout the plate is important to guarantee accurate results, any plate effect should be evaluated early during a bioassay development. The plate effect of the Anti-TIGIT ADCC bioassay was determined by analyzing the 8-point dose-response curve of the reference material loaded upright throughout the plate in three independent experiments. Data were fitted by

4PL algorithm considering different plate layout (1-5-9, 1-2-3, 2-3-4 that foresee the loading of standard and samples in triplicate and 1-2, 1-7, 2-3 and 2-7 in which both reference material and samples are analyzed in duplicate). One of the three independent experiments performed is shown in Figure 47 as representative result.



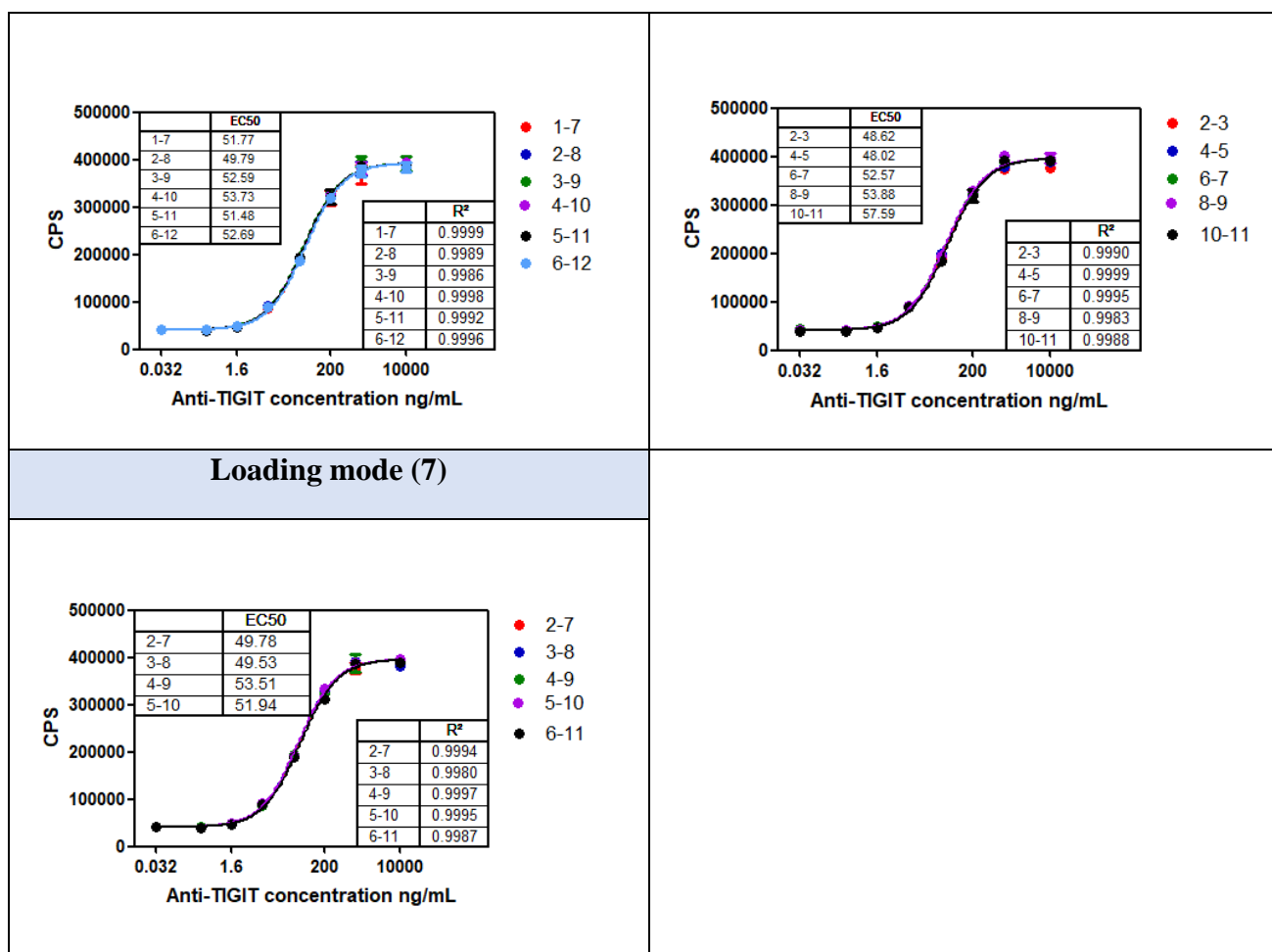


**Figure 47: Plate effect representative dose response curves.** All the possible layout combinations were checked and even if in all the tested loading modes the dose response curves showed comparable values in terms of bottom, top, hillslope and  $R^2$ , the layout 1-5-9 demonstrated less variability among  $EC_{50}$  values.

In all the analyzed plate layouts, the  $R^2$  of each of the curves was  $\geq 0.95$ , thus proving a good fitting of the 4PL model. Similar values of the Hillslope were observed between the curves of the same loading mode, indicating a comparable behavior of the sample throughout the plate. On the other hand, considering all the results obtained for fold increase,  $R^2$ ,  $EC_{50}$  values and the variability, the loading model 1 (1-5-9) was chosen as the best layout to perform and qualify the bioassay.

The performances of the developed method were evaluated according to the ICH guideline on the Validation of Analytical Procedures “Text and Methodology Q2 (R1)” and according to what is reported in Materials and Methods Chapter.

A qualification in terms of goodness of fitting, fold increase of the response, linearity and range, precision and accuracy was performed and evaluated as appropriate requirement to demonstrate the

assay suitability for characterization purposes. All analytical runs were independently performed in terms of day of execution, cells and reagents used. For the entire study CHO-S-myc-hu TIGIT ECD cells between the 15<sup>th</sup> and the 29<sup>th</sup> passage were used. Jurkat ADCC cells were used between 15<sup>th</sup> and the 29<sup>th</sup> passage. These ranges should be considered as just a key indication, until additional information will be collected, related to both cell lines passages working window. Results related to the assay performance qualification are reported in the following paragraphs.

#### 3.5.2.1 Linearity and Range

The linearity and range experiments were executed following the criteria described in table 5 in the section 3.3.1.2. Representative dose response curves of Reference material at different nominal concentrations and the elaboration of the three independent runs performed are reported in figure 48 and table 22 respectively.

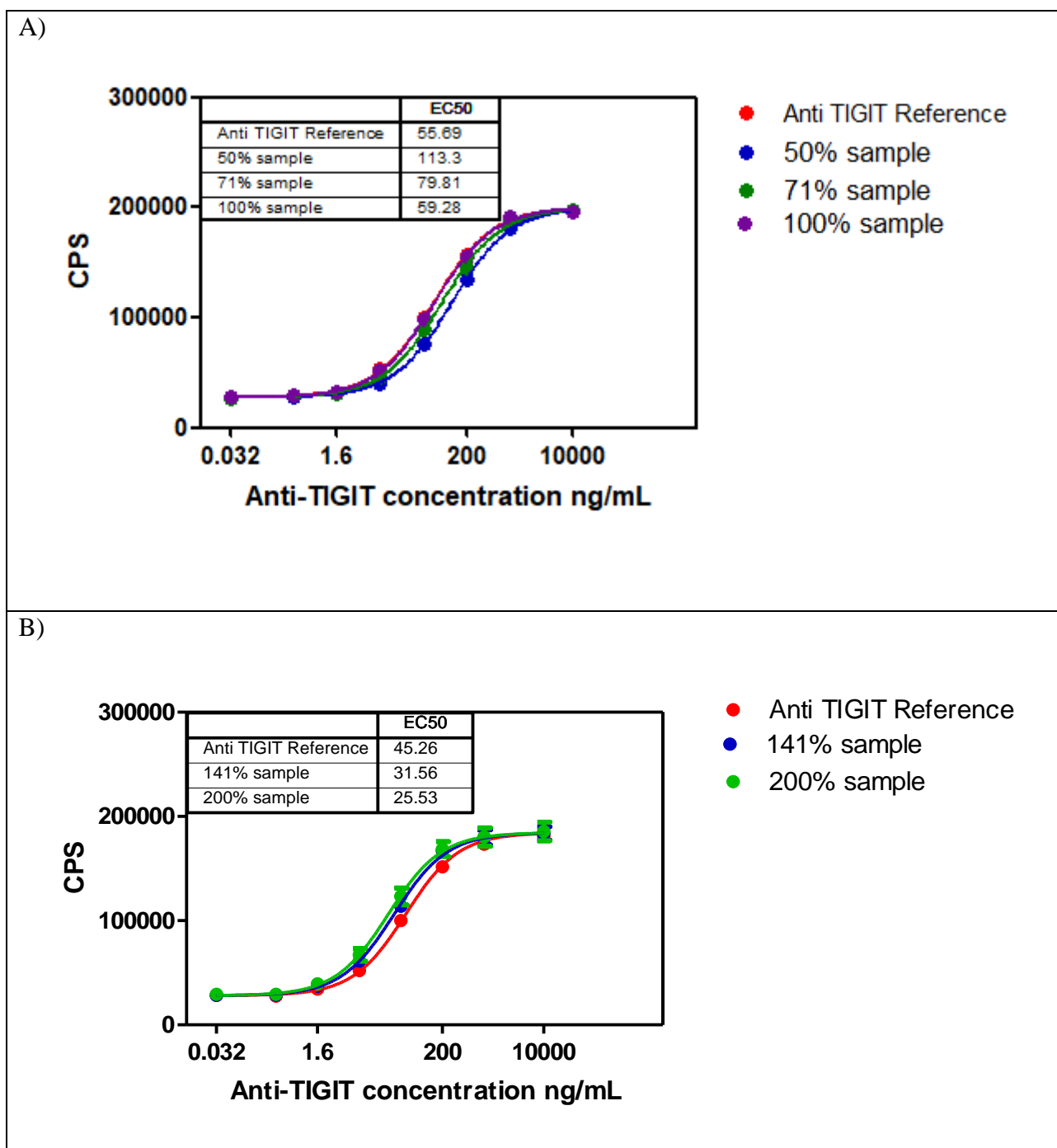
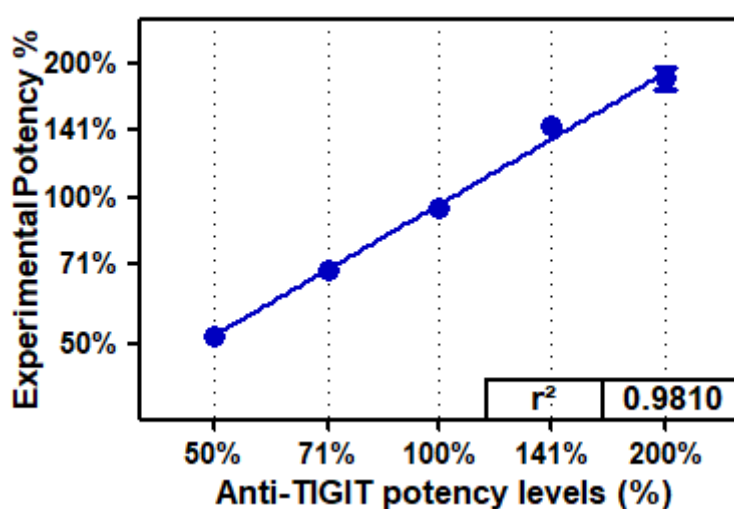


**Figure 48: Representative dose response curves at different nominal concentration of the Reference material.** All the dose response curves are well defined within the potency range 50%-200%. The reference material dose response curve is graphed in red. In the graph on the top the dose response curve of the sample at 50% is in blue, the one of the sample at 71% is graphed in green while the dose-response curve of the sample at 100% is graphed in violet. In the graph on the bottom in blue is represented the sample at 141% while in green the dose response curve of the sample at 200%. In both graphs also the EC50 values of each curve are reported.

**Table 22: Linearity and Range elaboration.** In the graph is represented the linear regression of the response obtained by plotting the calculated Potencies of Anti-TIGIT versus each nominal concentration (50%, 71%, 100%, 141% and 200%). In the table are shown the calculated Potencies values (Experimental Potency) at all the concentration levels coming from each run. The final Potency at every level is obtained as average of all the Potency measured. The values are shown without decimal numbers, but the calculations were performed considering seven significant digits that are the maximum that can be entered in GraphPad software.



Run	Experimental Potency				
	50%	71%	100%	141%	200%
1	47	63	98	157	206
2	50	74	92	132	172
3	49	70	94	143	177
<b>Average</b>	<b>49</b>	<b>69</b>	<b>95</b>	<b>144</b>	<b>185</b>
<b>CV (%)</b>	3	8	3	8	10

As the  $R^2$  of the linear regression curve is 0.9810 and all the acceptance criteria for the variability at each point were met ( $\leq 25\%$ ), the method was assessed to be able to give a linear response between

50% and 200% of Potency. Moreover, the values for Slope and Y-intercept when  $X = 0.0$  are 0.9021 to 1.066 and -0.1488 to 0.1815 respectively, at 95% of confidence intervals confirming the linearity.

#### 3.5.2.2 Accuracy and Precision

The experiments run for the linearity and range study were used to evaluate the accuracy of the method. Accuracy is a measure of the closeness of the experimental value to the real value. The Accuracy was calculated formulas showed in section 2.3.1.4 and was found between 93%÷103%.

The obtained values are within the acceptance criteria set for this parameter (75%-125%). The preliminary precision was evaluated using the experimental runs for the linearity and range study. The CV (Coefficient of Variance) was used as measure of the precision of the method for each percentage of reference material calculated. The maximum value obtained was 10%. This preliminary value is just a key indication of the suitability of the method and it will not be considered as an acceptance criterion, owing to the application of this method in characterization and in comparability exercises of samples/processes. At the end of the development study also the goodness of fit and fold increase were evaluated. All  $R^2$  values of the reference material generated within this study have been collected. In all the experiments the  $R^2$  were  $\geq 0.95$ , demonstrating the goodness of fitting of the applied model. For the fold increase evaluation, all the Top/Bottom ratio of the dose response curve of the reference material loaded in each plate, were considered. Results obtained within this study are reported with the cell passage number of effector and target cells in table 23.

**Table 23: Fold increase analysis.** All the FI obtained by dividing the Top and the Bottom of the reference dose-response curve are shown by highlighting the cell passage of both the target and the effector cells used for the experiment.

Exp. No.	Target Cells Passage	Effector Cells Passage	Fold Increase	Exp. No.	Target Cells Passage	Effector Cells Passage	Fold Increase
1	#20	#20	9.8	10	#27	#27	9.5
2	#20	#20	10.0	11	#28	#28	9.2
3	#21	#21	10.0	12	#28	#28	8.0
4	#23	#23	7.0	13	#28	#28	7.8
5	#23	#23	5.9	14	#28	#28	7.8
6	#23	#23	7.7	15	#29	#29	6.8
7	#23	#23	8.6	16	#16	#29	4.4
8	#24	#24	7.3	17	#20	#19	18.4
9	#24	#24	6.6	18	#21	#20	18.1

Abbreviations: Exp= experiment.

In all the experiments the obtained FI was always above the requirements confirming the ability of Anti-TIGIT to induce a significative and dose dependent response.

All together these data suggested that the developed method is fit for the purposes. Indeed, this assay is easier to use, showed good precision, physiological relevance and it is faster to execute with respect to other assay formats. In addition, the ADCC reporter assay using Jurkat/NFAT-luc/Fc $\gamma$ RIIIa is more suitable for release control, batch-to batch consistency and stability tests for mAbs with ADCC activity where accuracy and precision are important.

#### 4.6 Forced Degradation Study and Stability-indicating Bioassays

The study of the effect of a particular stress applied to a therapeutic mAb is referred to as forced degradation study or stress testing. Antibodies are prone to a variety of physical and chemical degradation pathways. In many cases, multiple degradation pathways can occur at the same time and the degradation mechanism may change depending on the stress conditions impacting different mAbs' properties. Therefore, stability studies under stress conditions or forced degradation studies play an important role in different phases of development and production of biopharmaceuticals.



FDA guidance states that stress testing should be performed in phase III of regulatory submission process. However, starting forced degradation studies early in preclinical phase or phase I of clinical trials is highly encouraged and should be conducted on drug substance to obtain enough time for identifying degradation products and structure elucidation as well as optimizing the stress conditions. These studies are mostly applicable for selection of suitable candidates and formulation developments, comparability studies, elucidation of possible degradation pathways and could give timely recommendations for making improvements in the manufacturing process (Blessy et al., 2014).

Here we used such studies to establish the stability indicating nature of the qualified cell-based methods (Anti-TIGIT ligand binding bioassay and ADCC RGA assay). According to FDA, a stability-indicating method is a validated quantitative analytical procedure that can be used to detect how the stability of the drug substances and drug products changes with time (Blessy et al., 2014).

This methods' feature should be demonstrated at the time of method development and before submission of the regulatory dossier to the FDA (Tamizi and Jouyban, 2016).

At that point, if methods do not indicate stability, there is still room to improve them enough to do so. In addition, the use of forced degradation samples can also help determine the critical method parameters. Moreover, since clinical consequences of different stress events are still under investigation, especially with regard to the immunogenicity potential, as several publications have shown for example an enhanced immune response due to aggregates formation (Le Basle et al., 2020), it is crucial to develop stability indicating analytical methods as early as possible.

Protein degradation can result from many different instability mechanisms that can be generally classified in chemical and physical instabilities. Those instabilities are closely interconnected since chemical reactions can lead to physical instability and physical instability may give access to chemically susceptible residues (Le Basle et al., 2020). Antibodies can show physical instability via two major pathways—denaturation and aggregation. A variety of chemical degradation pathways instead have been observed. The major chemical degradation pathways in an antibody include cross-linking, deamidation, isomerization, oxidation, and fragmentation (Wang et al., 2007) that may impact or not on protein's activity depending on the site of changes. The most commonly observed degradation pathways are summarized in the figure below (figure 49).

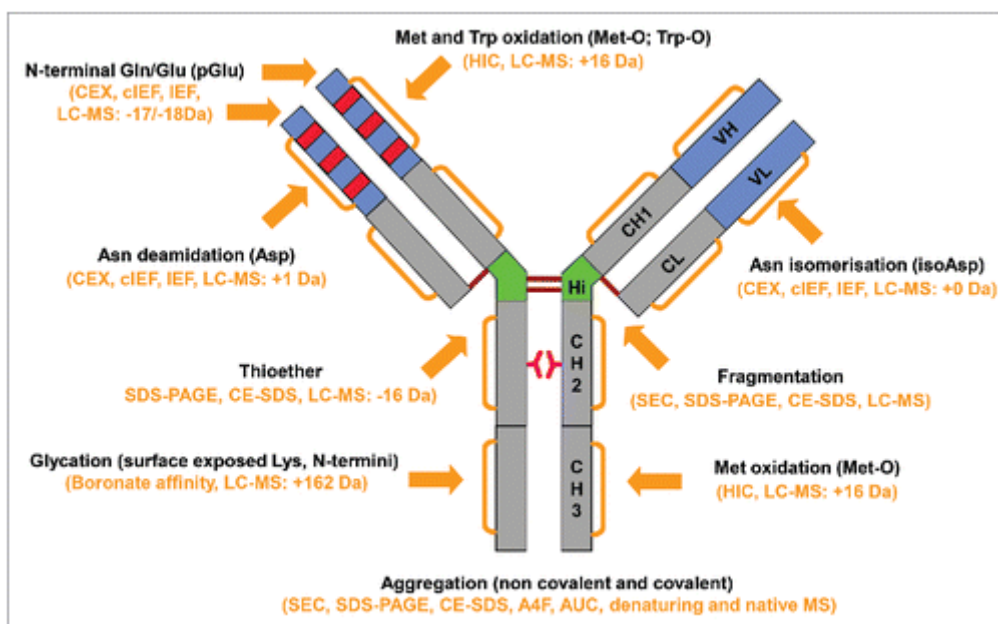


**Figure 49: Major degradation pathways of recombinant monoclonal antibodies.** Arrows indicate the main degradation sites. The commonly used methods to detect the degradation products are shown in the parenthesis. From Novak et al., 2017.

As reported in the review of Le Basle et al., three main axes should be developed: a physical stability that should comprehend an investigation on aggregation and fragmentation, as well as mAb's structure; a chemical stability study that should look for chemical degradations and a biological stability study which should corroborate the conservation of mAb's activity toward its target with its physicochemical stability (Le Basle et al., 2020).

As a consequence, cell-based release methods should be designed and performed to monitor and ensure the routine product quality and thus should have the ability to detect product degradation that could happen in various real-life conditions (e.g., during manufacturing, storage, handling etc.).

Degradation products tested should be representative of what could occur during real time and accelerated or excursion conditions in order to be relevant. In this sense, forced degradation conditions should be optimized to generate degradation products that are different only in terms of abundance, but not in species, as those formed during true processing and storage conditions (Nowak et al., 2017).

The commonly used forced degradation conditions comprehend high temperature, freeze-thaw, agitation, high pH, low pH, light exposure, oxidation and glycation. The applied conditions are usually harder compared to the naturally occurred ones in order to generate relevant degradation

trending within a short time and are chosen based on the likelihood that the products are potentially exposed to those detrimental conditions during processing, packaging, shipping and handling (Nowak et al., 2017). There is no specification and well-established protocols for the selection of stress conditions and required extent of degradation in regulatory guidelines, but it is generally agreed that the initial trial should have the aim to come upon the conditions that degrade the drug by approximately 10%.

Due to the present gap in the stability studies guidelines, it is the responsibility of researchers working in academia and biopharmaceutical industry to set up forced degradation experiments that could fulfill all the expectations from the stability studies of the biopharmaceutical under stress conditions.

Here, considering Anti-TIGIT sequence and structure (chapter 2.10), its manufacturing process (chapter 3, section 3.), its formulation and its normal storage the following stress conditions were selected to both assess the effect on Anti-TIGIT bioactivity and the stability indicating nature of the validated ligand binding bioassay: i) oxidation, ii) deamidation and iii) thermal and UV stress on the bioactivity of the treated samples (Table 24).

The stressed samples were obtained applying specific protocols to induce desired modifications. The batch BKAA-18-01-BDS was used for the variants production and has been included in the analysis of the stressed samples. The reference material is included in each assay plate as system suitability and for the potency measurement.

**Table 24: List of the stressed samples tested in this study together with their measured protein content.**

<b>Sample</b>	<b>Concentration mg/mL</b>
<b>Anti TIGIT Reference material</b>	19.42
<b>Thermal stress 50 °C 8 Week</b>	19.66
<b>Thermal stress 40 °C 8 Week</b>	19.08
<b>Deglycosylated</b>	15.51
<b>Oxidized</b>	17.81

Stressed samples were produced in MS Guidonia and have been tested also with other two different assays developed in the frame of this PhD study that are able to investigate different portions and

functions of Anti-TIGIT molecule. Each sample was analyzed in three independent runs applying the criteria defined during the method optimization.

### 3.6.1 Deglycosylation

Removal of oligosaccharides can induce significant structural changes. Structural changes have been demonstrated by the increased susceptibility of deglycosylated and non-glycosylated antibodies to proteases (Dwek et al., 1995, Tao and Morrison, 1989) and decreased thermal stability of antibodies and their Fc fragments (Ghirlando et al., 1999, Liu et al., 2006, Mimura et al., 2000, Mimura et al., 2001). The most dramatic differences between antibodies with and without oligosaccharides are Fc effector functions (Liu et al., 2008).

The deglycosylated sample has been tested as a negative control since, as it is reported in literature, deglycosylated mAbs completely loss their ADCC function. Data from chemical-physical characterization (Intact Molecule analysis by LC-MS, data not shown) confirmed that after the enzymatic treatment with PNGASE-F (under non-reducing condition) Anti-TIGIT antibody is fully deglycosylated. As expected, the sample shows no ADCC function since the glycans of the Fc region of the IgG1 have a key role in the binding to Fc $\gamma$ RIIIa (Raju, 2008; Hanson and Barb, 2015; Nimmerjahn and Ravetch, 2008).

A representative dose response curve of fully deglycosylated sample is reported in the figure below (Figure 50).

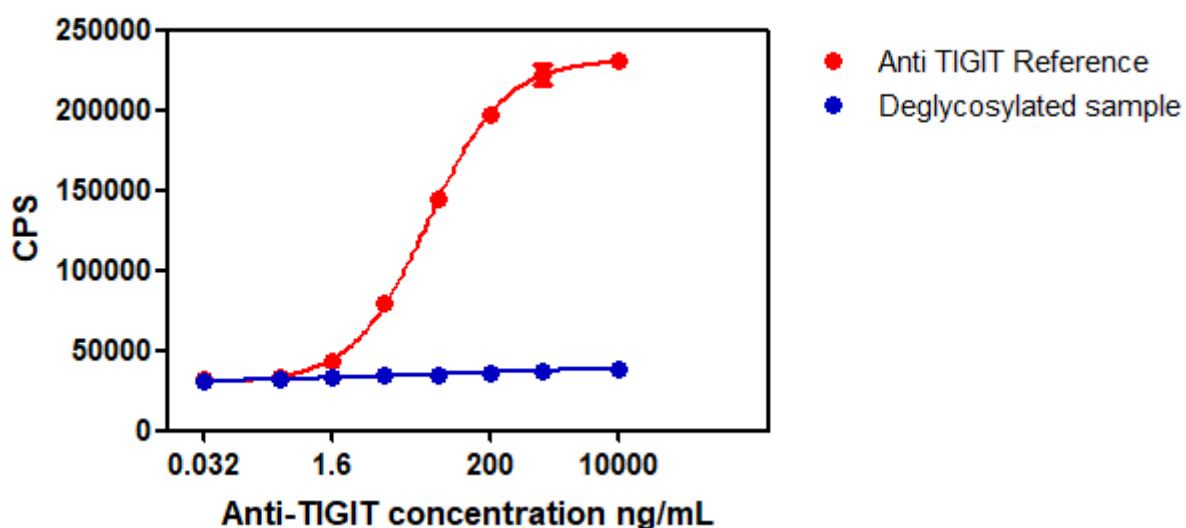
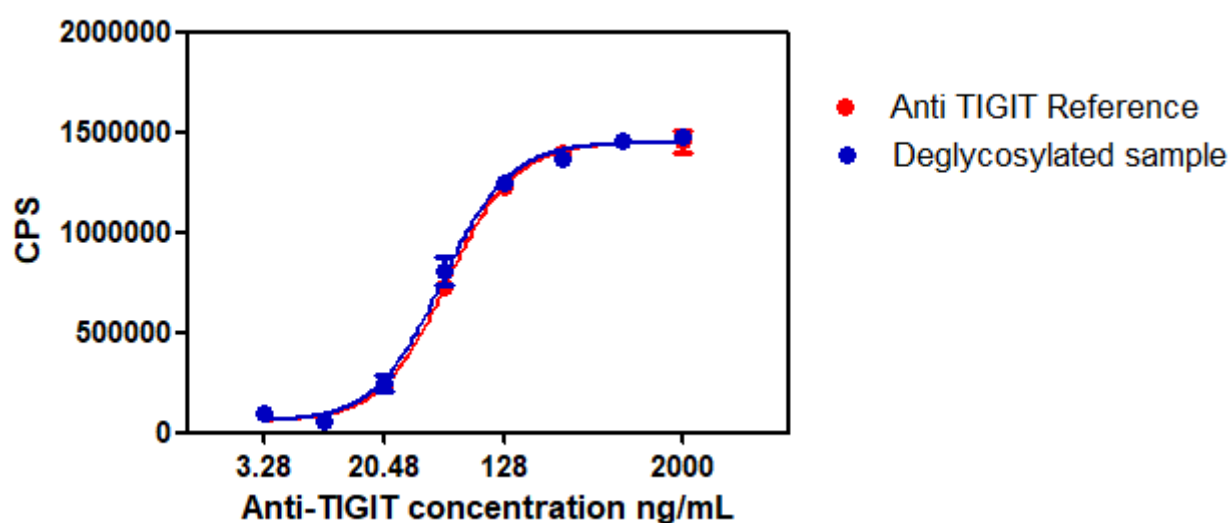


**Figure 50: ADCC Activity of deglycosylated Anti-TIGIT sample.** The dose response of the reference is graphed in red while the one of the deglycosylated sample is in blue. As expected, no ADCC activity has been detected in the deglycosylated sample.

As expected, since a proper dose-response curve for the deglycosylated Anti-TIGIT was not obtained, the final Potency of the sample could not be calculated. Possible effects of deglycosylation on Anti-TIGIT bioactivity were also explored with Anti-TIGIT ligand binding assay confirming that the potency is not affected by this stress as shown in the figure 51.



Sample	Potency	CV
Deglycosylated sample	106%	5%

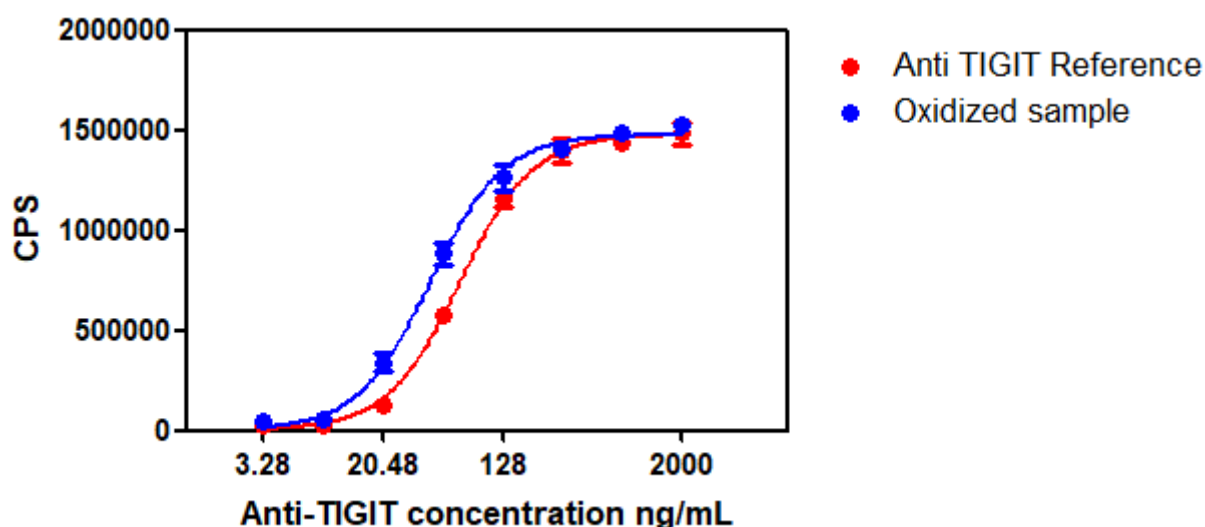
**Figure 51: Biological Activity of deglycosylated Anti-TIGIT sample.** As shown in the graph the dose response curve of the reference (in red) and the one of the deglycosylated sample (in blue) are completely overlapped. Indeed, the Potency of the sample is 106% as reported in the table on the bottom of the figure.

### 3.6.2 Oxidation

Oxidation is a common degradation pathway that may occur during the life cycle (production, purification, formulation, transportation, storage and handling) of proteins and peptides (Torosantucci et al., 2014). Indeed, during formulation and storage several excipients and impurities can directly or

indirectly favor oxidation. For instance, as reported by Torosantucci et al., impurities such as formaldehyde and hydrogen peroxide have been found in polymeric excipients such as polysorbate which is commonly encountered in mAbs formulation (Torosantucci et al., 2014). The generation of peroxides through autooxidation of these polymeric compounds might favor oxidation of amino acid residues. The presence of transition metals may also lead to oxidation, for example via the Fenton reaction (Mozziconacci et al., 2013). One option to prevent or at least reduce the probability of oxidation of the active protein is the addition of antioxidants, chelating agent, or radical scavengers to the formulation buffer, if acceptable from a toxicological and regulatory perspective use (Folzer et al., 2015). In literature it is reported how oxidation could lead to modifications of higher-order structures, including aggregate induction, and can generate products that are pharmacokinetically different, biologically less active and/or potentially more immunogenic than their native counterpart (Torosantucci et al., 2014). Moreover, oxidized forms of proteins have been shown to exhibit decreased chemical and physical stability (Sankar et al., 2018). It is therefore crucial during the pharmaceutical development of biotherapeutic proteins to comprehensively characterize oxidation products and evaluate their impact on the biological properties of the drug (Torosantucci et al., 2014) using stability indicating bioassays. Many amino acids (cysteine, histidine, tryptophan, and tyrosine) are susceptible to oxidation, but the reaction occurs considerably faster with methionine (Folzer et al., 2015). Oxidation of Met is a common non-enzymatic modification in proteins that can result from the conversion of Met to methionine sulfoxide (MetO) by reactive oxygen species (ROS) over a broad pH range (Sankar et al., 2018). The impact of oxidation on protein structure, function, and biological response, especially in the case of monoclonal antibodies (mAbs), where binding properties are essential to reach target antigen (Folzer et al., 2015), depends on the position of oxidized amino acids (especially if the oxidation occurs within the complementarity-determining region (CDR)). All methionine residues do not have the same effect on mAb functionality; some can be oxidized with no effects on antibody binding. Folzer et al. reported for example that oxidation of two methionine residues in the Fc section does not impact on antibody binding but may have a negative influence on interactions with Fc receptors, or components of the complement cascade, therefore affecting the necessary immune response processes (Folzer et al., 2015). Indeed, oxidation of Met residues in the constant domains of recombinant IgG1 antibodies such as Anti-TIGIT has been demonstrated to affect the in vitro interaction with protein A, the neonatal Fc receptor, and binding to the Fcγ receptors (Wang et al., 2011). So far, however, no susceptible Met residue within a CDR of recombinant IgG1 antibodies has been reported (Habberger et al., 2014). Anti-TIGIT sample has been oxidized with H<sub>2</sub>O<sub>2</sub> (see Materials and Methods chapter) and after the treatment it showed, through Peptide Mapping

LCMS/MS (data not shown), an increase of oxidation of Met257 (main species 62%), Met363 and Met433 of HC. These amino acids are in the Fc portion of the antibody and are not expected to affect the Fab activity. No other differences in respect to the not treated sample in post translational modifications (PTMs) and fragmentation profile have been detected. Firstly, the possible impact of oxidative stress on mAb's bioactivity were evaluated. Below a representative Anti-TIGIT treated sample dose-response curve obtained with the Ligand binding assay (Figure 52):



Sample	Potency	CV
Oxidized sample	176%	20%

**Figure 52: Biological Activity of oxidized Anti-TIGIT sample.** As shown in the graph both the dose response curves are well defined but the EC50 value of the curve of the oxidized sample depicted in blue is significantly lower respect to the one of the reference material (red curve) meaning that the biological activity of the stressed sample is increased. It is important to note that the final CV% of the potency value did not met the assay acceptance criteria ( $CV \leq 12\%$ ) highlighting the potency variability of the stressed sample.

Considering the Final Relative Potency value of 176%, an investigation to explain this anomalous value indicating an increased affinity of Anti-TIGIT to its target was done. In cell-based Ligand Binding assay layout, the protein A is used to coat the plate capturing the anti-TIGIT antibody via binding the Fc region. This binding is supposed to occur at the FcRn binding site (Loew et al., 2012; Maeda et al., 2017). Considering that either Met257 and Met433 are in FcRn binding region, the results obtained for the oxidized sample could be explained with a change in the specific binding site

of Protein A (Habberger et al., 2014) and not to an increase of the affinity binding to the target, determining a possible artifact. However, the potential artifact due to an increase in protein A capturing of anti-TIGIT was excluded with an ELISA assay, coating the protein A to the plate and incubating a dose response curve of Anti-TIGIT reference material and oxidized sample. The signal is detected with an HRP anti IgG antibody. Results reported in figure 53 indicate that the oxidation treatment does not affect the Protein A binding to Anti-TIGIT. This is visible by the overlapping of the dose response curves. At the top level the signal observed with the oxidized sample is even lower than the one observed with the reference material, excluding any impact on the increase in potency observed with the ligand binding assay.

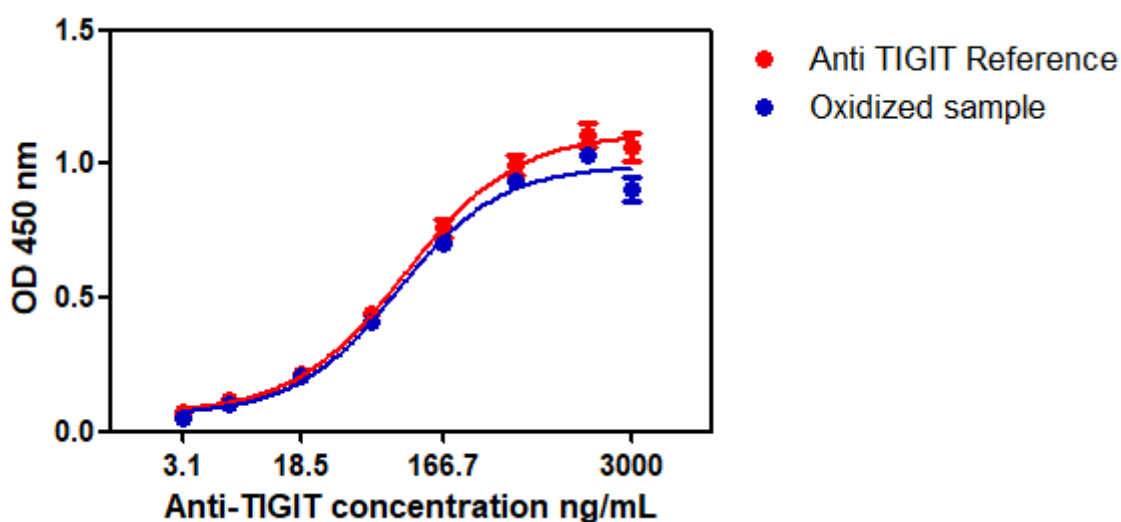


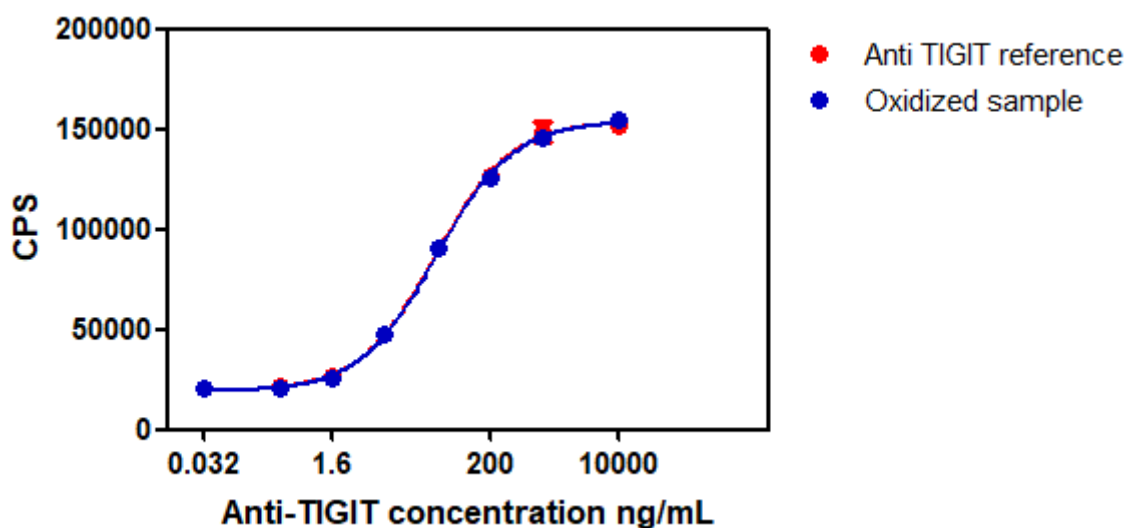
**Figure 53: ELISA detection of protein A-Anti-TIGIT binding capacity.** As shown in the graph Anti-TIGIT oxidation did not increase the binding to protein A with respect to the reference material as shown by the EC50 values of the two dose response curves. Indeed, the maximum signal obtained by the dose response curve of the treated sample is lower than the signal of the curve of Anti-TIGIT reference material.

Consequently, the results obtained using the ligand binding assay are indicative of an increase of the Potency of the oxidized sample demonstrating not only that the method is unbiased but also confirming its fitting as stability indicator assay. Further analysis will be necessary to elucidate the role of oxidization in the increase of the potency of Anti-TIGIT antibody.

For Anti-TIGIT ADCC activity, the two conserved methionine residues in its constant region should be considered. Previous studies revealed that methionine oxidation induces structural changes in the IgG Fc region, decreasing the binding affinity to FcRn, an Fc receptor regulating IgG recycling in



endothelial and blood cells and thus reducing the serum half-life of IgG. However, the effects of methionine oxidation in IgG Fc on FcγR activation are not yet fully understood (Tada et al., 2014). After the oxidation protocol applied (0.1% H<sub>2</sub>O<sub>2</sub>, 60 minutes) no effect was observed to Fc function monitored, as ADCC value is fully aligned to reference material. These results are also completely supported by the work of Tada et al demonstrating that oxidation in cetuximab (an IgG anti-Epidermal Growth Factor, EGFR) significantly decreased the EGFR binding-dependent activation of FcγRIIa-expressing reporter cells, but not that of FcγRIIIa-expressing reporter cells. A representative dose response curve obtained with ADCC RGA and the final potency of oxidized sample are reported in the figure below (Figure 54).



Sample	Potency	CV
Oxidized sample	100%	4%

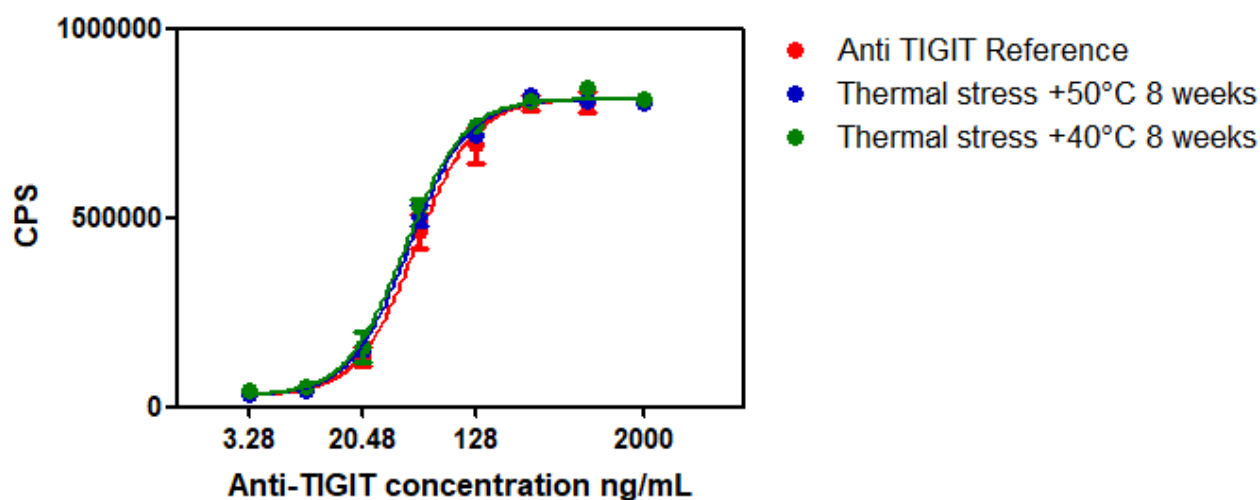
**Figure 54: ADCC activity of the oxidized Anti-TIGIT sample.** No effects in terms of potency are measured after sample oxidation. Indeed, the two dose-response curves (in red the one of the reference material and in blue the one of the stressed sample) are superimposed and the potency of the oxidized sample is 100% as shown in the table on the bottom of the picture.

### 3.6.3 Thermal stress

Stability studies are routinely performed under normal storage, accelerated or intermediate temperature conditions. In comparison, forced degradation under thermal stress is generally performed at temperatures exceeding the nominal storage and accelerated stability conditions. For

example, if the intended long-term storage condition for a mAb product is 2–8°C and the accelerated stability is 25°C, a thermal stress condition could be at 35°C or higher. The goal of using elevated temperature is to generate substantial levels of degradation within a short time period. High temperature stress is one of the most relevant conditions for providing information about potential long-term degradation at the intended storage condition. The effect of thermal stress has been monitored by applying two different conditions: +40°C and +50°C for eight weeks. Both stressing conditions induced an increasing of Anti-TIGIT fragmentation in terms of percentage of low molecular weights (%LMW) of the molecule and a decrease of %Purity as expected (the analysis have been performed with Whole molecule LC-MS and CGE-SDS, results not shown).

As expected, both thermally degraded samples show a strong decrease of the main isoform to the advantage of acid isoforms (measured with iCE, results not shown) (see the work of Nowak et al., 2017). The thermal treatment at +40°C and +50°C for 8 weeks produces comparable results: both temperatures have a negligible effect on the aggregation of the molecule, while a remarkable fragmentation is induced, with the formation of a LMW 1 with a molar mass 112-122 kDa that is ascribable to the monomer without a light chain, and a LMW 2, whose calculated mass is 52 kDa, probably due to the free Fc portion or to a dimer of the LC. Considering the structural effect of the thermal stress, the impact on Anti-TIGIT biological activity was detected. The final potency value confirmed that there is no impact on Anti-TIGIT's bioactivity as shown in the figure 55.



Sample	Potency	CV
Thermally stressed +50°C 8 weeks sample	98%	12%
Thermally stressed +40°C 8 weeks sample	112%	4%

**Figure 55: Biological activity of the two thermally stressed Anti-TIGIT samples.** In red is depicted the dose response curve of the reference material, in blue the one of the stressed sample at +50°C and in green the curve of the thermally stressed sample at +40°C. No significative impact of the high temperature exposure on Anti-TIGIT biological activity as shown in the potency table on the bottom of the figure.

However, the same thermal stresses impacted on ADCC activity of Anti-TIGIT. This effect is proportional to the increase of the temperature: the stress at +50°C determines a strong reduction of the ADCC activity of the molecule, while with a treatment at +40°C only a mild reduction is induced (figure 56).

The reduction of ADCC activity could be directly related to the monomer purity (up to about 78% for the stronger stress detected by mass spectrometry). In fact, ADCC biological activity seems to be strongly affected by the presence of fragmented species, showing a dependence from the stressing temperature applied as shown below (figure 56).

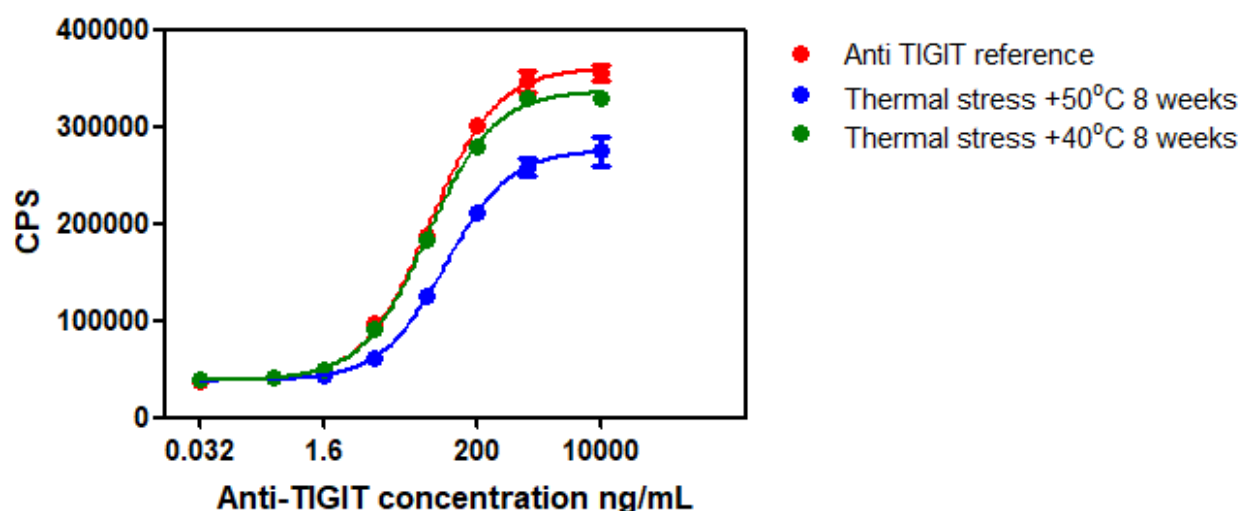


**Figure 56: ADCC activity of thermally stressed Anti-TIGIT samples.** Since the top of the curves of the treated samples (blue and green curves) differed from the one of the standard curve (in red) it was not possible to determine the final potency of the stressed samples. However, it is possible to conclude that the temperature has an impact on Anti-TIGIT ADCC activity. Indeed, a strong reduction in terms of signal intensity (CPS) is highlighted.

The mild stressed sample showed a different biological behavior compared to the reference standard mainly related to a decrease of the signal at the top of dose response curve. This effect is strongly enhanced for +50°C stressed sample with a high reduction of absolute response.

Together these data demonstrate that both assays, Cell-based Ligand Binding assay and ADCC RGA assay, are able to detect changes in Anti-TIGIT functions and to discriminate the intensity of the applied stress. This means that the validated Ligand Binding assay is applicable starting from pharmaceutical and industrial process development support to GMP studies like drug stability study and release and for the establishment of drug's specifications and shelf life. Also, ADCC reporter assay meets the requirements to be used as stability indicating bioassay during drug discovery, development and for characterization purposes. Moreover, both methods applied in early development phase could provide a background for the pre-formulation studies and the development of proper storage requirements.

## **5 DEVELOPMENT OF BIOASSAYS TO STUDY ANTI-TIGIT PREDICTIVE PHARMACOKINETICS**

### **5.1 Introduction and rationale**

According to what reported in the General Introduction in section 2.7 an in vitro FcRn binding assay is a highly valuable complementary tool to assess IgG antibody pharmacokinetics in IgG engineering and screening during the early optimization stage (Wu et al., 2015). In addition, it could be useful in biological characterization studies for antibody minor variants, process optimization, and comparability study at later stages of antibody development.

Assays suitable for sensitivity, precision and robustness, for the evaluation of FcRn-IgG interactions use real-time measurements through surface plasmon resonance (SPR) and bead-based proximity formats (AlphaScreen technology). Indeed, beside ELISA measurements or cell-based assays, these real-time measurements are often performed by several pharmaceutical companies to characterize FcRn in vitro binding (Eglen et al., 2008). In addition, with respect to cell-based assays these real-time techniques offer high-throughput sample processing and speed assay execution which make them particularly fit for drug candidate early screening.

However, in many cases, singular analytical methods cannot provide the complete picture for specific attributes and orthogonal methods (different methods intended to measure similar attributes) to confirm mAb properties become essential (Mitchell and Elder, 2016). An orthogonal analytical procedure is an additional method that measure the same parameter of the reference assay and it can be used to evaluate the performance of the primary method. If the two essentially different methods are used to measure the same phenomenon or parameter and the result turn out the same, then the measurement is considered reliable. As such, in pharmaceutical companies it is often desirable to evaluate one or more orthogonal (or complementary) methods. Indeed, herein we describe the development, qualification, and successful piloting of two novel biochemical-based high-throughput screening assays capable of surveying the interaction between canonical IgG1 and FcRn.

For this reason, two major goals were pursued: the first one was to develop and validate a reference SPR-based method to measure the binding between an IgG1 and FcRn receptor overcoming the issues of the SPR-based methods currently applied in the company and the second was to develop an orthogonal AlphaScreen procedure.

These assays will be then integrated into a platform to assess pharmacokinetics properties of new biological entities capable of screening the interaction of mAbs with FcRn to characterize biotherapeutic mAbs, their production intermediates as well as rank order lead candidates.

For such purpose the binding of Anti-TIGIT to FcRn using the two new in vitro assays has been investigated.

## **5.2 SPR PLATFORM**

The SPR technique is currently considered a fundamental analytical tool for interrogation of biomolecular interactions since it provides highly accurate results and real-time and label-free measurements (Olaru et al., 2015). SPR has been proven to be one of the most powerful technologies to determine specificity, affinity and kinetic parameters during the binding of macromolecules in many bond types. The ability to monitor almost any type of molecular interactions between different biological molecules allow SPR biosensors to be used in almost every step in pharmaceutical analysis which requires kinetic profile, target identification, or characterization (Olaru et al., 2015). Doubtless, this is the most robust and sensitive biosensing technique that has been successfully implemented in research pharmaceutical laboratories worldwide. It is already a gold standard in the field and in literature several SPR layouts are reported for the study of the binding of the Fc domain of IgG molecules to FcRn (Olaru et al., 2015; Wang et al., 2016).

Different SPR assay setups have been described in literature, where either the IgG or the receptor was used as immobilized ligand on the chip surface. In the first format, mAbs are directly immobilized on the biosensor chip, typically via amine coupling chemistry, and FcRn proteins in solution are injected over the sensor chip while in the second format the orientation is reversed so that the FcRn proteins are directly amine coupled on the biosensor chips, and mAbs are injected over the chips.

In order to identify the best SPR platform to be developed for the intended purposes, different intermediate objectives were pursued. Firstly, the SPR technology background and the features of the company currently applied SPR-based FcRn binding assays were studied. Upon that, a new innovative parental SPR method to determine the IgG/FcRn interaction for development process and product characterization has been introduced and successfully qualified.

### **5.1.1 Old SPR platform**

Despite the solid understanding of the SPR technique, the selection of suitable conditions for studying FcRn-IgG interactions using this methodology were quite challenging. Indeed, the reproducibility and precision observed with the old format presented intrinsic limitations when applied for the study of the binding between an IgG and FcRn. For a detailed description of the methods see chapter 3, section 3.5.1.

During method implementation several technical issues were encountered starting from the direct capturing approach of the ligand (FcRn). Many macromolecules can be directly immobilized as ligands on the sensor surface without significantly interfering with the interaction being studied (Schasfoort and Tudos, 2007). However, the ligand molecules are attached to the chip in random orientations and this could hide many of the ligand's binding sites to the analyte. Indeed, several published works like the one of Magistrelli et al. (Magistrelli et al., 2012). report that amine coupling led to random orientation and reduced functionality of the FcRn molecules on the sensor chip surface generating artifacts (Neuber et al., 2014).

Another drawback that was considered is that the method results time consuming. Indeed, the use of the multi-cycle analysis leads to a longer testing time since for each sample 6 different concentrations are run and between binding cycles regeneration of the surface needs to be performed. This approach could be limiting especially if applied to process or product support studies where a lot of samples are routinely tested.

Moreover, the attached ligand is the same for the entire analytical run and it is therefore subjected to the loss of activity introducing differences in the analyte response within the same analytical run.

For all the intrinsic limitations described above, the results generated applying this SPR platform were characterized by high variability as shown in figure 57. This highlighted the needs of a method optimization to be fit for the purpose.

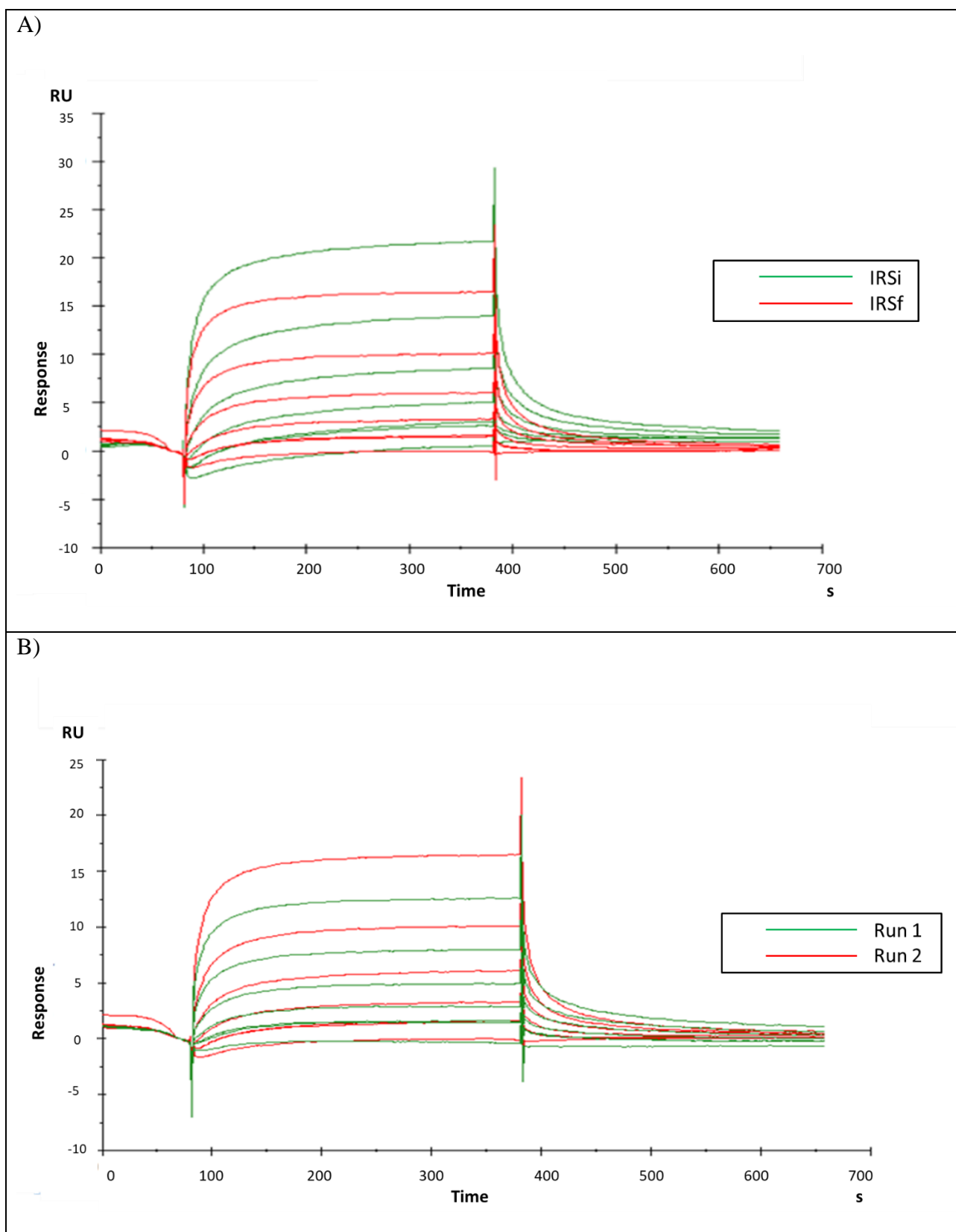


**Figure 57: Examples of the variability associated with the current SPR method both within the same run and between two runs of the same analytical session. A) Intraassay variability. In this figure, the high**



variability within a single run between the IRSi and IRSf is shown (in green the standard run at first position of each analytical sequence and in red the standard at the last position of each analytical sequence). The sensorgrams of the initial and the final standard, do not overlap, although is the same preparation. Moreover, a decrease trend of signal is observed within the analytical sequence. B) Inter assay variability. Graph B showed the high variability in an assay that includes two runs. The standard at the first position of each analytical sequence of the first run is graphed in green while the one of the second run in red. The sensorgrams of the initial standards of both runs, do not overlap, although is the same material.

IRS = interim reference material, IRSi = IRS initial, IRSf = IRS final

Considering the importance for our purposes to overcome these limits, two different technical solutions were explored.

The first method foresees the capture of the histidine tagged FcRn through specific and selective anti-His mAb. This assay format is a robust parental format used to assess protein-protein interactions and for which the regeneration conditions have been already optimized. However, despite the advantages in using this layout, it resulted not applicable for FcRn binding due to a fast dissociation of the tagged ligand from anti-His antibody (data not shown).

For this reason, an innovative approach for a regenerable use of the system Streptavidin/Biotin was explored as new SPR layout to be applied. So far, the streptavidin-biotin system seems to be the best choice for site-directed immobilization of biotinylated ligand in the SPR experiment since it ensures that all immobilized molecules are in the same orientation on the sensor chip (Li et al., 2006; Hutsell et al., 2010). However, since the affinity of streptavidin for biotin is extremely high, with an equilibrium dissociation constant (KD) of around  $10^{-15}$  M, the capturing will be essentially irreversible. Indeed, this strong interaction limits the application of the streptavidin-biotin approach as it is (Qureshi et al., 2001). To overcome this, a novel double capturing approach was proposed.

### **5.1.2 SPR method optimization**

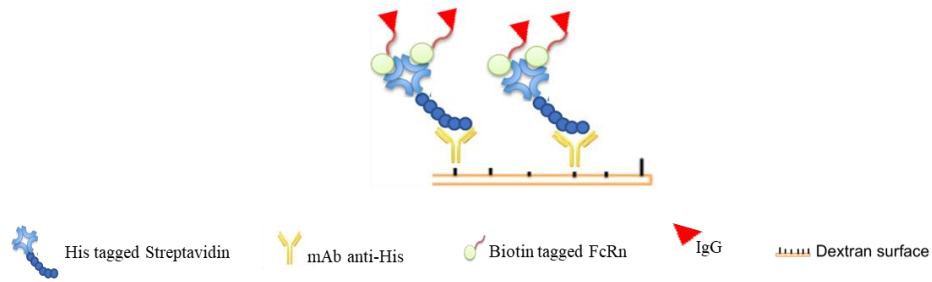
The innovative advantage of the new SPR method is based on combining the established technology of the his-tagged protein selectively recognized by anti-his antibodies with the well-known strong interaction between streptavidin and biotin that allows a stable FcRn capturing on the chip. In such approach, the binding is then very selective, avoiding nonspecific signals.

Moreover, with respect to covalent immobilization this type of capture does not require any chemical modification of the ligand and can be performed in physiological buffer conditions (Schasfoort and Tudos, 2007).

Despite the experimental complexity of the layout, this new method presents several advantages. As demonstrated in the work of Magistrelli et al., the single biotinylation site facilitated the directional immobilization of FcRn on the sensor chip and significantly increased the response level of the surface compared to amine coupling used in previous studies (Magistrelli et al., 2012). FcRn molecules can be conveniently immobilized at the desired surface density. Furthermore, this setup is probably a closer approximation to the *in vivo* situation of the receptor on the cell surface, as opposed to the reverse orientation (i.e., using the IgG as immobilized ligand and FcRn as the analyte). It is also more convenient for a characterization process in terms of higher throughput and lower material consumption (Neuber et al., 2014).

In detail, the new SPR method foresees the use of a double capturing approach as shown in figure 58A: biotin tag portion of FcRn (ligand) is captured by His tagged Streptavidin that is bound by the mAb anti-His tag immobilized onto the sensor surface through amine coupling. The IgG (analyte) is then injected over the FcRn at different concentrations through a single-cycle kinetic. In the analysis reference material is run at first and last position of each analytical sequence as a control in order to guarantee the performance of the FcRn throughout the analysis. The regeneration step, in order to reach the baseline again, occurs by simply interrupting the bond between the mAb anti-His tag and his tagged Streptavidin. The main steps of this new approach are graphed in the figure 58B.

A)



B)

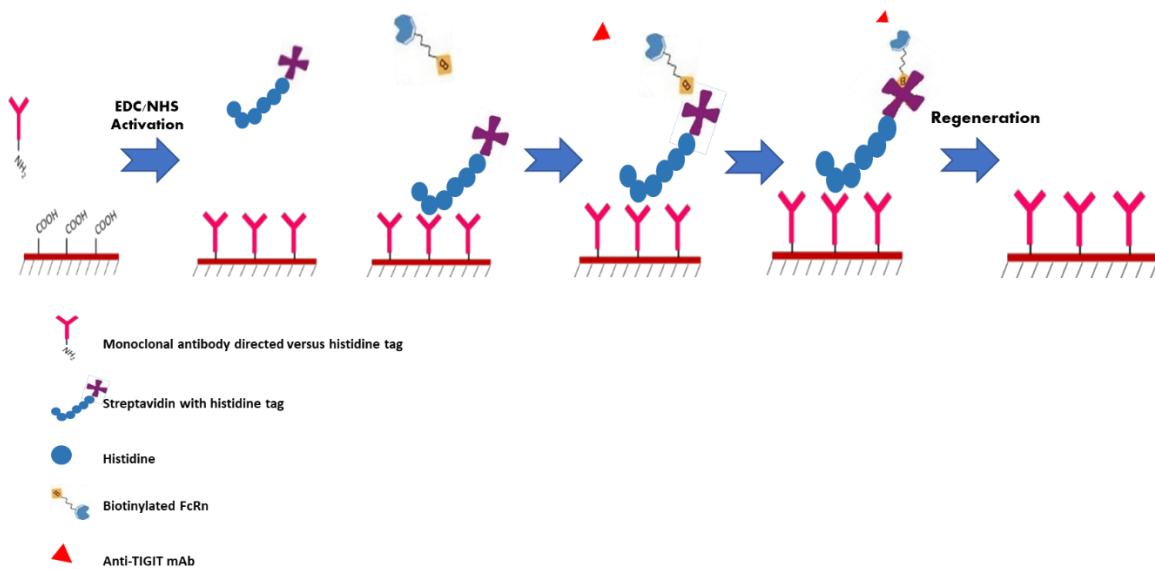
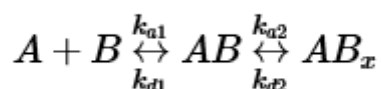


**Figure 58: Optimized SPR layout.** A) Schematic layout of the new SPR method and B) method steps representation. Biotinylated FcRn is used as ligand; its biotin tag portion is captured by His tagged Streptavidin that is bound by the Tetra anti-His Antibody immobilized onto the sensor surface.

Anti-TIGIT mAb is used as analyte, diluted in a range from 400 to 25 nM. Each cycle is composed by 5 sample injections (one for each concentration). At the end of each cycle, the surface is regenerated with two different regeneration solutions (10 mM pH 2.0 Glycine-HCl and 3 M Guanidine Hydrochloride).

The obtained sensorgram is elaborated applying the “two state reaction” fitting model in order to determine the KD value.

The two-state reaction model is described by the equation below:



Where the kinetic parameters are:

$k_{a1}$  - association rate constant for formation of AB

$k_{d1}$  - dissociation rate constant for complex AB

$k_{a2}$  - rate constant for conversion of AB to AB\*

$k_{d2}$  - rate constant for conversion of AB\* to AB

In this model, the analyte (A) binds to the ligand (B) to form an initial complex (AB) and then undergoes subsequent binding or conformational change to form a more stable complex (ABx) (Lund-Katz et al., 2010). This model describes a 1:1 binding of analyte to immobilized ligand followed by a conformational change that stabilizes the complex.

For a two-state reaction, an increase in the contact time between the analyte and the ligand decreases the dissociation rate since more of the stable ABx complex is formed.

Results are then generated as Absolute KD (nM) and Relative Binding (KD%) versus the reference material, according to the following formula:

$$KD (\%) = (KD \text{ Reference material} / KD \text{ sample}) * 100$$

The single-cycle approach (or kinetic titration) is particularly useful with interactions that are difficult to regenerate or when regeneration is detrimental to the ligand (Karlsson et al., 2006; Dougan et al., 1998). The analyte is injected from a low to high concentration with short dissociation times in between and a long dissociation time at the end (not shown here). All the injections are analyzed in one sensorgram.

This approach requires a shorter time for a complete analysis significantly reducing the demands on assay development and the time of analysis compared to multi-cycle kinetic. Moreover, it is no more required a new sensor chip preparation for each run, as the ligand is captured by the capturing molecule immobilized onto the sensor surface. The ligand is freshly injected in each cycle, thus, it has always the same activity.

The outputs observed applying this new SPR method are characterized by low variability that makes possible to discriminate differences in samples' affinity with high precision and accuracy. An

example of the low intra and inter assay variability is shown in the two representative sensorgrams reported in figure 59.

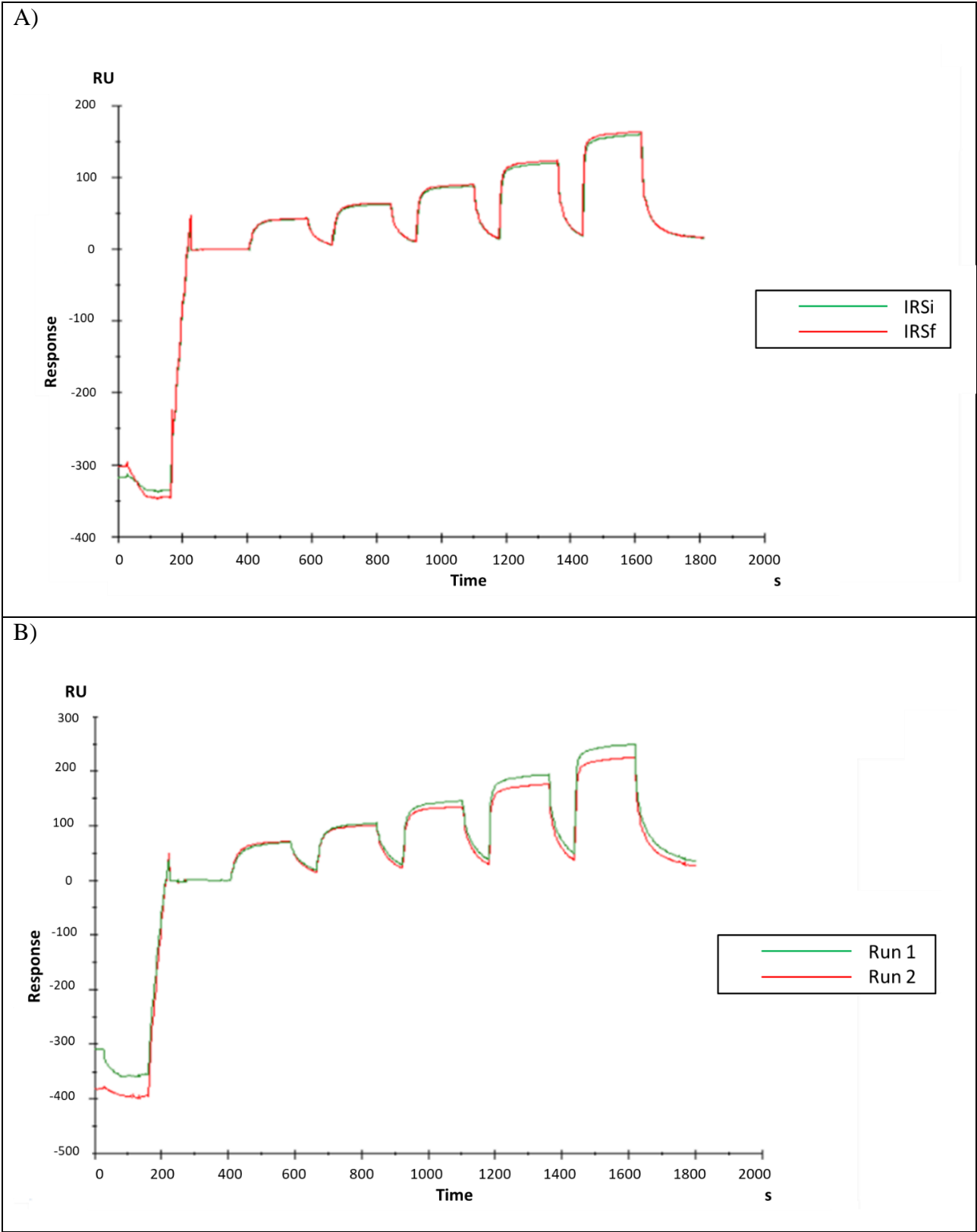


**Figure 59: Results obtained with the new SPR method showing a significative reduction of the variability within the same analysis (intra assay variability) and among two runs (inter assay variability).** A) Intra assay variability. The low variability within a single run is shown (in green the standard run at first position of each analytical sequence and in red the standard at the last position of each analytical sequence) The two sensorgrams are completely overlapped. B) Inter assay variability. An example of the low variability within a single assay including two runs is shown. The standard at the first position of the analytical sequence of the first run is graphed in green while the standard of the second run in red. Also this time, the sensorgrams of the two standards overlap. Abbreviations: IRS = interim reference material, IRSi = IRS initial, IRSf = IRS final

Once the layout was selected and all the reagents identified (see materials and methods chapter for further details), a series of experiments aimed at the fine tuning of the method were performed.

The new SPR method has been developed in house as a parental method using a generic IgG from Merck KGaA New Biological Entities (NBE) library and then it was optimized in order to be applied also to Anti-TIGIT samples.

All the measurements were performed at pH 6 as interaction of FcRn with IgG is dependent on acidic pH. Binding of Anti-TIGIT reference material was observed under these conditions. Furthermore, no nonspecific interaction of the reference material with the chip surface was observed.

The FcRn capturing level was selected in the range 200-400 RU. The selection of this range has been done by analyzing the variability of the KD values obtained for the IgG when changing FcRn capture levels (100 RU, 200 RU, 300 RU and 400 RU). When varying FcRn capture levels among 200 and 400 RU the KD values were consistent and reproducible while when FcRn capture level was below 200 RU KD values weren't uniform. Considering the KD values were reproducible among 200 and 400 RU, no further experiments with higher capture levels (>400 RU) were conducted since kinetics evaluation should be done with the lowest ligand density in order to give a good response without being disturbed by secondary factors such as mass transfer or steric hindrance.

Anti-TIGIT was tested with a dose-response curve from 400 nM to 25 nM with a step dilution 1:2 based on the results obtained during the feasibility study of this method testing different mAbs.

After assay's fast development, a more detailed feasibility study of this new SPR parental method has been done. Feasibility allowed us to gain familiarity with the method and evaluate the assay for attributes such as precision, linearity, accuracy and specificity with the hopes of avoiding protocol acceptance criteria failures. Indeed, the main questions to be answered were:

- Is the assay capable of measuring the analyte/effect?
- Is the assay usable in routine to determine IgG/FcRn interaction? Is the assay reliable for the intended purposes?

#### 5.1.2.1 Method feasibility study

To demonstrate the method suitability for characterization purposes, the method's throughput, precision, specificity and system suitability ( $\chi^2$ ) were checked. Furthermore, the method performance on Anti-TIGIT stressed samples has been verified to measure its ability to discriminate among variations. The key results are reported in table below.

**Table 25: Key results of method qualification**

Parameters	Results
<b>Throughput</b>	The maximum number of samples that could be tested in the same analytical run is 12
<b>Number of replicates</b>	The result is released as duplicate
<b>Precision</b>	Preliminary CV% < 15%
<b>Specificity</b>	The presence of contaminants (host cell proteins, HCPs) did not affect the final results highlighting the method specificity
<b>Stressed samples</b>	The method is stability indicating meaning that is capable to recognize degradation into the molecule impacting the affinity to FcRn receptor.
<b>System suitability</b>	$\chi^2$ of the standard $\leq 10\%$ of Rmax Preliminary range for absolute KD of the standard: 79 nM ÷ 104 nM

In order to determine the maximum number of samples that could be tested in the same analytical run, the method has been challenged testing serially the same Reference material curve solutions for all autosampler capability (12 replicates). Moreover, in this step the samples stability throughout the analysis was evaluated.

**Table 26: Parameters and acceptance criteria for assay's throughput.**

<b>Data analysis</b>	Obtained KD for each replicate of Reference material is assessed. The maximum number of samples is defined as the replicates that met the acceptance criteria.
<b>Acceptance criteria</b>	First and last Reference material KD variability: $\leq 10\%$
<b>No. of Analysts</b>	1
<b>No. of total runs</b>	3

The method throughput has been assessed by calculating the first and last reference material KD variability for all three runs, demonstrating the respect of the acceptance criteria stated in the table above (CV<10%, table 24). Moreover, the variability of KD values between the first and last Reference material run was less than 10% in each of the three runs, confirming samples stability inside the analysis during more than 14 hours.

Considering the low variability among the obtained results, it was also decided to test samples in duplicate instead of triplicates in order to increase method throughput.

The method has been also confirmed to be precise (both preliminary inter and intra assay variability were checked) with a CV< 15% for both absolute KD and relative binding KD%. To evaluate the factors that contribute to the method variability, different operators have been involved using different Biacore instruments, different batches of sensor chip and different preparations of the reagents.

Once method precision was demonstrated also method specificity was verified following the approaches summarized below (table 27).

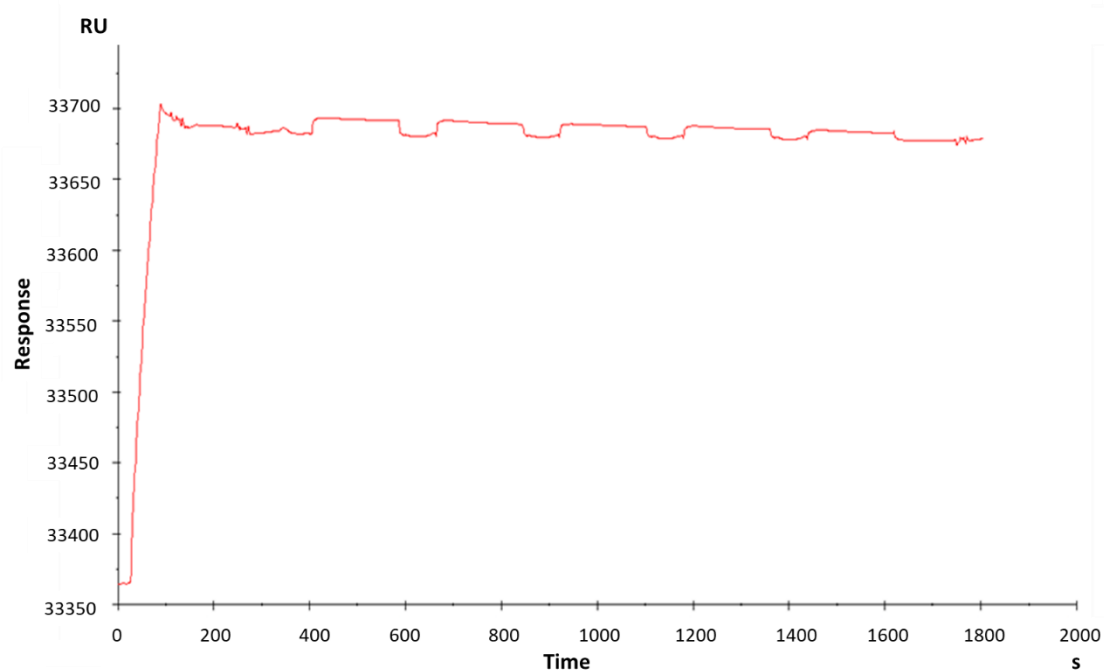
**Table 27: Parameters and acceptance criteria for specificity.**

<b>Approach</b>	Evaluation of the signal obtained on sensor chip surface and/or on the reference Flow cell verifying the Sensorgrams  Evaluation of the impact of possible contaminants on final results by spiking of typical impurities present in the samples
<b>Data analysis</b>	Elaboration of the curves generated with Biacore Evaluation software according to the fitting model provided for the method.
<b>Acceptance criteria</b>	No significant binding or impact on KD should be observed, respectively.
<b>No. of Analysts</b>	1
<b>No. of runs/Analyst</b>	2
<b>No. of total runs</b>	2

The possible unspecific binding on the sensor chip matrix has been excluded verifying the sensorgrams (measurement and reference) obtained during the testing of reference material. A representative behavior of Reference material is described in the figure 60.



A)



B)

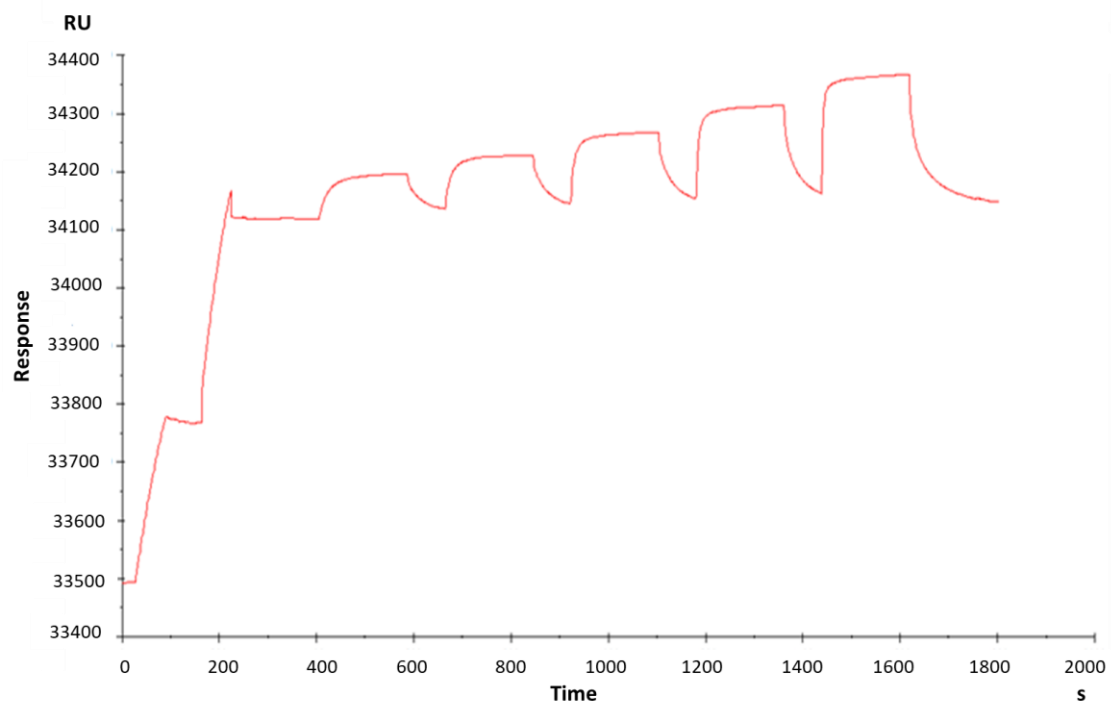


**Figure 60: Specificity analysis.** A) Binding measurement on the reference flow cell. As expected, no signal is detected throughout the five injections. B) Binding of Anti-TIGIT reference material to FcRn on the measurement flow cell.

The comparison of the two sensorgrams reported in Figure 63, obtained by simultaneously injecting the Reference material, highlights the absence of signal in the reference flow cell confirming the specificity of the signal on the measurement flow cell.

We also checked the impact of the possible presence of product contaminants in the drug including host cells proteins (HCPs) derived from the CHO cells that are a common expression system of biotherapeutic mAbs. This type of check is done for methods that are typically used for characterization purposes and that, for this reason, could be also applied for the analysis of samples that contain higher percentage of contaminants with respect to the final product. To create a similar contamination level to the one really found, reference material was spiked with CHO (Chinese Hamster Ovary cells) mock harvest. The results are shown in the table below (Table 28).

**Table 28: Specificity.** These results were generated during method qualification while testing the reference material with process impurities coming from CHO cells that are used to produce Anti-TIGIT therapeutic mAb. No impact on the final KD% value was detected. Abbreviations: IRS = Interim Reference Standard, HCP = Host Cell Proteins, IRS CTRL = IRS as a Control sample.

	KD %			
	1 run	2 run	Average	CV%
<b>IRS + HCP</b>	97	98	<b>98</b>	<b>1,2</b>
<b>IRS CTRL</b>	95	99	<b>97</b>	<b>3,1</b>

No significant impact on KD% was observed. Considering method variability, 98% of relative binding for the reference material plus HCP demonstrates that the spiking of typical impurities in the samples doesn't affect assay performance. This result is crucial considering that this method is also intended for in process control (IPC) testing. From this type of analysis, the manufacturer should obtain assurance that the product is of Pharmacopoeia quality conforming to the specifications. Indeed, in-process quality control tests are those tests carried out before manufacturing process is completed to ensure that established product quality is met before it is approved for consumption and marketing.

For the analyst dealing with in-process testing, there are some key challenges that include the many different sample matrices, the batch to batch differences and finally the presence of HCP. Indeed, these challenges can lead to modify the way the analytical methods are qualified (Wood, 2011). In this case no issues were found in the final KD% confirming the suitability of the developed SPR-based assay for these types of analysis.

Finally, in order to verify that the system is operating within the conditions tested during the qualification step and in order to define a specific range of critical parameters and a panel of acceptance criteria for each test, the following parameters have been evaluated:

- ✓ Goodness of fit ( $\text{Chi}^2$ ) of the kinetic elaboration
- ✓ KD of the reference material

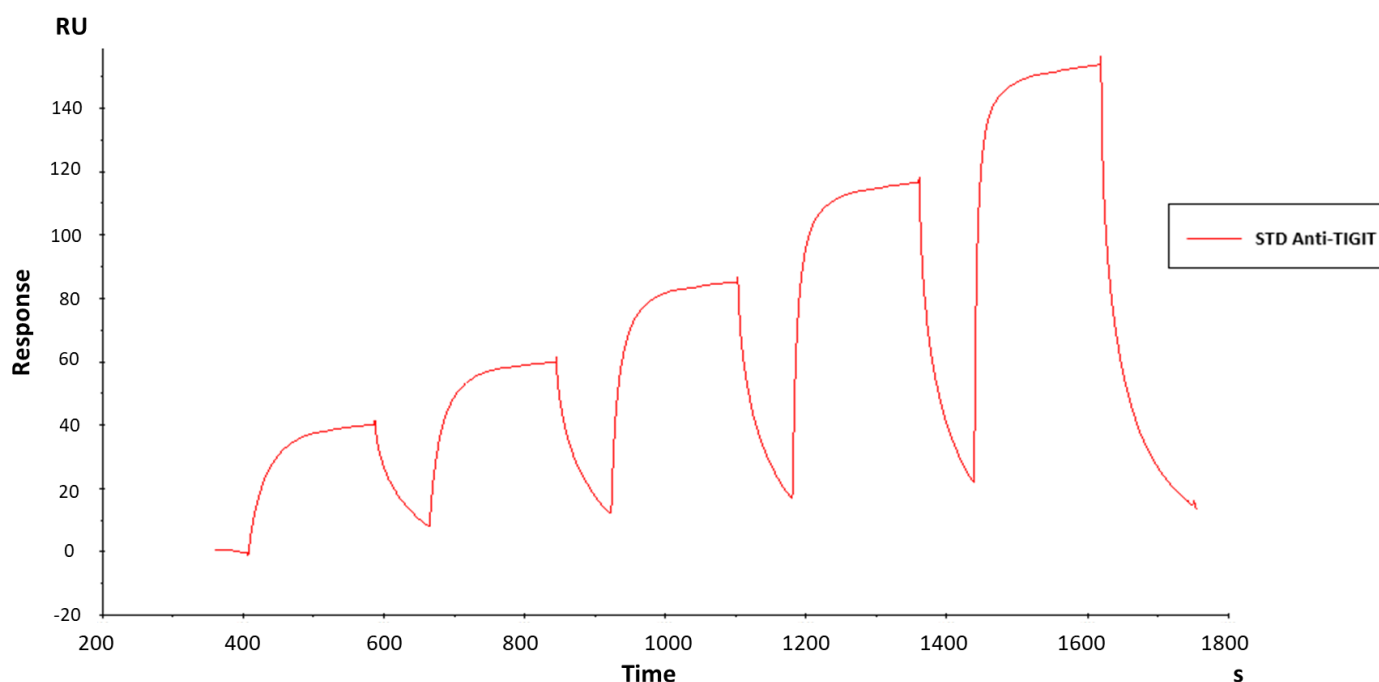
In the table (Table 29) below the applied approach is summarized.

**Table 29: Parameters and acceptance criteria for system suitability.** Abbreviations: SD = Standard deviation.

<b>Data analysis</b>	Ranges evaluated considering the reference results generated during the qualification study.
<b>Acceptance criteria</b>	<p>To be defined as follows:</p> <ul style="list-style-type: none"> <li>- Goodness of fit: <math>\text{Chi}^2 \leq 10\% \text{ Rmax}</math></li> <li>- KD of the reference material: average <math>\pm 3\text{xSD}</math></li> </ul> <p>In case the variability would not allow the 3SD approach to be applied, the Min and Max values obtained are considered.</p>

The goodness of fit was evaluated through  $\text{Chi}^2$  and Rmax values measured in all the experiments carried out during the study. Based on the obtained results, a  $\text{Chi}^2$  value of 10% of Rmax has been used for evaluating the performance of the assay (System and sample suitability). All KD values of the Reference material generated within this study have been collected and the final KD range obtained is 79-104 nM.

Below an example of the typical sensorgram obtained when analyzing Anti-TIGIT reference material binding to FcRn.



Curve	KD (M)	Rmax (RU)	Conc (M)	Flow (µl/min)	Chi <sup>2</sup> (RU <sup>2</sup> )
	<b>9,8E-08</b>	170,9347187			<b>3,03441</b>
Cycle: 12			2,5E-08	30	
			5E-08		
			1E-07		
			2E-07		
			4E-07		

**Figure 61: A typical Anti-TIGIT reference material binding to FcRn sensorgram together with the main information retrieved from the analysis.** Representative sensorgram of Anti-TIGIT binding to recombinant FcRn on Biacore assay at pH = 6.0.

In conclusion the newly developed SPR method fixes all the observed limitations associated with the formerly applied SPR methods performed in the laboratory. The main advantage of the new parental high throughput SPR method is the low variability that makes possible to discriminate differences in samples affinity with high precision and accuracy. Additionally, all SPR equipment existing on the market allow an automatized pipetting of assay components. This degree of automation reduces hands on time, ensures the high precision and accuracy of data and enables a good assay transferability between different sites using the same SPR system (Cooper, 2002; Mire-Sluis, 2001).

The method has been qualified in terms of throughput, number of replicates, precision, specificity and system suitability allowing its application starting from early phases of drug development. Considering the performance of the method measured during assay qualification, it could be also potentially applied for routine use in a GMP environment. Even if little published SPR-based data can be found for GMP-regulated quality assessment, instrument software and qualification procedures have been provided and the suitability of SPR using Biacore® for quality assessment has been demonstrated (Gassner et al., 2015).

Finally, as for bioactivity methods, also the stability indicating properties of this SPR qualified method were assessed. For this reason, from the reference material three stressed samples were generated: a deamidated sample, an oxidized sample at 0,1% and one at 0,01%. Oxidation samples were obtained by adding hydrogen peroxide (H<sub>2</sub>O<sub>2</sub>) to mAb formulation buffer accordingly to published protocols (Bertolotti-Ciarlet et al., 2009; Liu et al., 2008) while deamidated sample was obtained by adding an equal volume of 1 M ammonium bicarbonate pH 9.2 and incubating at +37°C for 3 days. For a more detailed description of samples preparation see materials and methods chapter. The stresses on the molecule were confirmed through Peptide mapping LC-MS/MS, iCE and CGE-SDS for deamidation and through Peptide mapping LC-MS/MS for oxidation (data not shown).

The oxidation stresses were selected based on the evidence in the literature that IgG1-Fc oxidation impairs FcRn binding and consequently affects pharmacokinetics of the therapeutic mAb while IgG1 deamidation should not affect the binding to the neonatal Fc receptor (Geuijen et al., 2017).

Three conserved methionine residues are present in the Fc portion of Anti-TIGIT: Met257, Met363 and Met433. Oxidized samples showed an increase of oxidation of all the three residues with a higher level on Met257. The oxidation of this Met residue has been reported to have the most deleterious effect of FcRn binding in the work of Gao et al. (Gao et al., 2017). Under this condition, no other differences in post translational modifications and no Fc degradation respect to the not treated sample have been detected. This result is consistent with other reports using similar forcing degradation conditions (Gao et al., 2017).

The analysis of the deamidated Anti-TIGIT sample showed no deamidation at the light chain while Asparagine deamidation was detected in the heavy chain. The most prone residue to deamidation was Asn320.

Below the obtained results:

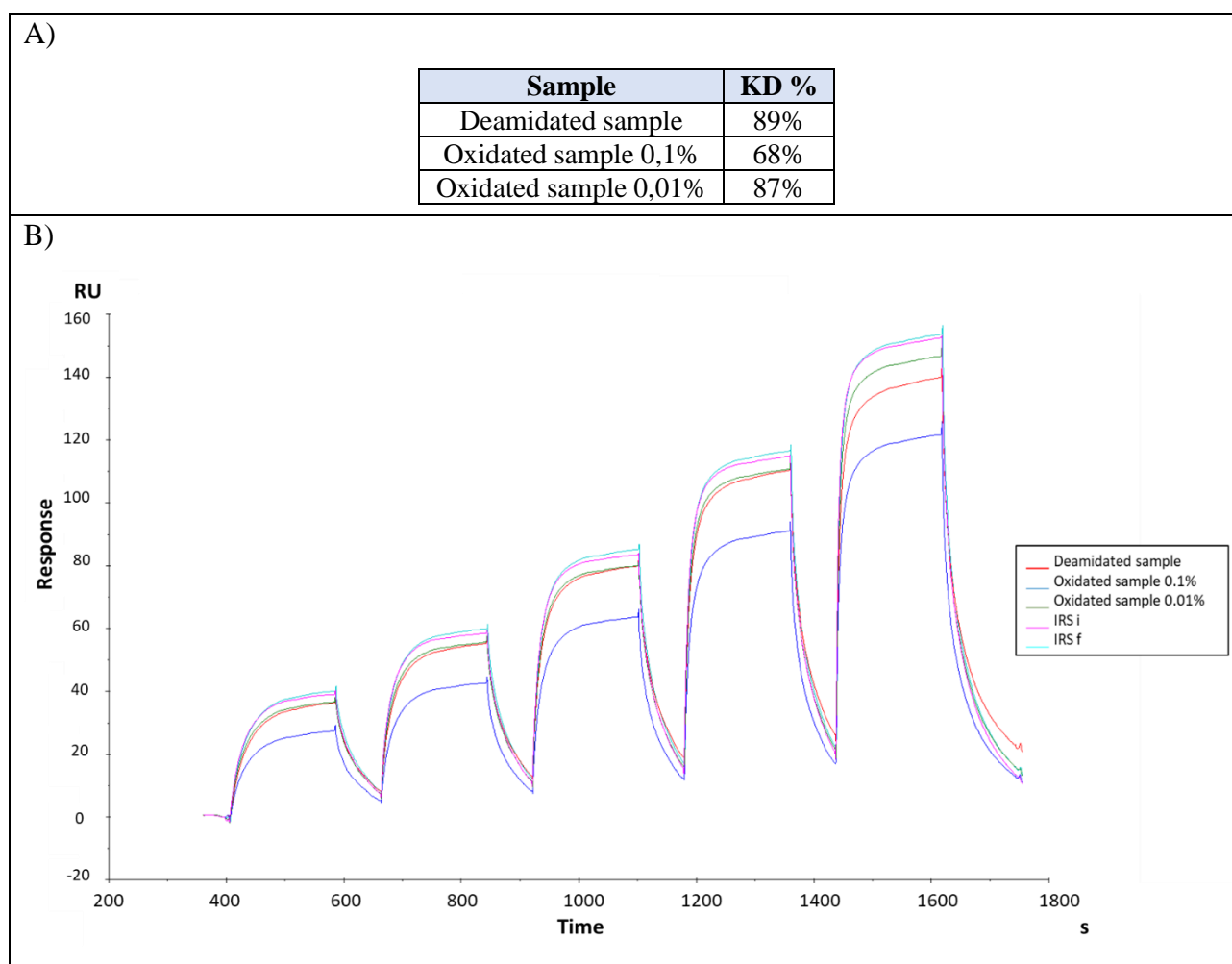


**Figure 62: Stressed samples analysis.** A) The table reported the KD% values obtained for the stressed samples. As expected, a high impact on FcRn binding was detected only for the sample undergone to a strong oxidation (0.1%). B) A representative sensorgram highlighting the differences in terms of response intensity among the 5 cycles for all the tested samples.

Abbreviations: IRS i = Interim Reference Standard initial; IRS f = Interim Reference Standard final

As expected, no effect on FcRn binding was detected for the deamidated sample. The same result was observed for the sample with a low oxidation level (0,01%).

As oxidation level increased from 0,01% to 0,1%, a notable decrease in terms of FcRn binding affinity was detected at pH 6. This result is consistent with previous studies (Wang et al., 2011) showing a reduction of the affinity to the receptor by about 80% when Methionine oxidation is nearly complete. This finding not only support us in defining the new SPR based assay as a stability indicating method but also emphasize the importance of monitoring Met oxidation in therapeutic mAbs having repercussions on the way these drugs are produced and stored to avoid Met oxidation. Taken together

all the results it is possible to conclude that this novel assay allows the highly precise and accurate determination of the interaction between an IgG1 like Anti-TIGIT and FcRn and is able to indicate mAb function-loss under specific conditions.

In conclusion, all the afore mentioned points indicate that the chosen assay format and SPR technology allow a very straightforward assay development, a highly informative assay for product and process characterization, and potential for routine use in a GMP environment. For this reason, the new parental SPR method has been introduced among the routine assays performed in the company so far to determine the IgG/FcRn interaction. The introduced SPR-based assay setup represents a generic approach for characterization of the FcRn binding of different IgG1 based biotherapeutics and it can be challenged also in the study of other interactions with the purpose to enlarge the analytical panel in terms of PK prediction to be applied in vitro for pharmaceutical process and product development.

### **5.3 ALPHA TECHNOLOGY**

Alpha technology (Amplified Luminescent Proximity Homogeneous Assay Screen) is a versatile assay technology, ease-of-use, developed to measure analytes using a homogenous protocol (Eglen et al., 2008).

Over the years, Alpha technology became an established detection technology in many academic and industrial settings. It has distinct features including consistent, reproducible results; simplified workflow; fast antibody detection and characterization (PerkinElmer Alpha user's guide). Alpha can detect a broad range of affinities with dissociation constants ( $K_d$ ) ranging from picomolar to low millimolar. Because the assay is homogeneous (no wash steps are required), transient interactions can be measured.

AlphaScreen technology offers several advantages. As Eglen et al reported in their work, the large distance for proximity allows one to capture very large molecules and study intractable interactions while using either simple or complex assay configurations, a task which is often difficult to accomplish using other popular homogeneous proximity technologies such as TR-FRET (Time-resolved fluorescence energy transfer) (Eglen et al., 2008).

Moreover, as reported by Qiang Wu et al (Wu, 2015), AlphaScreen technology provides sensitive detection of the low-affinity binding interaction between FcRn and IgG without needing any wash or secondary reagent, which could be a challenge with typical ELISA methods.

Among the advantages in using such technology we should also mention the high signal to background ratio. The signal generation process consists in a cascade reaction that produces a relevant

amplification of the signal resulting in high sensitivity. In addition, the background is low as a consequence of the excitation wavelength being in the red range at a higher wavelength than the emission signal. This reduces the auto-fluorescence generated by biomolecular components that is usually excited in the blue-green range. Moreover, thanks to the time delay between excitation and emission also auto-fluorescent noise is eliminated. Furthermore, being a homogeneous assay means that the detection of the bound donor-acceptor beads complex does not require physical separation from the unbound components to reduce the background. Consequently, it does not necessitate in-between separation or washing steps and can be executed with a simple add-and-read protocol. This reduces handling steps and makes Alphascreen more convenient and less time-consuming than other methods. Hence, it is particularly suited for automation-supported screening purposes and this is one of the reasons for its large adoption in drug discovery.

Finally, the assay can be downscaled and miniaturized. Indeed, it is easily adaptable and downscaled to a few  $\mu\text{L}$  with no change in assay robustness.

In the end, an Alpha assay is more sensitive, reproducible and has a higher throughput compared to other assays; therefore, facilitating therapeutic protein discovery and characterization (PerkinElmer Alpha user's guide).

Compared to SPR, in literature, fewer AlphaScreen methods are reported for the assessment of FcRn binding activity (Wu, 2015). In this study an AlphaScreen based method was developed to serve as a valid orthogonal technology to the reference standard SPR-based method and the assay turned out very easy-of-use, high-throughput, accurate and quick.

This AlphaScreen FcRn assay was also found to be versatile, as it involved the use of customized acceptor beads with a fragment Fab anti-IgG that allows the study of several kind of antibodies. This methodology can run up to 4 samples per plate in 2 hours which is both time and cost effective compared with other FcRn binding methods such as cell-based fluorescent activated cell scan and the previously described SPR. The generated data demonstrated that the assay is suitable for the purpose and moreover, it provides a platform approach that can be readily applied to various biotherapeutic antibodies.

The new method was challenged with a first feasibility check and then developed to set the optimal experimental conditions by using a human IgG1. Anti-TIGIT was here selected as prototype molecule to test the applicability of this method as a general platform for other IgG1.

The new AlphaScreen method was developed by testing two different approaches: competition assay where increasing concentrations of analyte are used to displace the tagged reagent from the assay, disrupting the association between the beads and saturation assay where one binding protein is titrated



across a range of concentrations to generate a saturation curve and the  $K_d$  can be derived from the data as the protein concentration at which half maximal signal is reached.

The second format was selected based on the feasibility data obtained that underlined an intrinsic higher variability and lower reproducibility of the data generated with the first layout (data not shown). Moreover, all the conditions needed to apply the second approach were satisfied (the  $K_d$  for the protein-protein interaction was far enough below the binding capacity of each bead so that all protein concentrations used to derive the  $K_d$  (usually up to 5X  $K_d$ ) fall below the bead binding capacities).

Below a table summarizing the layout of the saturation assay format (table 30).

**Table 30: Saturation assay format.**

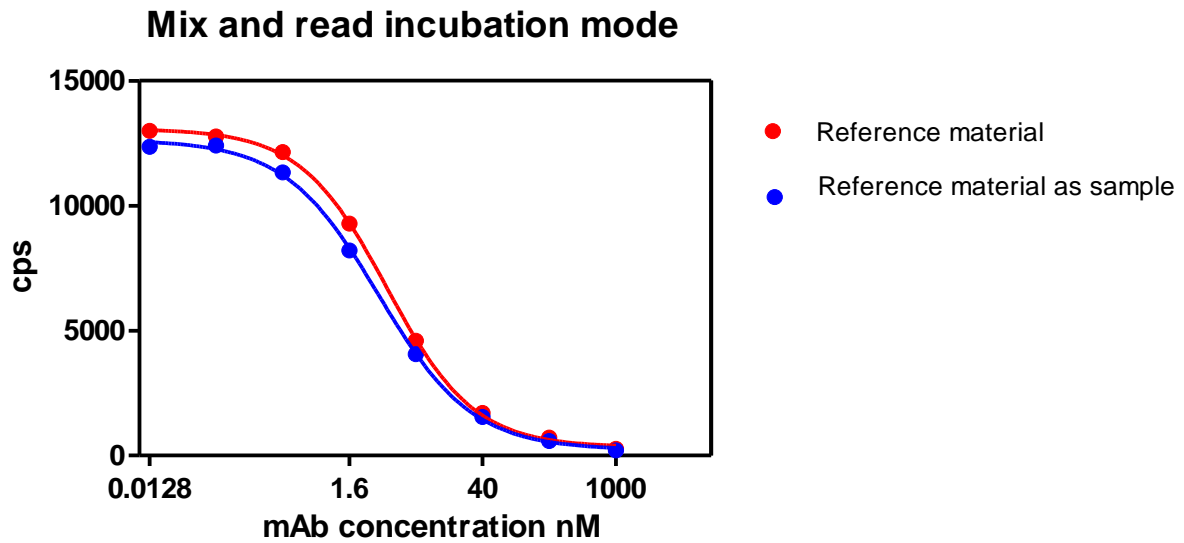
Layout	
AlphaScreen Acceptor Beads	Coated with Fab fragment direct to the whole IgG
AlphaScreen Donor Beads	Nickel, used to capture His-tagged FcRn
Ligand	FcRn His Tagged
Analyte	Biotherapeutic mAb
Curve layout	Vertical, 7 points plus the blank

Two protocols with different incubation mode have been compared:

- “mix and read” that foresees the simultaneous mix of analyte, receptor and beads, applying an incubation at 23°C in the dark for 1 hour.
- Initial incubation of 1 hour in which analyte and receptor reach the equilibrium followed by a second incubation in the dark for 1 hour in the presence of the beads’ mixture.

A representative result obtained when testing only reference material against itself applying these two incubation modes is graphed below (Figure 63).

A)



B)

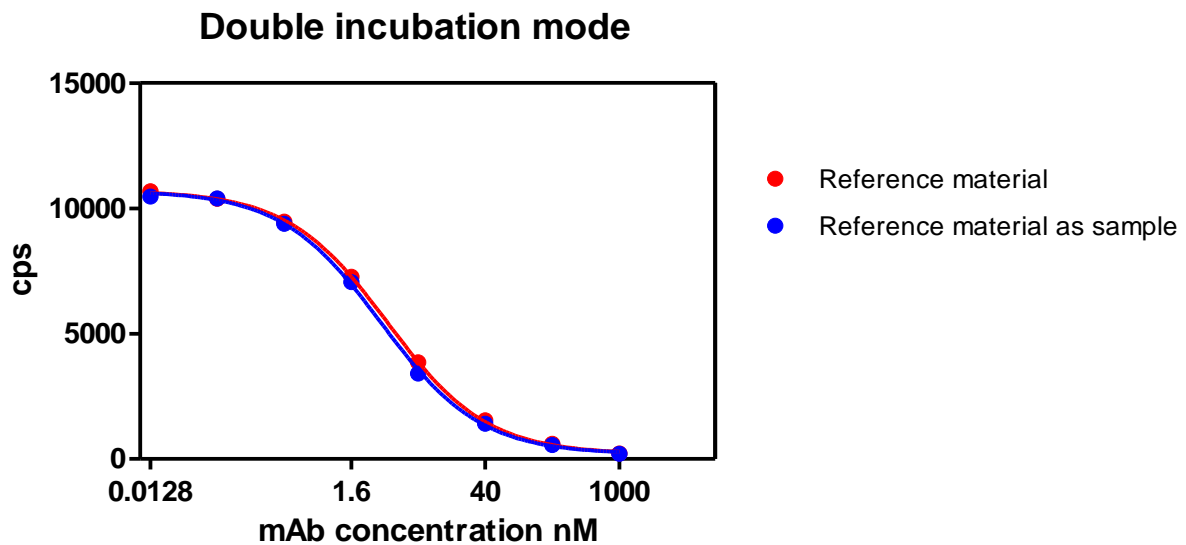


**Figure 63: Representative graphs showing the different outcome of the two incubation modes.** In both experiments the reference material is tested against itself. In A) is shown the comparison among the curves when using the “mix and read” incubation mode. When the two curves are compared for top, bottom and HillSlope, they are found statistically different ( $p\text{-value} < 0.0001$ ) even if the curves are obtained from the same material.

In B) is shown the comparison of the same curves obtained after the double incubation. The two curves are perfectly overlapped, and the calculated  $p\text{-value}$  is equal to 0.3231.

In the “mix and read” format the dose-response curve for the standard was found statistically different from the dose-response curve of the standard as a sample.

The fit of the curves was compared when selected parameters (bottom, top and HillSlope) are shared among all datasets with the fit when those parameters are fit individually to each dataset.

Indeed, bottom top and Hillslope of the two curves were compared by an extra sum of squares F test. The Extra sum-of-squares F test is based on traditional statistical hypothesis testing.

The null hypothesis is that the selected parameters are the same between the two curves. The F test compares the difference in sum-of-squares with the difference it is expected by chance. The result is expressed as the F ratio, from which a p-value is calculated.

If the P value is small, it is possible to conclude that the null hypothesis (three parameters are the same for each data set) is wrong and accept the other model (there is a difference among the two data sets). The threshold P value is set at its traditional value of 0.05. Since the P value is less than 0.05 ( $< 0.0001$ ), then the null model should be rejected and conclude that the two curves are different in terms of bottom top and HillSlope.

Probably, 1 hour of incubation is not enough to reach the equilibrium between analyte and receptor. In the format with the double incubation instead, the two dose-response curves are statistically similar in terms of Top, Bottom and HillSlope with a p-value of 0.3231. For this reason, the format with double incubation was preferred.

After the identification of the proper assay layout, the following concentrations for each reagent have been selected during the feasibility study.

**Table 31: List of all the reagents used in the assay and their concentrations.**

Reagent	Concentration
FcRn His tagged concentration	20 nM
Acceptor beads concentration	10 ug/mL
Donor beads concentration	10 ug/mL
Curve layout	Vertical, 7 points plus the blank
Analyte range	To be defined based on the analyte binding affinity to FcRn
Step dilution	To be defined based on the analyte

After the feasibility study the method was qualified in term of linearity and range, accuracy, precision, system suitability and the plate effect with another IgG1. For how the linearity and range, accuracy and precision of an analytical method were evaluated, and which were the criteria to be met, refer to the approach applied for the cell-based assays.

The method was found to be linear and accurate between 50% and 200% and the highest Intermediate Precision obtained among all the Potency levels tested was found to be 12%.

Before to apply it for the study of the interaction between Anti-TIGIT and FcRn, the proper mAb dose-response curve was determined and the plate effect and the specificity of the assay were assessed.

Moreover, with the aim to demonstrate that the method is able to discriminate changes in the FcRn binding affinity as a result of different stresses, that the method could really be applied for characterization purposes during the early phase of product development and that it gives results aligned with the Biacore method, the same stressed samples were tested.

Two Anti-TIGIT dose response curves were tested, one starting from 15 nM and the other starting from 20 nM, were analyzed. In both cases the curves were prepared with a step dilution 1:3. A representative result is graphed in figure 64.

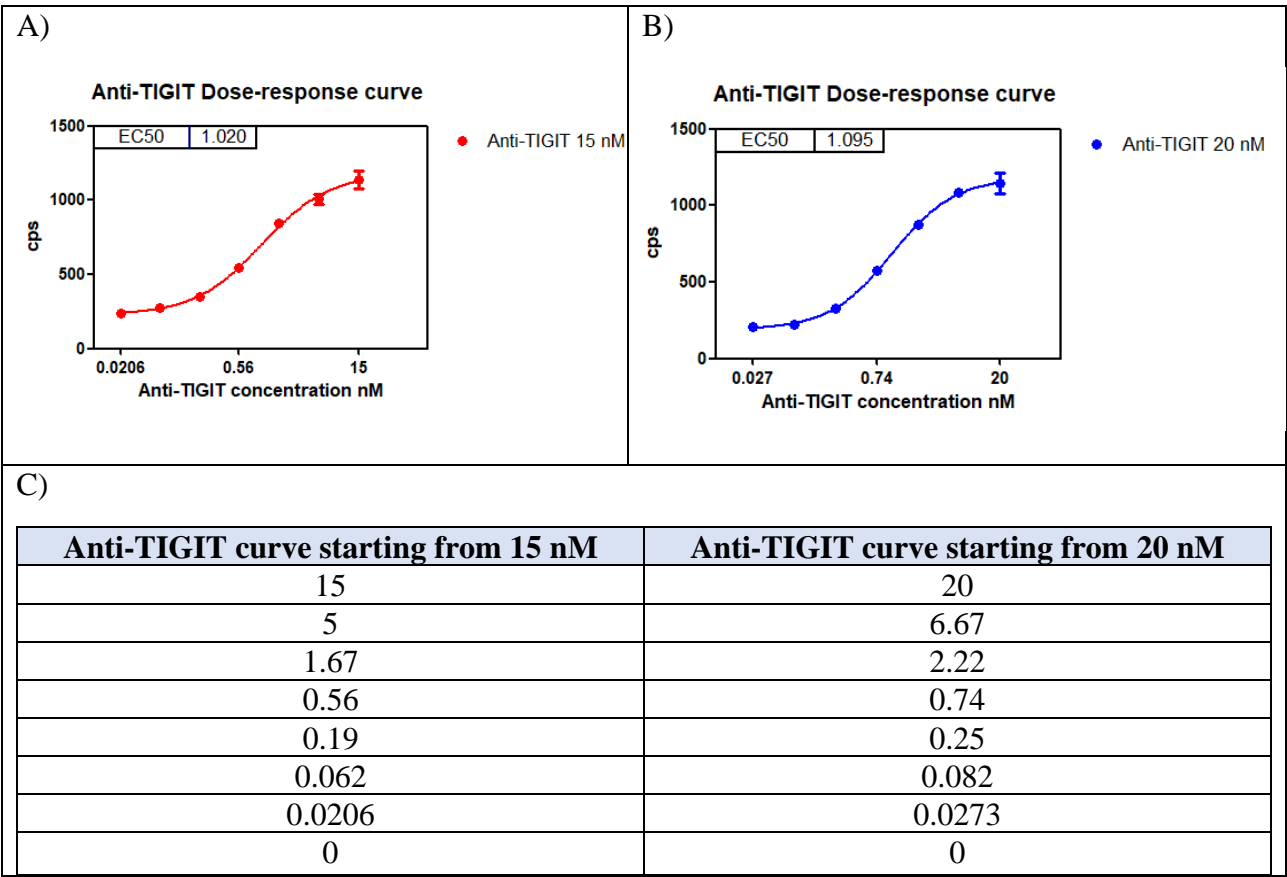


**Figure 64:** Anti-TIGIT AlphaScreen dose response curves. A) A representative dose response curve starting from 15 nM and B) a representative dose response curve starting from 20 nM. Considering that the two curves

are comparable in terms of EC<sub>50</sub>, curve A was selected since starting from a lower Anti-TIGIT concentration. C) In the table the Anti-TIGIT concentration points of the two dose response curves are reported.

Abbreviation: cps = count per second

Both dose response curves showed similar EC<sub>50</sub> values and considering that the curve starting from 15 nM of Anti-TIGIT starts from a lower amount of antibody, it was selected as the dose response curve for the AlphaScreen assay.

Finally, the plate effect was checked. Considering samples loaded in duplicate and the variability among the signal observed in the columns 1 and 12 of the assay plate (the so-called edge effect) a 2-7 layout has been selected. A representative result is shown below (Figure 65):

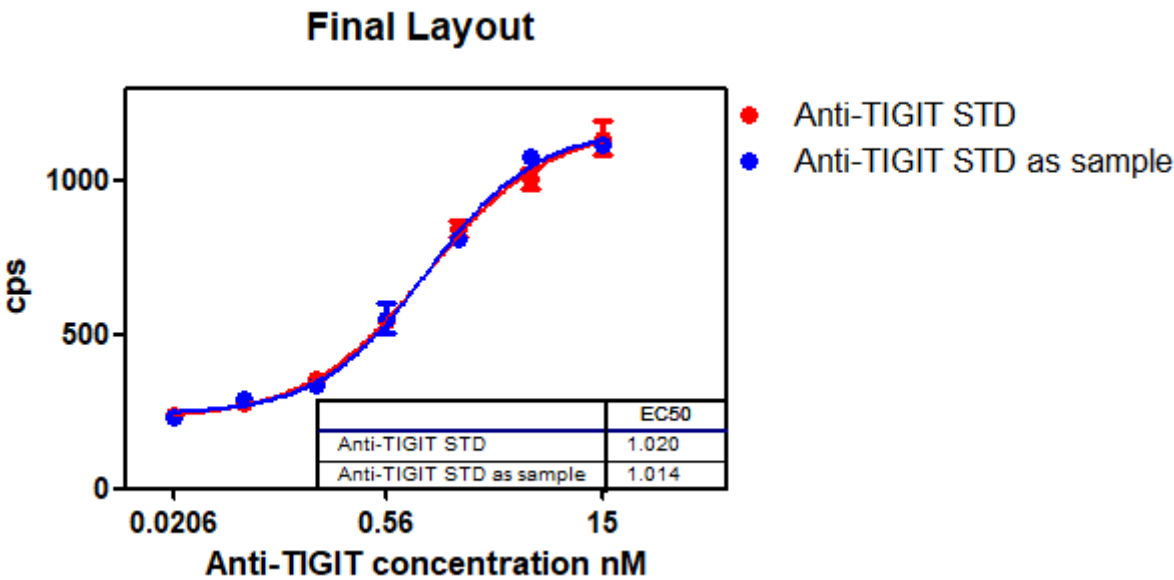


**Figure 65: Anti-TIGIT AlphaScreen assay plate layout.** A) A representative result showing that the selected layout gives well defined curves with no variability among the duplicates and with the same EC<sub>50</sub> value. Abbreviations: STD = Standard, cps = count per second

Once the main steps of the assay and the proper Anti-TIGIT dose response curve have been defined, as for the SPR-based method, also the specificity of the method response was demonstrated. The possible impact of contaminants on the results, through the spiking of typical impurities (HCP) in the samples was evaluated. Results are shown in the table below (Table 32).

**Table 32: Specificity results.** Considering the method variability, 99% of relative binding for HCP demonstrates that the spiking of typical impurities in the samples doesn't affect the assay.

Abbreviations: IRS = Interim Reference Standard; HCP = Host cell proteins; CV = coefficient of variation

	Potency %			
	1 run	2 run	Average	CV%
<b>IRS + HCP</b>	103	95	<b>99</b>	<b>6</b>

The final calculated Potency (99%) for the reference standard spiked with HCP from CHO cells confirmed the specificity of the AlphaScreen assay.

Finally, it was demonstrated the capability of the qualified assay to recognize degradation of the therapeutic antibody impacting the binding to the FcRn receptor.

Indeed, the same panel of stressed samples tested with Biacore have been evaluated with this orthogonal method. For the preparation of the stressed samples refer to chapter 3, Materials and Methods. Each sample was diluted in the assay diluent and tested in two assays according to the method procedure described in chapter 3. The results are shown in figure 66.

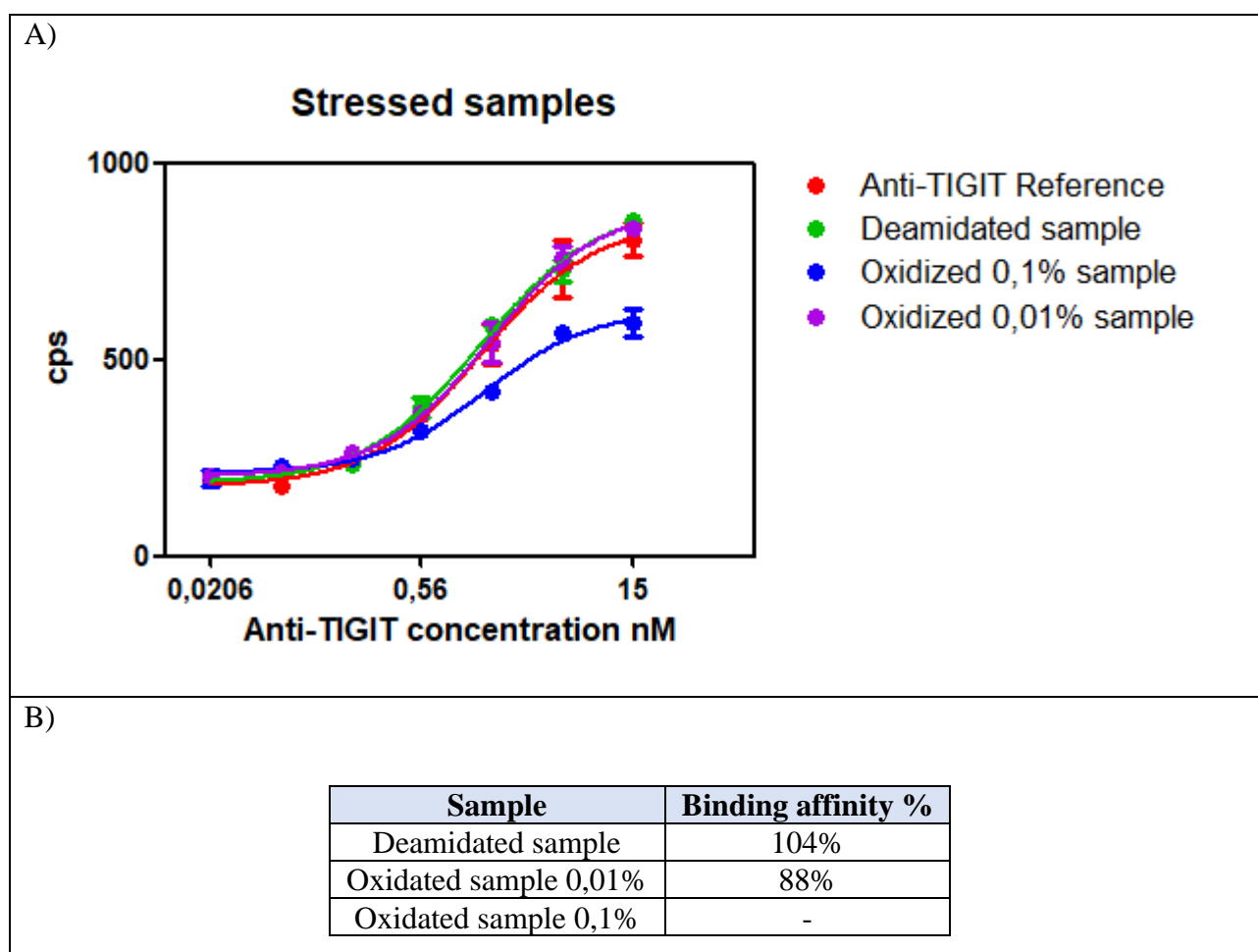


**Figure 66: Stressed samples results.** Two independent runs were performed. A) As shown from the representative graph Anti-TIGIT binding to FcRn is strongly reduced when a high level of oxidation is applied to the reference material. No effect of the deamidation as the dose response curve of the deamidated Reference material is completely overlapped to the non-treated Reference material. B) In the table the binding affinity to FcRn (%) is shown. Considering the strong differences among the dose response curve of the reference material and the one of the oxidized sample at 0.1% it was not possible to determine its binding affinity. However, based on the maximum signal generated from the 0.1% oxidized sample with respect to the reference material it is possible to conclude that the oxidation of Anti-TIGIT has a significant impact on its binding to FcRn.

Considering method variability (CV%), the results presented in figure 66 show that Anti-TIGIT samples subjected to deamidation at pH 9.2 and treatment with 0.01% of H<sub>2</sub>O<sub>2</sub> had activities similar to the control (104% and 88%, respectively). A high affinity reduction to FcRn instead is measured when testing Anti-TIGIT sample stressed with 0.1% of H<sub>2</sub>O<sub>2</sub>. Based on this finding is it possible to conclude that our novel AlphaScreen-based FcRn binding assay is able to detect the oxidation of the Fc methionine residues impacting FcRn binding.

These conclusions are also supported by the work of Qiang Wu et al (Wu et al., 2015). Indeed, when an IgG1 stressed with 1% of H<sub>2</sub>O<sub>2</sub> was tested with their AlphaScreen-based method, the estimated FcRn binding was about 4% compared with the untreated control sample.

With this study it was possible to demonstrate that the AlphaScreen-based FcRn binding assay is a simple and quick method that can be used to measure FcRn binding of IgGs as an orthogonal method to SPR providing an independent confirmation of protein FcRn binding properties. It is precise and stability indicating when critical residues for FcRn binding on the antibody are modified through different stresses.

In addition, the assay format was found to be readily applicable to other antibodies with minimal modifications confirming the broad versatility of the platform.

Finally, due its simplicity and high-throughput capability, the assay is now successfully used to support various studies where Biacore is used as the gold standard platform.

In summary, with this study it is shown how the acquisition of reliable kinetic parameters for the characterization of biomolecular interactions is an important component of the drug discovery and development process (Yang et al., 2016).

As suggested by Neuber et al. in their work, a single *in vitro* parameter alone cannot readily predict *in vivo* PK, but FcRn binding should be considered as one of the most important parameters that can influence the IgG PK *in vivo* (Neuber et al., 2014). For this reason, it is essential to analyze this interaction already during early antibody discovery using *in vitro* approaches that are sensitive, specific and accurate. Consequently, the two robust and high throughput platforms here qualified have been successfully implemented in the company for early characterization studies of the binding between the Merck NBEs and the FcRn.



## 6 POTENTIAL IMMUNOGENICITY *IN SILICO* ASSESSMENT

### 6.1 Introduction and rationale

As anticipated in the General Introduction (Chapter 2, section 3), monoclonal antibodies have numerous quality attributes that can potentially have an impact not only on the bioactivity, pharmacokinetic (PK) and safety but also on the immunogenicity of the product.

Despite the recent introduction of several approaches to reduce the immunogenicity potential of biotherapeutic antibodies, including the use of native human sequences, modification of known or potential immunogenic epitopes during drug design, production in mammalian cells, advanced manufacturing practices, and analytical characterization techniques, the human immune system can perceive as non-self the biologic drug products and launch specific immune responses against them (Shankar et al., 2014). This immune response could be characterized by T and/or B cell activation, cytokines' release and antibodies (ADA) production. As a result, pharmaceutical companies are more and more devising strategies to assess immune responses to protein therapeutics during the preclinical phases development (i.e. during designing of new sequences and lead selection). However, a proper risk-based approach should include also any liabilities due to drugs post-translational modifications as a consequence of process related changes associated with expression, purification, production cell line as well as formulation/excipient induced aggregation or degradation (Jawa et al., 2020).

Even if the world of analytical biochemistry applied to the field of potential immunogenicity evaluation is in continuous evolution, business strategies should be refined to support process needs. Indeed, when a change in the upstream or downstream process occurs, the possible impact on the drug are evaluated in analytics only in terms of protein structure, pharmacokinetics and bioactivity/potency of the drug candidate.

Therefore, the goal, recognizing the value of preclinical immunogenicity evaluation, is to incorporate *in silico* and *in vitro* immunogenicity assessment protocols into our product development strategy by defining a proper decisional/analytical workflow to be applied after critical quality attributes' assessment and/or each major production process change. This approach matches with the global intention to save time and reduce costs in the biotherapeutic drug development process by identifying the best drug candidate with the lower immunogenic potential or find mitigation strategies to avoid the unwanted product's variant or degradation product. The type of predictive immunogenicity study should be justified on the basis of the observed difference(s), the potential impact, and knowledge gained with the product and product class before (EMA guideline, 2008). To this aim Anti-TIGIT

will be firstly analyzed through an *in silico* software for potential immunogenicity evaluation and then, if potential T cell epitopes are detected, it will also be tested through the most suitable cell-based *in vitro* test to confirm *in silico* findings.

While there are many factors that contribute to protein immunogenicity, T cell- (thymus-) dependent (Td) responses appear to play a critical role in the development of antibody responses to biologic therapeutics (Jawa et al., 2013).

Because the T-cell epitopes presented by HLA Class II molecules are linear, sequence-based screening to evaluate the binding potential of overlapping peptides to the binding pockets of common HLA Class II alleles could be performed and the immunogenicity potential of the whole sequence can be scored. The advantages to use as a first step the *in silico* analysis instead of immediately begin with *in vitro* testing comprehend the relative low costs of the software, the high throughput of the analysis and the early identification, above all possible epitopes, of the most immunogenic ones.

## **6.2 *In silico* assessment**

HLA class II molecules are expressed by human professional antigen presenting cells (APCs) and can display peptides derived from exogenous antigens to CD4<sup>+</sup> T cells. These molecules are heterodimers consisting of an alpha chain and a beta chain encoded in one of three loci: HLA DR, DP and DQ. The DR locus can encode two beta chains DRB1 and DRB3-5; among them DRB1 encodes the most prevalent beta subunit in the population. Both alpha and beta chains can impact the distinct peptide binding specificity of an HLA class II molecule.

MHC class II peptide ligands that are recognized by T cells and trigger an immune response are referred to as immune epitopes (Smith-Garvin et al., 2009). Computational predictions of peptide binding to HLA molecules represent a powerful tool to identify these epitope candidates. The most comprehensive collection of epitope prediction and analysis tools is hosted by the Immune Epitope Database and Analysis Resource. In this study a Merck internal software based on IEDB MHC Class II binding prediction tool (Jensen et al., 2018) was used to assess the overall Anti-TIGIT immunogenic potential. Indeed, MHC class II binding is a prerequisite for T cell immunogenicity induction. The evaluation approach is briefly described here to illustrate the basic process of screening Anti-TIGIT therapeutic for immunogenicity. Upon submission, the mAb sequence (shown in chapter 2, section 10) was first parsed into all possible overlapping 15-mer peptide frames, each of which was then evaluated for binding potential to each of the 27 common class II HLA alleles covering more than 95% of the population (Greenbaum et al., 2011).

Then the software generates a percentile rank by comparing the peptide's predicted binding affinity against that of a large set of 15mers randomly selected from the SWISS-PROT database. This way the percentile score provides a uniform scale allowing comparisons across different predictors. A lower percentile rank indicates higher affinity. The IEDB currently recommends making selections of the binders based on a consensus percentile rank of the top 10% (percentile rank  $\leq 10$ ). However, only the peptides with a percentile rank  $< 2$  (Top 2% binders) are considered high binders and should be further investigated with *in vitro* analysis.

After software data processing, the attention was focused on the most common, representative set of eight class II HLA DR alleles (DRB1\*0101, 0301, 0401, 0701, 0801, 1101, 1301, and 1501). Indeed, T helper epitopes are presented to CD4<sup>+</sup> T cells predominantly by a subset of HLA DR class II molecules (Jawa et al., 2020).

As a second step, all Anti-TIGIT peptides containing only germline amino acids (a total of 74 peptides) were removed from the final consideration. Indeed, germline peptides will be predicted to bind but are expected to be tolerated by the human immune system and were, therefore, considered “false-positive” predictions. Among the non-germline peptides, the ones with a score  $< 10$  were then selected, and peptide binders able to bind more than one HLA allele (the so-called promiscuous binders) were identified. The significance of this selection is given by the fact that promiscuous binders are associated with stronger antigenicity and larger population coverage; identifying these peptides could therefore be important in reducing the immunogenicity of a therapeutic protein. The same strategy could also be utilized for example to compare the relative predicted binding potential of different proteins and related variants.

The strongest predicted binder is peptide H\_110 (sequence VWGQGTLVTVSSAST) that is located in the variable region (framework sequence after CDR3) of mAb's HC (heavy chain). *In silico* analysis showed high affinity to HLA-DRB1\*07:01 with a score of 2.1. The same peptide resulted also the highest promiscuous binder since it is predicted to bind 5 out of the 8 alleles considered (HLA-DRB1\*04:01, HLA-DRB1\*07:01, HLA-DRB1\*08:02, HLA-DRB1\*11:01, HLA-DRB1\*15:01) with a percentile rank between 2.1 and 4.5.

Since no strong binding peptides were detected by the software, no cell-based *in vitro* analysis was necessary to confirm Anti-TIGIT *in silico* results.

Taken together, these observations demonstrate that *in silico* analysis could help making informed decisions about the likelihood that a protein will provoke an immune response. Moreover, this and similar tools can identify potentially immunogenic regions (known as epitope clusters) within each protein sequence and map individual amino acids which contribute to the immunogenic potential of

the cluster helping a possible de-immunization of the mAb's sequence. *In silico* analysis gives a good first pass approach to immunogenicity, enabling detailed inspection of certain molecular features using *vitro* methods when required. However, these innovative tools cannot always be used as stand-alone tools since assessing only sequence-based risk without informing on other factors pertaining immunogenicity such as patient-, formulation- and treatment-related factors. Moreover, the fact that the peptide is predicted to bind to MHC class II molecules do not ensure that the mAb is phagocytosed and naturally processed by APC cells. This could be only confirmed through *in vitro* testing. As a consequence, to strengthen the output of the prediction, analysis on biotherapeutic proteins with a well-established rate of immunogenicity potential will be performed in the future to use them as proof of concept molecules for the development and qualification of cell-based assays to be use for *in silico* findings confirmation when necessary.

The critical quality attributes of a given biotherapeutic monoclonal antibody (mAb), its molecular characterization, functional assessment and effector function analysis should be defined and profiled in detail during the life cycle of a drug. In the past, this product characterization was simple and standardized. In today's complex world of biologics, success of product launch in the market demands a more thoughtful approach and drug developers are investing in advanced analytics much earlier in the development process. Indeed, these investments in early developmental phases may mitigate risks by confirming that the drug candidate has the required basic characteristics and functionality. Therefore, recognizing the added value of an early functional characterization of NBEs in the pharmaceutical industry, this work is focused on the development and qualification of sophisticated and state of the art *in silico* and *in vitro* methodologies defining the proper analytical characterization approach for a new therapeutic monoclonal antibody. Key binding properties and functional assays should be established as early as possible in development since during early phase much about the drug's quality attributes is unknown and therefore must be evaluated empirically (Emmerich et al., 2020). As a consequence, with the aim to achieve a level of product knowledge ensuring the quality of the final drug, sensitive and robust analytical assays are critical. An Anti-TIGIT monoclonal IgG1 was selected as proof of concept molecule. Such model has been selected considering that in the current range of licensed antibodies, the majority are IgG1. This allowed the establishment of platform assays that could be rapidly adapted to other biotherapeutic candidates. Monoclonal antibodies have multiple described mechanisms of action associated with the antigen binding (Fab) and crystallizable (Fc) fragments. In the case of Anti-TIGIT, crucial information includes how strongly the drug binds its target(s) and to what extent it engages the immune system to bring about cell-mediated cytotoxic effects. The first part of this work (chapter 4) was therefore focused on the identification of *in vitro* assays that reflect Anti-TIGIT biological activity and effector functions. Understanding of all the possible biological activities in relation to the antibody's intended action(s) and therapeutic effect enables selection of the most appropriate characterization method for that product. The first mechanism of action of Anti-TIGIT is based on the inhibition of the interaction between TIGIT and its binding partner CD155. Current published methods used to measure the activity of biologic drugs targeting TIGIT rely on primary human T cells and measurement of functional endpoints such as cell proliferation, cell surface marker expression, and interferon gamma (IFN $\gamma$ ) and interleukin-2 (IL-2) production. These assays are laborious and highly variable due to their reliance on donor primary cells and complex assay protocols. As a result, these assays are limited in their ability to provide a mechanism of action-based quantitative measure of drug-induced cellular

response with the assay precision and accuracy required for use in a quality control environment. Regulatory agencies generally agreed that a phase-bases approach to the development of bioassays can be accepted. Based on this assumption, on the collected information on Anti-TIGIT and on regulatory requirements for bioassay for the bioactivity determination of a drug candidate, a cell-based ligand binding bioassay has been identified as the best option. This method is based on the binding between Anti-TIGIT and its main target (TIGIT) and the known affinity of the Fc portion of antibodies to protein A (Boyle and Reis, 1987) that was used as coating solution. The main steps of the optimization phase were the cell line selection and the identification of the proper Anti-TIGIT reference material dose-response curve. The selected target cells for the Anti-TIGIT Ligand Binding Bioassay (CBA) are the CHO-s-myc-huTIGIT ECD cells which are engineered and immortalized Chinese hamster ovary (CHO) cells that constitutively express on their surface the extracellular portion of human TIGIT. These cells could be cultured both in suspension and in adhesion by simply adding FBS to the cell medium. To select the best condition for the cell-based assay an experiment testing the two cell lines in the Anti-TIGIT CBA assay was performed indicating that even if the mAb response curve was the same, the signal intensity obtained with the suspension cells was three fold higher with respect to the adherent cells. As a consequence, suspension growing cells were chosen. Then the proper Anti-TIGIT dose-response curve was identified (ranging from 2000 to 3.28 ng/ml) so the assay was ready to be tested for the preliminary performance verification meaning that preliminary linearity and range, accuracy and precision were assessed. The assay met all the acceptance criteria set at the beginning of the study and therefore it was validated without changes. At the end of the validation study the Anti-TIGIT ligand binding bioassay resulted linear between 50% and 200% of Potency, accurate with a bias between -13% and +15% and precise with a final  $CV\% \leq 12\%$ . In addition to method accuracy and precision, its specificity was also evaluated: no matrix interference on the active drug and on the assay were detected. Moreover, also the system suitability criteria were defined in order to apply the assay also for quality control purposes and stability studies. Considering that the complexities of biological manufacturing, the large size of the molecules, and the product heterogeneity introduced by cellular expression systems present significant challenges to measure the quality of a biologic drug, the qualified assay should also provide an insight into how heterogeneity or other situations that could occur during product manufacturing and storage may affect the biological functionality of the molecule. For this reason, also the stability indicating properties of Anti-TIGIT CBA were verified testing thermal stressed, oxidized and deglycosylated Anti-TIGIT samples. The obtained results not only confirmed the ability of the bioassay to detect changes in biological activity of the drug after different stresses but also

helped in determining the significance of structural attributes and variability on the drug's biological function. Since classical cell-based ligand binding bioassays are not the first choice for regulatory authorities for biotherapeutic products, also other alternative options that could be more fit for purpose and more mimicking of the MOA of the drug were explored. Among these, two possible formats were selected: Anti-TIGIT competitive ELISA assay and TIGIT/CD155 Blockade Bioassay. The ELISA method that has been developed consists in a competition between a labeled molecule (biotinylated CD155) and the antibody (Anti-TIGIT) for the binding to the antigen (TIGIT) captured on the plate. Several method fine tuning steps were required considering the complexity of the assay layout but finally a proper Anti-TIGIT dose-response curve was obtained and the reproducibility of the assay was demonstrated. However, the robustness of the system and its stability indicating properties before using it as an orthogonal method to Anti-TIGIT CBA should be demonstrated. The second option, the TIGIT/CD155 Blockade Bioassay developed by Promega, consists of two genetically engineered cell lines. TIGIT Effector Cells (Jurkat T cells) expressing human TIGIT with a luciferase reporter driven by a native promoter that can respond to both TCR activation and CD226 co-stimulation and CD155 aAPC/CHO-K1 Cells (CHO-K1 cells) engineered to express human CD155 with an engineered cell-surface protein designed to activate the TCR complex in an antigen-independent manner. When the two cell types are co-cultured, TIGIT inhibits CD226 activation and promoter-mediated luminescence. Addition of Anti-TIGIT antibody blocks the interaction of TIGIT with CD155 or inhibits the ability of TIGIT to prevent CD226 homodimerization, resulting in promoter-mediated luminescence. As a consequence, this assay should detect not only the binding between Anti-TIGIT and TIGIT but also the resultant biological effects. During the method optimization several issues were encountered: no proper detection instrument sensitivity, difficulties in the establishment of Anti-TIGIT reference dose-response curve, variability in the results, low fold increase and low signal to cite a few. The main root cause was identified in the low potency of the tested compound with respect to an external positive control used by Promega to develop the commercially available blockade bioassay. This hypothesis was confirmed with the cell-based assay by testing both compounds in the same run. Considering the results of the investigation, it was possible to conclude that the low binding affinity was the main cause of the Anti-TIGIT behavior in the TIGIT/CD155 Blockade Bioassay explaining the difficulties encountered in the development of such assay. Therefore, the development of this functional cell-based assay for Anti-TIGIT was stopped as the method is not fit for the purpose. All together these results showed a stepwise approach to be used for bioassay development and validation of a novel drug candidate and the main difficulties that could be encountered by bioassay developers. Moreover, when combined with physical/structural

data, all these binding and biological activity data could also help to establish whether the product has suitable attributes for its intended use in the clinic.

In a case like Anti-TIGIT, knowing that multiple immune system-mediated effects are important suggests that early inclusion of effector function capability testing in the characterization package may provide valuable insight. Moreover, the assessment of effector functions becomes mandatory in later phases for manufacturing process control. For this reason, to test for these Anti-TIGIT potential effector functions, a cell based ADCC assay has been developed and qualified. ADCC assays required at least an effector cell, an antigen-bearing target cell, mAbs, and a readout to measure cytotoxicity (Lewis et al., 2019). Killing of targets is an endpoint of ADCC pathway activation and is used in classic ADCC bioassays. As effector cells classic methods use primary donor peripheral blood mononuclear cells (PBMCs) or purified natural killer (NK) cells that express Fc Receptors on their surface. In this study, two different assay formats involving different types of effector cells have been explored during the development stage, to obtain the best compromise between assay performance, high throughput and work time for single assay. The two types of effector cells selected for the evaluation of ADCC activity of Anti-TIGIT are FcγRIIIA engineered NK cells and FcγRIIIA/NFAT-RE/luc2 engineered Jurkat T cells. CHO-S-myc-hu TIGIT ECD cell line has been used as target cell for both the tested formats. Both assay formats overcome many of the limitations of traditional methods by eliminating the requirement for primary cell culture and do not use radioactive materials. The main purpose of the study was to rationalize which of these ADCC effector cells best simulate the expected response in human subjects and to identify which effector cells and assay best fit ADCC bioassay needs during antibody drug development. In the first approach engineered NK cells were used as bioassay effector cells in order to try to mimic the in vivo situation. This assay is considered a valid alternative to <sup>51</sup>Cr release assay since it shows comparable sensitivity for cytotoxicity assays without using radioactive compounds (Blomberg et al., 2011). However, several technical limitations were encountered during bioassay development and none of the mitigation actions taken provided satisfactory results. In details, the low fluorescent dye retain of target cells and the poor growth condition of effector cell line were the major root causes of the assay optimization failure. For this reason, the second ADCC assay format was explored.

ADCC Reporter Gene Assay is a bioluminescent cell-based assay using Jurkat T cells that express the FcγRIIIa receptor and a luciferase reporter driven by an NFAT-response element (NFAT-RE). These engineered effector cells have been implemented to address need for improved precision and accuracy of classic NK cell ADCC bioassays (Hsieh et al., 2017). The ADCC Reporter Gene Assay



measures reporter gene signal generated by ADCC pathway activation in engineered Jurkat T effector cells. This format is a surrogate ADCC assay measuring relevant pathway activation in the effector cells as an alternative to measuring target cell death (Cheng et al., 2014). Therefore, ADCC reporter Bioassay provides partial but relevant indication of ADCC MOA process. Its biological relevance with respect to PBMC ADCC assays has been already discussed in the literature (Parekh et al., 2012). In addition, as underlined by Cheng et al. (Cheng et al., 2014), this ADCC reporter gene assay is widely used in drug development for its high stability and precision and ability to ensure a good throughput of analysis. For the intended aim, the assay would be appropriate, upon development and qualification, to support side by side testing and antibody characterization for industrial purposes. Briefly, target cells are seeded with Anti-TIGIT antibody and after the incubation Jurkat effector cells are added. The Fc $\gamma$ RIIIa/Anti-TIGIT binding results in the activation of NFAT-RE-mediated luciferase activity. The bioluminescent signal is then detected and quantified. A preliminary assessment study has been performed before starting the development of the assay to identify the best Effector/Target cells ratio and the best Anti-TIGIT dose response curve. During the following development study, the presence of a plate effect was checked together with the preliminary performance assessment where linearity and range, accuracy, precision and specificity were verified applying the same approach of the Anti-TIGIT cell-based ligand binding assay. Finally, the system suitability criteria were defined based on the development study results. All together these data suggested that the developed method is fit for the purposes. Indeed, this assay is easier to use, showed good precision, physiological relevance and it is faster to execute with respect to other assay formats. Moreover, the same stressed Anti-TIGIT samples previously tested with the CBA assay were also analysed here providing more complete knowledge and judgment on the stability indicating properties of the developed ADCC assay.

After understanding the primary mechanism of action of the drug, the attention in chapter 5 was then turned to the secondary features. Indeed, to achieve a level of product understanding that enables risk reduction, the analyses on mAbs' biological activity and effector functions described earlier, must be complemented with sensitive binding assays that reflect the possible drug's pharmacokinetics *in vivo*. This is often done using a panel of assays that test binding of mAb Fc regions to the neonatal Fc receptor (FcRn), providing insights into the real-time kinetics of these binding interactions. FcRn is a critical contributor to the half-life of therapeutic antibodies (Jones et al., 2019). Therefore, an accurate, precise, specific, and user-friendly *in vitro* FcRn binding assay is a current need industry wide. Indeed, it would facilitate the support of antibody engineering, process development, comparability studies, and biological characterization of pharmaceutical molecules. Moreover,

modulating FcRn-IgG interaction could allow changing the therapeutic antibody's half-life and improving its efficacy. In this study it is described the development, qualification, and successful piloting of two novel biochemical-based high-throughput screening assays capable of surveying the interaction between canonical IgG1 and FcRn: an SPR-based format and a bead-based proximity format (AlphaScreen technology). Both methods presented here provide a platform approach that can be readily applied to various antibodies. The SPR technique is currently considered a fundamental analytical tool for interrogation of biomolecular interactions since it provides highly accurate results and real-time and label-free measurements (Olaru et al., 2015). In this work, SPR technology background and the features of SPR-based FcRn binding assays were studied by challenging the in-house experience. Upon that, a novel parental SPR method to determine the IgG/FcRn interaction for development process and product characterization has been introduced. Firstly, different SPR assay layouts currently applied in house were explored and their limitations highlighted. Then, an innovative approach based on a regenerable use of the system Streptavidin/Biotin was explored as new SPR layout to be applied. The innovative advantage of the new SPR method is based on combining the established technology of the his-tagged protein selectively recognized by anti-his antibodies with the well-known strong interaction between streptavidin and biotin that allows a stable FcRn capturing on the chip. In such approach, the binding is then very selective, avoiding nonspecific signals. In detail, the new SPR method foresees the use of a double capturing approach: biotin tag portion of FcRn (ligand) is captured by His tagged Streptavidin that is bound by the mAb anti-his tag immobilized onto the sensor surface through amine coupling. The IgG (analyte) is then injected over the FcRn at different concentrations through a single-cycle kinetic. The obtained sensorgram is elaborated applying the “two state reaction” fitting model in order to determine the  $K_D$  value. This new method presents several advantages. As demonstrated in the work of Magistrelli et al. (Magistrelli et al., 2012), the single biotinylation site facilitated the directional immobilization of FcRn on the sensor chip and significantly increased the response level of the surface compared to amine coupling used in previous studies and it represents a closer approximation to the in vivo situation. During assay set up all the reagents were selected (running buffer, regeneration buffer, His-tag Streptavidin and biotinylated FcRn) and the FcRn capturing level was fixed in the range 200-400 RU. After the identification of the principal assay conditions, the full-dose response curve for Anti-TIGIT was established. Indeed, this method was developed as a parental method using a generic human IgG from our New Biological Entities (NBE) library and then it was optimized in order to be applied also to Anti-TIGIT samples. Method feasibility allowed us to gain familiarity with the novel assay and evaluate it for attributes such as throughput, precision, accuracy, specificity and system

suitability ( $\chi^2$ ). Optimization of the assay revealed a high level of precision ( $CV \leq 15\%$ ), accuracy and specificity. The absence of an impact given by possible presence of product contaminants in the drug including host cells proteins (HCPs) derived from the CHO cells that are a common expression system of biotherapeutic mAbs was also verified. This type of check was done considering the possibility that the method could be also used for process characterization purposes and that, for this reason, could be also applied for the analysis of samples that contain higher percentage of contaminants with respect to the final product. Moreover, upon analysis of different stressed Anti-TIGIT samples it was shown that the assay is able to indicate mAb's function-loss. In conclusion, the chosen assay format displays robust qualification parameters, is specific for the biotherapeutic, and is also highly informative being able to indicate molecular stability of the drug candidate. For all these reasons, the new parental SPR method has been introduced among the routine assays performed by the company so far to determine the IgG/FcRn interaction. Moreover, its setup represents a generic approach for characterization of the FcRn binding of different IgG1 based biotherapeutics and it can be challenged also in the study of other interactions with the purpose to enlarge the analytical panel in terms of PK prediction to be applied in vitro for pharmaceutical process and product development. Compared to SPR, in literature, fewer AlphaScreen methods are reported for the assessment of FcRn binding activity (Wu, 2015). In this study an AlphaScreen based method was successfully developed to serve as a valid orthogonal technology to the reference standard SPR-based method and the assay turned out very easy-of-use, high-throughput, accurate and quick. This AlphaScreen FcRn assay was also found to be versatile, as it involves the use of customized acceptor beads with a fragment Fab anti-IgG that allows the study of several kind of biotherapeutic antibodies. The new method was challenged with a first feasibility check and then developed to set the optimal experimental conditions. Anti-TIGIT was here selected as prototype molecule to test the applicability of this method as a general platform for other IgG1. This methodology can run up to 4 samples per plate in 2 hours which is both time and cost effective compared with other FcRn binding methods. In this study using the AlphaScreen-based assay, a double incubation layout was chosen: His tag FcRn is incubated with Anti-TIGIT and then after a proper incubation at room temperature a mixture of Nickel donor beads and acceptor beads coated with a Fab fragment anti-human IgG is added. The close proximity among the beads bound to the FcRn-Anti-TIGIT complex enables the transfer of 1  $O_2$  from donor beads excited at 680 nm to acceptor beads emitting a signal at 520–620 nm. In the end, the binding of the Anti-TIGIT sample to FcRn results in a different emitting signal for different sample IgG dilutions. During assay development the full dose response curve of Anti-TIGIT was determined in a range from 15 nM to 0.0206 nM with a step dilution 1:3. Then the assay was further characterized

by conducting a study to evaluate the assay accuracy and precision. The method was found to be linear and accurate between 50% and 200% and the highest Intermediate Precision obtained among all the Potency levels tested was found to be 12%. After the method accuracy, precision, and specificity were verified, the ability of the assay to detect changes in Fc domain modification was evaluated using the same panel of stressed Anti-TIGIT samples that had been previously tested with SPR-based method.

Eventually, in chapter 6 also the potential immunogenicity of biotherapeutic mAbs was taken into account. Indeed, any liabilities due to drugs post-translational modifications as a consequence of process related changes associated with expression, purification, production cell line as well as formulation/excipient induced aggregation or degradation (Jawa et al., 2020) should be evaluated not only in terms of mAbs' bioactivity, effector functions and predictive PK but also from the point of view of the immunogenic potential. Currently, when a change in the upstream or downstream process occurs, the most common strategy is to evaluate in analytics the possible impact on the drug only in terms of its protein structure, pharmacokinetics and bioactivity/potency. Therefore, the main goal here was to incorporate *in silico* and *in vitro* immunogenicity assessment protocols into our product development strategy by defining a proper decisional/analytical workflow to be applied after critical quality attributes' assessment and/or each major production process change. To this aim Anti-TIGIT was first analyzed through a Merck *in silico* tool based on IEDB software to identify the peptides that are most likely to bind MHC class II molecules. The results showed no strong binding peptides (rank score <2) in the drug's sequence supporting clinical trials results. However, considering the low immunogenic potential of Anti-TIGIT, the development of cell-based assays was not necessary. In addition, from the analytical perspective, this antibody would be not appropriate for method development since a low T cell response was expected. For this reason, to complete the analytical panel for immunogenicity assessment, analysis on biotherapeutic proteins with a well-established rate of immunogenicity potential will be performed in the future to utilize them as proof of concept molecules for the development and qualification of cell-based assays to be use for *in silico* findings confirmation when necessary.

## 8

## CONCLUSIONS

Biologics testing is a critical process during development and production as these large molecules are sensitive to and altered by changes in their manufacturing process and therefore quality, safety, and efficacy must be continually monitored in order to meet strict regulatory requirements. Method development and validation of fit-for-purpose analytical methods is critical to the successful development of new pharmaceuticals. Indeed, implementation of Quality-by-Design (QbD), and its wider acceptance in the industry is creating a need for more sophisticated means of analysis. Here we offered an insight into bioassays and binding assays, where they intersect, how they differ, and why developers would use one over another. A deeper exploration of specific assays is also reported and accompanied by a discussion of the stepwise approach to be applied for assay development and validation together with the best practices to comply with regulatory requirements and the latest trends. A schematic representation of the analytical developed strategy is reported below:

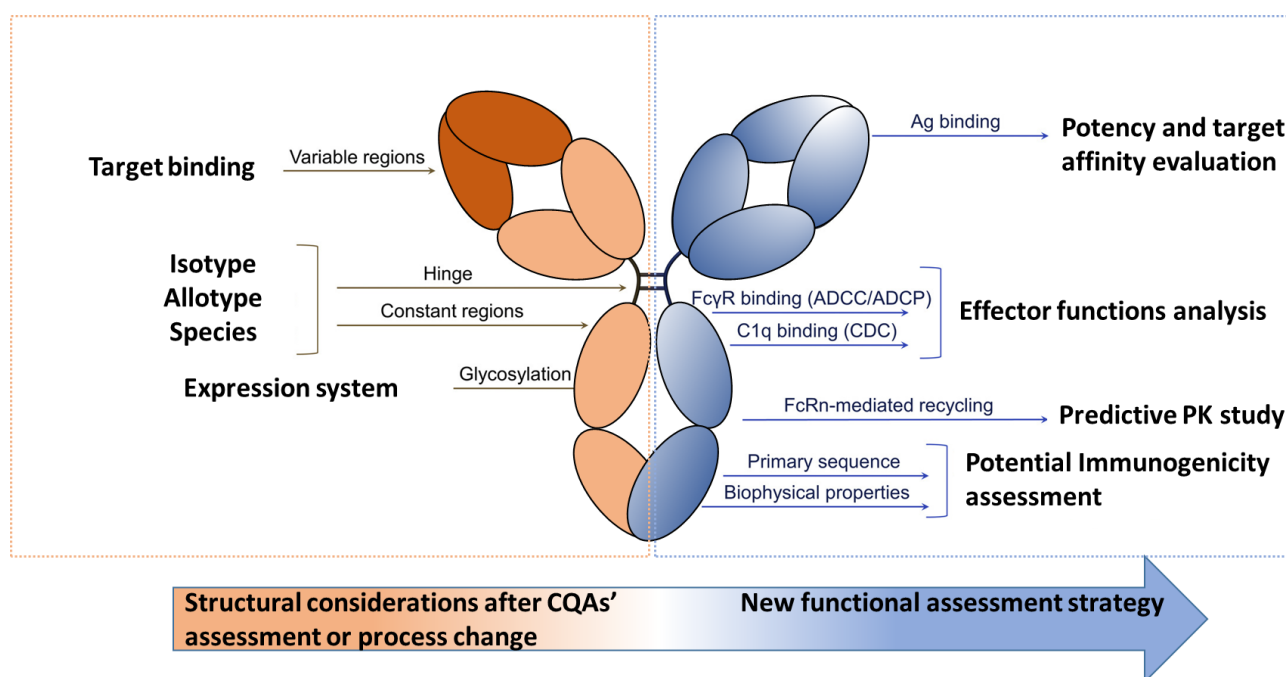


**Figure 70: Comprehensive analytical strategy to be applied after biopharmaceuticals' CQAs assessment or after each major process change.**

Modified from Goulet D.R., Atkins W.M., 2019.

In conclusion this work provided customized, stand-alone analytical solutions throughout the drug development process focusing on biopharmaceutical mAbs' bioactivity, predictive pharmacokinetics and potential immunogenicity. A subset of these methods is currently used for lot release and stability

testing in GMP manufacturing of drug substances for the clinic and to support comparability studies following changes in manufacturing.

- Akinleye, A., Rasool, Z. Immune checkpoint inhibitors of PD-L1 as cancer therapeutics. *Journal of Hematology & Oncology* 12, 92 (2019). Doi: 10.1186/s13045-019-0779-5.
- Alt N., Zhang T.Y., Motchnik P., Tatischev R., Quarmby V., Schlothauer T, Beck H., Emrich T., Harris R.J. Determination of critical quality attributes for monoclonal antibodies using quality by design principles. *Biologicals*, 44(5):291-305 (2016). Doi: 10.1016/j.biologicals.2016.06.005.
- Anderson, A.C., Joller, N., & Kuchroo, V. Lag-3, Tim-3, and TIGIT: Co-inhibitory Receptors with Specialized Functions in Immune Regulation. *Immunity*, 44, 989-1004 (2016). Doi: 10.1016/j.immuni.2016.05.001
- Andrews L.P., Yano H., Vignali D.A.A. Inhibitory receptors and ligands beyond PD-1, PD-L1 and CTLA-4: breakthroughs or backups. *Nature Immunology*, 20(11):1425-1434 (2019). Doi: 10.1038/s41590-019-0512-0.
- Avery L.B., Wade J., Wang M., Tam A., King A., Piche-Nicholas N., Kavosi M.S, Penn S., Cirelli D., Kurz J.C., Zhang M., Cunningham O., Jones R., Fennell B.J., McDonnell B., Sakorafas P., Apgar J., Finlay W.J., Lin L., Bloom L., O'Hara D.M. Establishing in vitro in vivo correlations to screen monoclonal antibodies for physicochemical properties related to favorable human pharmacokinetics. *MAbs*, 10(2):244-255 (2018). Doi: 10.1080/19420862.2017.1417718.
- Baek Y., Emami P., Singh N., Ilott A., Sahin E., & Zydney A. Stereospecific Interactions between Histidine and Monoclonal Antibodies. *Biotechnology and Bioengineering* (2019). Doi: 10.1002/bit.27109.
- Bajardi-Taccioli A., Blum A., Xu C., Sosic Z., Bergelson S., Feschenko M. Effect of protein aggregates on characterization of FcRn binding of Fc-fusion therapeutics. *Molecular Immunology*, 67(2 Pt B):616-24 (2015). Doi: 10.1016/j.molimm.2015.06.031.
- Baker M.P., Jones, T.D. Identification and removal of immunogenicity in therapeutic proteins. *Current Opinion in Drug Discovery & Development* 10(2): 219– 227 (2007).
- Barbosa M.D.F.S., Celis E. Immunogenicity of protein therapeutics and the interplay between tolerance and antibody responses. *Drug Discovery Today* 12(15–16): 674– 681 (2007). Doi: 10.1016/j.drudis.2007.06.005.

- Beck A., Wurch T. & Corvaia N. Therapeutic antibodies and derivatives: from the bench to the clinic. *Current pharmaceutical biotechnology* 9(6) 421-2 (2008). Doi: 10.2174/138920108786786420
- Bendtzen K., Immunogenicity of Anti-TNF- $\alpha$  Biotherapies: II. Clinical Relevance of Methods Used for Anti-Drug Antibody Detection. *Frontiers in Immunology*, 6:109 (2015). Doi:10.3389/fimmu.2015.00109
- Bertolotti-Ciarlet A., Wang W., Lownes R., Pristatsky P., Fang Y., McKelvey T., Li Y., Li Y., Drummond J., Prueksaritanont T., Vlasak J. Impact of methionine oxidation on the binding of human IgG1 to Fc  $\gamma$ 1 and Fc  $\gamma$ 3 receptors. *Molecular Immunology*, 46(8-9):1878-82 (2009). Doi: 10.1016/j.molimm.2009.02.002.
- Blessy M., Patel R.D., Prajapati P.N., Agrawal Y.K. Development of forced degradation and stability indicating studies of drugs-A review. *Journal of Pharmaceutical Analysis*, 4(3):159-165 (2013). Doi: 10.1016/j.jpha.2013.09.003.
- Bloem K., Hernandez-Breijo B., Martinez-Feito A., Rispens T. Immunogenicity of therapeutic antibodies: monitoring antidrug antibodies in a clinical context. *Therapeutic Drug Monitoring*, 39:327–32 (2017). Doi: 10.1097/FTD.0000000000000404
- Blomberg K.R., Mikkilä V.M., Hakala H.H., Mäkinen P.H., Suonpää M.U., Hemmälä I.A. A dissociative fluorescence enhancement technique for one-step time-resolved immunoassays. *Analytical and Bioanalytical Chemistry*, 399(4):1677–1682 (2011). Doi:10.1007/s00216-010-4485-y
- Borghaei H., Robinson M.K., Weiner L.M. Monoclonal Antibody Therapy of Cancer. In: Disis M.L. (eds) *Immunotherapy of Cancer. Cancer Drug Discovery and Development*. Humana Press (2006). <https://doi.org/10.1385/1-59745-011-1:487>
- Boyle M., Reis K. Bacterial Fc Receptors. *Nature Biotechnology* 5, 697–703 (1987). <https://doi.org/10.1038/nbt0787-697>
- Brinks V., Jiskoot W., Schellekens H. Immunogenicity of therapeutic proteins: the use of animal models. *Pharmaceutical Research*, (10):2379-85 (2011). Doi: 10.1007/s11095-011-0523-5
- Caldwell, G.W., Yan, Z., Masucci, J.A., Hageman W., Leo G., Ritchie D. M. Applied Pharmacokinetics in Drug Development. *Pharmaceutical Development and Regulation* 1, 117–132 (2003). <https://doi.org/10.1007/BF03257371>



Camacho-Sandoval R., N. Sosa-Grande E., González-González E., Tenorio-Calvo A., López-Morales C.A., Velasco-Velázquez M., Pavón-Romero L., Mayra Pérez-Tapia S., Medina-Rivero E. Development and validation of a bioassay to evaluate binding of adalimumab to cell membrane-anchored TNF $\alpha$  using flow cytometry detection, *Journal of Pharmaceutical and Biomedical Analysis*, Volume 155, 2018, Pages 235-240, ISSN 0731-7085, <https://doi.org/10.1016/j.jpba.2018.03.057>.

Cantoni O., Sestili P., Brandi G., Cattabeni F. The L-histidine-mediated enhancement of hydrogen peroxide-induced cytotoxicity is a general response in cultured mammalian cell lines and is always associated with the formation of DNA double strand breaks. *FEBS Letters* Oct 10;353(1):75-8 (1994). Doi: 10.1016/0014-5793(94)01010-2.

Cavallo F, Calogero R.A., Forni G. Are oncoantigens suitable targets for anti-tumour therapy? *Nature Reviews Cancer* 2007 Sep;7(9):707-13. Doi: 10.1038/nrc2208.

Chamberlain P., Rup B. Immunogenicity Risk Assessment for an Engineered Human Cytokine Analogue Expressed in Different Cell Substrates. *AAPS Journal* 22, 65 (2020). <https://doi.org/10.1208/s12248-020-00443-2>

Chames P., Van Regenmortel M., Weiss E., Baty D. Therapeutic antibodies: successes, limitations and hopes for the future. *British Journal of Pharmacology*. 2009;157(2):220-233. Doi:10.1111/j.1476-5381.2009.00190.x

Chauvin J.M., Pagliano O., Fourcade J., Sun Z., Wang H., Sander C., Kirkwood J..M, Chen T.H., Maurer M., Korman A.J., Zarour H.M. TIGIT and PD-1 impair tumor antigen-specific CD8<sup>+</sup> T cells in melanoma patients. *Journal of Clinical Investigation*. 2015 May;125(5):2046-58. Doi: 10.1172/JCI80445.

Chirino, A., Mire-Sluis, A. Characterizing biological products and assessing comparability following manufacturing changes. *Nature Biotechnology* 22, 1383–1391 (2004). <https://doi.org/10.1038/nbt1030>

Chung S., Nguyen V., Lin Y.L., Lafrance-Vanasse J., Scales S.J., Lin K., Deng R., Williams K., Sperinde G., Li J.J., Zheng K., Sukumaran S., Tesar D., Ernst J.A., Fischer S., Lazar G.A., Prabhu S., Song A. An in vitro FcRn- dependent transcytosis assay as a screening tool for predictive assessment of nonspecific clearance of antibody therapeutics in humans. *MAbs*. 2019 Jul;11(5):942-955. Doi: 10.1080/19420862.2019.1605270.

Cook D., Brown D., Alexander R., March R., Morgan P., Satterthwaite G., Pangalos M.N. Lessons learned from the fate of AstraZeneca's drug pipeline: a five-dimensional framework. *Nature Reviews Drug Discovery* 2014 Jun;13(6):419-31. Doi: 10.1038/nrd4309.

Cooper, M. Optical biosensors in drug discovery. *Nature Reviews Drug Discovery* 1, 515–528 (2002). <https://doi.org/10.1038/nrd838>

Cromwell M.E., Hilario E., Jacobson F. Protein aggregation and bioprocessing. *AAPS Journal* 2006; 8(3):E572-E579. Doi:10.1208/aapsj080366

Dall'Acqua W.F., Woods R.M., Ward E.S., Palaszynski S.R., Patel N.K., Brewah Y.A., Wu H., Kiener P.A., Langermann S. Increasing the affinity of a human IgG1 for the neonatal Fc receptor: biological consequences. *The Journal of Immunology* 2002 Nov 1;169(9):5171-80. Doi:10.4049/jimmunol.169.9.5171.

Debnath M., Prasad G.B., Bisen P.S. (2010) *Molecular Diagnostics: Promises and Possibilities*. Springer, 2010 Dordrecht. [https://doi.org/10.1007/978-90-481-3261-4\\_5](https://doi.org/10.1007/978-90-481-3261-4_5)

Delves P.J., Roitt I.M. The immune system. Second of two parts. *The New England Journal of Medicine* 2000 Jul 13;343(2):108-17. Doi: 10.1056/NEJM200007133430207.

Deuss F.A., Gully B.S., Rossjohn J., Berry R. Recognition of nectin-2 by the natural killer cell receptor T cell immunoglobulin and ITIM domain (TIGIT). *Journal of Biological Chemistry* 2017 Jul 7;292(27):11413-11422. Doi: 10.1074/jbc.M117.786483.

Dobson C.L., Devine P.W., Phillips J.J., Higazi D.R., Lloyd C., Popovic B., Arnold J., Buchanan A., Lewis A., Goodman J., van der Walle C.F., Thornton P., Vinall L., Lowne D., Aagaard A., Olsson L.L., Ridderstad Wollberg A., Welsh F., Karamanos T.K., Pashley C.L., Iadanza M.G., Ranson N.A., Ashcroft A.E., Kippen A.D., Vaughan T.J., Radford S.E., Lowe D.C. Engineering the surface properties of a human monoclonal antibody prevents self-association and rapid clearance in vivo. *Scientific Reports* 2016 Dec 20;6:38644. Doi: 10.1038/srep38644.

Dostalek M., Prueksaritanont T., Kelley R.F. Pharmacokinetic de-risking tools for selection of monoclonal antibody lead candidates. *MAbs*. 2017 Jul;9(5):756-766. Doi: 10.1080/19420862.2017.1323160.

Dougan D.A., Malby R.L., Gruen L.C., Kortt A.A., Hudson P.J. Effects of substitutions in the binding surface of an antibody on antigen affinity. *Protein Engineering*. 1998 Jan;11(1):65-74. Doi: 10.1093/protein/11.1.65.

Duensing T.D., Watson S.R. Complement-Dependent Cytotoxicity Assay. *Cold Spring Harbor Protocols* 2018 Feb 1;2018(2). Doi: 10.1101/pdb.prot093799.

Dunnington, K., Benrimoh, N., Brandquist, C., Cardillo-Marricco, N., Spirito, M.D., & Grenier, J. (2018). Application of Pharmacokinetics in Early Drug Development. From “Pharmacokinetics and Adverse Effects of Drugs - Mechanisms and Risks Factors”. Doi: 10.5772/intechopen.74189

Dwek R.A., Lellouch A.C., Wormald M.R. Glycobiology: 'the function of sugar in the IgG molecule'. *Journal of Anatomy* vol. 187 ( Pt 2),Pt 2 (1995): 279-92.

Ecker D.M., Jones S.D., Levine H.L. The therapeutic monoclonal antibody market. *MAbs*. 2015;7(1):9-14. Doi: 10.4161/19420862.2015.989042.

Ederveen J., “A practical approach to biological assay validation”, 2010

Eglen R.M., Reisine T., Roby P., Rouleau N., Illy C., Bossé R., Bielefeld M. The use of AlphaScreen technology in HTS: current status. *Current Chemical Genomics* 2008 Feb 25;1:2-10. Doi: 10.2174/1875397300801010002.

Elloumi J., Jellali K., Jemel I., Aifa S. Monoclonal antibodies as cancer therapeutics. *Recent Patents on Biotechnology* 2012 Apr;6(1):45-56. Doi: 10.2174/187220812799789190.

EMA, Guideline on immunogenicity assessment of biotherapeutic proteins, 18 May 2017

Emmerich, C.H., Gamboa, L.M., Hofmann, M.C.J., Bonin-Andresen M., Arbach O., Schendel P., Gerlach B., Hempel K., Bessalov A., Dirnagl U., Parnham M.J. Improving target assessment in biomedical research: the GOT-IT recommendations. *Nature Reviews Drug Discovery* 20, 64–81 (2021). <https://doi.org/10.1038/s41573-020-0087-3>

Eriksson E.M., Keh C.E., Deeks S.G., Martin J.N., Hecht F.M., Nixon D.F. Differential expression of CD96 surface molecule represents CD8<sup>+</sup> T cells with dissimilar effector function during HIV-1 infection. *PLoS One* 2012; 7(12):e51696. Doi: 10.1371/journal.pone.0051696.

FDA, Potency Tests for Cellular and Gene Therapy Products. Final Guidance for Industry: JANUARY 2011.

Fleri W., Paul S., Dhanda S.K., Mahajan S., Xu X., Peters B., Sette A. The Immune Epitope Database and Analysis Resource in Epitope Discovery and Synthetic Vaccine Design. *Frontiers in Immunology* 2017 Mar 14;8:278. Doi: 10.3389/fimmu.2017.00278.

Folzer E., Diepold K., Bomans K., Finkler C., Schmidt R., Bulau P., Huwyler J., Mahler H.C., Koulov A.V. Selective Oxidation of Methionine and Tryptophan Residues in a Therapeutic IgG1 Molecule. *Journal of Pharmaceutical Sciences* 2015 Sep;104(9):2824-31. Doi: 10.1002/jps.24509.

Gabrielson J.P., Kendrick B.S., Young J.A. Universal Qualification of Analytical Procedures for Characterization and Control of Biologics. *Journal of Pharmaceutical Sciences* 2020 Aug;109(8):2413-2425. Doi: 10.1016/j.xphs.2020.05.012.

Gao J., Yin D.H., Yao Y., Sun H., Qin Z., Schoneich C., Williams T.D., Squier T.C. Loss of conformational stability in calmodulin upon methionine oxidation. *Biophysical Journal*, 74 (1998), pp. 1115-1134

Gao X., Ji J.A., Veeravalli K., Wang Y.J., Zhang T., McGreevy W., Zheng K., Kelley R.F., Laird M.W., Liu J., Cromwell M. Effect of individual Fc methionine oxidation on FcRn binding: Met252 oxidation impairs FcRn binding more profoundly than Met428 oxidation. *Journal of Pharmaceutical Sciences* 2015 Feb;104(2):368-77. Doi: 10.1002/jps.24136.

Gassner C., Lipsmeier F., Metzger P., Beck H., Schnueriger A., Regula J.T., Moelleken J. Development and validation of a novel SPR-based assay principle for bispecific molecules, *Journal of Pharmaceutical and Biomedical Analysis*, Volume 102, Pages 144-149, ISSN 0731-7085 (2015). <https://doi.org/10.1016/j.jpba.2014.09.007>.

Gazzano-Santoro H., Chan L.G., Ballard, M.S. & Young, J.C. Ready-to-use cryopreserved primary cells: A novel solution for QC lot release potency assays. *BioProcess International Magazine* 12. 28-39 (2014).

Geuijen K.P.M, Oppers-Tiemissen C., Egging D.F., Simons P.J., Boon L., Schasfoort R.B.M., Eppink M.H.M. Rapid screening of IgG quality attributes - effects on Fc receptor binding. *FEBS Open Bio*. 2017 Sep 5;7(10):1557-1574. Doi: 10.1002/2211-5463.12283.

Ghirlando R., Lund J., Goodall M., Jefferis R. Glycosylation of human IgG-Fc: influences on structure revealed by differential scanning micro-calorimetry. *Immunology Letters* 1999 May 3;68(1):47-52. Doi: 10.1016/s0165-2478(99)00029-2.

Goetze A.M., Liu Y.D., Zhang Z., Shah B., Lee E., Bondarenko P.V., Flynn G.C. High-mannose glycans on the Fc region of therapeutic IgG antibodies increase serum clearance in humans. *Glycobiology* 2011 Jul;21(7):949-59. Doi: 10.1093/glycob/cwr027.

Goetze A.M., Schenauer M.R., Flynn G.C. Assessing monoclonal antibody product quality attribute criticality through clinical studies. *MAbs*. 2010 Sep-Oct;2(5):500-7. Doi: 10.4161/mabs.2.5.12897.

Golay J., Introna M. Mechanism of action of therapeutic monoclonal antibodies: promises and pitfalls of in vitro and in vivo assays. *Archives of Biochemistry and Biophysics*. 2012 Oct 15;526(2):146-53. Doi: 10.1016/j.abb.2012.02.011.

Gong J.H., Maki G., Klingemann H.G. Characterization of a human cell line (NK-92) with phenotypical and functional characteristics of activated natural killer cells. *Leukemia*. 1994 Apr;8(4):652-8. PMID: 8152260.

Goulet D.R., Atkins W.M. Considerations for the Design of Antibody-Based Therapeutics. *Journal of Pharmaceutical Sciences* 2020 Jan;109(1):74-103. Doi: 10.1016/j.xphs.2019.05.031.

Greenbaum J., Sidney J., Chung J., Brander C., Peters B., Sette A. Functional classification of class II human leukocyte antigen (HLA) molecules reveals seven different supertypes and a surprising degree of repertoire sharing across supertypes. *Immunogenetics*. 2011 Jun;63(6):325-35. Doi: 10.1007/s00251-011-0513-0.

Groell F., Jordan O., Borchard G. In vitro models for immunogenicity prediction of therapeutic proteins. In: *European Journal of Pharmaceutics and Biopharmaceutics*, 2018, vol. 130, p. 128-142. Doi: 10.1016/j.ejpb.2018.06.008

Haberger M., Bomans K., Diepold K., Hook M., Gassner J., Schlothauer T., Zwick A., Spick C., Kepert J.F., Hienz B., Wiedmann M., Beck H., Metzger P., Mølhøj M., Knoblich C., Grauschopf U., Reusch D., Bulau P. Assessment of chemical modifications of sites in the CDRs of recombinant antibodies: Susceptibility vs. functionality of critical quality attributes. *MAbs*. 2014 Mar-Apr;6(2):327-39. Doi: 10.4161/mabs.27876.

Hansel T.T., Kropshofer H., Singer T., Mitchell J.A., George A.J. The safety and side effects of monoclonal antibodies. *Nature Reviews Drug Discovery*. 2010 Apr;9(4):325-38. Doi: 10.1038/nrd3003.

Hanson Q.M., Barb A.W. A perspective on the structure and receptor binding properties of immunoglobulin G Fc. *Biochemistry*. 2015 May 19;54(19):2931-42. Doi: 10.1021/acs.biochem.5b00299.

Harjunpää H., Guillerey C. (2019). TIGIT as an emerging immune checkpoint. *Clinical & Experimental Immunology*. 2020. May;200(2):108-119. Doi: 10.1111/cei.13407.

Hsieh Y.T., Aggarwal P., Cirelli D., Gu L., Surowy T., Mozier N.M. Characterization of FcγRIIIA effector cells used in in vitro ADCC bioassay: Comparison of primary NK cells with engineered NK-92 and Jurkat T cells. *Journal of Immunological Methods*. 2017 Feb;441:56-66. Doi: 10.1016/j.jim.2016.12.002.

<https://specialcarepr.com/en/game-changers-immuno-oncology-treatment/>

<https://www.cancer.gov/about-cancer/treatment/types/immunotherapy/checkpoint-inhibitors>

Hunter S.A., Cochran J.R. Cell-Binding Assays for Determining the Affinity of Protein-Protein Interactions: Technologies and Considerations. *Methods Enzymology*. 2016;580:21-44. Doi: 10.1016/bs.mie.2016.05.002.

Hutsell S. Q., Kimple R. J., Siderovski D. P., Willard F. S., & Kimple A. J. (2010). High-affinity immobilization of proteins using biotin- and GST-based coupling strategies. *Methods in molecular biology* (Clifton, N.J.), 627, 75-90. [https://doi.org/10.1007/978-1-60761-670-2\\_4](https://doi.org/10.1007/978-1-60761-670-2_4)

ICH guideline Q5E: comparability of biotechnological/biological products subject to changes in their manufacturing process. EMA/CPMP/ICH/5721/03

ICH guideline Q8 (R2) on pharmaceutical development

ICH guidelines, Q1A (R2): Stability Testing of New Drug Substances and Products (revision 2), International Conference on Harmonization

ICH Q2 (R1), Validation of analytical procedures (definitions and terminology); 2005; pp. 9-10.

Ifandi V., Al-Rubeai M. Stable transfection of CHO cells with the c-myc gene results in increased proliferation rates, reduces serum dependency, and induces anchorage independence. *Cytotechnology*. 2003;41(1):1-10. Doi:10.1023/A:1024203518501

Igawa T., Tsunoda H., Kuramochi T., Sampei Z., Ishii S., Hattori K. Engineering the variable region of therapeutic IgG antibodies. *MAbs*. 2011 May-Jun;3(3):243-52. Doi: 10.4161/mabs.3.3.15234.

Irani V., Guy A.J., Andrew D., Beeson J.G., Ramsland P.A., Richards J.S. Molecular properties of human IgG subclasses and their implications for designing therapeutic monoclonal antibodies against infectious diseases. *Molecular Immunology*. 2015 Oct;67(2 Pt A):171-82. Doi: 10.1016/j.molimm.2015.03.255.

Jahn E.M., Schneider C.K. How to systematically evaluate immunogenicity of therapeutic proteins - regulatory considerations. *Nature Biotechnology*. 2009 Jun;25(5):280-6. Doi: 10.1016/j.nbt.2009.03.012.

Janeway C. A., Travers P.J., Walport M., and Shlomchik M.J. *Immunobiology*, 5th edition: The Immune System in Health and Disease. Garland Science, 2001 ISBN-10: 0-8153-3642-X

Jawa V., Cousens L.P., Awwad M., Wakshull E., Kropshofer H., De Groot A.S. T-cell dependent immunogenicity of protein therapeutics: Preclinical assessment and mitigation, *Clinical Immunology*, Volume 149, Issue 3, Part B, 2013, Pages 534-555, ISSN 1521-6616, <https://doi.org/10.1016/j.clim.2013.09.006>.

Jawa V., Terry F., Gokemeijer J., Mitra-Kaushik S., Roberts B.J., Tourdot S., De Groot A.S. T-Cell Dependent Immunogenicity of Protein Therapeutics Pre-clinical Assessment and Mitigation-Updated Consensus and Review 2020. *Frontiers in Immunology*. 2020 Jun 30;11:1301. Doi: 10.3389/fimmu.2020.01301. PMID: 32695107; PMCID: PMC7338774.

Jensen K.K., Andreatta M., Marcatili P., Buus S., Greenbaum J.A., Yan Z., Sette A., Peters B., Nielsen M. Improved methods for predicting peptide binding affinity to MHC class II molecules. *Immunology*. 2018 Jul;154(3):394-406. doi: 10.1111/imm.12889.

Jiang X.R., Song A., Bergelson S., Arroll T., Parekh B., May K., Chung S., Strouse R., Mire-Sluis A., Schenerman M. Advances in the assessment and control of the effector functions of therapeutic antibodies. *Nature Reviews Drug Discovery*. 2011 Feb;10(2):101-11. Doi: 10.1038/nrd3365.

Jiskoot W., Kijanka G., Randolph T.W., Carpenter J.F., Koulov A.V., Mahler H.C., Joubert M.K., Jawa V., Narhi L.O. Mouse Models for Assessing Protein Immunogenicity: Lessons and Challenges. *Journal of Pharmaceutical Sciences*. 2016 May;105(5):1567-1575. Doi: 10.1016/j.xphs.2016.02.031.

Johnston R.J., Comps-Agrar L., Hackney J., Yu X., Huseni M., Yang Y., Park S., Javinal V., Chiu H., Irving B., Eaton D.L., Grogan J.L. The immunoreceptor TIGIT regulates antitumor and antiviral CD8(+) T cell effector function. *Cancer Cell*. 2014 Dec 8;26(6):923-937. Doi: 10.1016/j.ccell.2014.10.018.

Joller N., Hafler J.P., Brynedal B., Kassam N., Spoerl S., Levin S.D., Sharpe A.H., Kuchroo V.K. Cutting edge: TIGIT has T cell-intrinsic inhibitory functions. *Journal of Immunology*. 2011 Feb 1;186(3):1338-42. Doi: 10.4049/jimmunol.1003081.

Jones H.M., Zhang Z., Jasper P., Luo H., Avery L.B., King L.E., Neubert H., Barton H.A., Betts A.M., Webster R. A Physiologically-Based Pharmacokinetic Model for the Prediction of Monoclonal Antibody Pharmacokinetics From In Vitro Data. *CPT Pharmacometrics & Systems Pharmacology*. 2019 Oct;8(10):738-747. Doi: 10.1002/psp4.12461.

Kanda Y., Yamada T., Mori K., Okazaki A., Inoue M., Kitajima-Miyama K., Kuni-Kamochi R., Nakano R., Yano K., Kakita S., Shitara K., Satoh M. Comparison of biological activity among nonfucosylated therapeutic IgG1 antibodies with three different N-linked Fc oligosaccharides: the high-mannose, hybrid, and complex types. *Glycobiology*. 2007 Jan;17(1):104-18. Doi: 10.1093/glycob/cwl057.

Karlsson R., Katsamba P.S., Nordin H., Pol E., Myszka D.G. Analyzing a kinetic titration series using affinity biosensors, *Analytical Biochemistry*, Volume 349, Issue 1, 2006, Pages 136-147, ISSN 0003-2697, <https://doi.org/10.1016/j.ab.2005.09.034>.

Klingemann H., Boissel L., Toneguzzo F. Natural Killer Cells for Immunotherapy - Advantages of the NK-92 Cell Line over Blood NK Cells. *Frontiers in Immunology*. 2016 Mar 14;7:91. Doi: 10.3389/fimmu.2016.00091.

Koene H.R., Kleijer M., Algra J., Roos D., von dem Borne A.E., de Haas M. Fc gammaRIIIa-158V/F polymorphism influences the binding of IgG by natural killer cell Fc gammaRIIIa, independently of the Fc gammaRIIIa-48L/R/H phenotype. *Blood* 1997; 90:1109 – 14. PMID: 9242542.

Koren E., De Groot A.S., Jawa V., Beck K.D., Boone T., Rivera D., Li L., Mytych D., Koscec M., Weeraratne D., Swanson S., Martin W. 2007. Clinical validation of the “in silico” prediction of immunogenicity of a human recombinant therapeutic protein. *Clinical Immunology* 124: 26– 32. Doi: 10.1016/j.clim.2007.03.544.

Kosmas C., Stamatopoulos K., Stavroyianni N., Tsavaris N., Papadaki T. Anti-CD20-based therapy of B cell lymphoma: state of the art. *Leukemia*. 2002 Oct;16(10):2004-15. Doi: 10.1038/sj.leu.2402639. PMID: 12357351.



- Krishna M., Nadler S.G. Immunogenicity to biotherapeutics—the role of anti-drug immune complexes. *Frontiers in Immunology*. (2016) 7:21. Doi: 10.3389/fimmu.2016.00021
- Kurtulus S., Sakuishi K., Ngiow S.F., Joller N., Tan D.J., Teng M.W., Smyth M.J., Kuchroo V.K., Anderson A.C. TIGIT predominantly regulates the immune response via regulatory T cells. *J Clin Invest*. 2015 Nov 2;125(11):4053-62. Doi: 10.1172/JCI81187.
- Le Basle Y., Chennell P., Tokhadze N., Astier A., Sautou V. Physicochemical Stability of Monoclonal Antibodies: A Review. *Journal of Pharmaceutical Sciences*. 2020 Jan;109(1):169-190. Doi: 10.1016/j.xphs.2019.08.009.
- Lewis G.K., Ackerman M.E., Scarlatti G., Moog C., Robert-Guroff M., Kent S.J., Overbaugh J., Reeves R.K., Ferrari G., Thyagarajan B. Knowns and Unknowns of Assaying Antibody-Dependent Cell-Mediated Cytotoxicity Against HIV-1. *Frontiers in Immunology*. 2019 May 10;10:1025. Doi: 10.3389/fimmu.2019.01025.
- Li M., Xia P., Du Y., Liu S., Huang G., Chen J., Zhang H., Hou N., Cheng X., Zhou L., Li P., Yang X., Fan Z. T-cell immunoglobulin and ITIM domain (TIGIT) receptor/poliovirus receptor (PVR) ligand engagement suppresses interferon- $\gamma$  production of natural killer cells via  $\beta$ -arrestin 2-mediated negative signaling. *Journal of Biological Chemistry*. 2014 Jun 20;289(25):17647-57. Doi: 10.1074/jbc.M114.572420.
- Li Y.J., Bi L.J., Zhang X.E., Zhou Y.F., Zhang J.B., Chen Y.Y., Li W., Zhang Z.P. Reversible immobilization of proteins with streptavidin affinity tags on a surface plasmon resonance biosensor chip. *Analytical and Bioanalytical Chemistry*. 2006 Nov;386(5):1321-6. Doi: 10.1007/s00216-006-0794-6.
- Liu D., Ren D., Huang H., Dankberg J., Rosenfeld R., Cocco M.J., Li L., Brems D.N., Remmele R.L. Jr. Structure and stability changes of human IgG1 Fc as a consequence of methionine oxidation. *Biochemistry*. 2008 May 6;47(18):5088-100. Doi: 10.1021/bi702238b.
- Liu H., Gaza-Bulseco G., Xiang T., Chumsae C. Structural effect of deglycosylation and methionine oxidation on a recombinant monoclonal antibody. *Molecular Immunology*. 2008 Feb;45(3):701-8. Doi: 10.1016/j.molimm.2007.07.012.
- Liu H., Saxena A., Sidhu S.S., Wu D. Fc Engineering for Developing Therapeutic Bispecific Antibodies and Novel Scaffolds. *Frontiers in Immunology*. 2017 Jan 26;8:38. Doi: 10.3389/fimmu.2017.00038.

- Liu S., Zhang H., Li M., Hu D., Li C., Ge B., Jin B., Fan Z. Recruitment of Grb2 and SHIP1 by the ITT-like motif of TIGIT suppresses granule polarization and cytotoxicity of NK cells. *Cell Death & Differentiation* 2013 Mar;20(3):456-64. Doi: 10.1038/cdd.2012.141.
- Loew C., Knoblich C., Fichtl J., Alt N., Diepold K., Bulau P., Goldbach P., Adler M., Mahler H.C., Grauschopf U. Analytical protein a chromatography as a quantitative tool for the screening of methionine oxidation in monoclonal antibodies. *Journal of Pharmaceutical Sciences*. 2012 Nov;101(11):4248-57. Doi: 10.1002/jps.23286.
- Lu R.M., Hwang Y.C., Liu I.J., Lee C.C., Tsai H.Z., Li H.J., Wu H.C. Development of therapeutic antibodies for the treatment of diseases. *Journal of Biomedical Science*. 2020 Jan 2;27(1):1. Doi: 10.1186/s12929-019-0592-z.
- Lundholt B.K., Scudder K.M., Pagliaro L. A simple technique for reducing edge effect in cell-based assays. *Journal of Biomolecular Screening*. 2003 Oct;8(5):566-70. Doi: 10.1177/1087057103256465.
- Lund-Katz S., Nguyen D., Dhanasekaran P., Kono M., Nickel M., Saito H., & Phillips M. (2009). Surface plasmon resonance analysis of the mechanism of binding of apoA-I to high density lipoprotein particles. *Journal of lipid research*. 51. 606-17. Doi: 10.1194/jlr.M002055.
- Luo S., Levine R.L. Methionine in proteins defends against oxidative stress. *FASEB Journal*. 2009;23(2):464-472. Doi:10.1096/fj.08-118414
- Maeda A., Iwayanagi Y., Haraya K., Tachibana T., Nakamura G., Nambu T., Esaki K., Hattori K., Igawa T. Identification of human IgG1 variant with enhanced FcRn binding and without increased binding to rheumatoid factor autoantibody. *MAbs*. 2017 Jul;9(5):844-853. Doi: 10.1080/19420862.2017.1314873.
- Magistrelli G., Malinge P., Anceriz N., Desmurs M., Venet S., Calloud S., Daubeuf B., Kosco-Vilbois M., Fischer N. Robust recombinant FcRn production in mammalian cells enabling oriented immobilization for IgG binding studies. *Journal of Immunological Methods*. 2012 Jan 31;375(1-2):20-9. Doi: 10.1016/j.jim.2011.09.002.
- Mahmood I., Green M.D. Pharmacokinetic and pharmacodynamic considerations in the development of therapeutic proteins. *Clinical Pharmacokinetics*. 2005;44(4):331-47. Doi: 10.2165/00003088-200544040-00001.

- Mahoney K.M., Rennert P.D., Freeman G.J. Combination cancer immunotherapy and new immunomodulatory targets. *Nature Reviews Drug Discovery*. 2015 Aug;14(8):561-84. Doi: 10.1038/nrd4591.
- Manieri N.A., Chiang E.Y., Grogan J.L. TIGIT: A Key Inhibitor of the Cancer Immunity Cycle. *Trends in Immunology*. 2017 Jan;38(1):20-28. Doi: 10.1016/j.it.2016.10.002.
- Martin A.C.R. (2010) Protein Sequence and Structure Analysis of Antibody Variable Domains. In: Kontermann R., Dübel S. (eds) *Antibody Engineering*. Springer Protocols Handbooks. Springer, Berlin, Heidelberg. [https://doi.org/10.1007/978-3-642-01147-4\\_3](https://doi.org/10.1007/978-3-642-01147-4_3)
- Mathur A., Arora T., Liu L., Crouse-Zeineddini J., Mukku V. Qualification of a homogeneous cell-based neonatal Fc receptor (FcRn) binding assay and its application to studies on Fc functionality of IgG-based therapeutics. *Journal of Immunological Methods*. 2013 Apr 30;390(1-2):81-91. Doi: 10.1016/j.jim.2013.01.011.
- Melero I., Berman D.M., Aznar M.A., Korman A.J., Pérez Gracia J.L., Haanen J. Evolving synergistic combinations of targeted immunotherapies to combat cancer. *Nature Reviews Cancer*. 2015 Aug;15(8):457-72. Doi: 10.1038/nrc3973.
- Mimura Y., Church S., Ghirlando R., Ashton P.R., Dong S., Goodall M., Lund J., Jefferis R. The influence of glycosylation on the thermal stability and effector function expression of human IgG1-Fc: properties of a series of truncated glycoforms. *Molecular Immunology*. 2000 Aug-Sep;37(12-13):697-706. Doi: 10.1016/s0161-5890(00)00105-x.
- Mimura Y., Sondermann P., Ghirlando R., Lund J., Young S.P., Goodall M., Jefferis R. Role of oligosaccharide residues of IgG1-Fc in Fc gamma RIIb binding. *Journal of Biological Chemistry*. 2001 Dec 7;276(49):45539-47. Doi: 10.1074/jbc.M107478200.
- Mire-Sluis A.R. Progress in the use of biological assays during the development of biotechnology products. *Pharmaceutical Research*. 2001 Sep;18(9):1239-46. doi: 10.1023/a:1013067424248.
- Mitchell J. and Elder D., *The Role of Complimentary Methods in Analytical Quality Control*, American Pharmaceutical Review, 2016.
- Mohammed R., Milne A., Kayani K., Ojha U. How the discovery of rituximab impacted the treatment of B-cell non-Hodgkin's lymphomas. *Journal of Blood Medicine*. 2019 Feb 27;10:71-84. Doi: 10.2147/JBM.S190784.

Mould D.R., Meibohm B. Drug Development of Therapeutic Monoclonal Antibodies. *BioDrugs* 30, 275–293 (2016). <https://doi.org/10.1007/s40259-016-0181-6>

Mozziconacci O., Ji J.A., Wang Y.J., Schöneich C. Metal-catalyzed oxidation of protein methionine residues in human parathyroid hormone (1-34): formation of homocysteine and a novel methionine-dependent hydrolysis reaction. *Molecular Pharmacology*. 2013 Feb 4;10(2):739-55. Doi: 10.1021/mp300563m.

Neuber T., Frese K., Jaehrling J., Jäger S., Daubert D., Felderer K., Linnemann M., Höhne A., Kaden S., Kölln J., Tiller T., Brocks B., Ostendorp R., Pabst S. Characterization and screening of IgG binding to the neonatal Fc receptor. *MAbs*. 2014 Jul-Aug;6(4):928-42. Doi: 10.4161/mabs.28744.

Nimmerjahn F., Ravetch J.V. Fcγ receptors as regulators of immune responses. *Nature Reviews Immunology*. 2008 Jan;8(1):34-47. Doi: 10.1038/nri2206. PMID: 18064051.

Nowak C., K Cheung J., M Dellatore S., Katiyar A., Bhat R., Sun J., Ponniah G., Neill A., Mason B., Beck A., Liu H. Forced degradation of recombinant monoclonal antibodies: A practical guide. *MAbs*. 2017 Nov/Dec;9(8):1217-1230. Doi: 10.1080/19420862.2017.1368602.

Olaru A., Bala C., Jaffrezic-Renault N, & Aboul-Enein H.Y. Surface Plasmon Resonance (SPR) Biosensors in Pharmaceutical Analysis, *Critical Reviews in Analytical Chemistry*, 45:2, 97-105, (2015) Doi: 10.1080/10408347.2014.881250

Parekh B.S., Berger E., Sibley S., Cahya S., Xiao L., LaCerte M.A., Vaillancourt P., Wooden S. & Gately D. Development and validation of an antibody-dependent cell-mediated cytotoxicity-reporter gene assay, *MAbs*, 4:3, 310-318 (2012). Doi: 10.4161/mabs.19873

Patching Simon G., Surface plasmon resonance spectroscopy for characterisation of membrane protein–ligand interactions and its potential for drug discovery, *Biochimica et Biophysica Acta (BBA) - Biomembranes*, Volume 1838, Issue 1, Part A, 2014, Pages 43-55, ISSN 0005-2736, <https://doi.org/10.1016/j.bbamem.2013.04.028>.

Paul S., Kolla R.V., Sidney J., Weiskopf D., Fleri W., Kim Y., Peters B., Sette A. Evaluating the Immunogenicity of Protein Drugs by Applying In Vitro MHC Binding Data and the Immune Epitope Database and Analysis Resource, *Journal of Immunology Research*, vol. 2013, Article ID 467852, 7 pages, 2013. <https://doi.org/10.1155/2013/467852>

- Paul S., Sidney J., Sette A., Peters B. TepiTool: A Pipeline for Computational Prediction of T Cell Epitope Candidates. *Current Protocols in Immunology*. 2016; 114:18.19.1-18.19.24. Published 2016 Aug 1. Doi:10.1002/cpim.12
- Porter S., Human immune response to recombinant human proteins. *Journal of Pharmaceutical Sciences*. 2001 Jan;90(1):1-11. Doi: 10.1002/1520-6017(200101)90:1<1::aid-jps1>3.0.co;2-k.
- Putnam W.S., Prabhu S., Zheng Y., Subramanyam M., Wang Y-M.C. Pharmacokinetic, pharmacodynamic and immunogenicity comparability assessment strategies for monoclonal antibodies. *Trends in Biotechnology*. (2010) 28:509–16. Doi: 10.1016/j.tibtech.2010.07.001
- Qin S., Xu L., Yi M., Yu S., & Wu K., & Luo S. Novel immune checkpoint targets: Moving beyond PD-1 and CTLA-4. *Molecular Cancer*. 18, 155 (2019). Doi: 10.1186/s12943-019-1091-2.
- Qureshi M.H., Yeung J.C., Wu S.C., Wong S.L. Development and characterization of a series of soluble tetrameric and monomeric streptavidin muteins with differential biotin binding affinities. *Journal of Biological Chemistry*. 2001 Dec 7;276(49):46422-8. Doi: 10.1074/jbc.M107398200.
- Rajasekaran N., Chester C., Yonezawa A., Zhao X., & Kohrt H. E. Enhancement of antibody-dependent cell mediated cytotoxicity: a new era in cancer treatment. *ImmunoTargets and therapy*, 4, 91–100 (2015). <https://doi.org/10.2147/ITT.S61292>
- Raju T.S. Terminal sugars of Fc glycans influence antibody effector functions of IgGs. *Current Opinion in Immunology*. 2008 Aug;20(4):471-8. Doi: 10.1016/j.coi.2008.06.007.
- Rathore A., Weiskopf A. & Reason A. (2015). Defining Critical Quality Attributes for Monoclonal Antibody Therapeutic Products. *BioPharm International*. Vol 27(7):34-43 (2014).
- Rathore A.S., Roadmap for implementation of quality by design (QbD) for biotechnology products. *Trends in Biotechnology*. 2009 Sep;27(9):546-53. Doi: 10.1016/j.tibtech.2009.06.006.
- Ravisankar P., Sankar R. A Review on Step-by-Step Analytical Method Validation. Volume 5, Issue 10, pp 7-19 (2015).
- Redman J.M., Hill E.M., AlDeghaither D., Weiner L.M. Mechanisms of action of therapeutic antibodies for cancer. *Molecular Immunology*. 2015 Oct;67(2 Pt A):28-45. Doi: 10.1016/j.molimm.2015.04.002.
- Reichert J.M., Rosensweig C.J., Faden L.B., Dewitz M.C. Monoclonal antibody successes in the clinic. *Nature Biotechnology*. 2005 Sep;23(9):1073-8. Doi: 10.1038/nbt0905-1073.

- Ritter N., Advant S.J., Hennessey J., Simmerman H., McEntire J., Mire-Sluis A., and Joneckis C. What is test method qualification? Proceedings of the WCBP CMC Strategy Forum, 24 July 2013. BioProcess International 2014
- Robinson J., Sadick M., Deming S., Estdale S., Bergelson S., Little L. Assay acceptance criteria for multiwell-plate-based biological potency assays. *BioProcess Technology*. 12(1), 30–41 (2014).
- Rodgers K.R., Chou R.C. Therapeutic monoclonal antibodies and derivatives: Historical perspectives and future directions. *Biotechnol Advances*. 2016 Nov 1;34(6):1149-1158. Doi: 10.1016/j.biotechadv.2016.07.004.
- Roselle C., Verch T., Shank-Retzlaff M. Mitigation of microtiter plate positioning effects using a block randomization scheme. *Analytical and Bioanalytical Chemistry*. 2016 Jun;408(15):3969-79. Doi: 10.1007/s00216-016-9469-0.
- Rosenberg A.S. Effects of protein aggregates: an immunologic perspective. *AAPS Journal*. 2006 Aug 4;8(3):E501-7. Doi: 10.1208/aapsj080359. PMID: 17025268; PMCID: PMC2761057.
- Rosenberg A.S., Worobec A. A risk-based approach to immunogenicity concerns of therapeutic protein products, Part I: Considering consequences of the immune response to a protein. *BioPharm Int* 17(11): 22– 26 (2004).
- Rossignol A., Bonnaudet V., Clémenceau B., Vié H., Bretaudeau L. A high-performance, non-radioactive potency assay for measuring cytotoxicity: A full substitute of the chromium-release assay targeting the regulatory-compliance objective. *MAbs*. 2017 Apr;9(3):521-535. Doi: 10.1080/19420862.2017.1286435.
- Rudnick S.I., Adams G.P. Affinity and avidity in antibody-based tumor targeting. *Cancer Biotherapy and Radiopharmaceuticals*. 2009 Apr;24(2):155-61. Doi: 10.1089/cbr.2009.0627.
- Sabir A., Moloy M., Bhasin P. HPLC METHOD DEVELOPMENT AND VALIDATION: A REVIEW. *International Research Journal of Pharmacy*. 4. 39-46 (2015). Doi: 10.7897/2230-8407.04407.
- Sanchez-Correa B., Valhondo I., Hassouneh F., Lopez-Sejas N., Pera A., Bergua J.M., Arcos M.J., Bañas H., Casas-Avilés I., Durán E., Alonso C., Solana R., Tarazona R. DNAM-1 and the TIGIT/PVRIG/TACTILE Axis: Novel Immune Checkpoints for Natural Killer Cell-Based Cancer Immunotherapy. *Cancers (Basel)*. 2019 Jun 23;11(6):877. Doi: 10.3390/cancers11060877.

- Sankar K., Hoi K.H., Yin Y., Ramachandran P., Andersen N., Hilderbrand A., McDonald P., Spiess C., Zhang Q. Prediction of methionine oxidation risk in monoclonal antibodies using a machine learning method. *MAbs*. 2018 Nov-Dec;10(8):1281-1290. Doi: 10.1080/19420862.2018.1518887.
- Saxena N. Validation of Analytical Methods used for the Characterization, Physicochemical and Functional Analysis and of Biopharmaceuticals.2010
- Schasfoort R. & Tudos A. (2007). Handbook Of Surface Plasmon Resonance. Doi: 10.1039/9781847558220.
- Schellekens H. Bioequivalence and the immunogenicity of biopharmaceuticals. *Nature Reviews Drug Discovery*. 2002 Jun;1(6):457-62. Doi: 10.1038/nrd818. PMID: 12119747.
- Schellekens H. Factors influencing the immunogenicity of therapeutic proteins. *Nephrology Dialysis Transplantation* (2005) 20 [Suppl 6]: vi3–vi9. Doi:10.1093/ndt/gfh1092
- Schlothauer T., Rueger P., Stracke J.O., Hertenberger H., Fingas F., Kling L., Emrich T., Drabner G., Seeber S., Auer J., Koch S., Papadimitriou A. Analytical FcRn affinity chromatography for functional characterization of monoclonal antibodies. *MAbs*. 2013 Jul-Aug;5(4):576-86. Doi: 10.4161/mabs.24981.
- Scott A.M., Allison J.P., Wolchok J.D. Monoclonal antibodies in cancer therapy. *Cancer Immunology*. 2012;12:14. PMID: 22896759; PMCID: PMC3380347.
- Shah D.D., Zhang J., Maity H., Mallela K.M.G. Effect of photo-degradation on the structure, stability, aggregation, and function of an IgG1 monoclonal antibody. *International Journal of Pharmaceutics*. 2018 Aug 25;547(1-2):438-449. Doi: 10.1016/j.ijpharm.2018.06.007.
- Shankar G., Arkin S., Cocea L., Devanarayan V., Kirshner S, Kromminga A., Quarmby V., Richards S., Schneider C.K., Subramanyam M., Swanson S., Verthelyi D., Yim S. American Association of Pharmaceutical Scientists. Assessment and reporting of the clinical immunogenicity of therapeutic proteins and peptides-harmonized terminology and tactical recommendations. *AAPS Journal*. 2014 Jul;16(4):658-73. Doi: 10.1208/s12248-014-9599-2.
- Sharma, S., Goyal S. & Chauhan K. A review on analytical method development and validation. *International Journal of Applied Pharmaceutics*. 10. 8. (2018). Doi: 10.22159/ijap.2018v10i6.28279.
- Shields R.L., Lai J., Keck R., O'Connell L.Y., Hong K., Meng Y.G., Weikert S.H., Presta L.G. Lack of fucose on human IgG1 N-linked oligosaccharide improves binding to human FcγRIII and

antibody-dependent cellular toxicity. *Journal of Biological Chemistry*. 2002 Jul 26;277(30):26733-40. Doi: 10.1074/jbc.M202069200.

Sibénil S., Ménez R., Jorieux S., de Romeuf C., Bourel D., Fridman W.H., Ducancel F., Stura E.A., Teillaud J.L. Effect of zinc on human IgG1 and its FcγR interactions. *Immunology Letter*. 2012 Mar 30;143(1):60-9. Doi: 10.1016/j.imlet.2012.02.002. PMID: 22553781.

Singh S.K. Impact of product-related factors on immunogenicity of biotherapeutics. *Journal of Pharmaceutical Sciences*. 2011 Feb;100(2):354-87. Doi: 10.1002/jps.22276.

Singh S.K., Afonina N., Awwad M., Bechtold-Peters K., Blue J.T., Chou D., Cromwell M., Krause H.J., Mahler H.C., Meyer B.K., Narhi L., Nesta D.P., Spitznagel T. An industry perspective on the monitoring of subvisible particles as a quality attribute for protein therapeutics. *Journal of Pharmaceutical Sciences*. 2010 Aug;99(8):3302-21. Doi: 10.1002/jps.22097.

Smith-Garvin J.E., Koretzky G.A., Jordan M.S. T cell activation. *Annual Review of Immunology*. 2009; 27:591-619. Doi: 10.1146/annurev.immunol.021908.132706.

Songara R., Prakashkumar A. Overview of analytical method validation in Pharmaceutical industries, *IJPI Journal of Analytical Chemistry*, vol 1:5 (2010) ISSN 2229-6867

Steinitz M. Quantitation of the blocking effect of tween 20 and bovine serum albumin in ELISA microwells. *Analytical Biochemistry*. 2000 Jul 1;282(2):232-8. Doi: 10.1006/abio.2000.4602. PMID: 10873278.

Suzuki M., Kato C., Kato A. Therapeutic antibodies: their mechanisms of action and the pathological findings they induce in toxicity studies [published correction appears in *Journal of Toxicologic Pathology*. 2016 Jan;29(1):74]. *J Toxicol Pathol*. 2015;28(3):133-139. Doi:10.1293/tox.2015-0031

Syedbasha M., Linnik J., Santer D., O'Shea D., Barakat K., Joyce M., Khanna N., Tyrrell D.L., Houghton M., Egli A. An ELISA Based Binding and Competition Method to Rapidly Determine Ligand-receptor Interactions. *Journal of Visualized Experiments*. 2016 Mar 14;(109):53575. Doi: 10.3791/53575.

Tabrizi M.A., Tseng C.M., Roskos L.K. Elimination mechanisms of therapeutic monoclonal antibodies. *Drug Discovery Today*. 2006 Jan;11(1-2):81-8. Doi: 10.1016/S1359-6446(05)03638-X.



Tada M., Ishii-Watabe A., Suzuki T., Kawasaki N. Development of a cell-based assay measuring the activation of FcγRIIa for the characterization of therapeutic monoclonal antibodies. *PLoS One*. 2014 Apr 21;9(4):e95787. Doi: 10.1371/journal.pone.0095787.

Tamizi E., Jouyban A., Forced degradation studies of biopharmaceuticals: Selection of stress conditions, *European Journal of Pharmaceutics and Biopharmaceutics*, Volume 98, 2016, Pages 26-46, ISSN 0939-6411, <https://doi.org/10.1016/j.ejpb.2015.10.016>.

Tao M.H., Morrison S.L. Studies of aglycosylated chimeric mouse-human IgG. Role of carbohydrate in the structure and effector functions mediated by the human IgG constant region. *Journal of Immunology*. 1989 Oct 15;143(8):2595-601. PMID: 2507634.

Torosantucci R., Schöneich C., Jiskoot W. Oxidation of therapeutic proteins and peptides: structural and biological consequences. *Pharmaceutical Research*. 2014 Mar;31(3):541-53. Doi: 10.1007/s11095-013-1199-9.

Turnis M.E., Andrews L.P., Vignali D.A. Inhibitory receptors as targets for cancer immunotherapy. *European Journal of Immunology*. 2015 Jul;45(7):1892-905. Doi: 10.1002/eji.201344413. PMID: 26018646; PMCID: PMC4549156.

User's guide to Alpha assays protein:protein interactions, PerkinElmer  
[http://www.blossombio.com/pdf/products/UG\\_Alphatech.pdf](http://www.blossombio.com/pdf/products/UG_Alphatech.pdf)

#### USP <1033> Biological Assay Validation

Vaisman-Mentesh A., Rosenstein S., Yavzori M., Dror Y., Fudim E., Ungar B., Kopylov U., Picard O., Kigel A., Ben-Horin S., Benhar I., Wine Y. Molecular Landscape of Anti-Drug Antibodies Reveals the Mechanism of the Immune Response Following Treatment With TNFα Antagonists. *Frontiers in Immunology*. 2019 Dec 18;10:2921. Doi: 10.3389/fimmu.2019.02921.

Van Erp E.A., Luytjes W., Ferwerda G., van Kasteren P.B. Fc-Mediated Antibody Effector Functions During Respiratory Syncytial Virus Infection and Disease. *Frontiers in Immunology*. 2019 Mar 22;10:548. Doi: 10.3389/fimmu.2019.00548.

Van Walle I., Gansemans Y., Parren P.W., Stas P., Lasters I. 2007. Immunogenicity screening in protein drug development. *Expert Opinion Biological Therapy*. 2007;7(3):405–418. Doi: 10.1517/14712598.7.3.405.

- Vidarsson G., Dekkers G., Rispens T. IgG subclasses and allotypes: from structure to effector functions. *Frontiers in Immunology*. 2014 Oct 20;5:520. Doi: 10.3389/fimmu.2014.00520.
- Wadhwa M., Knezevic I., Kang H.N., Thorpe R. Immunogenicity assessment of biotherapeutic products: An overview of assays and their utility. *Biologicals*. 2015 Sep;43(5):298-306. Doi: 10.1016/j.biologicals.2015.06.004.
- Walker D.K. The use of pharmacokinetic and pharmacodynamic data in the assessment of drug safety in early drug development. *British Journal of Clinical Pharmacology*. 2004 Dec;58(6):601-8. Doi: 10.1111/j.1365-2125.2004.02194.x.
- Wang M., Bu J., Zhou M., Sido J., Lin Y., Liu G., Lin Q., Xu X., Leavenworth J.W., Shen E. CD8+T cells expressing both PD-1 and TIGIT but not CD226 are dysfunctional in acute myeloid leukemia (AML) patients. *Clinical Immunology*. 2018 May;190:64-73. Doi: 10.1016/j.clim.2017.08.021.
- Wang P., Sidney J., Kim Y., Sette A., Lund O., Nielsen M., Peters B. Peptide binding predictions for HLA DR, DP and DQ molecules. *BMC Bioinformatics*. 2010 Nov 22;11:568. Doi: 10.1186/1471-2105-11-568.
- Wang W., Erbe A.K., Hank J.A., Morris Z.S., Sondel P.M. NK Cell-Mediated Antibody-Dependent Cellular Cytotoxicity in Cancer Immunotherapy. *Frontiers in Immunology*. 2015;6:368. Doi:10.3389/fimmu.2015.00368
- Wang W., Singh S., Zeng D.L., King K., Nema S. Antibody structure, instability, and formulation. *Journal of Pharmaceutical Sciences*. 2007 Jan;96(1):1-26. Doi: 10.1002/jps.20727. PMID: 16998873.
- Wang W., Vlasak J., Li Y., Pristatsky P., Fang Y., Pittman T., Roman J., Wang Y., Prueksaritanont T., Ionescu R. Impact of methionine oxidation in human IgG1 Fc on serum half-life of monoclonal antibodies. *Molecular Immunology*. 2011 Mar;48(6-7):860-6. Doi: 10.1016/j.molimm.2010.12.009.
- Wang X., An Z., Luo W., Xia N., Zaho Q. Molecular and functional analysis of monoclonal antibodies in support of biologics development. *Protein Cell* 9, 74–85 (2018). <https://doi.org/10.1007/s13238-017-0447-x>
- Wang X., McKay P., Yee L.T., Dutina G., Hass P.E., Nijem I., Allison D., Cowan K.J., Lin K., Quarmby V., Yang J. Impact of SPR biosensor assay configuration on antibody: Neonatal Fc receptor binding data. *MAbs*. 2017 Feb/Mar;9(2):319-332. Doi: 10.1080/19420862.2016.1261774.

- Weinberg W.C., Frazier-Jessen M.R., Wu W.J., Weir A., Hartsough M., Keegan P., Fuchs C. Development and regulation of monoclonal antibody products: challenges and opportunities. *Cancer Metastasis Reviews*. 2005 Dec;24(4):569-84. Doi: 10.1007/s10555-005-6196-y.
- White J.R., Abodeely M., Ahmed S., Debaue G., Johnson E., Meyer D.M., Mozier N.M., Naumer M., Pepe A., Qahwash I., Rocnik E., Smith J.G., Stokes E.S., Talbot J.J., Wong P.Y. Best practices in bioassay development to support registration of biopharmaceuticals. *Biotechniques*. 2019 Sep;67(3):126-137. Doi: 10.2144/btn-2019-0031.
- Wood C. In-Process Control Testing. *Separation Science and Technology* (2011). Doi:10.1016/B978-0-12-375680-0.00010-3.
- Woof J., Burton D. Human antibody–Fc receptor interactions illuminated by crystal structures. *Nature Review Immunology* 4, 89–99 (2004). <https://doi.org/10.1038/nri1266>
- Wu Q., Lee H.Y., Wong P.Y., Jiang G., Gazzano-Santoro H. Development and applications of AlphaScreen-based FcRn binding assay to characterize monoclonal antibodies. *Journal of Immunological Methods*. 2015 May; 420:31-7. Doi: 10.1016/j.jim.2015.03.012.
- Wu J., Edberg J.C., Redecha P.B., Bansal V., Guyre P.M., Coleman K., Salmon J.E., Kimberly R.P. A novel polymorphism of FcγRIIIa (CD16) alters receptor function and predisposes to autoimmune disease. *Journal Clinical Investigations*. 1997 Sep 1;100(5):1059-70. Doi: 10.1172/JCI119616.
- Xu Y., Wang D., Mason B., Rossomando T., Li N., Liu D., Cheung J.K., Xu W., Raghava S., Katiyar A., Nowak C., Xiang T., Dong D., Sun J., Beck A., Liu H. Structure, heterogeneity and developability assessment of therapeutic antibodies, *MAbs*, 11:2, 239-264, (2019). Doi: 10.1080/19420862.2018.1553476
- Yang D., Singh A., Wu H., Kroe-Barrett R. Comparison of biosensor platforms in the evaluation of high affinity antibody-antigen binding kinetics, *Analytical Biochemistry*, Volume 508, 2016, Pages 78-96, ISSN 0003-2697, <https://doi.org/10.1016/j.ab.2016.06.024>.
- Yang L., Biswas M.E., Chen P. Study of binding between protein A and immunoglobulin G using a surface tension probe. *Biophysical Journal*. 2003 Jan;84(1):509-22. Doi: 10.1016/S0006-3495(03)74870-X.

- Yeh W-I., Seay H., Mathews C., Brusko T. (2018). Costimulatory Molecules CD226 and TIGIT Impact CD8<sup>+</sup> T-Cell Activity and Function during Type 1 Diabetes. *Diabetes* 2018; 67(1) Doi: 10.2337/db18-96-OR.
- Yu M., Brown D., Reed C., Chung S., Lutman J., Stefanich E., Wong A., Stephan J-P., Bayer R. Production, characterization, and pharmacokinetic properties of antibodies with N-linked mannose-5 glycans. *MAbs*. 2012;4:475–487. Doi:10.4161/mabs.20737.)
- Yu X., Harden K., Gonzalez L.C., Francesco M., Chiang E., Irving B., Tom I., Ivelja S., Refino C.J., Clark H., Eaton D., Grogan J.L. The surface protein TIGIT suppresses T cell activation by promoting the generation of mature immunoregulatory dendritic cells. *Nature Immunology*. 2009 Jan;10(1):48-57. Doi: 10.1038/ni.1674.
- Zafir-Lavie, I., Michaeli, Y. & Reiter, Y. Novel antibodies as anticancer agents. *Oncogene* 26, 3714–3733 (2007). <https://doi.org/10.1038/sj.onc.1210372>
- Zahavi D., AlDeghaither D., O’Connell A., Weiner L.M. Enhancing antibody-dependent cell-mediated cytotoxicity: a strategy for improving antibody-based immunotherapy, *Antibody Therapeutics*, Volume 1, Issue 1, June 2018, Pages 7–12, <https://doi.org/10.1093/abt/tby002>
- Zhu Y., Paniccia A., Schulick A.C., Chen W., Koenig M.R., Byers J.T., Yao S., Bevers S., Edil B.H. Identification of CD112R as a novel checkpoint for human T cells. *Journal of Experimental Medicine*. 2016 Feb 8;213(2):167-76. Doi: 10.1084/jem.20150785.
- Zhuang Y., Chen D., Sharma A., Xu Z. Risk-Based Comparability Assessment for Monoclonal Antibodies During Drug Development: A Clinical Pharmacology Perspective. *AAPS Journal*. 2018 Oct 15;20(6):109. Doi: 10.1208/s12248-018-0268-8.